

AD-A009 228

ELECTROMAGNETIC-PULSE HANDBOOK FOR
ELECTRIC POWER SYSTEMS

Edward F. Vance

Stanford Research Institute

Prepared for:

Defense Nuclear Agency

4 February 1975

DISTRIBUTED BY:



National Technical Information Service
U. S. DEPARTMENT OF COMMERCE

ACCESSION FOR

NTIS	White Section <input checked="" type="checkbox"/>
DOC	Off. Section <input type="checkbox"/>
UNAP CUBED	<input type="checkbox"/>
JUSTRIFICATION	
BY DISTRIBUTOR AVAILABILITY CODES	
DIST.	REF ID: A6110000000000000000
A	

**Destroy this report when it is no longer
needed. Do not return to sender.**



UNCLASSIFIED

SECURITY CLASSIFICATION OF THIS PAGE (When Data Entered)

DD FORM 1 JAN 73 1473

Reproduced by
**NATIONAL TECHNICAL
INFORMATION SERVICE**
U.S. Department of Commerce
Springfield, VA. 22151

UNCLASSIFIED

SECURITY CLASSIFICATION OF THIS PAGE (When Data Entered)

UNCLASSIFIED

SECURITY CLASSIFICATION OF THIS PAGE(When Data Entered)

20. ABSTRACT (Continued)

The emphasis of the handbook is on the EMP effects of concern to the power user, but much of the information contained in the handbook can also be used to evaluate the effects of the EMP on electric power systems.

UNCLASSIFIED

SECURITY CLASSIFICATION OF THIS PAGE(When Data Entered)

SUMMARY

This handbook has been prepared primarily for the power, communications, and systems engineer who must be concerned with the effects of the nuclear electromagnetic pulse on his system. The power engineer should be aware of the effects of EMP on his transmission and distribution system, and the power users must protect their equipment from the pulse conducted into their facilities on the power lines. The contents of this handbook draw heavily on the results of research conducted at Stanford Research Institute for the Air Force Weapons Laboratory under Contract F29601-69-C-0127 and on the extensive work conducted by D. B. Nelson, J. K. Baird, and J. H. Marable at the Oak Ridge National Laboratory.

This handbook was prepared under the auspices of the Defense Nuclear Agency under Contract DNA001-73-C-0238. Project Officers for this task were Maj. Frank Vajda and Maj. William Adams.

PREFACE

The author gratefully acknowledges the constructive criticism of the draft by A. L. Whitson, L. Schlessinger, J. E. Bridges, J. H. Marable, and R. V. Hugo, and by Maj. William Adams. Their many suggestions have, without doubt, contributed to a more useful handbook. Special credit should also be given to Maj. Frank Vajda who initiated the program for preparation of this handbook.

TABLE OF CONTENTS

Chapter One	EFFECTS OF THE EMP ON POWER SYSTEMS	
1.1	Introduction	21
1.2	Characteristics of the Nuclear EMP	22
1.2.1	Generation of the EMP	22
1.2.2	Characteristics of the High-Altitude EMP	24
1.2.3	Comparison with Lightning	25
1.2.4	Technology Applicable to EMP Analysis	28
1.3	Description of a Power System	29
1.4	Contents and Use of the Handbook	34
1.4.1	Subjects Covered	34
1.4.2	Conventions Used in the Handbook	38
1.5	Cited References	40
Chapter Two	COUPLING TO TRANSMISSION LINES	
2.1	Transmission-Line Configurations	42
2.1.1	General	42
2.1.2	Construction of Transmission Lines	43
2.1.3	Transmission-Line Cable	45
2.1.4	Line Insulators	46
2.1.5	Interaction of the EMP with Transmission Lines	49
2.2	Coupling to Horizontal Conductors	50
2.2.1	Semi-Infinite Line	50
2.2.1.1	General Approach	50
2.2.1.2	General Analysis of Transmission Lines	51
2.2.1.3	Open-Circuit Voltage in the Frequency Domain	56
2.2.1.4	Transient Waveforms for an Exponential Pulse	62
2.2.1.5	Parametric Variation of the Open-Circuit Voltage	62

2.2.2	Line of Finite Length	66
2.2.2.1	Uniform Plane Wave	66
2.2.2.2	Spherical Wave at Grazing Incidence	68
2.2.3	Rate of Rise of the Open-Circuit Voltage	73
2.3	Response of a Vertical Element	77
2.3.1	Current at Top of Vertical Element	77
2.3.2	Current at Base of Vertical Element	81
2.3.3	Comparison of Voltage in Vertical and Horizontal Elements	83
2.3.4	General Analysis of Vertical Elements	84
2.3.5	Impedance of a Ground Rod	86
2.3.6	Response of Horizontal Conductor with Vertical Risers	88
2.3.7	Periodically Grounded Line	91
2.4	Transmission Properties of Power Lines	98
2.4.1	Attenuation and Phase Characteristics	98
2.4.2	Junctions in Transmission Lines	106
2.4.3	Bends in Power Lines	109
2.4.4	Other Effects	112
2.5	Differential Coupling to Horizontal Conductors	116
2.5.1	Wires in a Horizontal Plane	116
2.5.2	Wires in a Vertical Plane	121
2.5.3	Mode Conversion at the Load	125
2.6	High-Voltage Properties of Transmission-Line Components	126
2.6.1	General	126
2.6.2	Insulator Flashover Characteristics	127
2.6.3	Lightning-Arrester Firing Characteristics	129
2.6.4	Corona Threshold of Conductors	131
2.7	Cited References	133

Chapter Three **CONSUMER'S SERVICE ENTRANCE**

3.1	Introduction	136
3.1.1	Description of the Service Entrance.	136
3.1.2	Ground-Based Transformer Installation	138
3.1.3	Pole-Mounted Transformer Installations	140
3.1.4	Effect of Service Entrance on EMP Coupling	143
3.2.	Transmission Through Conduits and Cables	145
3.2.1	Transfer Functions for Conduits and Shielded Cables	145
3.2.2	Thevenin-Equivalent Source	153
3.2.3	Characteristic Impedance of Conductors in a Conduit	153
3.2.4	Characteristic Impedance of Shielded Cables	157
3.3	Coupling Through Steel Conduit Walls	158
3.3.1	General Considerations	158
3.3.2	Bulk Currents Induced in Buried Conduits	161
3.3.2.1	General	161
3.3.2.2	Current Far from the Ends of a Long Conduit	161
3.3.2.3	Current Near the End of a Long Bare Conduit	165
3.3.2.4	Current in an Electrically Short Conduit	170
3.3.3	Current and Voltage Induced on Internal Conductors	173
3.3.3.1	Transfer Impedance of Steel Conduit	173
3.3.3.2	Internal Voltage Induced in an Electrically Short Conduit - Uniform Exponential Current	176
3.3.3.3	Internal Voltage from Incident Field	181
3.3.3.4	Saturation of Steel Conduit	182
3.4	Cables in Nonmetallic Conduit	184
3.4.1	General Considerations	184
3.4.2	Current Induced on Cables	185
3.4.3	Transfer Impedance of Cable Shields	194
3.5	Cited References	199

Chapter Four**PROPERTIES OF DISTRIBUTION TRANSFORMERS**

4.1	Introduction	201
4.1.1	Effects of Transformers and Lightning Arresters	201
4.1.2	Transformer Construction	203
4.1.3	Lightning-Arrester Construction	209
4.2	Linear Characteristics of Transformers	211
4.2.1	Analysis of Transformer Coupling Characteristics	211
4.2.2	Distribution of Voltage Along the Windings	217
4.2.3	CW Measurements of Transformer Characteristics	219
4.2.4	Linear Transient Test Results	231
4.3	Nonlinear Characteristics of Transformers	241
4.3.1	Transformer Responses	241
4.3.2	Lightning-Arrester Firing Characteristics	244
4.3.3	Summary of Transformer and Lightning-Arrester Properties	248
4.4	Cited References	249

Chapter Five**LOW-VOLTAGE CIRCUITS**

5.1.	General Description of the Low-Voltage System	251
5.1.1	Installation Practice	251
5.1.2	Distribution of the EMP-Induced Signal	254
5.2	Linear Analysis of Conduit Circuits	258
5.2.1	Transmission-Line Analysis (Common-Mode)	258
5.2.2	Determination of the Properties of Conduit Circuits	264
5.2.2.1	Characteristic Impedance	264
5.2.2.2	Propagation Factor and Length	267
5.2.2.3	Stray Inductance of Leads	267
5.2.2.4	Load Impedances	268
5.2.3	Multiconductor-Transmission-Line Analysis	273
5.3	Cited References	275

Chapter Six GROUNDING SYSTEMS

6.1	General Description of Grounding Systems	276
6.1.1	Power-System Grounding	277
6.1.2	Grounding Low-Voltage Wiring	279
6.1.3	Grounding Electronic Equipment	280
6.2.	Evolution of a Facility Grounding System	280
6.3	Principles of Grounding	285
6.3.1	Single-Point vs. Distributed Ground	285
6.3.2	Ground Impedance	287
6.3.3	Tree Ground	288
6.3.4	Distributed Ground	291
6.3.5	Star Ground	291
6.3.6	Some Guidelines for System Design	292
6.4	Grounding Counterpoise	294
6.5	Cited References	297

Chapter Seven POWER-SYSTEM PRACTICES FOR EMP PROTECTION

7.1	Introduction	298
7.2	Protection from the Power System	300
7.2.1	EMP Protection of the Consumer	300
7.2.2	Voltage Limiters and Filters	300
7.2.3	Selection and Installation of Surge Arresters	301
7.2.4	Selection and Installation of Line Filters	306
7.2.5	Auxiliary Power Systems	310
7.2.5.1	Function of Auxiliary Power Systems	310
7.2.5.2	The Automatic Transfer Switch	311
7.3	Protection of the Power System	315
7.4	Cited References	317

Chapter Eight	TESTS OF COMPONENTS AND FACILITIES	
8.1	Introduction	318
8.2	Standard Insulation Tests	320
8.3	EMP Tests of Equipment	321
8.3.1	Purpose of Equipment Tests	321
8.3.2	Direct-Injection Tests	324
8.4	EMP Tests of Facilities	327
8.4.1	Excitation of the Service Entrance	327
8.4.2	Observation of the System Response	329
8.5	Cited References	334
INDEX		335

ILLUSTRATIONS

1-1	Mechanism for Generation of the EMP	23
1-2	Two-Exponential Representation of the High-Altitude Map Waveform	26
1-3	Magnitude of the Spectrum of the Two-Exponential Waveform	26
1-4	Last Pole of Distribution Spur Showing Lightning Arresters, Potheads, and Entrance Conduit	30
1-5	Ground-Based Distribution Transformers: Primary Side and Distribution Potheads	31
1-6	Ground-Based Distribution Transformers: Secondary Side and Service-Entrance Weatherheads	33
1-7	Typical Rural Power Distribution System	35
1-8	Block Diagram of a Typical Power Generation, Transmission, and Distribution System	36
1-9	Breakdown of the Power System for Presentation in Handbook	37
2-1	Wood Pole Construction for Distribution and Subtransmission Lines	43
2-2	Wood Pole Construction for Transmission Lines at Voltages up to 161 kV	44
2-3	Grounding Methods for Wood-Pole Lines	44
2-4	Steel Tower Construction for Transmission Lines at Voltages of 69 kV and Above	45
2-5	Transmission-Line Cable Construction	47
2-6	Transmission-Line Insulators	48
2-7	Coordinates Defining Azimuth and Elevation Angles of Incidence	51
2-8	Equivalent Transmission-Line Circuit	52

2-9	Comparison of the Transmission-Line Approximation and the Exact Solution for the Current in a Wire Over a Perfectly Conducting Ground Plane -- Step-Function Incident Field, Horizontally Polarized	56
2-10	Power-Line Directivity Patterns for Vertical Polarization	58
2-11	Power-Line Directivity Patterns for Horizontal Polarization	59
2-12	Open-Circuit Terminal Voltage Induced in an Infinite Transmission Line by a Vertically Polarized Incident Field of 1 V/m	60
2-13	Open-Circuit Terminal Voltage Induced in a Semi-Infinite Transmission Line by a Horizontally Polarized Incident Field of 1 V/m	61
2-14	Open-Circuit Voltage at the End of a Semi-Infinite Line for Various Soil Conductivities	63
2-15	Open-Circuit Voltage at the End of a Semi-Infinite Line for Various Line Heights	64
2-16	Open-Circuit Voltage at the End of a Semi-Infinite Line for Various Incident Pulse Decay Time Constants	65
2-17	Transmission Line of Finite Length	67
2-18	Open-Circuit Voltage Waveform at the Terminals of a 150-m-Long Line Open-Circuited at Both Ends	69
2-19	Physical Arrangement that Produces a Vertically Polarized Wave with End-On Incidence	69
2-20	Open-Circuit Voltage at the Terminals of a Line 1000 m Long and 1000 m from the Source with 1 V/m Incident on the End Nearest the Source ($Z_0 = 300 \Omega$, $z_1 = 1000$ m, $z_2 = 2000$ m, exponential pulse)	73
2-21	Rate of Rise of the Open-Circuit Voltage at the Terminals of a Semi-Infinite Line	75
2-22	Minimum Length of Line Required to Obtain an Open-Circuit Voltage of 100 kV with 50-kVm Field Incident at Small Angle	76

2-23	Vertical Element at the End of a Transmission Line	77
2-24	Short-Circuit Current at Top of Lossless Vertical Element Terminated in Soil at the Base	80
2-25	Current Delivered to a Matched Lead at the Top of a Vertical Riser by a Vertically Polarized Incident Wave	80
2-26	Short-Circuit Current Induced at the Base of a Vertical Riser by a Vertically Polarized Incident Wave	82
2-27	Open-Circuit Voltage Induced at the Base of Vertical Element by a Unit Step Incident Wave	84
2-28	Illustration of a Vertical Ground Rod of Circular Cross Section	87
2-29	Variation of $\log(\sqrt{2\delta/\gamma_0 a})$ with Frequency and Conductor Radius	87
2-30	Variation of dc Resistance of Vertical Ground Rod With Length	88
2-31	Transmission Line Terminated with Vertical Risers at Both Ends	89
2-32	Current Components Induced on Horizontal Line and Vertical Risers, and Total Current	92
2-33	Steps in the Analysis of a Periodically Grounded Transmission Line	93
2-34	Open-Circuit Voltage at Terminals of Finite Horizontal Transmission Line	98
2-35	Frequency-Domain Response of a Periodically Grounded Line	99
2-36	Time Constant τ_h as a Function of Soil Conductivity and Line Height'	101
2-37	Attenuation Constant α as a Function of Frequency for Various Line Heights and Soil Conductivities	102
2-38	Normalized Attenuation Constant α/k and Propagation Factor β/k as a Function of Frequency, Line Height, and Soil Conductivity	103

2-39	Wave Front of Unit Step Current After Propagation for a Distance of 10 km (6.2 miles) Along Copper Conductors of 1 mm and 1 cm Radius	105
2-40	Wave Front of Unit Step Current After Propagation for a Distance of 10 km (6.2 miles) Along a Copper Conductor of 1 mm Radius at a Height of 10 m, for Various Soil Conductivities	106
2-41	Symmetrical Junction in a Transmission Line	107
2-42	Two-Conductor Transmission Line Over Ground Plane (Common- Mode Excitation)	109
2-43	Reflection and Transmission Coefficient at a Symmetrical Junction, Where $h = 40$ ft	110
2-44	Two-Wire Line with a Bend	111
2-45	Comparison of Calculated and Measured Reflection Coefficients of a Bend as a Function of Bend Angle	112
2-46	Reflection and Transmission Coefficient of a Bend in a Single-Wire Line Over Ground as a Function of Bend Angle	113
2-47	Reflection Coefficient for a 90° Bend as a Function of Radius of Curvature	114
2-48	Variation in Characteristic Impedance Caused by Line Sag	115
2-49	Geometry of Two-Wire Transmission Line for Differential-Coupling Analysis	117
2-50	Open-Circuit, Differential Voltage Induced in a Semi-Infinite Two-Wire Line by an Exponential Pulse (Wires in a Horizontal Plane)	121
2-51	Two-Wire Line Lying in a Vertical Plane	122

2-52	Open-Circuit Differential-Voltage Waveform Induced in a Semi-Infinite, Two-Wire Line by an Exponential Pulse (Wires in a Vertical Plane)	124
2-53	Asymmetrical Load on a Four-Wire Line with a Common-Mode Voltage	125
2-54	Impulse Flashover Characteristics of Particular Types of Apparatus Insulators on Positive and Negative $1\frac{1}{2}$ X 40 Waves at Standard Air Conditions	128
2-55	Impulse Flashover Characteristics of Suspension Insulators for $1\frac{1}{2}$ X 40 Waves at 77°F, 30-Inch Barometric and 0.6085-Inch Vapor Pressure	129
2-56	Breakdown Voltage as a Function of Time-to-Fire for Lightning Arresters	130
2-57	9-kV-Distribution Lightning-Arrester Firing Characteristics for Fast Rates of Rise	131
2-58	Corona-Threshold Voltage of a Wire Over Ground with Standard Air Conditions	133
3-1	Typical Power Service Entrances	138
3-2	Potheads for Single- and Three-Conductor Cables	140
3-3	Shielded Cables for Service Entrance	142
3-4	Pole-Mounted Service Entrance	142
3-5	Approximate Equivalent Circuit for Analysis of Transmission Through Shielded Cable or Conduit Feeder Circuits	146
3-6	Feeder Transfer Functions for Resistive Loads	147
3-7	Feeder Transfer Functions for Inductive Loads	148
3-8	Feeder Transfer Functions for Capacitive Loads	149
3-9	Voltage Across a Resistive Load Produced by a Unit Step Source	150
3-10	Voltage Across an Inductive Load Produced by a Unit Step Source	151

3-11	Voltage Across a Capacitive Load Produced by a Unit Step Source	154
3-12	Feeder Source Translated to the Load Terminals	155
3-13	Characteristic Impedance of Conductors in a Metal Conduit	156
3-14	Variation of Characteristic Impedance of Eccentric Coaxial Cable	157
3-15	Illustration of Coordinates for Conduit and Angle of Arrival of Transient Wave	162
3-16	Skin Depth δ in Soil as a Function of Frequency and Soil Conductivity σ	163
3-17	Waveforms of Incident Field, Cable Current, and Open-Circuit Voltage Between the Shields	165
3-18	Variation of Peak Conduit Current as Azimuth (ϕ) and Elevation (ψ) Angle of Incidence Change	166
3-19	Peak Conduit Current as a Function of Soil Conductivity and Incident Exponential Pulse-Decay Time Constant τ	167
3-20	Variation of Log ($\sqrt{2\delta/\gamma_0 a}$) with Frequency and Conductor Radius	168
3-21	Waveform of the Conduit Current Near the End when Conduit End is Open-Circuit	169
3-22	Magnitude of the Transfer Impedance of Rigid Steel Conduit	175
3-23	Voltage Waveforms produced by an Exponential Pulse $L_0 e^{-t/\tau}$ of Current in the Shield	178
3-24	Variation of Peak Open-Circuit Voltage and Rise Time of Conductor Voltage as a Function of Exponential Conduit- Current-Decay Time Constant τ	179
3-25	Core-to-Shield Voltage Waveforms Induced in Conductors in a Buried Conduit by an Incident Plane-Wave Exponential Pulse $e^{-t/\tau}$	182
3-26	Buried Insulated Conductor	186

3-27	Characteristic Impedance Z_0 and Propagation Factor β for Conductors in a Buried Nonmetallic Conduit	190
3-28	A Dispersion Constant α for Conductors in a Buried Non-Metallic Conduit	191
3-29	Short-Circuit Current and Open-Circuit Voltage Induced In Conductors in a Buried, Nonmetallic Conduit	193
3-30	Illustration of Parameters for a Single-Layer Tape-Wound Shield	196
3-31	Magnitude of the Transfer Impedance Computed for a Tape-Wound Shield	197
4-1	Typical Power-Distribution Transformers	204
4-2	Photographs of the Windings and Core of the 25-kVA GE Transformer	205
4-3	Internal Construction of a Valve-Type Lightning Arrestor	210
4-4	Lightning-Arrester Styles Used in Conjunction with the Transformer HV Transient Tests	211
4-5	Transmission-Line Model for Coupled Transformer Windings	213
4-6	Low-Frequency Equivalent Circuits for a Transformer	215
4-7	High-Frequency Equivalent Circuits for a Transformer	217
4-8	Spatial Distribution of Winding Voltage at Early Times	218
4-9	Voltage Distribution Along Primary Winding at Late Times	219
4-10	Voltage Distribution Along Secondary Winding at Late Times	219
4-11	Power-Transformer Configurations and Equivalent T-Networks Used to Obtain CW Transfer-Function Data	221
4-12	Magnitude of Transfer Function Relating Common-Mode Primary Voltage to Common-Mode Secondary Voltage Across a 100-ohm Load for the Test Transformers	223

4-13	Magnitude of Transfer Function Relating Common-Mode Primary Voltage to Differential-Mode Secondary Voltage Across a 100-ohm Load for the Test Transformers	225
4-14	Magnitude of Transfer Function Relating Differential-Mode Primary Voltage to Common-Mode Secondary Voltage Across a 100-ohm Load for the Test Transformers	227
4-15	Magnitude of Transfer Function Relating Differential-Mode Primary Voltage to Differential-Mode Secondary Voltage Across a 100-ohm Load for the Test Transformers	229
4-16	Schematic Diagram of Transformer Test Circuits	232
4-17	Waveform of Excitation Voltage Applied to Transformer	233
4-18	Waveform of Pulser Capacitor Discharge Current (which includes the current through the 100-ohm pulser load)	234
4-19	Secondary Output-to-Ground Voltage Observed at X1 for Common-Mode Excitation and Loading for Four of the Transformers	235
4-20	Secondary Output-to-Ground Voltage Observed at X3 for Common-Mode Loading	238
4-21	Differential Voltage Appearing Between Secondary Terminals X1 and X3 for Common-Mode Loading	239
4-22	Secondary Output-to-Ground Voltage Observed at X1 for Differential-Mode Loading	240
4-23	Secondary Output-to-Ground Voltage Observed at X1 for Common-Mode Excitation and Loading	243
4-24	Peak Secondary Voltage as a Function of Primary Excitation for Various Transformer Configurations	245
4-25	Lightning-Arrester Firing Characteristics for Fast Rates of Rise	247

5-1	Single-Line Diagram of Internal Low-Voltage Circuits	252
5-2	Surge-Protection Techniques for Low-Voltage Circuits	254
5-3	Typical Low-Voltage Wiring in Rigid Steel Conduit	255
5-4	Low-Voltage Wiring Inside a Main Circuit-Breaker Panel	256
5-5	Transmission-Line Model of Low-Voltage Wiring in Metal Conduit	259
5-6	Steps in Translating Load Impedances Toward Driving Source	261
5-7	Steps in Translating Driving Current and Voltage Toward Loads	265
5-8	Techniques for Determining the Characteristic Impedance Experimentally	266
5-9	Inductance per Unit Length of a Wire Over a Ground Plane	268
5-10	Characteristic Impedance, and Capacitance and Inductance per Inch	270
5-11	Line-to-Case Impedance of 7½-hp Induction-Motor Winding	271
5-12	Line-to-Case Impedance of ½-hp Induction-Motor Winding	272
5-13	Line-to-Case Impedance of ½-hp Single-Phase Capacitor-Start Motor Winding	273
6-1	Typical Grounding Arrangement for a Transmission System	278
6-2	Three-Phase Distribution Transformer Connections	278
6-3	Grounding System for a Telephone Switching Center	281
6-4	Examples of Grounds for a Simple Radio Receiver	282
6-5	Simple Receiver Separated into Modules Interconnected by Shielded Cables	283

6-6	Single-Point Tree Ground System	284
6-7	Loop Formed by Cable Shields and Metal Floor or Walls	285
6-8	Single-Point Ground and One Trunk	286
6-9	Impedance of Metal Ground Planes and of a Ground Cable	289
6-10	Tree with Trunk and Two Branches	290
6-11	Junction Grounded to Reduce Coupling Through Trunk	290
6-12	Trunk Eliminated to Form a Star Ground	292
6-13	Behavior of a Ring Counterpoise at Low and High Frequencies	296
7-1	Use of Secondary Lightning Arresters and Filters to Suppress EMP-Induced Transients on Low-Voltage Circuits	302
7-2	Illustration of Secondary Lightning Arresters at the Main Circuit-Breaker Cabinet	304
7-3	Impulse Test for Evaluating Power-Line Filters for EMP Applications	309
7-4	Determination of the Insertion Loss of a Line Filter	310
7-5	Illustration of Power-Line Filters in an Entry Vault on Wall of Shielded Structure	312
7-6	Schematic of a Simplified "Uninterruptible Power System" (UPS)	313
7-7	Circuit Diagram of an Automatic Transfer Switch	314
8-1	Impulse-Test Waveform Showing Method of Specifying Rise Time and Time-to-Half-Peak	322
8-2	Conductors Entering or Leaving an Equipment Cabinet	323
8-3	Impedance Matrix Used to Inject Common-Mode Voltages	326
8-4	Capacitors Used to Inject Common-Mode Voltages	327
8-5	Current Transformer to Inject Current on a Grounded Cable Shield	328

8-6	Schematic Diagram of Power-Line Pulser and Coupler	330
8-7	Power-Line Coupler Unit	331
8-8	Probe Adapters for a Tektronix P-6047 Passive Voltage Probe	332
8-9	Definition of the Excitation for an Internal Equipment Component	333

TABLES

2-1	Some Typical Properties of Above-Ground Power Lines	46
2-2	Tentative AIEE Standard on Insulation Tests for Outdoor Air Switches, Insulator Units, and Bus Supports	126
3-1	Suggested Withstand Impulse Voltages for Cables with Metallic Covering	141
3-2	Common-Mode Characteristic Impedance of Four 300-MCM Insulated Conductors in a Three-Inch-Diameter Conduit	155
3-3	Characteristic Impedances of Paper-Insulated Shielded Power Cables	159
3-4	Properties of Standard Galvanized or Enamelled Rigid Steel Conduit	174
3-5	Shielding Parameters for Rigid Steel Conduit	180
4-1	Standard Insulation Classes and Dielectric Tests for Distribution and Power Transformers	208
4-2	Properties of Class OA Transformers Used in CW and Transient Measurements	220
4-3	Comparison of Peak Voltage at Secondary Terminal X1 for a One-Volt, 7.5- μ s Exponential Pulse Applied to the Primary	237
5-1	Maximum Number of Conductors in Trade Sizes of Conduit or Tubing	257

Chapter One

EFFECTS OF THE EMP ON POWER SYSTEMS

1.1 INTRODUCTION

Until a few years ago, the nuclear EMP community gave little attention to commercial power systems other than to recommend surge arrestors and line filters for the power lines. It is now recognized, however, that the commercial power system can be a major path for coupling the EMP into ground-based systems. The power distribution system forms a very large, completely exposed antenna system that is hard-wired into the consumer's facility. Thus extremely high voltages may be developed on the power conductors, and even if the commercial power is not relied on for system survival these voltages may be delivered to the system either before commercial power is lost, or by the ground or neutral system after transferring to auxiliary power.

In the last few years, considerable research has been performed on EMP coupling to commercial power systems in an effort to characterize the power distribution lines as EMP collectors and to determine the effects of major components, such as transformers, lightning

arresters, and low-voltage wiring, on the penetration of the received signal into ground-based facilities. This research has entailed development and experimental verification of the theory of coupling to transmission lines, and even though considerable research is still continuing on the EMP interaction with power systems, it is felt that the preparation of a handbook on the interaction of EMP with commercial power systems is in order so that designers and systems engineers can benefit from the results of extensive data already accumulated.

1.2 CHARACTERISTICS OF THE NUCLEAR EMP

1.2.1 GENERATION OF THE EMP

The nuclear electromagnetic pulse (EMP) is produced by the products of a nuclear detonation interacting with air molecules to produce a sudden separation of electrical charge. This process is illustrated in Figure 1-1(a) for a surface detonation and in Figure 1-1(b) for a high-altitude detonation. Very-high-energy γ -rays (photons) are produced by the nuclear detonation and propagated radially away from the burst point. These γ -rays eventually collide with air molecules to produce relativistic Compton electrons which also move in the radial direction. The heavier positive ions are left behind, so that a separation of the negative electrons from the positive ions occurs. This is the charge separation mechanism by which the electromagnetic pulse is initiated. As the Compton electrons travel through the air, however, they collide with neutral air molecules to produce secondary electrons, and lose their energy in this process. The air soon becomes fairly highly ionized and the separated charge begins to discharge as a result of current flowing through the ionized air. At large distances from a surface burst, this charge separation and relaxation has the appearance of a transient electric dipole.

The charge-separation mechanisms are similar for the high-altitude detonation, but because the probability of the γ -ray (photon) colliding with an air molecule is relatively low until it has reached the more dense atmosphere, most of the Compton electron production and charge separation occurs in or below the region of the upper atmosphere containing the ionosphere D-layer. In this region, the distance that a Compton electron travels

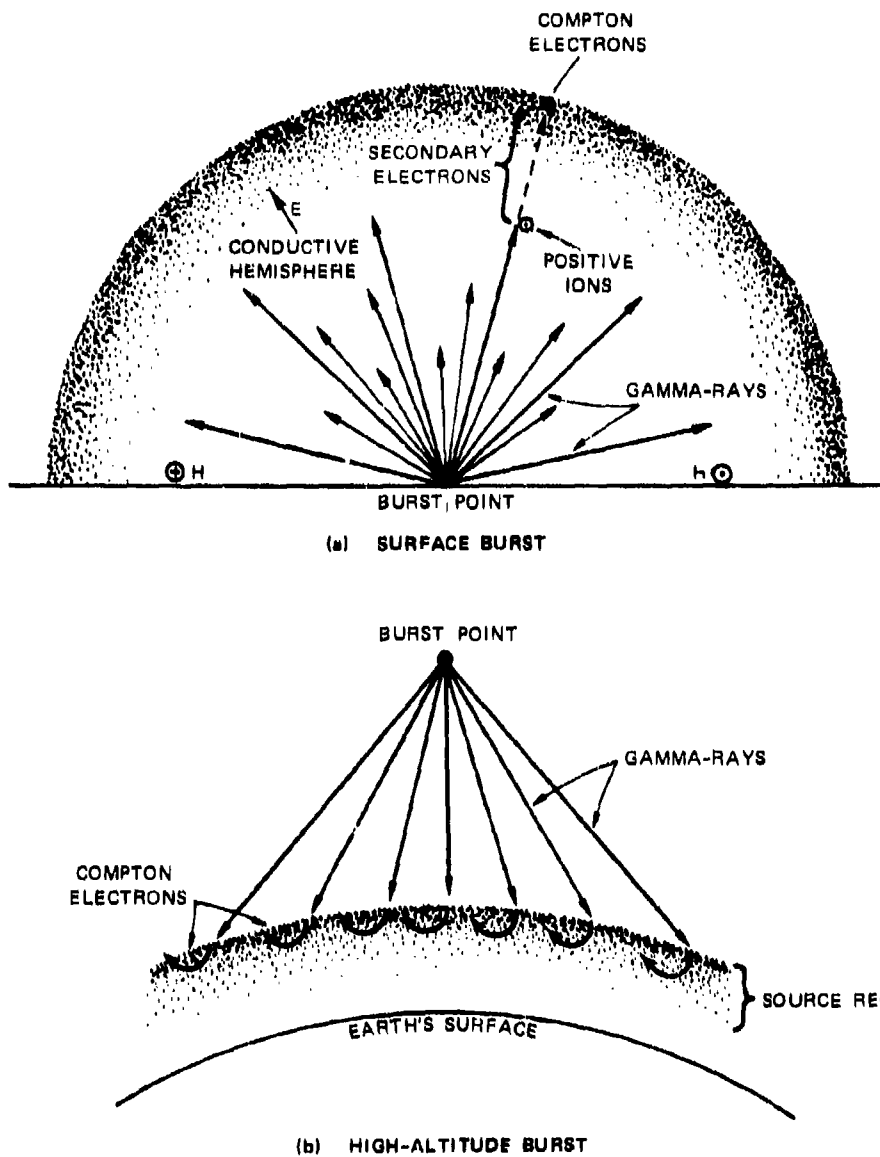


Figure 1-1 MECHANISM FOR GENERATION OF THE EMP

before it loses its energy through collisions is great enough that the curvature of its path produced by the earth's magnetic field and the resultant magnetic dipole moment, are also significant, as is indicated in Figure 1-(b). As is also illustrated in Figure 1-1(b) the source region where the charge separation occurs can cover a very large area, so that the EMP produced by a single high-altitude detonation may be quite strong over a region with dimensions of several hundred miles.

1.2.2 CHARACTERISTICS OF THE HIGH-ALTITUDE EMP

The detailed characteristics of the high-altitude EMP waveform vary with weapon characteristics and the positions of the observer relative to the burst point, but for the purposes of most EMP coupling analysis a simple, approximate waveform is adequate. A useful approximation for the incident electric field strength to be used in coupling calculations is the two-exponential pulse given by

$$E(t) = E_0 (e^{-t/\tau_1} - e^{-t/\tau_2}) \quad (1-1)$$

where τ_1 is the pulse-decay time constant and τ_2 is the rise time constant. Since $\tau_1 \gg \tau_2$, E_0 is approximately the peak value of the incident electric field strength. The values given by Marable et al.^{1*} for E_0 , τ_1 , and τ_2 are

$$E_0 \approx 5.2 \times 10^4 \text{ V/m}$$

$$\tau_1 \approx 6.7 \times 10^{-7} \text{ s}$$

$$\tau_2 \approx 3.8 \times 10^{-9} \text{ s}$$

A sketch of the waveform plotted from Eq. (1-1) using these values is shown in Figure 1-2.

The Fourier transform of the two-exponential pulse is

$$E(\omega) = E_0 \frac{\tau_1 - \tau_2}{(1 + j\omega\tau_1)(1 + j\omega\tau_2)} \quad (1-2)$$

* References are listed in the last section of each chapter.

A plot of the magnitude of the field $E(\omega)$ for the values of E_0 , τ_1 , and τ_2 given above is shown in Figure 1-3.

From this approximate waveform and its Fourier transform, it is apparent that the EMP produced by a high-altitude detonation is characterized by a very fast rise to a peak electric field strength of the order of 50 kV/m, and that the duration of the pulse is of the order of 1 μ s. The spectrum of the pulse contains significant energy at frequencies approaching 100 MHz.

The magnetic field strength (outside the region of ionization) associated with the EMP is related to the electric field through the intrinsic impedance of air (120π), so that the incident magnetic field is

$$H(t) = \frac{E_0}{120\pi} (e^{-t/\tau_1} - e^{-t/\tau_2}) \quad (1-3)$$

1.2.3 COMPARISON WITH LIGHTNING

Because both the nuclear EMP and lightning produce large electromagnetic transients it is natural to compare their properties and characteristics. As is well known, lightning is produced by the discharge of static electricity accumulated in clouds. The discharge occurs as a long arc between the cloud and the earth, in which peak currents of tens of kA (but occasionally hundreds) and charge transfers of about 1 coulomb occur.^{2, 3} Typical current rise times are of the order of 1 μ s, and the duration of individual current pulses (time to decay to half the peak value) is of the order of 40 μ s. Each lightning flash normally consists of several strokes or pulses of current. The lightning stroke-current rise-time and duration are thus much greater than those of the EMP fields.

The effects of lightning are most severe when a direct strike is incurred. These effects are often manifested as molten metal, charred insulation, and exploded timber—the result of a high energy density delivered by the stroke to its point of attachment. Lightning

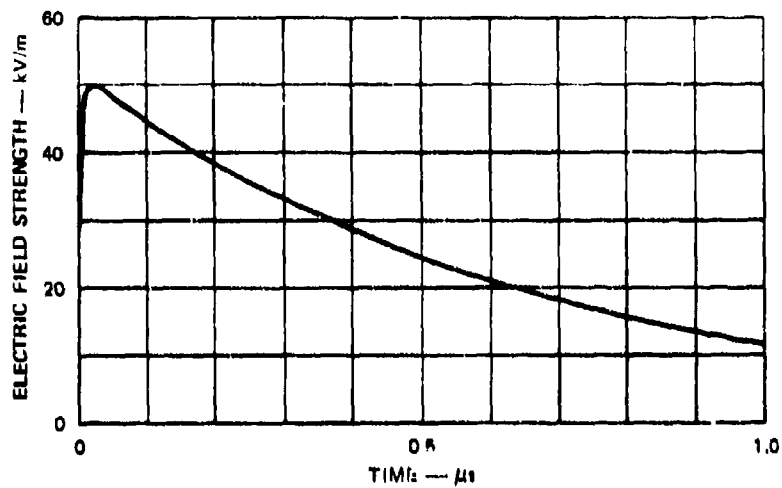


Figure 1-2 TWO-EXPONENTIAL REPRESENTATION OF THE HIGH-ALTITUDE MAP WAVEFORM

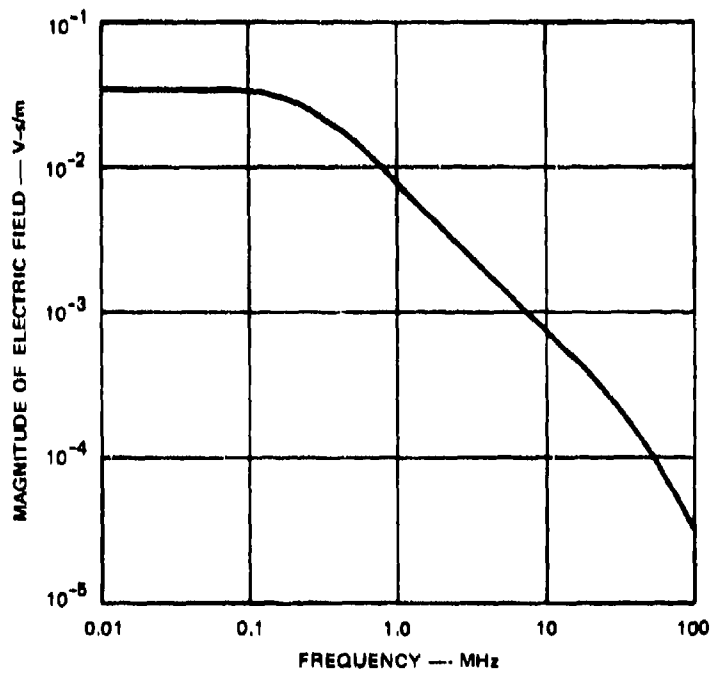


Figure 1-3 MAGNITUDE OF THE SPECTRUM OF THE TWO-EXPONENTIAL WAVEFORM

transients propagated along transmission lines often produce peak voltages of several hundred kilovolts with pulse rise-times of about 10 μ s and durations of 50 μ s or more. This transient is not necessarily a common-mode (zero-sequence) voltage, since the stroke may attach to only one conductor; the voltages induced in the remaining conductors are produced by mutual coupling.⁴

Because the nuclear EMP arrives at the surface as a plane, propagating wave, rather than as a stroke channel, the melting, charring, and splintering effects associated with direct lightning strikes do not usually occur with the EMP. The EMP exerts its influence through induced effects; the very large electromagnetic fields of the EMP induce large voltages or currents in antenna-like elements of equipment. For example, a 5-meter-high vertical conductor (monopole antenna) exposed to a 50-kV/m incident electric field will have an open-circuit voltage of 500 kV induced at its base. The reader should adjust his thinking to accommodate the fact that the very fast rise time of the EMP implies that conductors over a few feet long are no longer electrically short. Thus, although a 20-ft-long ground wire on a transformer pole may be treated as a lumped inductance for lightning transients, 20 ft is twice the distance a wave will propagate during the buildup time of the EMP. Conductors over a few feet long must therefore be analyzed as transmission lines, rather than lumped elements, in the investigation of EMP effects. In addition, small inductances and capacitances that are negligible in lightning analysis become important in EMP analysis because of the large rates of change associated with the leading edge of the EMP.

The primary effect of the EMP is, therefore, the production of large voltages or currents in conductors such as power lines, buried cables, antennas, etc. These induced currents and voltages may then cause secondary effects such as insulation flashover and electronic component damage or malfunction. Electronic logic circuits, in which information is transferred as a train of pulses, are particularly susceptible to transients of the type induced by the EMP. Even small transients in these circuits can cause a false count or status indication that will lead to an error in the logic output, and large transients can destroy the junctions of the solid-state devices used in these circuits. Furthermore, the techniques used for protecting equipment from the slowly rising lightning transients are not necessarily effective against the fast-rising EMP-induced transients.

1.2.4 TECHNOLOGY APPLICABLE TO EMP ANALYSIS

Because the EMP is a transient whose spectrum is significant at frequencies approaching 100 MHz, the analysis of EMP effects is a transient analysis. Hence, although some differences between the EMP and lightning have been noted above, the results of extensive transient analysis related to lightning are beneficial to the analysis of EMP effects on power systems and components. One of the problems encountered in the analysis of the coupling and propagation of EMP-induced transients is that of determining the electrical properties of components such as transformers, motors, etc. at frequencies other than their normal operating frequencies (60 Hz). For many transmission-line components, however, analytical techniques and component characteristics have been developed for lightning and switching transient analysis that are applicable for the frequency spectrum below 1 MHz.⁴⁻⁷ Engineers familiar with conventional transient analysis of power systems should therefore be well equipped to perform EMP analysis.

Some data are also available for system and component characteristics in the 50-to-150-kHz range used for power-line carrier applications.⁸ Although much of the supervisory control, telemetering, and relaying is now carried on microwave links, power-line carriers are still in use and much data on the transmission properties of lines and components are available to supplement the data available from lightning and switching transient analysis. Because of the fairly narrow band of frequencies used for power-line carrier operations, however, these data are of somewhat limited value.

Because the usual treatment of lightning and switching transients is not concerned with frequencies above about 1 MHz, high-frequency techniques must be invoked for analyzing the power system's response to the EMP. Most useful in the EMP analysis at frequencies above 1 MHz is a good understanding of the fundamentals of electromagnetic waves and transmission lines.⁹⁻¹¹ As was indicated in Section 1.2.3 above, many conductors that are electrically small at 1 MHz (300-meter wavelength) are large at 100 MHz (3-meter wavelength). Thus the EMP analyst must be acutely aware of wave propagation times and the transmitted and reflected waves at discontinuities in conductor configurations. To illustrate this point, consider a lightning transient with a 1.5- μ s time-to-peak. The toe of this transient has propagated 1500 ft beyond an observer by the time the peak arrives. For a 1- μ s-wide pulse with a 10-ns time-to-peak, however, the toe of the pulse has propagated only 10 ft by the time the peak arrives, and by the time the toe has propagated 1500 ft beyond the

observer the trailing edge of the pulse has passed and propagated 500 ft beyond the observer (the velocity of propagation is approximately 1 ft/ns). One consequence of this difference is that the current at the top of a vertical ground wire on a pole may be radically different from the current only 30 ft away at the base of the pole.

1.3 DESCRIPTION OF A POWER SYSTEM

The power system is described from the viewpoint of a consumer who is concerned about the EMP-induced transients entering his facility on the power conductors. As viewed by the consumer, the most important parts of the power system are those that are closest to his facility. Thus the service entrance, the distribution transformer, and the last mile of distribution line are quite important, but parts of the distribution and transmission system over a mile away decrease in interest as the distance increases.

Typical service at the end of a distribution line is shown in Figure 1-4 for service with ground-based transformers. The 3-phase aerial distribution line ends on the guyed pole, where the line is spliced to shielded cable, which enters a conduit running down the pole and underground to the transformer. The top of the pole is shown in Figure 1-4 to illustrate the installation of the lightning arresters, disconnect switches, and potheads. Rigid steel conduit is normally used to protect the conductors on the drop down the pole, but often fiber duct is used for a segment of the buried horizontal run between the pole and the transformers. There is almost always a ground wire for the lightning arresters running down the pole to a ground rod or butt wrap at the base of the pole.

The other end of the conduit and the distribution transformers are shown in Figure 1-5. In the case shown, the transformers are mounted outdoors on a concrete pad and protected by a chain-link fence. The shielded cables exit the conduit through a moisture barrier and are terminated in potheads. Connecting leads between the pothead terminals and the transformer terminals can be seen in the figure. Three single-phase transformers are used to reduce the distribution voltage (13.2 kV) to the consumer's voltage (440 V). The neutral conductors and the transformer cases are grounded to ground rods just off the concrete pad.

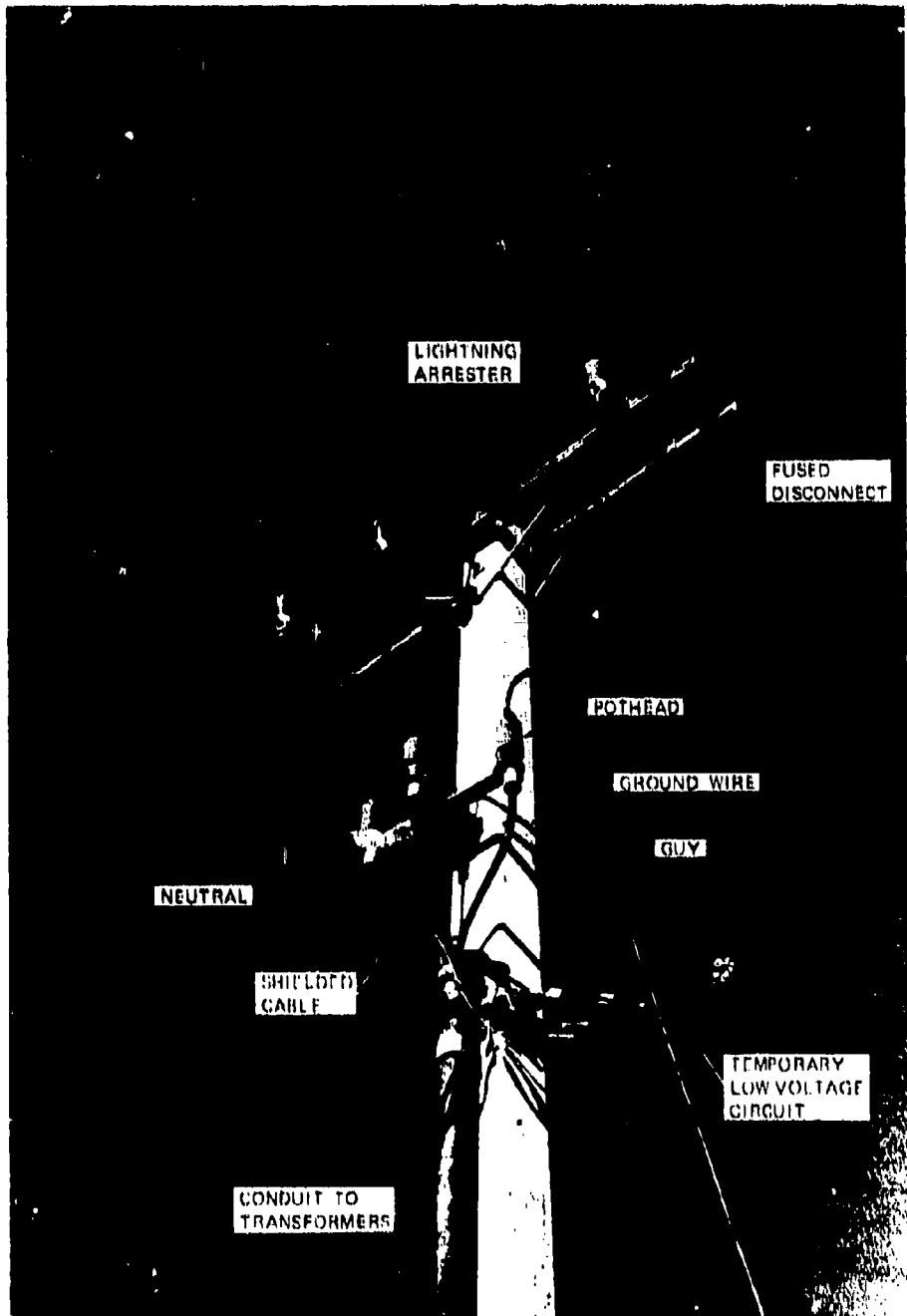


Figure 1-4 LAST POLE OF DISTRIBUTION SPUR SHOWING LIGHTNING ARRESTERS, POTHEADS, AND ENTRANCE CONDUIT

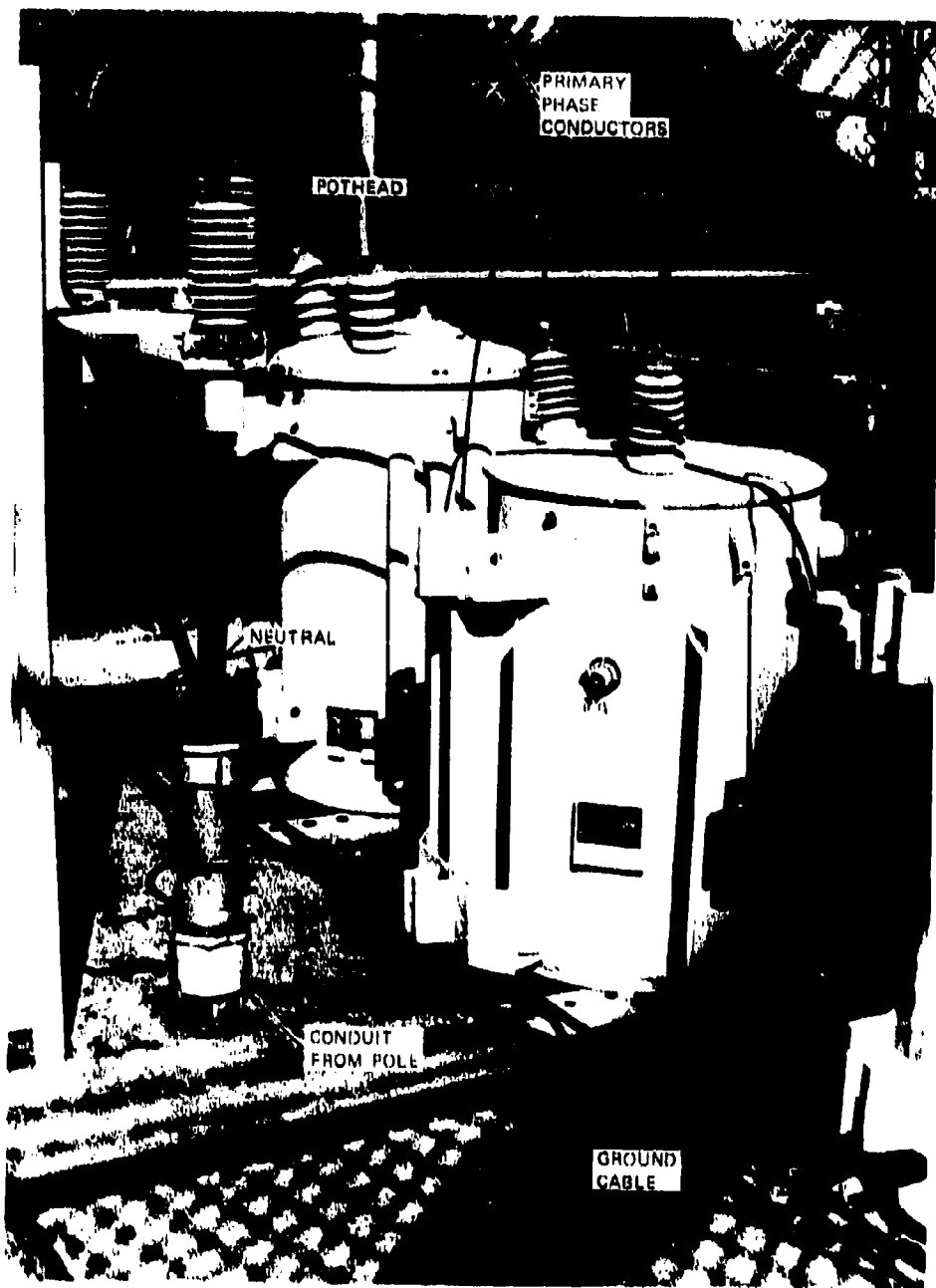


Figure 1-5 GROUND-BASED DISTRIBUTION TRANSFORMERS: PRIMARY SIDE AND DISTRIBUTION POTHEDS

A view of the secondary side of the transformers and the low-voltage conductors entering the weatherheads is shown in Figure 1-6. In the installation shown in this figure, several conductors are used for each phase, so that three entrance conduits are required. These conduits also may be either steel, part steel and part fiber duct, or fiber duct all the way. The conduits are normally run underground into the building where they terminate in the main circuit-breaker panel. The length of the conduit between the top of the pole and the transformers ranges from about 50 ft to about 1000 ft, but a typical distance is about 100 ft. The length of the conduit between the transformers and the main circuit-breaker panel is typically 20 or 30 ft, but it can vary from about 10 ft up to about 200 ft.

The outdoor transformer arrangement shown in Figures 1-5 and 1-6 is quite common, but other common practices include installing the transformers in steel cabinets or sheds outside the building or in a vault inside the building. Pole-mounted transformers are common for light loads and at sites where real estate for ground-based installations is limited.

Some of the features of the service that are important in the analysis of EMP coupling to the building electrical circuits are:

- (1) The height and separation of the conductors of the distribution lines. These affect the coupling of the EMP to the line.
- (2) The lightning arresters. These protect the potheads and shielded cables from insulation breakdown.
- (3) The characteristic impedance of the shielded cables. A large mismatch between the aerial line and the shielded cables limits the voltage delivered to the cables.
- (4) The conduit between the pole and the transformers. If the conduit is all steel, the cables will be protected from the fields in the ground, but if it is partly plastic or fiber duct, additional coupling may occur along this path.
- (5) The transformers and connecting leads. These behave as bandpass filters that limit the very high frequencies and the very low frequencies. If the secondary leads are exposed for significant lengths, however, some of the high-frequency spectrum may be restored by direct coupling to the EMP.

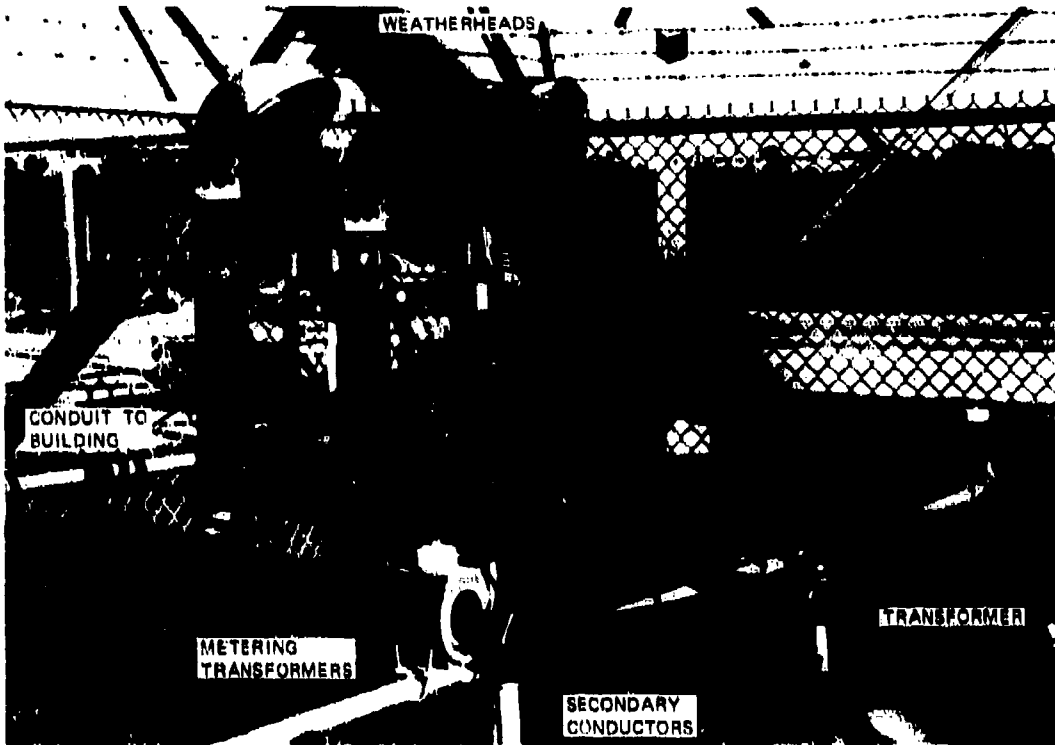


Figure 1-6 GROUND-BASED DISTRIBUTION TRANSFORMERS: SECONDARY SIDE AND SERVICE-ENTRANCE WEATHERHEADS

- (6) The conduit between the transformers and the main circuit-breaker panel. If the conduit is steel, the conductors are well shielded, but if partly plastic or fiber, significant coupling to the conductors can occur.
- (7) The lead lengths between the aerial lines and the shielded cables and between the transformer terminals and the conduits. The inductance of these leads limits the rise time of the transient propagating toward the building.

The distribution system supplying a facility is likely to be unique to each facility. A typical rural distribution system is shown in Figure 1-7. The distribution network shown is that provided by one rural electric cooperative serving customers within a 10-mile radius of its distribution substation. Note that there is a mixture of single-phase service and 3-phase service, and the distribution system is interconnected with neighboring systems. Of interest is the fact that most customers are at the ends of segments of transmission line that are at least 1000 ft long, and many are served by spur lines over a mile long. In the network shown

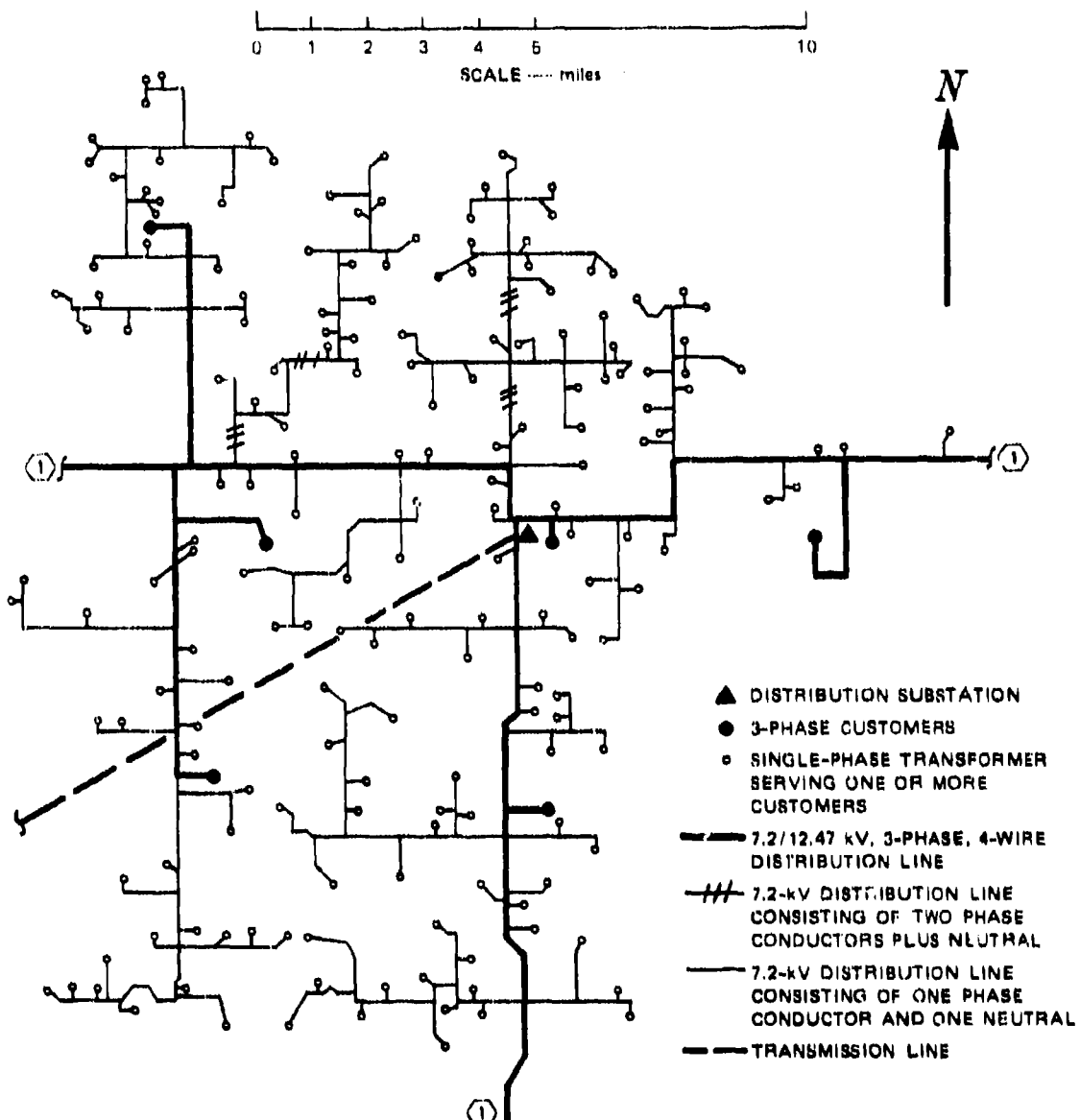
In Figure 1-7, only one 3-phase customer is close enough to the substation to be even remotely concerned with EMP coupled to the subtransmission line. Also noteworthy is the fact that even in this rather sparsely populated service area, the distance between branches or spur lines is typically only about one mile. This fact is important in assessing the buildup of induced current propagating into a facility from great distances, since spurs, branches, or bends tend to limit the buildup and propagation of this current. In more densely populated urban and suburban areas, of course, the distance between spurs and branches is much less than that shown in Figure 1-7.

Although the consumer is seldom concerned with the generation and transmission system, this part of the power system is exposed to the EMP and may be susceptible to the EMP-induced transients. The generation and transmission system is shown schematically in Figure 1-8 to illustrate the hierarchy of the system. In practice, however, there are many interties at the transmission, subtransmission, and distribution levels, so that the transmission and subtransmission systems form very complicated networks. These systems also contain feedback in the form of supervisory control and relaying, so that a disturbance, (e.g., load shedding, generator shutdown) in one part of the system causes changes in the remainder of the system.

1.4 CONTENTS AND USE OF THE HANDBOOK

1.4.1 SUBJECTS COVERED

The goal of this handbook is to provide the formulas and numerical examples necessary to evaluate the principal coupling problems a power-consumer might encounter, and to provide some general information on grounding theory, protection techniques, and test methods. Because it has been prepared as a handbook, rather than a treatise, the complete derivation of coupling formulas has not been provided, although some of the more important formulas have been partially derived, and an attempt has been made to provide references to sources where the subjects are treated in more detail.



(1) POINT WHERE THE DISTRIBUTION SYSTEM IS INTERCONNECTED WITH A NEIGHBORING DISTRIBUTION SYSTEM. THE BREAK CONSISTS OF MANUALLY OPERATED ISOLATING SWITCHES NORMALLY IN THE OPEN POSITION.

Figure 1-7 TYPICAL RURAL POWER DISTRIBUTION SYSTEM

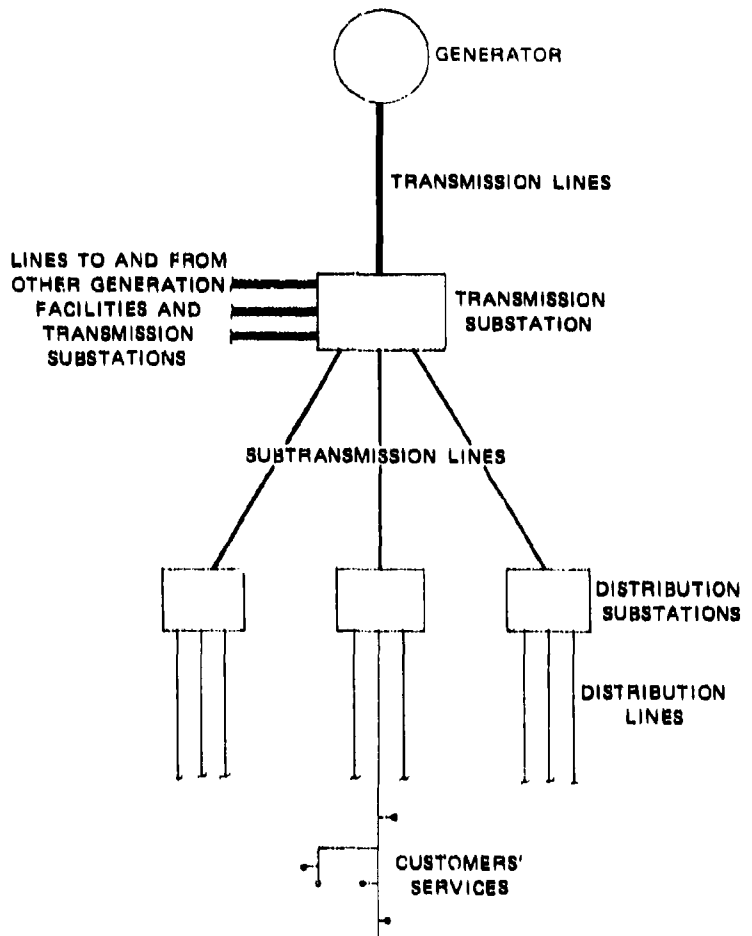


Figure 1-8 BLOCK DIAGRAM OF A TYPICAL POWER GENERATION, TRANSMISSION, AND DISTRIBUTION SYSTEM

Coupling of the EMP to transmission lines and through the distribution transformer and entrance conduits is covered in Chapters Two, Three, and Four. The partition of the power system among these chapters is illustrated in Figure 1-9. Chapter Two contains formulas and results for coupling to aerial transmission lines and includes the effects of soil parameters and of polarization and angle of incidence of the EMP, as well as the effects of vertical elements such as ground wires and service-entrance conduits.

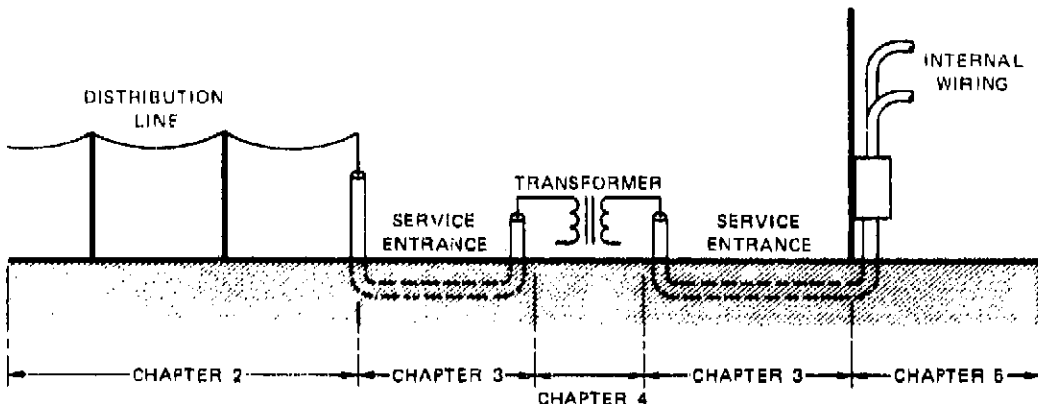


Figure 1-9 BREAKDOWN OF THE POWER SYSTEM FOR PRESENTATION IN HANDBOOK

Chapter Three treats the transmission of the transient through the entrance conduits. Included in this chapter are transmission-line formulas for passive metal conduit systems and for fiber conduits along which additional coupling occurs. Also discussed in this chapter are the shielding properties of rigid steel conduit and tape-wound shields. Examples of the waveforms delivered to the load-end of transmission lines simulating service-entrance conduits are given for resistive, capacitive, and inductive loads.

The linear and nonlinear characteristics of transformers and lightning arresters are given in Chapter Four. Although the data available on transformers and lightning arresters are still somewhat limited, the trends are evident and the bandpass behavior of the transformers and data on firing voltage versus time to fire available are presented in this chapter.

Chapter Five discusses some aspects of coupling through internal building wiring. Because the electrical wiring in a typical building has extremely complex high-frequency characteristics, detailed analytical procedures for handling this part of the coupling are very cumbersome and generally not very accurate. Nevertheless, some general guidelines and aids to estimating major coupling parameters are presented.

Chapters Six, Seven, and Eight treat grounding, protection, and testing, respectively. Grounding theory and practice are reviewed in Chapter Six in a more or less qualitative manner, primarily for the user who is not familiar with the subject. Effective and economical protection methods using arresters and filters are described in Chapter Seven. Techniques

for evaluating component susceptibility to EMP-induced transients and for proof-testing facilities are described in Chapter Eight.

1.4.2 CONVENTIONS USED IN THE HANDBOOK

Throughout this handbook coupling formulas in the frequency domain and the time domain are used. Because of its wide use by electrical engineers, the Fourier transform has been used for frequency-domain representations. The Fourier transform pair, as used throughout this handbook, can be written as follows:

$$F(\omega) = \int_0^\infty f(t)e^{-j\omega t} dt \quad (1-4)$$

$$f(t) = \frac{1}{2\pi} \int_{-\infty}^{\infty} F(\omega)e^{j\omega t} d\omega \quad (1-5)$$

For those more accustomed to the Laplace transform, the transition is very simple since the Fourier variable $j\omega$ and the Laplace variable s are interchangeable for all applications encountered in this handbook. This is apparent from a comparison of Eqs. (1-4) and (1-5) with the Laplace transform pair:

$$F(s) = \int_0^\infty f(t)e^{-st} dt \quad (1-6)$$

$$f(t) = \frac{1}{2\pi j} \int_{\delta-j\infty}^{\delta+j\infty} F(s)e^{st} ds \quad (1-7)$$

for the limiting case where $\delta \rightarrow 0$. (However, this simple change of variable cannot be used for waveforms that are not zero for negative time.)

The time dependence of alternating fields, voltages, and currents used in the handbook is $e^{j\omega t}$, consistent with common electrical engineering usage. This time dependence is consistently suppressed (by the Fourier transform), however, so that the expression for a propagating field that represents

$$E(t) = E_0 e^{j(\omega t - kz)}$$

is written

$$E(\omega) = E_0 e^{-jkz}.$$

The important effect of the $e^{j\omega t}$ time-dependence is that it makes inductive impedances positive imaginary quantities ($j\omega L$), and capacitive impedances negative imaginary quantities ($-j/\omega C$).

The rationalized mks system of units is used exclusively in the analysis and formulas presented, although dimensions and distances are sometimes discussed in the more familiar English or engineering terms (e.g., feet, miles, mils). In the rationalized mks system, the following dimensions and constants apply:

<u>Quantity</u>	<u>Unit</u>	<u>Abbreviation</u>
potential	volt	V
current	ampere	A
impedance	ohm	Ω
electric field strength	volt/meter	V/m
magnetic field strength	ampere/meter	A/m
inductance	henry	H
capacitance	farad	F
permeability $(\mu_0 = 4\pi \times 10^{-7} \text{ H/m})$	henry/meter	H/m
permittivity $(\epsilon_0 = 8.85 \times 10^{-12} \text{ F/m})$	farad/meter	F/m
conductivity	mho/m	

Conventional abbreviations for factors of $10^{\pm n}$ are used:

<u>Prefix</u>	<u>Symbol</u>	<u>Meaning</u>
pico	p	$\times 10^{-12}$
nano	n	$\times 10^{-9}$
micro	μ	$\times 10^{-6}$
milli	m	$\times 10^{-3}$
kilo	k	$\times 10^3$
mega	M	$\times 10^6$

One exception to this convention occurs in the discussion of cable sizes, where MCM is used to abbreviate "thousand circular mils."

1.5 CITED REFERENCES

1. J. H. Marable, J. K. Baird, and D. B. Nelson, "Effects of Electromagnetic Pulse (EMP) on a Power System," ORNL-4836, Oak Ridge National Laboratory, Oak Ridge, Tennessee (December 1972).
2. N. Clanos and E. T. Pierce, "A Ground-Lightning Environment for Engineering Usage," Technical Report 1, SRI Project 1834, Contract L.S.-2817-A3, Stanford Research Institute, Menlo Park, California (August 1972).
3. M. A. Uman, *Lightning* (McGraw-Hill Book Co., Inc., New York 1969).
4. L. V. Bewley, *Traveling Waves on Transmission Systems* (Dover Publications, Inc., New York, N.Y., 1963).
5. R. Rudenberg, *Electrical Shock Waves in Power Systems* (Harvard University Press, Cambridge, Mass., 1968).
6. A. Greenwood, *Electrical Transients in Power Systems* (John Wiley & Sons, Inc. New York, N.Y., 1971).
7. E. D. Sunde, *Earth Conduction Effects in Transmission Systems* (Dover Publications, Inc., New York, N.Y., 1968).
8. *Electrical Transmission and Distribution Book*, 4th Ed., 5th printing (Westinghouse Electric Corporation, East Pittsburgh, Penn., 1964).

9. S. Ramo and J. R. Whinnery, *Fields and Waves in Modern Radio*, 2nd Ed. (John Wiley & Sons, New York, N.Y., 1953).
10. S. A. Schelkunoff, *Antennas: Theory and Practice* (John Wiley & Sons, Inc., New York, N.Y., 1952).
11. R. W. P. King, *Transmission Line Theory* (Dover Publications, Inc. New York, N.Y., 1965).

Chapter Two

COUPLING TO TRANSMISSION LINES

2.1 TRANSMISSION-LINE CONFIGURATIONS

2.1.1 GENERAL

Overhead lines for power transmission, subtransmission, and distribution are used to carry 3-phase, 60-Hz power from the generating station to the consumer. The lines may vary in length from a fraction of a mile to hundreds of miles and may transmit 60-Hz voltages varying from a few kilovolts to a few hundred kilovolts. Although it is doubtful that the power lines will be damaged by the EMP, they are very large, exposed collectors of the EMP that can funnel the EMP energy into the consumer's facility, the substations that control line relaying and load control, and the generating stations. A primary consideration in the analysis of coupling to the power lines is, therefore, the EMP-induced voltages or currents available from the ends of the lines that might affect critical components in the terminal facilities of the consumer or the power system. A second consideration, however, is the possibility that the EMP-induced voltages might produce insulation breakdown along the

line and thereby induce faults or protective reactions that cause widespread load-shedding or similar responses that the power system cannot cope with.

In this section, a brief description of the physical construction of power lines and power-line components will be given. The emphasis in this description will be on those aspects of the power lines that are believed to be important in the coupling and propagation of EMP-induced transients — namely, their geometry and insulation.

2.1.2 CONSTRUCTION OF TRANSMISSION LINES

Wood pole construction is used almost exclusively for overhead distribution lines that transmit power from the distribution substation to the consumer. Wood poles are also

very widely used for subtransmission lines that carry power from the bulk-power source to the distribution substations. Typical wood-pole line configurations for 3-phase transmission are shown in Figure 2-1. The conductors are supported on crossarms, on pin or post type insulators. A wood-pole line may carry a single 3-phase circuit as shown in Figure 2-1(a) or two 3-phase circuits as illustrated in Figure 2-1(b).

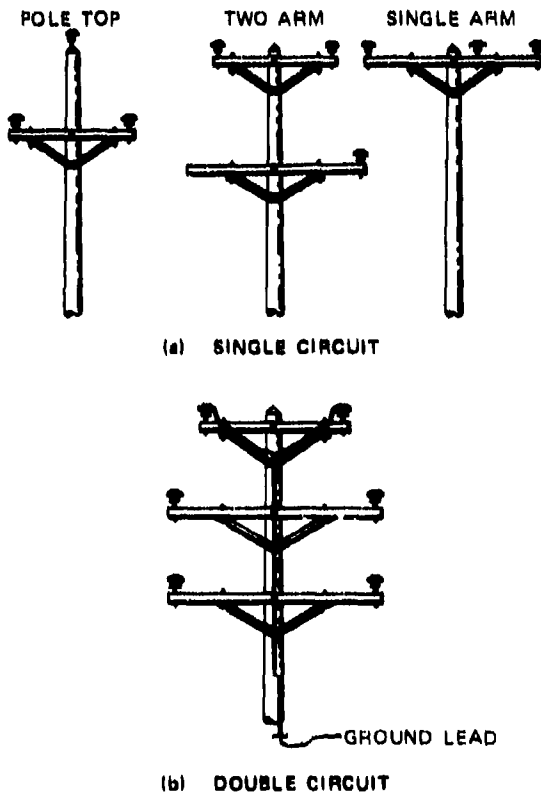


Figure 2-1 WOOD POLE CONSTRUCTION FOR DISTRIBUTION AND SUBTRANSMISSION LINES

Wood poles are also used for transmission lines at voltages up to 161 kV.^{1,2} Typical construction of these lines is illustrated in Figure 2-2. The conductors are usually supported on suspension insulators at these voltages, and at the higher voltages where large conductor spacing is required, the H-frame construction illustrated in Figure

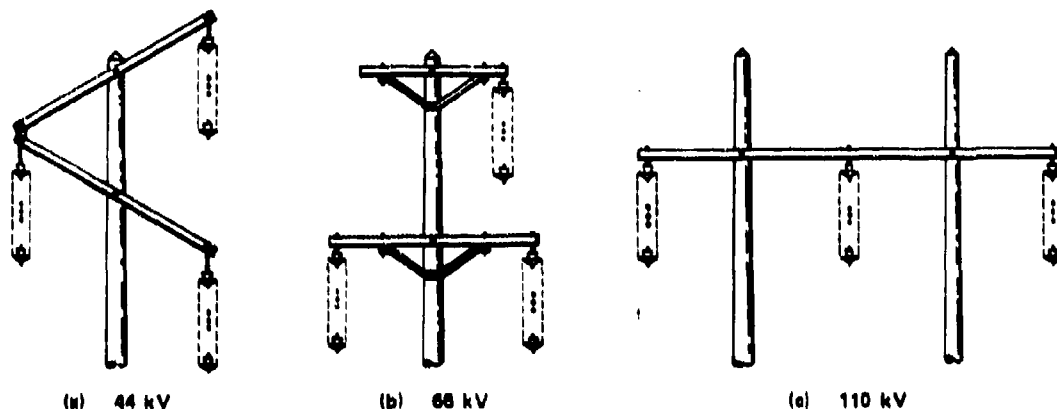


Figure 2-2 WOOD POLE CONSTRUCTION FOR TRANSMISSION LINES AT VOLTAGES UP TO 161 kV

2-2(c) is common. Modern transmission lines designed for lightning protection are provided with ground wires above the phase conductors (at the top of each pole in the H-frame construction, for example). These ground wires are grounded at each pole by wrapping several turns around the butt of the pole

below the ground level as illustrated in Figure 2-3(a). Grounding at the pole may also be achieved with a butt plate attached to the bottom of the pole and, occasionally, with ground rods driven near the base of the pole as illustrated in Figures 2-3(b) and (c).

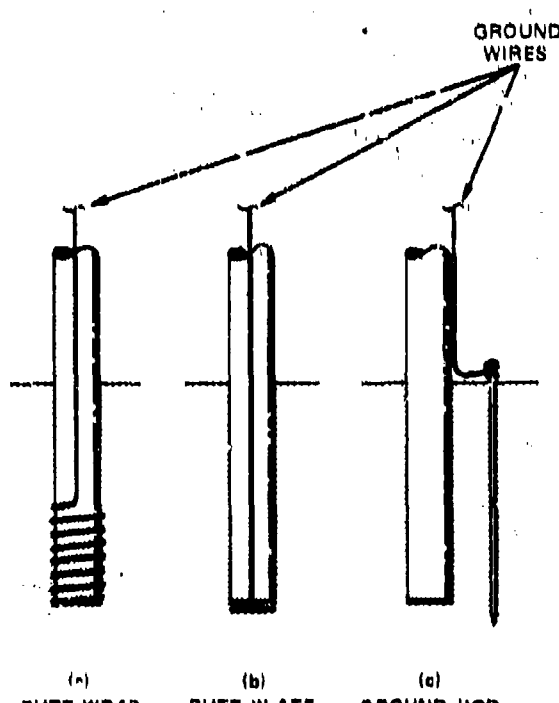


Figure 2-3 GROUNDING METHODS FOR WOOD-POLE LINES

High-voltage transmission lines supported on steel towers are common for bulk-power transmission from major generating plants to utility customers or within a utility's power network.^{1,2} Typical steel tower supports for single and double circuits are illustrated in Figure 2-4. Overhead ground wires for lightning protection (at the points atop the towers in Figure 2-4) are widely used on these transmission

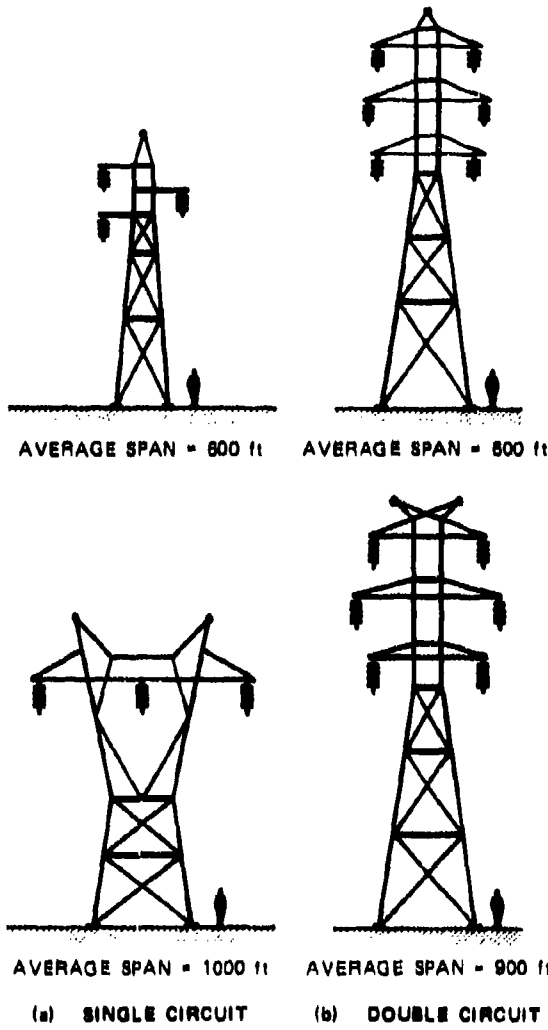


Figure 2-4 STEEL TOWER CONSTRUCTION FOR TRANSMISSION LINES AT VOLTAGES OF 69 KV AND ABOVE

impedance of typical power lines is 300 to 600 ohms.

lines. Counterpoises at the tower footings are used to minimize the surge impedance of the base of the tower. Counterpoise and insulation are designed to permit the tower or overhead ground wires to accommodate a direct lightning stroke without the tower-to-phase-conductor voltage exceeding the insulation flashover voltage. Although some older transmission lines use horn gaps or expulsion-tube lightning arresters to protect the phase conductors, modern lightning protection design relies on overhead ground wires and tower footing counterpoises to reduce the probability of flashover of the phase-conductor insulators.

Some of the properties of wood-pole and steel-tower transmission lines are given in Table 2-1. The 60-Hz transmission voltage is given in the left-hand column, followed by the basic insulation level, the height (at the pole or tower) of the lowest conductors, the span between poles, and typical transmission-line lengths. The common-mode (zero sequence) surge

2.1.3 TRANSMISSION-LINE CABLE

Conductors for power lines are usually stranded cable of copper, aluminum, or copperweld (copper-clad steel), although the conductors for the higher voltages may be of

Table 2-1
SOME TYPICAL PROPERTIES OF ABOVE-GROUND POWER LINES

Voltage (kV)	Basic Insulation Level (kV)	Height of Lowest Conductor (ft)		Span (ft)		Typical Length (miles)	Type
		Wood Poles	Steel Tower	Wood Poles	Steel Tower		
2.4	45	25-35	—	160-200*	—	0-3	Distribution
4.8	60	25-35	—	100-200*	—	0-5	Distribution
7.2		30-40	—	100-200*	—	1-10	Distribution
12.5	95	30-40	—	100-200*	—	5-20	Distribution
23	150	30-40	—	200*	—	5-30	& Subtransmission
34.5	200	40	—	300*	—	10-40	
69	350	45	40-60	500	600	25-100	Transmission
115	550	50	40-60	600	700	25-100	Transmission
138	650	50	50-80	600	800-900	25-140	Transmission
161	750	50	50-80	600	900-1000	—	Transmission
230	1050	—	60-100	—	900-1000	45-260	Transmission
287.5	1300	—	70-120	—	900-1000	—	—

* Longer spans are often used in rural areas.

the hollow type HH (Hederheim) construction.^{1,2} Some typical power cables are illustrated in Figure 2-5. Cable sizes range from No. 8 AWG (16,510 circular mils) for short lines with light loads, to the equivalent of 1,000,000 circular mils of copper for long, high-power lines. Cable for high-voltage transmission lines is of the hollow or rope-core construction illustrated in Figures 2-5(c) through (f) to give the cable a larger radius for a given cross section. The larger radius is required for high-voltage lines to increase the corona threshold of the conductor. Some of the larger hollow cables are over 2 inches in diameter.

2.1.4 LINE INSULATORS

Insulators for transmission lines are made of glazed porcelain and shaped to provide long surface leakage paths, wet or dry. Hardware for attaching the insulator to the supporting

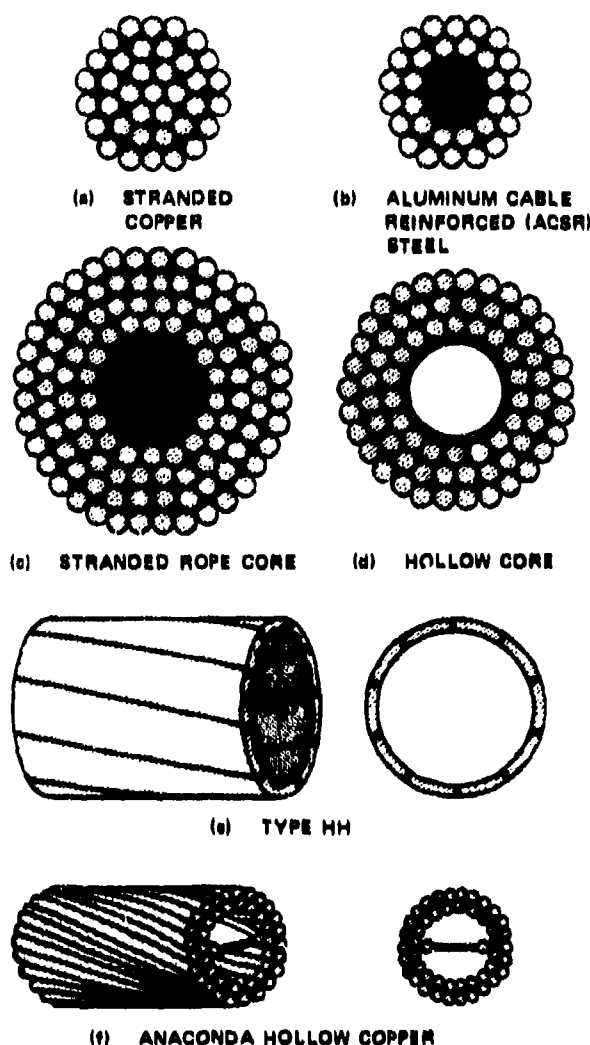


Figure 2-6 TRANSMISSION-LINE CABLE CONSTRUCTION

age is considerably larger than the transmission voltage, yet low enough that the lightning arrester fires before insulator flashover.^{1,2,3} On older transmission lines, expulsion-type lightning arresters were used along the line (at each support) to protect the insulators against direct strikes to the phase conductors. Modern transmission lines use the overhead ground wire to protect the phase conductors against direct strikes along the line. Lightning arresters are then used only at the ends of the line to protect the terminal equipment (transformers, substations, etc.). Many distribution and subtransmission lines are essentially unprotected.

structure and for attaching the power conductor to the insulator are provided. Figure 2-6 illustrates some typical power-line insulators. The pin-type insulators shown in Figure 2-6(a) and the post-type shown in Figure 2-6(b) are used for distribution, subtransmission, and low-voltage transmission lines. Strings of suspension-type insulators, such as those illustrated in Figure 2-6(c) are used for all high-voltage transmission lines. Such strings may be provided with arcing horns and grading rings on some of the older transmission lines. As can be seen in Table 2-1, the basic insulation level for transmission lines, which indicates the peak $1.5 \times 40 \mu\text{s}$ impulse voltage the system can withstand without flashover, is much higher than the 60-Hz transmission voltage, even for transmission voltages greater than 100 kV. This margin of safety (on the transmission voltage) permits the use of lightning arresters whose firing volt-

against lightning strikes along the line, but terminal equipment is almost always protected with lightning arresters.

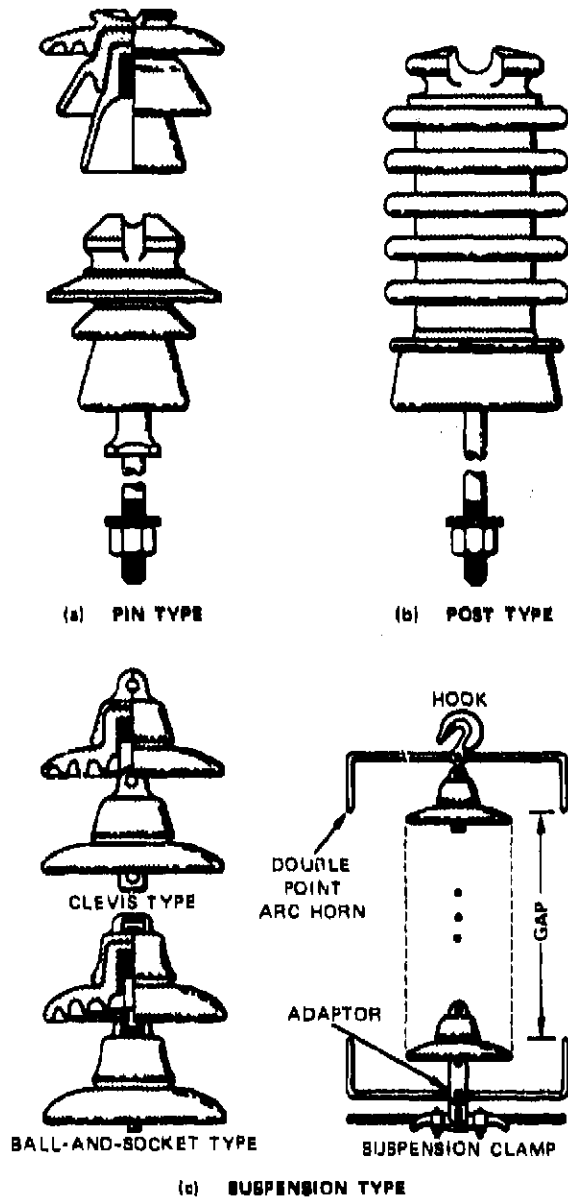


Figure 2-6 TRANSMISSION-LINE INSULATORS

2.1.5 Interaction of the EMP with Transmission Lines

The EMP wave induces current in the horizontal conductors strung on poles or towers, and it induces current in the vertical elements, such as steel towers, ground wires on wood poles, or vertical runs of cable or conduit at the customer's service. It is in these parts of the transmission line that the EMP induced currents are generated. The amount delivered to a particular pair of terminals depends on the length and height of these elements as well as the magnitude, waveform, and angle of incidence of the EMP and the conductivity of the soil. In addition, the propagation characteristics of the transmission line and junctions and bends in the vicinity of the terminals also influence the manner in which the induced currents propagate to the terminals. Formulas for evaluating these effects are contained in the following sections.

The common-mode currents and voltages induced in the horizontal conductors are treated in Section 2.2 for long lines (extending from the terminals to infinity) and for lines of finite length. The currents induced in the horizontal conductors usually have the largest peak values and the longest durations because they can propagate in from great distances, and for small angles of incidence of the EMP these currents can build up to large peak values (of the order of 10 kA for the high altitude EMP).

The currents and voltages induced in the vertical elements are treated in Section 2.3. For poorly conducting soil, the current induced in vertical elements such as towers or ground wires on poles is smaller than that induced in the horizontal line (unless the line is very short), but for highly conducting soils, the peak current induced in the vertical element may be comparable to that in the horizontal line. However, the latter result is because the peak current in the horizontal line is smaller for highly conducting soils, rather than because the current induced in the vertical element is larger. The peak current induced in a 10m high vertical element by the high altitude EMP is typically a few kA.

The propagation characteristics of transmission lines are treated in Section 2.4. Included in this section are the attenuation and phase factors for long, uniform lines over finitely conducting soil and the effects of bends junctions, line sag, and some other deviations from the ideal transmission line. The topics discussed in this section are useful for refining the estimates of induced current or voltage made from the formulas in Sections 2.2 and 2.3.

Differential coupling to transmission lines is treated in Section 2.5. The differential voltage is the voltage induced between the wires of, say, a single-phase distribution line by the EMP. This voltage is usually considerably smaller than the common mode voltage induced between both conductors and ground. The differential voltage is often of secondary interest; however, it may be necessary for the evaluation of stress on insulators and metering transformers.

Some general information on high-voltage properties of insulators, lightning arresters, and transmission line conductors is given in Section 2.6. These data are useful in evaluating the probable effects of the EMP induced voltages on the performance of these transmission line components.

2.2 COUPLING TO HORIZONTAL CONDUCTORS

2.2.1 SEMI-INFINITE LINE

2.2.1.1 General Approach

Common-mode (zero sequence) coupling of a plane wave to above-ground transmission lines has been analyzed by several methods.⁴⁻¹⁷ These include the solution of the boundary-value problem for a cylinder over a plane,^{5,6} the solution for the scattering by a conducting filament over a ground plane,⁹⁻¹⁴ and the solution for a transmission line with a distributed voltage source.^{4,7,8} The transmission-line solution is the least complicated, and it is quite accurate for EMP transients on power line configurations.^{7,8} The results presented here will therefore be based primarily on the transmission-line approximation.

Two additional approximations considerably simplify the calculation of the current or voltage induced on the line without much loss of accuracy. The first is the assumption that the soil behaves as a good conductor (i.e., $\sigma > \omega c$) for all frequencies of interest. The second is that the rise time of the incident wave may be considered zero if it is small compared to the round-trip propagation time between the wire and ground. The latter approximation permits fast-rising two-exponential pulses to be treated as single-exponential pulses. The assumption that the soil behaves as a good conductor causes some

distortion of the leading edge of the induced pulse after the ground-reflected wave returns, but this distortion is often negligible — particularly if the pulse is filtered by the service transformers and low-voltage circuits before it reaches the customer's equipment.

The coordinate system used in the mathematical analysis of the transmission lines is illustrated in Figure 2-7. The angle of incidence of the wave is defined by an azimuth angle φ measured from the projection of the wire on the ground, and an elevation angle ψ measured from the horizontal ground plane.

2.2.1.2 General Analysis of Transmission-Lines

In the analysis of the coupling of electromagnetic waves to above-ground transmission lines and similar structures, the source of the voltage that drives the line is distributed along the length of the transmission line. In this section we will develop the differential equations that describe transmission lines with distributed voltage sources, and show general forms of the solutions to these differential equations.

A transmission line with a distributed source voltage is, by definition, one that has an increment of source voltage in each increment of line length. An element, dz , in length, of such a transmission line is illustrated in Figure 2-8. Except for the source labeled

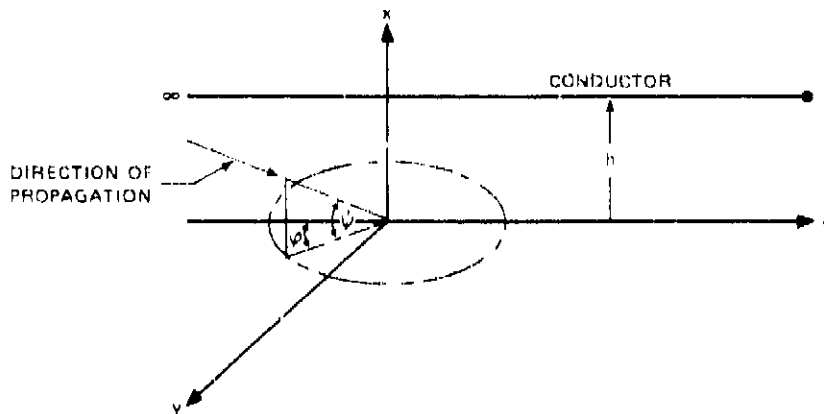


Figure 2-7 COORDINATES DEFINING AZIMUTH AND ELEVATION ANGLES OF INCIDENCE

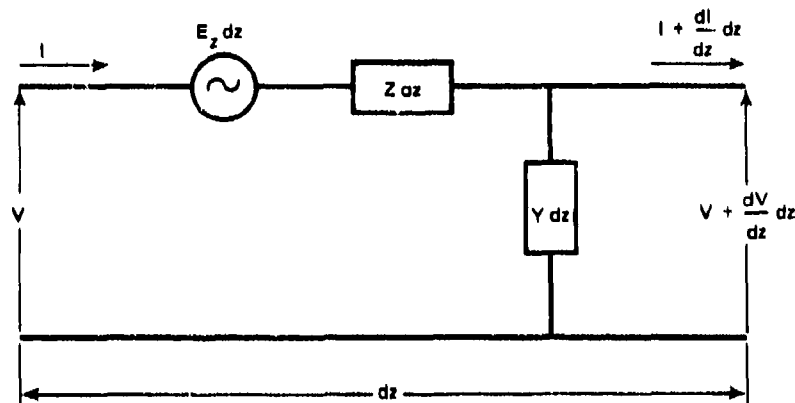


Figure 2-8 EQUIVALENT TRANSMISSION-LINE CIRCUIT

E_z in Figure 2-8, this transmission line is identical to classical transmission lines, and the techniques for determining the impedance per unit length Z and the admittance per unit length Y are the same as for classical transmission lines. The source term has been labeled E_z because it has the units of electric field strength (V/m).

The coupling calculations are based on the assumption that the height of the horizontal conductor over ground can be considered small, in terms of wavelengths, so that circuit analysis can be used. This assumption allows the low-frequency characteristic impedance of the line to be used. In the circuit analysis, radiation from the line and the existence of transmission modes other than the single simple TEM mode are also ignored.

The differential equations for the voltage and current along the transmission line of Figure 2-8 for harmonically varying signals ($e^{j\omega t}$) are

$$\frac{dV}{dz} = E_z - IZ \quad (2-1a)$$

$$\frac{dI}{dz} = -VY. \quad (2-1b)$$

By differentiating one and substituting the other, the second-order differential equations can be obtained:

$$\frac{d^2V}{dz^2} - \gamma^2 V = \frac{dE_z}{dz} \quad (2-2a)$$

$$\frac{d^2I}{dz^2} - \gamma^2 I = -YE_z \quad (2-2b)$$

where $\gamma^2 = ZY$. Except for the terms containing E_z , Eqs. (2-1) and 2-2) are identical to the equations for the more classical transmission-line formulation. The solutions to Eqs. (2-2) are^{4,7}

$$I(z) = [K_1 + P(z)]e^{-\gamma z} + [K_2 + Q(z)]e^{\gamma z} \quad (2-3a)$$

$$V(z) = Z_0 \left\{ [K_1 + P(z)]e^{-\gamma z} - [K_2 + Q(z)]e^{\gamma z} \right\} \quad (2-3b)$$

where

$$P(z) = \frac{1}{2Z_0} \int_{z_1}^z e^{\gamma v} E_z dv \quad (2-4a)$$

$$Q(z) = -\frac{1}{2Z_0} \int_z^{z_2} e^{-\gamma v} E_z dv \quad (2-4b)$$

K_1 and K_2 are coefficients determined from the terminating impedances Z_1 and Z_2 , at the ends of the line at $z = z_1$ and $z = z_2$ ($z_2 > z_1$), respectively, and $Z_0 = \sqrt{Z/Y}$ as in conventional transmission lines. K_1 and K_2 are constants given by

$$K_1 = \mu_1 e^{\gamma z_1} \frac{\mu_2 P(z_2)e^{-\gamma z_2} - Q(z_1)e^{\gamma z_2}}{e^{\gamma(z_2-z_1)} - \mu_1 \mu_2 e^{-\gamma(z_2-z_1)}} \quad (2-5a)$$

$$K_2 = \rho_2 e^{-\gamma z_2} \frac{\rho_1 Q(z_1) e^{\gamma z_1} - P(z_2) e^{-\gamma z_1}}{e^{\gamma(z_2-z_1)} - \rho_1 \rho_2 e^{-\gamma(z_2-z_1)}} \quad (2-5b)$$

in which the reflection coefficients ρ_1 and ρ_2 are given by

$$\rho_1 = \frac{Z_1 - Z_0}{Z_1 + Z_0}, \quad \rho_2 = \frac{Z_2 - Z_0}{Z_2 + Z_0} \quad (2-6)$$

The electric field $E_z(v)$ in Eqs. (2-4) is the "undisturbed" field that would exist at the wire height if the wire were not there. This resultant field is written $E_z^u(h, z)$ below to indicate that it is the z -component of the undisturbed field at height h . For an incident field of amplitude E_i , the resultant field is

$$E_z^u(h, z) = E_i e^{-jkz \cos \psi \cos \varphi} \left(1 - R_v e^{-jk2h \sin \psi} \right) \sin \psi \cos \varphi \quad (2-7a)$$

for a vertically polarized incident wave (magnetic vector parallel to the surface), and

$$E_z^u(h, z) = E_i \sin \varphi \left(1 + R_h e^{-jk2h \sin \psi} \right) e^{-jkz \cos \psi \cos \varphi} \quad (2-7b)$$

for a horizontally polarized incident wave (electric vector parallel to the surface). The phase is referred to the phase of the incident wave at the wire height when $z = 0$. In these expressions $k = \omega \sqrt{\mu_0 \epsilon_0}$ is the propagation factor for the wave in free space, and R_v and R_h are the reflection factors for wave reflection at the air/earth interface. These reflection factors are given by^{18,19}

$$R_h = \frac{\sin \psi - \sqrt{\epsilon_r \left(1 + \frac{\sigma}{j\omega \epsilon} \right) - \cos^2 \psi}}{\sin \psi + \sqrt{\epsilon_r \left(1 + \frac{\sigma}{j\omega \epsilon} \right) - \cos^2 \psi}} \quad (2-8a)$$

and

$$R_v = \frac{\epsilon_r \left(1 + \frac{\sigma}{j\omega \epsilon} \right) \sin \psi - \sqrt{\epsilon_r \left(1 + \frac{\sigma}{j\omega \epsilon} \right) - \cos^2 \psi}}{\epsilon_r \left(1 + \frac{\sigma}{j\omega \epsilon} \right) \sin \psi + \sqrt{\epsilon_r \left(1 + \frac{\sigma}{j\omega \epsilon} \right) - \cos^2 \psi}} \quad (2-8b)$$

It is convenient to separate the term $1 + R e^{-jk2h \sin \psi}$ in Eqs. (2-7) into two parts – one given by $1 - e^{-jk2h \sin \psi}$ that depends on the line height and a phase-shifted term given by $e^{-jk2h \sin \psi} (1 + R)$ that depends on the properties of the soil. Here $R = -R_v$ for vertical polarization and $R = R_h$ for horizontal polarization. For $\sigma \gg \omega \epsilon \sin^2 \psi$, the terms $1 + R$ reduce to

$$1 + R_h \approx \frac{2 \sin \psi}{\sqrt{\frac{\sigma}{j\omega \epsilon_0}}} \quad (2-9a)$$

$$1 - R_v \approx \frac{2}{\sqrt{\frac{\sigma}{j\omega \epsilon_0}} \sin \psi} \quad (2-9b)$$

These expressions can be used to obtain two components of the resultant field $E_x^u(h, z)$ from Eqs. (2-7) – one, depending on line height h , that would be obtained if the ground were perfectly reflecting ($|R| = 1$), and one, depending on the soil properties contained in $1 + R$, that is, in effect, a correction term to account for the fact that the ground is an imperfect reflector of the incident wave. These two components can be used in Eqs. (2.4), and thence in Eqs. (2.3), to obtain two solutions for the current or voltage.

The approximations of line height small compared to wavelength, negligible radiation loss, and no non-TEM propagation mode have been demonstrated to introduce very small errors in the results computed with the transmission-line approximation given above. Figure 2-9, for example, shows the current induced in an infinite line by a step function $E_0 u(t)$ of incident field calculated by the transmission-line method (dashed curves) and by an exact method (solid curves).^{5,7} It is apparent from this illustration that the transmission-line approximation is a good approximation to the current induced in a wire over a perfect ground plane even for the zero-rise-time step function. For realizable finite-rise-time pulses, the difference between the exact solution and the transmission-line approximation is so small that it is difficult to detect experimentally. The exact solution does provide interesting insight into the behavior of the scattered waves before the structure "settles down" to behave as a transmission line. In Figure 2-9, for example, one can see the discontinuity that occurs as the ground-reflected wave arrives at $(2h \sin \psi)/c$, a second discontinuity when the scattered direct wave reflected from the ground returns at $2h/c$, and a third discontinuity when the ground-reflected wave scattered from the wire reflected back

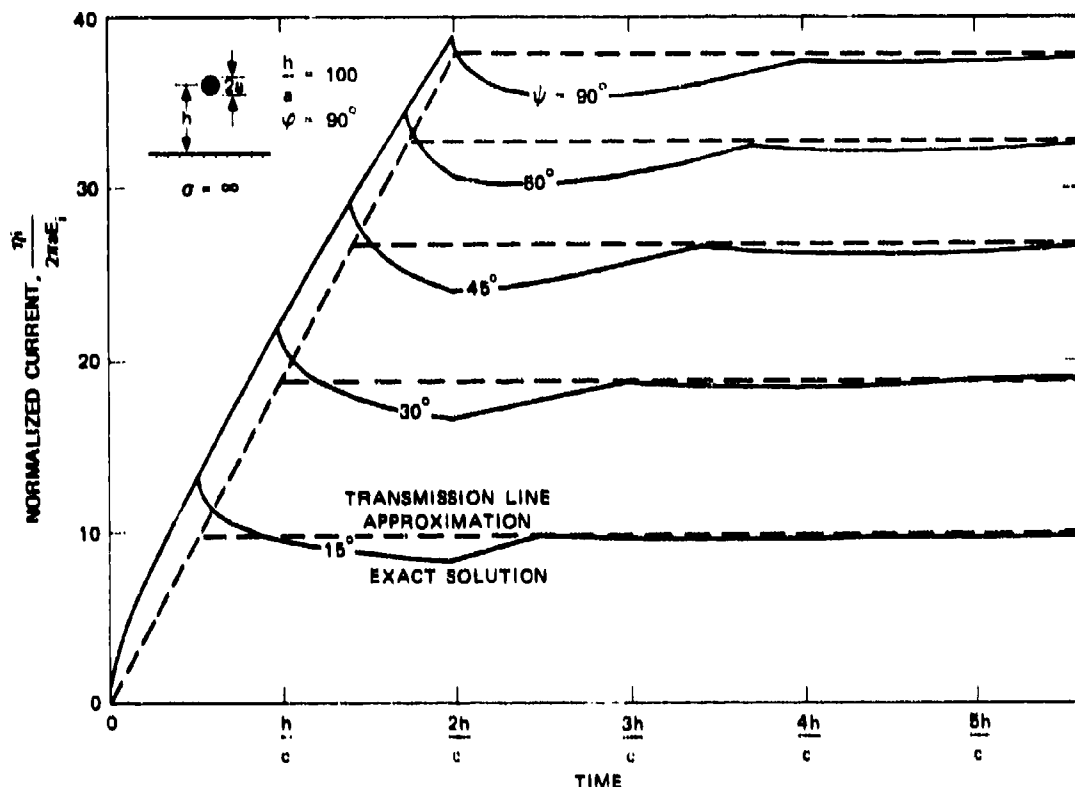


Figure 2-9 COMPARISON OF THE TRANSMISSION-LINE APPROXIMATION AND THE EXACT SOLUTION FOR THE CURRENT IN A WIRE OVER A PERFECTLY CONDUCTING GROUND PLANE — STEP-FUNCTION INCIDENT FIELD, HORIZONTALLY POLARIZED

from the ground arrives at $(1 + \sin \psi) 2h/c$. Subsequent multiply-scattered waves have a very weak influence, but they eventually bring the exact late-time response into coincidence with the transmission-line solution.

2.2.1.3 Open-Circuit Voltage in the Frequency Domain

The open-circuit voltage developed at the end of a semi-infinite transmission line of height h above a perfectly reflecting ground ($|R| = 1$) by a 1 V/m plane incident wave is⁷

$$V_\infty = cD(\psi, \varphi) \frac{1 - e^{-j\omega t_0}}{j\omega} \quad (2-10)$$

where c is the speed of light, $\omega = 2\pi f$ is the radian frequency, $t_0 = (2h \sin \psi)/c$, and $D(\psi, \varphi)$ is a directivity function defined by

$$D(\psi, \varphi) = \frac{\sin \psi \cos \varphi}{\frac{\alpha c}{j\omega} + \frac{\beta}{k} - \cos \psi \cos \varphi} \quad (\text{vertical polarization})$$

$$= \frac{\sin \varphi}{\frac{\alpha c}{j\omega} + \frac{\beta}{k} - \cos \psi \cos \varphi} \quad (\text{horizontal polarization}) \quad (2-11)$$

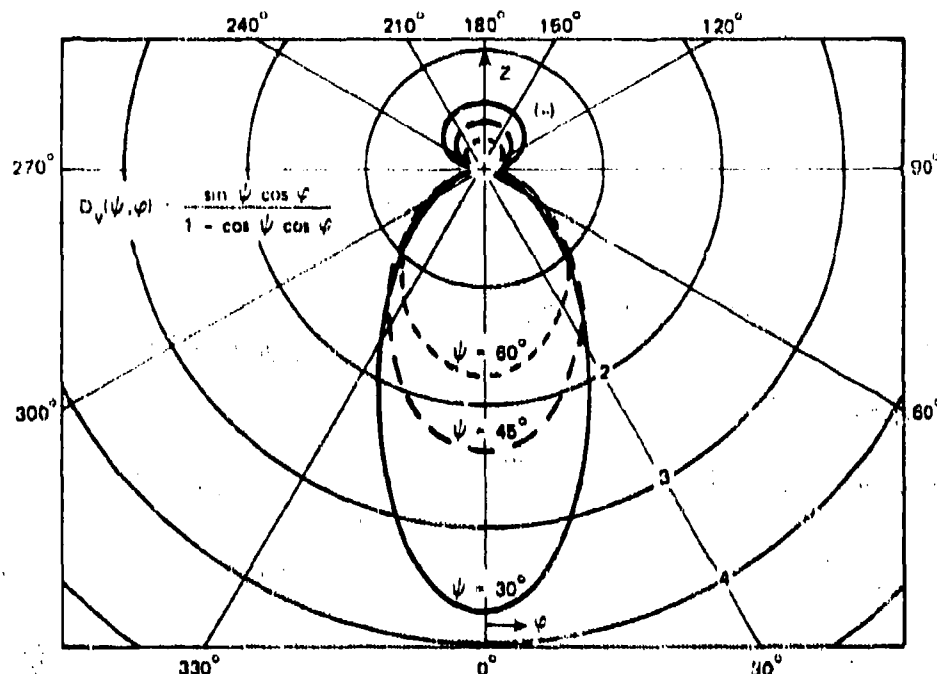
where α and β are the attenuation and phase factors for the transmission line (for perfect conductors, $\beta = k$ and $\alpha = 0$). Although α , β , and k are in general frequency-dependent, the value of $D(\psi, \varphi)$ depends primarily on the angles of incidence, and it is almost independent of frequency for many power line configurations. Plots of the directivity functions are shown in Figures 2-10 and 2-11 for $\beta/k = 1$ and for α/k negligible or constant. The assumptions that $\beta/k = 1$ and α/k is negligible are valid for finite soil conductivity if $h \geq \delta$ and the angles of incidence ψ and φ are large. For small angles of incidence, however, $\cos \psi \cos \varphi \rightarrow 1$, and the assumption that $\beta = k$ may cause an overestimate of $D(\psi, \varphi)$, and thus of the induced voltage and current, particularly at low frequencies. The value of β/k for conductors over soil are given in Section 2.4.1.

The correction that must be applied to V_{∞} to account for the imperfect reflection from the soil when $|R_{h,v}| \neq 1$ and $v \gg \omega t_0$ is

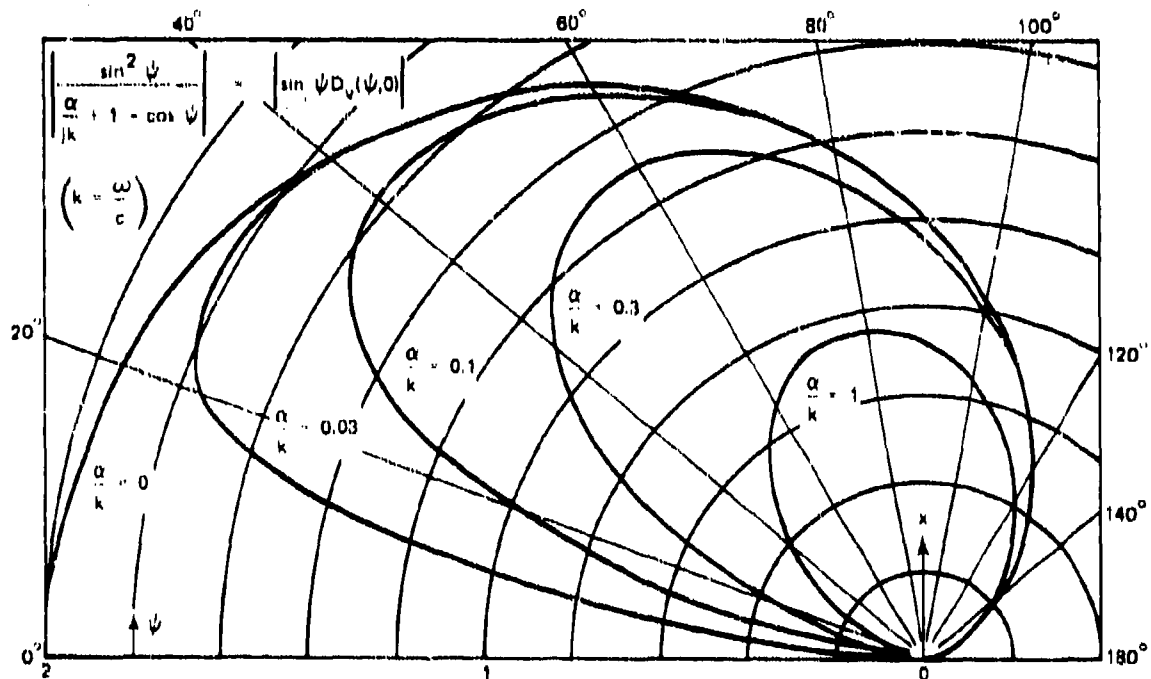
$$\Delta V = c\sqrt{\tau_e} D(\psi, \varphi) \frac{2}{\sin \psi} \frac{e^{-j\omega t_0}}{\sqrt{j\omega}} \quad (\text{vertical polarization})$$

$$= c\sqrt{\tau_e} D(\psi, \varphi) 2 \sin \psi \frac{e^{-j\omega t_0}}{\sqrt{j\omega}} \quad (\text{horizontal polarization}) \quad (2-12)$$

where $\tau_e = \epsilon_0/\sigma$, σ is the soil conductivity and ϵ_0 is the permittivity of free space.



(a) DIRECTIVITY FUNCTION FOR VERTICAL POLARIZATION (α negligible)



(b) PATTERN FOR $\sin \psi D_v(\psi, 0)$ AT ZERO AZIMUTHAL ANGLE

Figure 2-10 POWER-LINE DIRECTIVITY PATTERNS FOR VERTICAL POLARIZATION.
Source: Ref. 8.

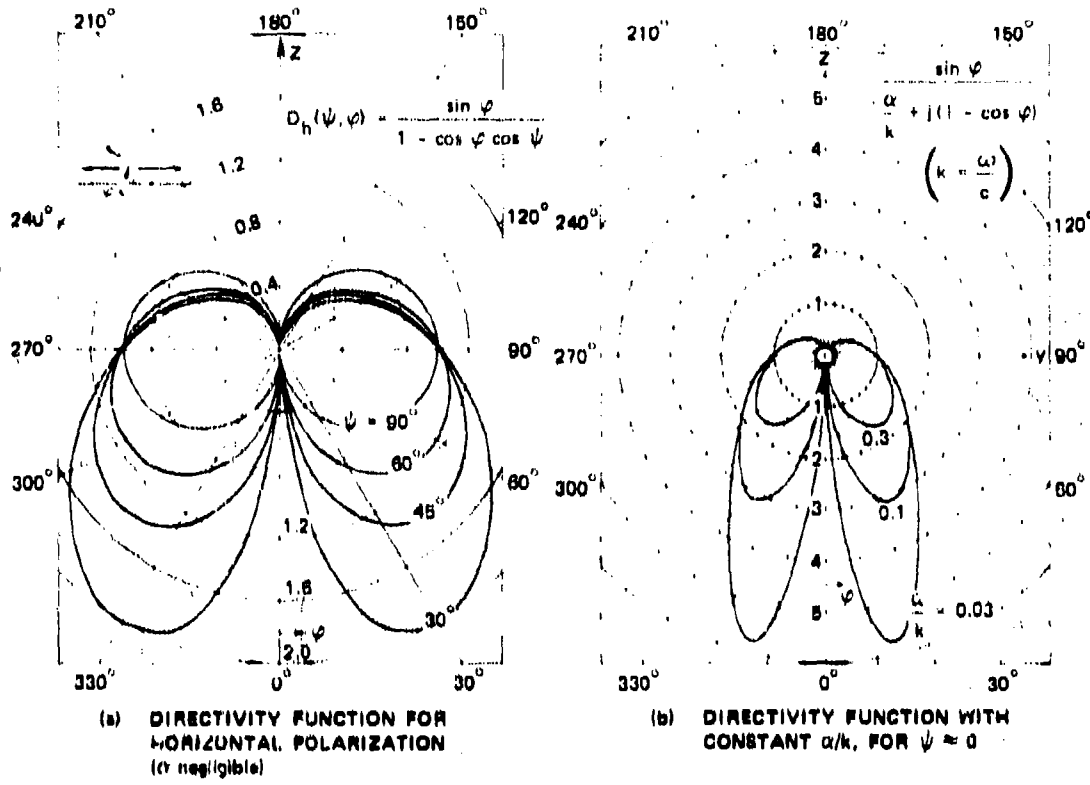


Figure 2-11 POWER-LINE DIRECTIVITY PATTERNS FOR HORIZONTAL POLARIZATION.
Source: Ref. 8.

The total open-circuit voltage is then?

$$V_{oc} = V_{in} + jV = c D(\psi, \varphi) \left[\frac{1 - e^{-j\omega t_0}}{j\omega} + 2\sqrt{\tau_0} (\sin \psi)^{+1} \frac{e^{-j\omega t_0}}{\sqrt{j\omega}} \right] \quad (2-13)$$

where the exponent +1 is associated with horizontal polarization, and -1 is associated with vertical polarization. The voltage given by Eq. (2-13) is caused by the horizontal component of the electric field. For vertical polarization, there is an additional component of voltage produced by the vertical component of the electric field. This component is discussed in Section 2.3, where the voltage and current induced in the vertical elements of the transmission line are discussed. Plots of the open-circuit voltage calculated from Eq. (2-13) are shown in Figure 2-12 for vertical polarization and in Figure 2-13 for horizontal polarization.

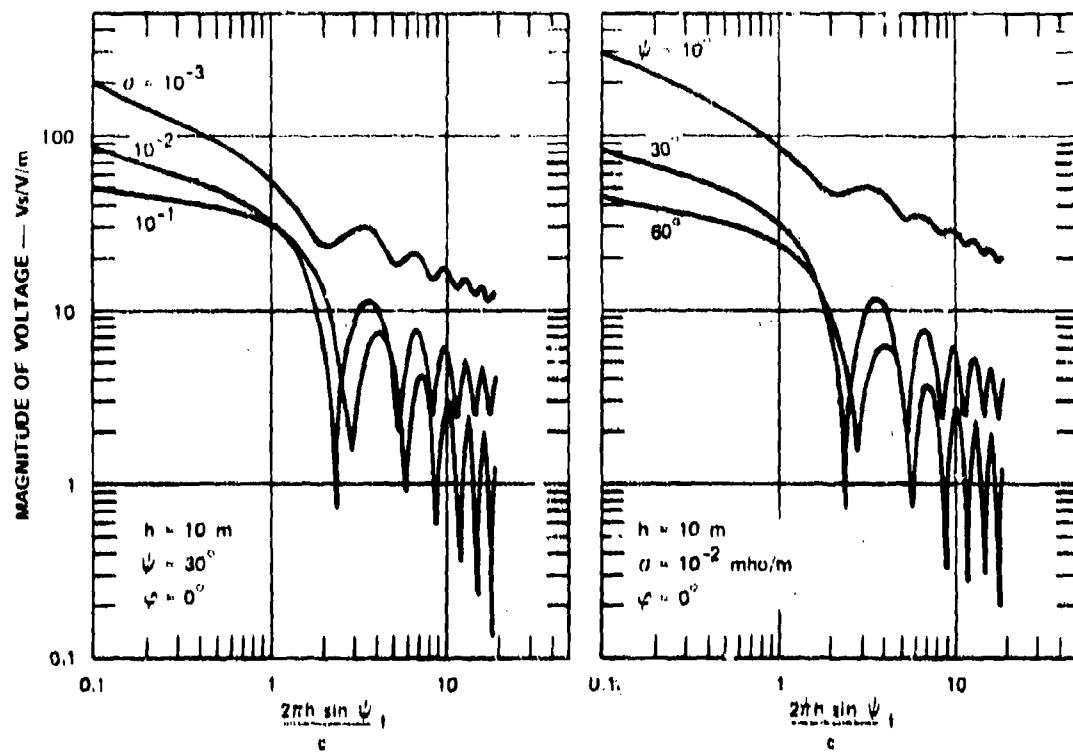


Figure 2-12 OPEN-CIRCUIT TERMINAL VOLTAGE INDUCED IN AN INFINITE TRANSMISSION LINE BY A VERTICALLY POLARIZED INCIDENT FIELD OF 1 V/m

The source impedance for the semi-infinite transmission line is simply its characteristic impedance $Z_0 = \sqrt{Z/Y}$. For typical power transmission-line configurations, this impedance deviates very little from^{20,21}

$$Z_0 = \frac{\eta_0}{2\pi} \log \frac{2h}{a} \quad (h \gg a) \quad (2-14)$$

where a is the radius (or effective radius) of the power conductors and $\eta_0 = \sqrt{\mu_0/c_0}$ is the intrinsic impedance of free space. The Thevenin equivalent circuit of the transmission line is thus the open-circuit voltage given by Eq. (2-13) in series with Z_0 . The Norton equivalent circuit is a current source V_{oc}/Z_0 in parallel w/ Z_0 .

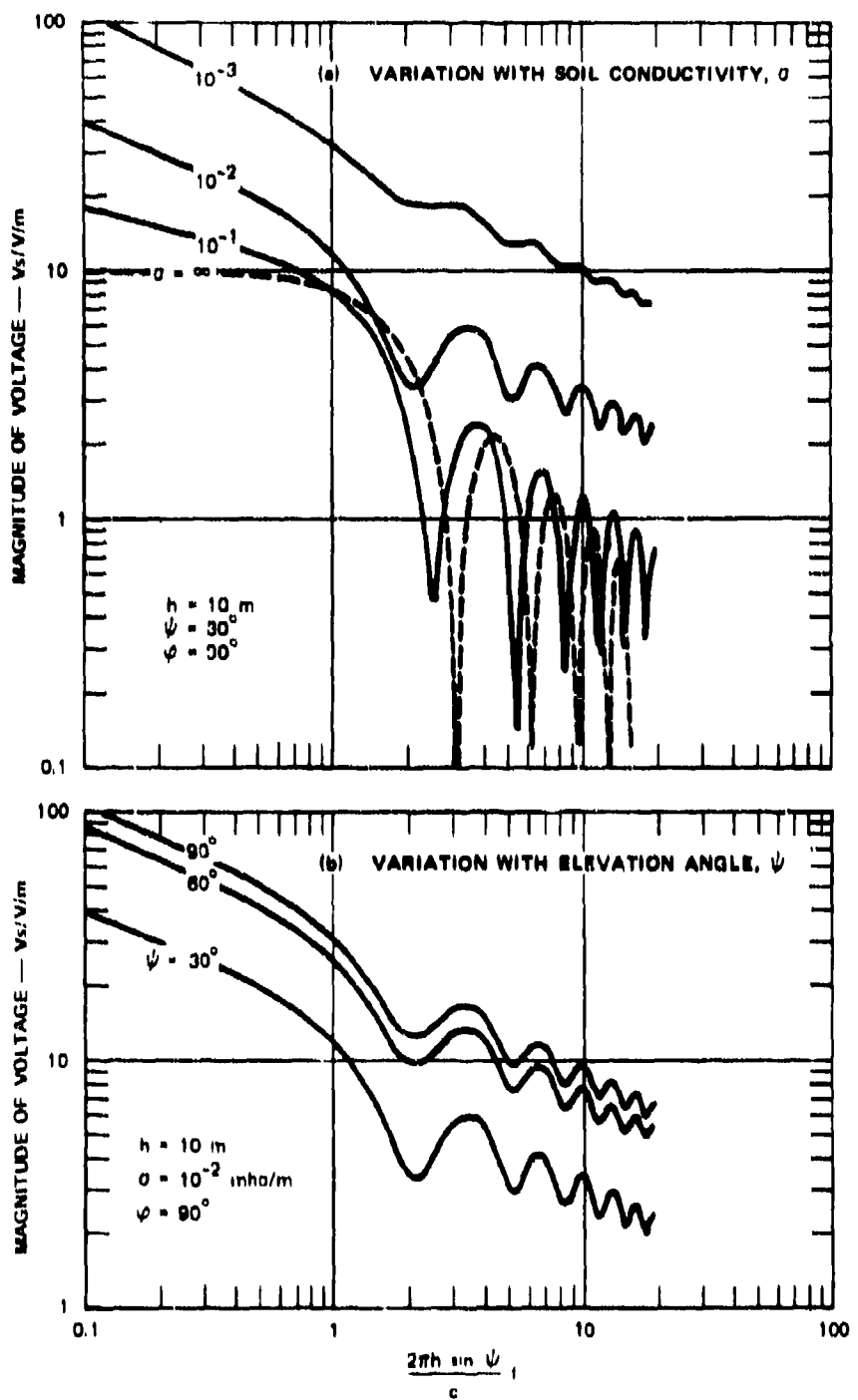


Figure 2-13 OPEN-CIRCUIT TERMINAL VOLTAGE INDUCED IN A SEMI-INFINITE TRANSMISSION LINE BY A HORIZONTALLY POLARIZED INCIDENT FIELD OF 1 V/m

2.2.1.4 Transient Waveforms for an Exponential Pulse

For an incident exponential pulse $E_0 e^{-t/\tau}$ whose Fourier transform is

$$E(\omega) = E_0 \frac{1}{|\omega + 1/\tau|} \quad (2-16)$$

the open-circuit voltage at the end of a semi-infinite line is

$$V_{oc}(\omega) = E_0 c D(\psi, \varphi) \left[\frac{1 - e^{-|\omega t_0}}{|\omega|(\omega + 1/\tau)} + \frac{2\sqrt{\tau_e} (\sin \psi)^{1/2}}{\sqrt{|\omega|(\omega + 1/\tau)}} \frac{e^{-|\omega t_0}}{\sqrt{|\omega|(\omega + 1/\tau)}} \right] \quad (2-16)$$

From the inverse transforms,²² the voltage waveform is

$$\begin{aligned} V_{oc}(t) &= E_0 c \tau D(\psi, \varphi) (1 - e^{-U\tau}) \quad (0 \leq t \leq t_0) \\ &= E_0 c \tau D(\psi, \varphi) \left\{ (e^{t_0/\tau} - 1) e^{-U\tau} - \frac{4 (\sin \psi)^{1/2}}{\pi} \sqrt{\frac{\tau_e}{\tau}} e^{-t'/\tau} \right. \\ &\quad \left. \times \int_0^{\sqrt{t'/\tau}} e^{u^2} du \right\} \quad (t \geq t_0) \end{aligned} \quad (2-17)$$

where $t' = t + t_0$, and $t_0 = (2h \sin \psi)/c$. The first term in the braces in Eq. (2-17) is due to the geometry (line height and angle of incidence) and is independent of the properties of the soil. The second term contains the effect of the soil conductivity in $\tau_e = r_0/a$, as well as geometric effects.

2.2.1.5 Parametric Variation of the Open-Circuit Voltage

The open-circuit voltage $v_{oc}(t)$ is plotted in Figure 2-14 for both polarizations with soil conductivity varying from 10^{-3} to ∞ mho/m. The waveform for $a = \infty$

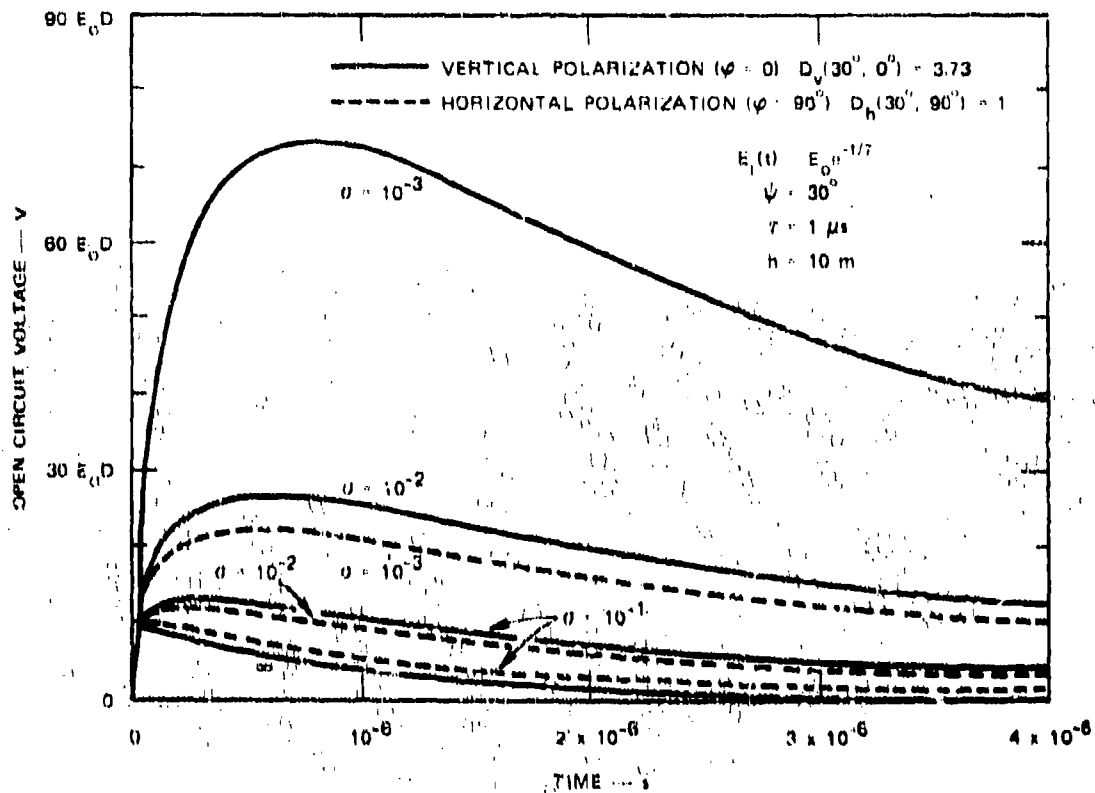


Figure 2-14 OPEN-CIRCUIT VOLTAGE AT THE END OF A SEMI-INFINITE LINE FOR VARIOUS SOIL CONDUCTIVITIES. Source: Ref. 7.

($r_g = 0$) is produced by the first term of Eq. (2-17) alone. The deviations of the other waveforms from that for $\sigma = \infty$ are caused by imperfect reflection of the incident wave by the ground. The coupling caused by the ground effect is larger than the coupling caused by the line height for vertical polarization and soil conductivities less than 10^{-2} mho/m. It is also apparent that the ground-effect coupling to vertical polarization is considerably greater than the coupling to horizontal polarization. The difference is even greater than the waveforms in Figure 2-14 indicate because the directivity function $D(\psi, \varphi)$ is greater for vertical polarization than for horizontal polarization.

In Figure 2-14 and in other illustrations of induced waveforms that follow, the amplitude of the open-circuit voltage is normalized to $D(\psi, \varphi)$. The values of $D(\psi, \varphi)$ are shown for end-on incidence ($\varphi \approx 0$) with vertical polarization and broadside incidence ($\varphi \approx 90$ degrees) with horizontal polarization, although the results can be applied to any azimuth angle of incidence φ . However, because the ground-effect term depends on

$(\sin \psi)^{\pm 1}$, as well as on $D(\psi, \varphi)$, the results shown are applicable to only the 30 degree elevation angle of incidence.

The effect of line height on the open-circuit voltage waveform is illustrated in Figure 2-15, where the waveforms are plotted for vertical polarization incident on soil with a conductivity of 10^{-2} mho/m. Also shown as dashed curves in Figure 2-15 are the waveforms with $\sigma = \infty$; only this portion of the waveforms is proportional to the line height. For the soil conductivity of 10^{-2} mho/m, the ground effect is larger than the height effect, and changing the height of the line does not have a large effect on the peak open-circuit voltage.

The effect of incident pulse duration (decay time constant) on the open-circuit voltage waveform is illustrated in Figure 2-16, where the open-circuit voltage is

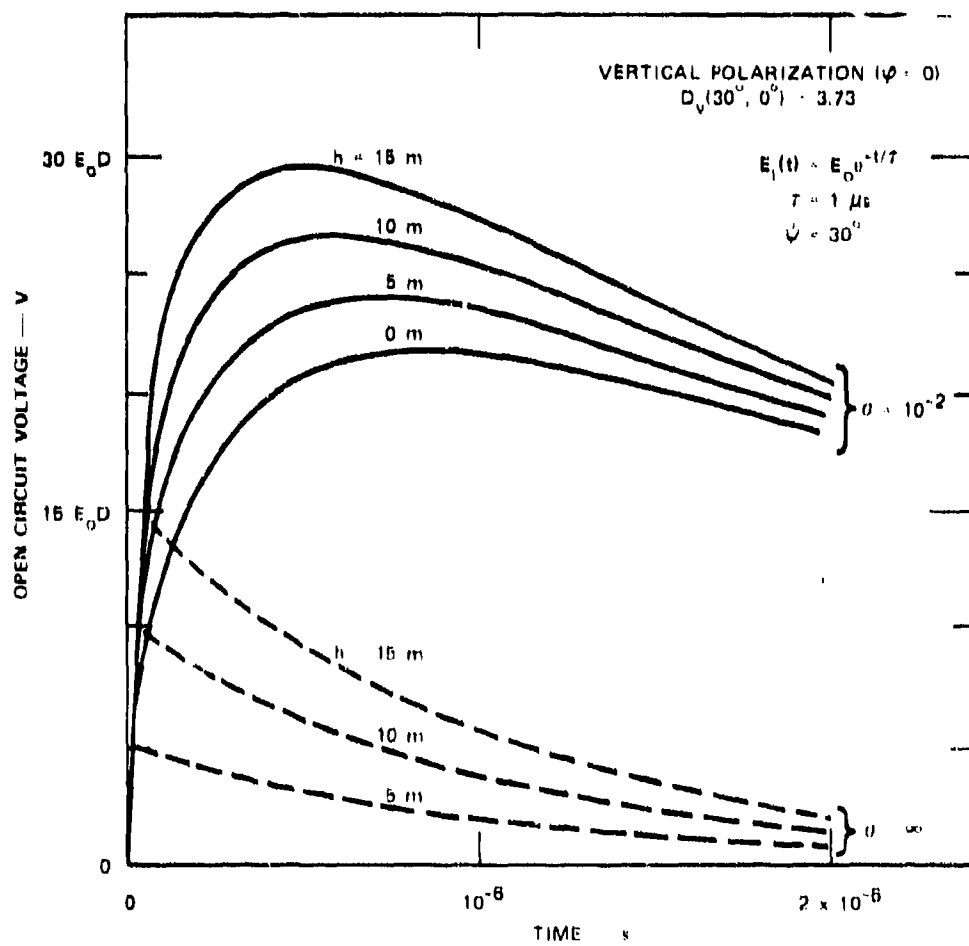


Figure 2-15 OPEN-CIRCUIT VOLTAGE AT THE END OF A SEMI-INFINITE LINE FOR VARIOUS LINE HEIGHTS. Source: Ref. 7.

plotted for incident pulse decay time constants of 0.25, 0.5, and 1.0 μ s. As is apparent from Eq. (2-17), the waveform for a given soil conductivity, line height, and angle of incidence can be plotted as a function of a normalized time t/τ , in which case the pulse decay time constant τ affects only the relative magnitudes of the two terms in braces in Eq. (2-17). However, it is apparent in Figure 2-16 that the pulse duration affects both the peak voltage and the time required to reach the peak value. The wider the pulse, the larger the peak voltage because the wider the pulse, the longer the segment of line near the terminals over which the ground effect is integrated. Note that for perfect ground (dashed curves in Figure 2-16) the pulselength has little effect on the peak voltage, and the open-circuit voltage

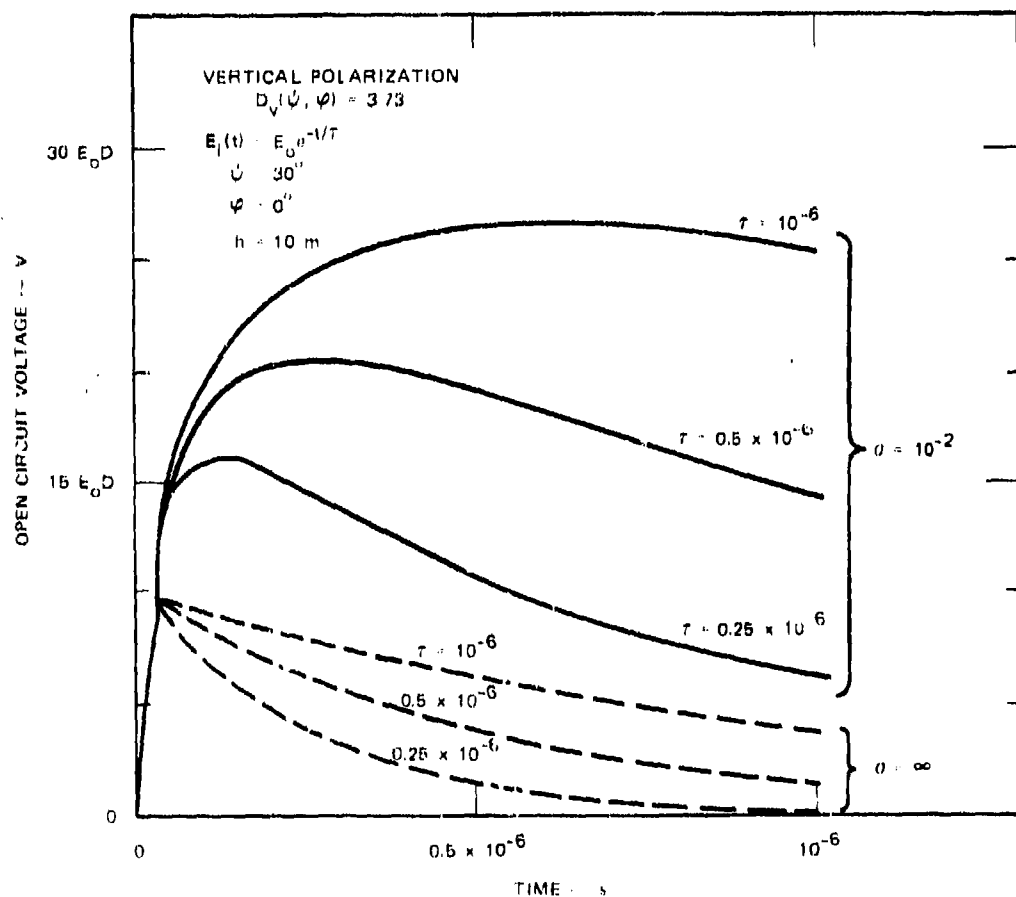


Figure 2-16 OPEN-CIRCUIT VOLTAGE AT THE END OF A SEMI-INFINITE LINE FOR VARIOUS INCIDENT PULSE DECAY TIME CONSTANTS. Source: Ref. 7.

waveform is essentially the incident-field waveform except for the finite rise time $t_0 = (2h \sin \psi)/c$.

In Figures 2-14, 2-15, and 2-16, the waveforms for vertical polarization have been plotted for an elevation angle $\psi = 30^\circ$ and an azimuth angle $\varphi = 0^\circ$, while the waveforms for the horizontally polarized incident wave in Figure 2-14 were plotted for $\psi = 30^\circ$ and $\varphi = 90^\circ$ (broadside). In all three illustrations, it was assumed that $\alpha/k \ll 1$ and that α/k is not frequency-dependent. It is also important to recognize that changing the angles of incidence in Eq. (2-13) affects the relative magnitude of the ground effect through the $(\sin \psi)^{\pm 1}$ coefficient as well as affecting the directivity function $D(\psi, \varphi)$ and the delay time t_0 . In effect, there are two directivity functions — one for the response with perfect ground, $D(\psi, \varphi)$, and one for the correction term, $(\sin \psi)^{\pm 1} D(\psi, \varphi)$.

2.2.2 LINE OF FINITE LENGTH

2.2.2.1 Uniform Plane Wave

The open-circuit voltage induced at the terminals of a horizontal transmission line of a finite length ℓ as illustrated in Figure 2-17 by a uniform plane wave is⁸

$$V_{oc}(\omega) = V_{oc}(\omega) \left\{ [1 - e^{-(\gamma - |k'|)\ell}] - [\rho_\ell e^{-\gamma 2\ell} - e^{-(\gamma - |k'|)\ell}] \right. \\ \times \left. \frac{D(\psi, \varphi + \pi)}{D(\psi, \varphi)} \right\} \times \sum_{n=0}^{\infty} [\rho_\ell e^{-\gamma 2\ell}]^n \quad (2-18)$$

where $V_{oc\infty}(\omega)$ is the voltage induced in a semi-infinite line, and

$$\gamma \approx \alpha + j\omega/c$$

$$k' = \frac{\omega}{c} \cos \psi \cos \varphi$$

$$\rho_L = \frac{Z_L - Z_0}{Z_L + Z_0}.$$

The open-circuit voltage $V_{oc\infty}(\omega)$ for the semi-infinite line is given by Eq. (2-13), the directivity functions $D(\psi, \varphi)$ are given by Eq. (2-11), and the characteristic impedance Z_0 is given by Eq. (2-14). The reflection factor ρ_L at the end of the line opposite the terminals is a function of the load impedance Z_L at that end of the line (see Eq. (2-6)).

When the line attenuation α is negligible, the exponential terms in Eq. (2-18) become of the form $\exp[-j\omega(1 - \cos \psi \cos \varphi) L/c]$ or $\exp[-j\omega 2L/c]$, which transform into delays in the time domain. Thus the open-circuit voltage waveform of the finite-length line is identical to that for the semi-infinite line until the first end-effect arrives at $(1 - \cos \psi \cos \varphi) L/c$. Between this time and $2L/c$, the waveform is that for the semi-infinite line, modified by the factor $-\rho_L \frac{D(\psi, \varphi + \pi)}{D(\psi, \varphi)}$. After $2L/c$, the waveform repeats, as illustrated in Figure 2-18 where the waveform for a line 150 m long, open-circuited at both ends, and having negligible attenuation, is shown for an exponential pulse of incident field. When the attenuation of the line is not neglected, the abrupt changes shown in Figure 2-18 become more rounded, and the amplitude of the oscillations becomes smaller with increasing time.

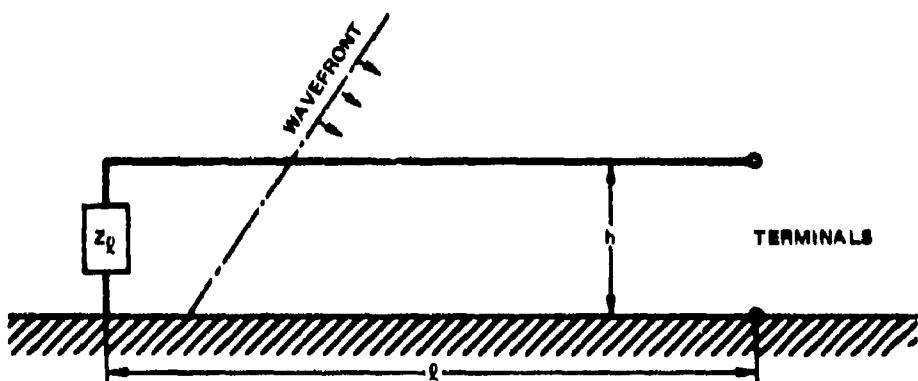


Figure 2-17 TRANSMISSION LINE OF FINITE LENGTH

The source impedance at the terminals of a line of finite length is

$$Z(0) = Z_0 \frac{1 + \rho_\ell e^{-2\gamma l}}{1 - \rho_\ell e^{-2\gamma l}} \quad (2-19)$$

and the short-circuit current at the terminals is $I_{sc}(\omega) = V_{oc}(\omega) / Z(0)$. The open-circuit voltage given by Eq. (2-18) is only that part induced in the horizontal conductor by the horizontal component of the incident electric field. If a vertical element is included, the vertical component of the electric field (in the case of a vertically polarized incident wave) will induce a voltage in this vertical element. The voltage induced in the vertical element is discussed in Section 2.3.

2.2.2.2 Spherical Wave at Grazing Incidence

Consider a vertically polarized wave is incident at $\psi = \varphi = 0$, as illustrated in Figure 2-19, where the EMP is generated by a surface burst on the transmission line (or an extension of the line). Near the source point (in the close-in region), the radiation from the weapon will ionize the air sufficiently to cause it to behave as a conductor ($\sigma \gg \omega \epsilon_0$), and further away (in the intermediate region), the ionization will be weaker but still sufficient to produce significant attenuation of signals propagating away from the source on the line. Here we discuss only the coupling that occurs outside these regions, where the EMP wave behaves as a vertically polarized wave propagating outward from the source at the speed of light.

The transmission-line axis is assumed to extend from the point z_1 to the terminals at $z_2 > z_1$, as illustrated in Figure 2-19. The wave in the air is assumed to propagate as though the ground were a perfect conductor so that $E_x = \eta_0 H_y$, where η_0 is the intrinsic impedance of free space, and $E_x = (E_0 e^{-jkz})/z$. However, for a finitely conducting ground there will be a z-component of the electric field at the surface whose value is $E_z(0,z) = \eta H_y(0,z)$, where η is the intrinsic impedance of the soil, and $\eta_0 \gg \eta > 0$.

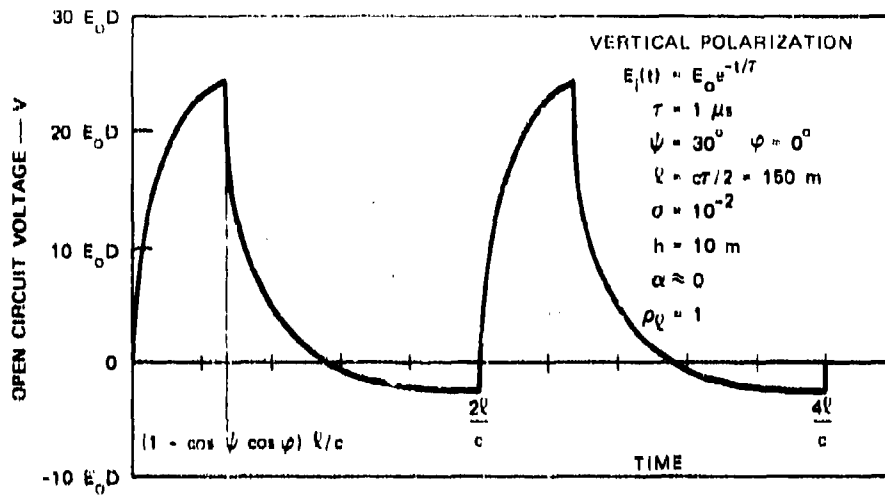


Figure 2-18 OPEN-CIRCUIT VOLTAGE WAVEFORM AT THE TERMINALS OF A 150-m-LONG LINE OPEN-CIRCUITED AT BOTH ENDS

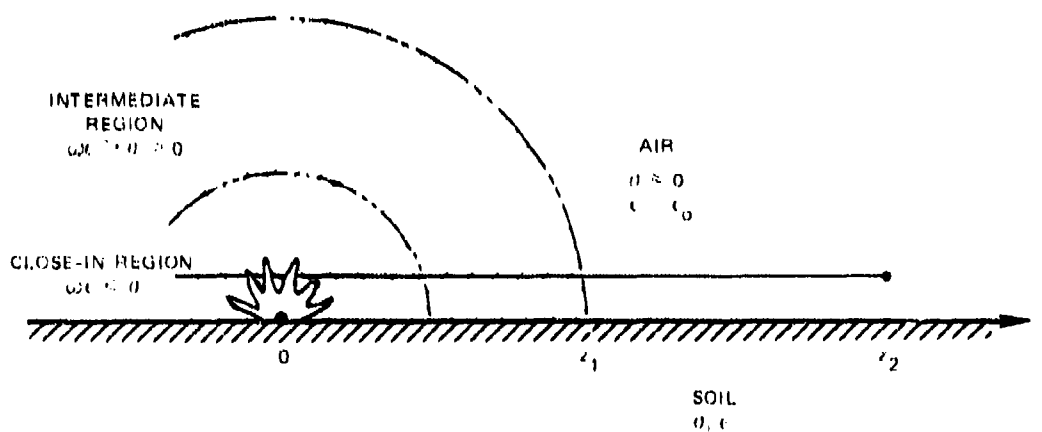


Figure 2-19 PHYSICAL ARRANGEMENT THAT PRODUCES A VERTICALLY POLARIZED WAVE WITH END-ON INCIDENCE

The horizontal component of the field at the wire height is⁷

$$E_z(h,z) \approx \left(\frac{\eta}{\eta_0} - \frac{h}{z} \right) \frac{E_0 e^{-jkz}}{z} \quad (2-20)$$

where $\eta_0 = \sqrt{\mu_0/\epsilon_0}$ and $\eta = \sqrt{\omega\mu_0/(v + j\omega\epsilon)}$, if we neglect attenuation of the wave due to losses to the ground, and apply a first-order correction to the field at the surface to obtain the field at the wire height. (E_0 is the total vertical electric field, so that it corresponds to $2E_0$ in the space-wave case discussed in Section 2.2.1.)

The open-circuit voltage induced at the terminals at $z = z_2$ by this horizontal electric field is, from Eq. (2-3),

$$V_{oc}(\omega) = \frac{E_0 h Z(0) e^{-\gamma z_2}}{Z_0} \left\{ \frac{e^{(\gamma-jk)z_2}}{z_2} - \frac{e^{(\gamma-jk)z_1}}{z_1} + \left[\frac{\eta}{h\eta_0} - (\gamma-jk) \right] \right.$$

$$\left. \times \int_{z_1}^{z_2} \frac{e^{(\gamma-jk)v}}{v} dv \right\} \quad (2-21)$$

where γ , $Z(0)$, and k are the propagation factor, the source impedance given by Eq. (2-19), and the free-space phase factor, respectively.

The coupling to the wire can be resolved into three components according to the nature of coupling: geometric, ground-effect, and phase-disparity. If the wire and soil were perfect conductors, then $\eta = 0$ and $\gamma = jk$, and the open-circuit voltage on the wire at z_2 would be

$$V_g(z_2) = -\frac{E_0 h Z(0) e^{-jkz_2}}{Z_0} \left(\frac{1}{z_2} - \frac{1}{z_1} \right) \left(\begin{array}{l} \eta = 0 \\ \gamma = jk \end{array} \right). \quad (2-22)$$

The coupling in this case is the geometric component caused by the nonuniformity in the magnitude of the incident electric field along the wire, which causes the potential at the wire height at z_1 to differ from the potential at the wire height at z_2 .

If $\gamma = jk$ and $\eta \neq 0$, we obtain an additional ground-effect component

$$V_\alpha(z_2) = \frac{E_0 \eta Z(0)}{Z_0 \eta_0} e^{-jkz_2} \log \frac{z_2}{z_1} \quad (2-23)$$

which is caused by the finite conductivity of the soil ($\eta \approx \sqrt{\omega \mu / \sigma}$). This component is the integral (between z_1 and z_2) of the z-component of the electric field induced in the finitely conducting soil by the incident wave.

Finally, if $\gamma \neq jk$, both the geometric component and the ground-field component are modified, and a third component, caused by the disparity in the propagation characteristics of the incident wave and the induced responses, is obtained. This phase-disparity component is

$$V_\beta(z_2) = -\frac{E_0 h Z(0)}{Z_0} e^{-\gamma z_2} (\gamma - jk) \int_{z_1}^{z_2} \frac{e^{(\gamma - jk)v}}{v} dv \quad (2-24)$$

which exists only if there is a disparity between the phase factors of the incident wave and those of the transmission line.

For typical soil conductivities and line lengths, the geometric term given by Eq. (2-22) is significant only at very low frequencies unless the line is very high or very close to the source, and the phase-discrepancy term given by Eq. (2-24) is small compared to the ground-effect term given by Eq. (2-23). The open-circuit voltage induced in the transmission line by an exponential pulse $(E_0/z)e^{-t/\tau}$ is thus

$$V(z_2) \approx \frac{E_0 Z(0)}{Z_0 \sqrt{\epsilon_r}} \log \frac{z_2}{z_1} \left[\frac{1}{j\omega + \frac{1}{\tau}} \right] \left(\omega \gg \frac{1}{\epsilon_r \tau_e} \right)$$

$$\approx \frac{E_0}{Z_0} \sqrt{\tau_e} \log \frac{z_2}{z_1} \left[\frac{\sqrt{j\omega}}{j\omega + \frac{1}{\tau}} \right] \left(\omega \ll \frac{1}{\epsilon_r \tau_e} \right)$$

(2-25)

where $\tau_e = \epsilon_0 / \sigma$, when phase is referred to the terminals at z_2 .

The voltage waveform is

$$\begin{aligned}
 v(z_2, t) &\approx \frac{E_0 Z(0)}{Z_0 \sqrt{\epsilon_r}} \log \frac{z_2}{z_1} e^{-t/\tau} & (t < \epsilon_r \tau_0) \\
 &\approx \frac{E_0 Z(0)}{Z_0} \sqrt{\frac{\tau_0}{\pi r}} \log \frac{z_2}{z_1} \left[\sqrt{\frac{\tau}{t}} - 2e^{-t/\tau} \int_0^{\sqrt{t/\tau}} e^{u^2} du \right] & (t > \epsilon_r \tau_0)
 \end{aligned} \tag{2-26}$$

for a zero-rise-time exponential pulse. For a two-exponential pulse with non-zero rise time, the voltage waveform can be obtained by superposing two solutions such as in Eq. (2-26). The waveforms for single and double exponential transient fields are shown in Figure 2-20 for a pulse decay time constant of 1 μ s and soil conductivities varying from 10^{-1} to 10^{-3} mho/m. The line is assumed to be terminated in its characteristic impedance at the end z_1 opposite the terminals. For the two-exponential pulse (solid curves), the rise-time constant τ_r is 4 ns. The early-time and late-time approximations, which do not meet at $t = \epsilon_r \tau_0$ for the lower conductivities, have been joined by a vertical line. The dashed curves are the zero rise time (single exponential) responses.

The waveforms of Figure 2-18 are such short, high-amplitude pulses that it was necessary to plot them on a log-log scale to view significant details. Note that the peak value and the time to reach the peak value both increase as soil conductivity decreases, because the more poorly conducting soil behaves as a dielectric longer and supports a larger z-component of electric field when it behaves as a conductor.

Comparison of Figures 2-20 and 2-14 shows that the peak voltages obtained with end-on illumination of a semi-infinite line can be much greater than those obtained with oblique illumination of a line of finite length. Although some of the difference between these two cases can be attributed to the nonuniform illumination, most of it can be attributed to the length of the line. On the semi-infinite line, the peak voltage contains voltage that was induced at a distance $c t_{pk} / (1 - \cos \psi)$ away from the terminals. Therefore, unless the transmission line is straight and at least $c t_{pk} / (1 - \cos \psi)$ long, the open-circuit voltage will never attain the peak value predicted for a semi-infinite line. One should therefore use caution in applying the currents and voltages predicted for semi-infinite lines with small angles of incidence.

2.2.3 RATE OF RISE OF THE OPEN-CIRCUIT VOLTAGE

The rate of rise of the line voltage is important in evaluating lightning arrester performance and insulation flashover characteristics. For typical line heights such that the transit time h/c is large compared to the rise time of the EMP and small compared to the pulselength, the rate of rise of the voltage in response to a step-field is a useful measure of the early-time behavior of the line voltage. The open-circuit voltage induced at the end of a semi-infinite line by a step of incident field $E_0 u(t)$ is

$$v(t) = 2E_0 h \sin \psi D(\psi, \varphi) \frac{t}{t_0} \quad (0 < t < t_0) \quad (2-27)$$

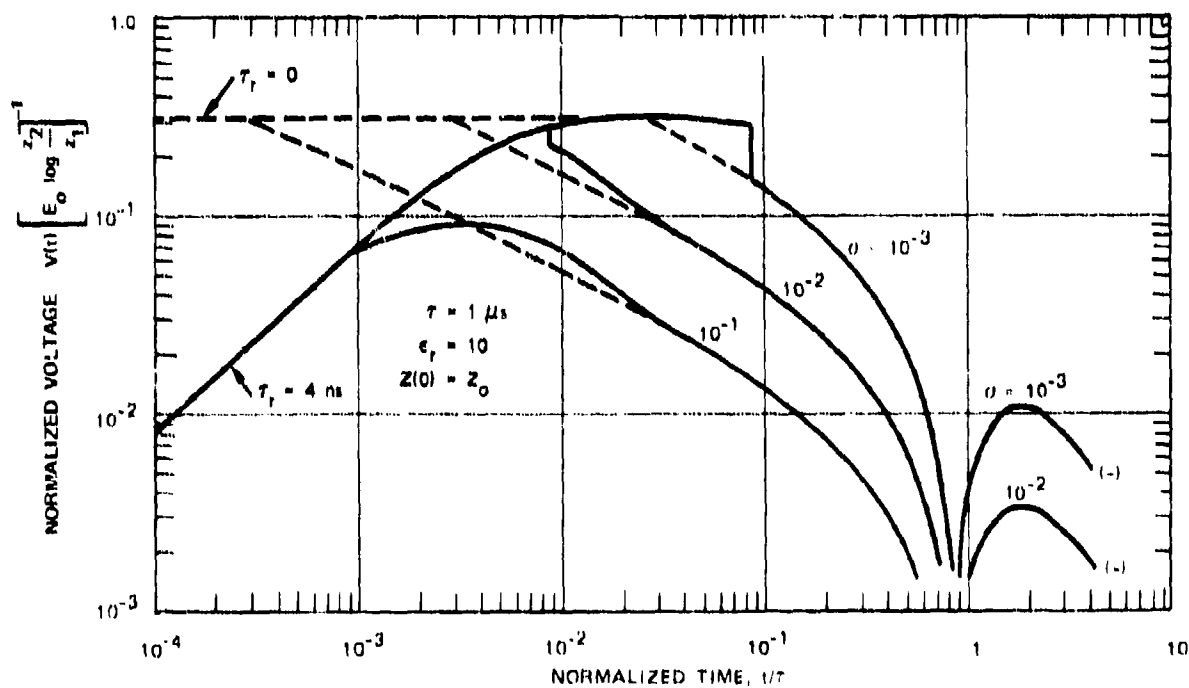


Figure 2-20 OPEN-CIRCUIT VOLTAGE AT THE TERMINALS OF A LINE 1000 m LONG AND 1000 m FROM THE SOURCE WITH 1 V/m INCIDENT ON THE END NEAREST THE SOURCE ($Z_0 \approx 300 \Omega$, $z_1 \approx 1000 \text{ m}$, $z_2 \approx 2000 \text{ m}$, exponential pulse). Source: Ref. 7.

where $t_0 = (2h \sin \psi)/c$. At $t = t_0$, the reflection of the incident wave from the ground returns to the wire and the form of the voltage changes. At this time, however, the open-circuit voltage for small ψ and φ (where $D(\psi, \varphi)$ is large) can already be $2E_0h$, which, for typical EMP field strengths and line heights, is of the order of 1 MV. The time required to reach this voltage is t_0 for a zero-rise-time step function; for a finite-rise-time EMP, however, the minimum rise time is the rise time τ_r of the EMP. The maximum rate of rise of the open-circuit voltage is therefore

$$\boxed{\frac{\Delta v}{\Delta t} \approx \frac{2E_0h}{\tau_r} \quad (\tau_r > t_0)} \quad . \quad (2-28)$$

For $E_0 = 5 \times 10^4$ V/m, $h = 10$ m, and $\tau_r \approx 10$ ns, the maximum rate of rise is 100 kV/ns. This rate of rise occurs for either horizontal or vertical polarization for grazing, end-on incidence on a semi-infinite low-loss transmission line. (For vertical polarization, the maximum net voltage between the end of the horizontal conductor and the top of the vertical element between the ground and the horizontal conductor at $t = t_0$ is $2E_0h$; for horizontal polarization the total voltage of the horizontal conductor is $2E_0h$ and none is induced in the vertical element.)

For angles of incidence such that $\tau_r < (2h \sin \psi)/c$, the rate of rise of the open circuit voltage is

$$\boxed{\frac{\Delta v}{\Delta t} = E_0 c D(\psi, \varphi) \quad (\tau_r < t < t_0)} \quad . \quad (2-29)$$

where $D(\psi, \varphi)$ is given by Eq. (2-11). For $E_0 = 5 \times 10^4$ V/m, $\Delta v/\Delta t \approx 15 D(\psi, \varphi)$ kV/ns. Figure 2-21 shows, for various constant values of α/k , plots of $\Delta v/\Delta t$ with vertical polarization incident at an azimuth angle of $\varphi = 0$, where $D(\psi, \varphi)$ is maximum (dashed curves) and with horizontal polarization incident at $\varphi = \psi$, where $D(\psi, \varphi)$ is maximum (solid curves). As is apparent in Figure 2-21 the rate of rise of the open-circuit voltage is strongly dependent on angle of incidence, with the values approaching 100 kV/ns occurring only for small angles of incidence.

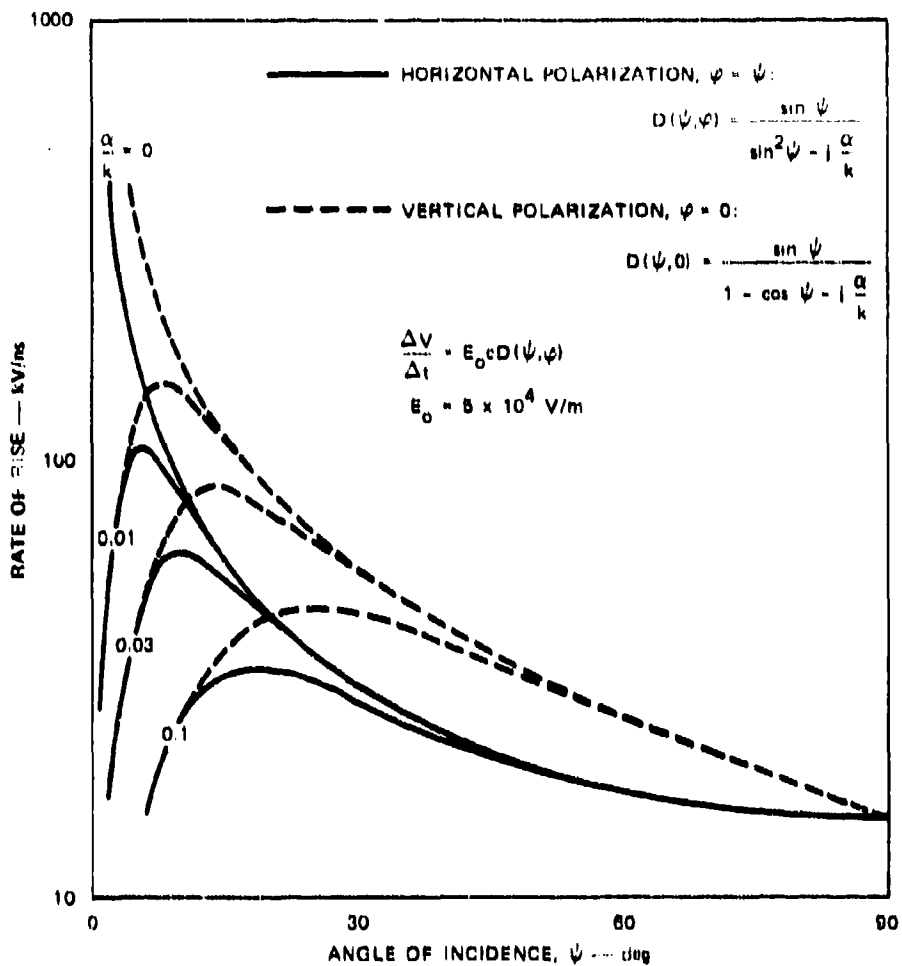


Figure 2-21 RATE OF RISE OF THE OPEN-CIRCUIT VOLTAGE AT THE TERMINALS OF A SEMI-INFINITE LINE

Although the initial rate of rise of the voltage is not dependent on the length of the line, the time that this rate of rise lasts and the final voltage obtained are dependent on line length. For a line of finite length ℓ , therefore, the rate of rise $E_0 c D(\psi, \varphi)$ lasts only for a time

$$t_1 = \ell (1 - \cos \psi \cos \varphi) / c \quad (2-30)$$

and the maximum voltage obtained with this rate of rise is

$$V_{DC} = E_0 \ell \times \begin{cases} \sin \psi \cos \varphi & (\text{vertical polarization}) \\ \sin \varphi & (\text{horizontal polarization}) \end{cases} \quad (2-31)$$

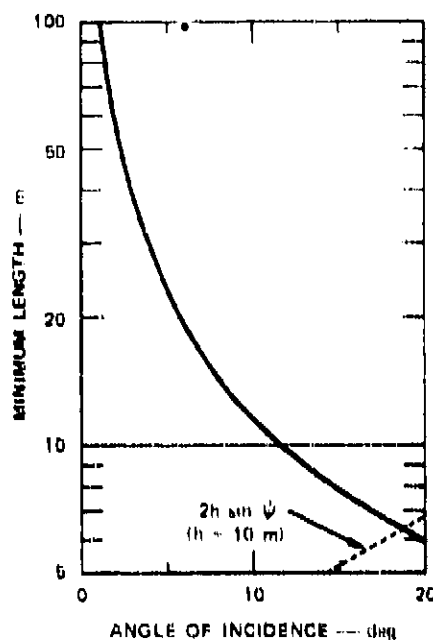


Figure 2-22 MINIMUM LENGTH OF LINE REQUIRED TO OBTAIN AN OPEN-CIRCUIT VOLTAGE OF 100 KV WITH 50-kVm FIELD INCIDENT AT SMALL ANGLE

example, the maximum rate of rise of the voltage across the 50 pF bushing capacitances of three delta-connected transformers supplied from a 300 ohm line is

$$\frac{\Delta v}{\Delta t} = \frac{2E_0 h}{Z_0 C} = \frac{2 \times 5 \times 10^4 \times 10}{300 \times 6 \times 50 \times 10^{-12}} = 11 \text{ kV/ns}$$

for $E_0 = 5 \times 10^4 \text{ V/m}$ and $h \sim 10 \text{ m}$. For the same conditions, the rate of rise of the voltage across three 20-ohm shielded cables would be

$$\frac{\Delta v}{\Delta t} = \frac{2E_0 h}{Z_r} + \frac{Z_{oc}/3}{Z_0 + Z_{oc}/3} = \frac{2 \times 5 \times 10^4 \times 10}{10^{-8}} + \frac{20/3}{300 + 20/3} = 2.2 \text{ kV/ns}$$

Thus the maximum rate of rise of the voltage actually applied to equipment terminals is of the order of 10 kV/ns.

if $t_1 < t_0$. If this open-circuit voltage is quite small, the rate of rise may not be important even though it is quite large. Note that the open-circuit voltage is smallest for the angles of incidence that produce the largest rate of rise. Figure 2-22 shows the minimum length of time required to develop 100 kV at the small angles of incidence before end-effects alter the rate of rise (assuming $t_1 < t_0$). In Figure 2-22, $\varphi = 0$ and ψ is varied for vertical polarization, and φ is varied for horizontal polarization (i.e., the angle of incidence is ψ for vertical polarization and φ for horizontal polarization).

It should be emphasized that the rates of rise given by Eqs. (2-28) through (2-31) are rates of rise of the open-circuit voltage at the end of a long line. The actual rate of rise across the terminals of distribution transformers or across the potheads is much smaller. For

2.3 RESPONSE OF A VERTICAL ELEMENT

2.3.1 CURRENT AT TOP OF VERTICAL ELEMENT

Vertical elements such as ground wires and service-entrance conduits also interact with the incident wave and therefore have current induced in them. Because only the vertically polarized wave has a component of electric field in the vertical direction, the vertical elements actively interact with only the vertically polarized wave; for horizontally polarized waves, the vertical elements behave as passive impedances with delay times associated with their length. The vertical element is considered to be a biconic transmission line with its upper end terminated in its characteristic impedance and its lower end short-circuited to the ground (see Figure 2-23). The current induced in the vertical element opposes the current induced in the horizontal conductor when $|\varphi| < \pi/2$ and aids it when $|\varphi| > \pi/2$. Since the coupling to the horizontal conductor is greatest for $|\varphi| < \pi/2$ — when $D(\psi, \varphi)$ is large — the current induced in the vertical element tends to reduce the maximum current calculated for the horizontal conductor alone.

For a vertically polarized wave incident at an elevation angle ψ on a vertical element of height h , the current at the top of a lossless vertical element will be^{7,8}

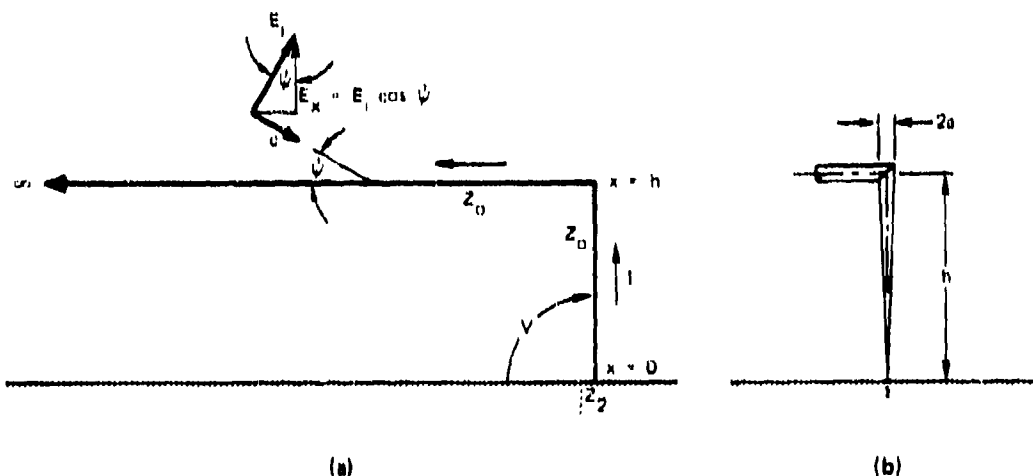


Figure 2-23 VERTICAL ELEMENT AT THE END OF A TRANSMISSION LINE

$$I(h, \omega) = \frac{E_0 c \cos \psi}{2Z_0} \left[\frac{1}{j\omega} \left[\frac{1 - e^{-j\omega \frac{2h}{c} (1 + \sin \psi)}}{1 + \sin \psi} \right] + \frac{e^{-j\omega \frac{2h}{c} \sin \psi}}{1 - \sin \psi} \left[\frac{-e^{-j\omega \frac{2h}{c}}}{j\omega + 1/r} \right] \right] \quad (2-32)$$

for an exponential pulse $E_0 e^{-t/\tau}$ and a semi-infinite horizontal line. In the expression above, the ground is assumed to be a perfect conductor, and Z_0 is the characteristic impedance of the biconic transmission line given by¹⁸

$$Z_0 \approx \frac{\eta_0}{2\pi} \log \frac{2h}{a} \quad (2-33)$$

where a is the radius of the riser and h is its height. Note that Z_0 for the vertical element is essentially the same as the characteristic impedance of the horizontal conductor of radius a and height h . The waveform of the current at the top of the vertical element is^{7,8}

$$I(h, t) = \frac{E_0 c r \cos \psi}{2Z_0} \left\{ \frac{1}{1 + \sin \psi} \left[(1 - e^{-t/\tau})_{t>0} - (1 - e^{-(t-t_1)/\tau})_{t>t_1} \right] + \frac{1}{1 - \sin \psi} \left[(1 - e^{-(t-t_2)/\tau})_{t>t_2} - (1 - e^{-(t-t_3)/\tau})_{t>t_3} \right] \right\} \quad (2-34)$$

where $t_1 = 2h/c (1 + \sin \psi)$, $t_2 = (2h/c)\sin \psi$, and $t_3 = 2h/c$.

For a vertically polarized wave at grazing incidence ($\psi = 0$),

$$I(h, t) = \frac{E_0 c r}{Z_0} \left[(1 - e^{-t/\tau})_{t>0} - (1 - e^{-(t-t_3)/\tau})_{t>t_3} \right]. \quad (2-35)$$

The source impedance of the vertical element viewed from the top and terminated in soil at the base is

$$Z(h) \approx Z_0 \frac{1 + \rho_0 e^{-j\omega \frac{2h}{c}}}{1 - \rho_0 e^{-j\omega \frac{2h}{c}}} \quad (2-36)$$

where ρ_0 is the reflection coefficient at the base and losses in the vertical element are negligible. For many power-system applications it can be assumed that the soil is a perfect conductor, for which $\rho_0 = -1$. (For the impedance of ground rods, see Section 2.3.5.) The open-circuit voltage developed at the top of the vertical element is

$$V_{oc}(h) = I(h) [Z(h) + Z_0] \quad (2-37)$$

and the short-circuit current is

$$I_{sc}(h) = \frac{Z(h) + Z_0}{Z(h)} I(h) . \quad (2-38)$$

A plot of the short-circuit current at the top of a 10-m-high element that is terminated in the base by extending the conductor 2 m into the soil is shown in Figure 2-24. The base resistance was calculated from Eq. (2-50) with $\ell = 2$ m, $a = 10^{-2}$ mho/m, and $a = 2$ mm (81 mils). The short-circuit current shown in Figure 2-23 is for a uniform incident field of 1 V/m at all frequencies, rather than for the exponential pulse spectrum.

Plots of the current waveform are shown in Figure 2-25 for $\psi = 0$ and $\psi = 30^\circ$ for an incident exponential pulse with a decay time constant $\tau = 1 \mu s$ and a riser height $h = 10$ m. The waveforms for these two angles of incidence are quite similar, but the leading edge of the waveform for $\psi = 30^\circ$ is more complex because of the difference in the time of arrival of the upward and downward traveling current waves induced by the direct and ground-reflected electric-field waves.

It is noted that the current given here is that induced in the vertical element only; this current must be added to any current induced in the horizontal line with proper regard

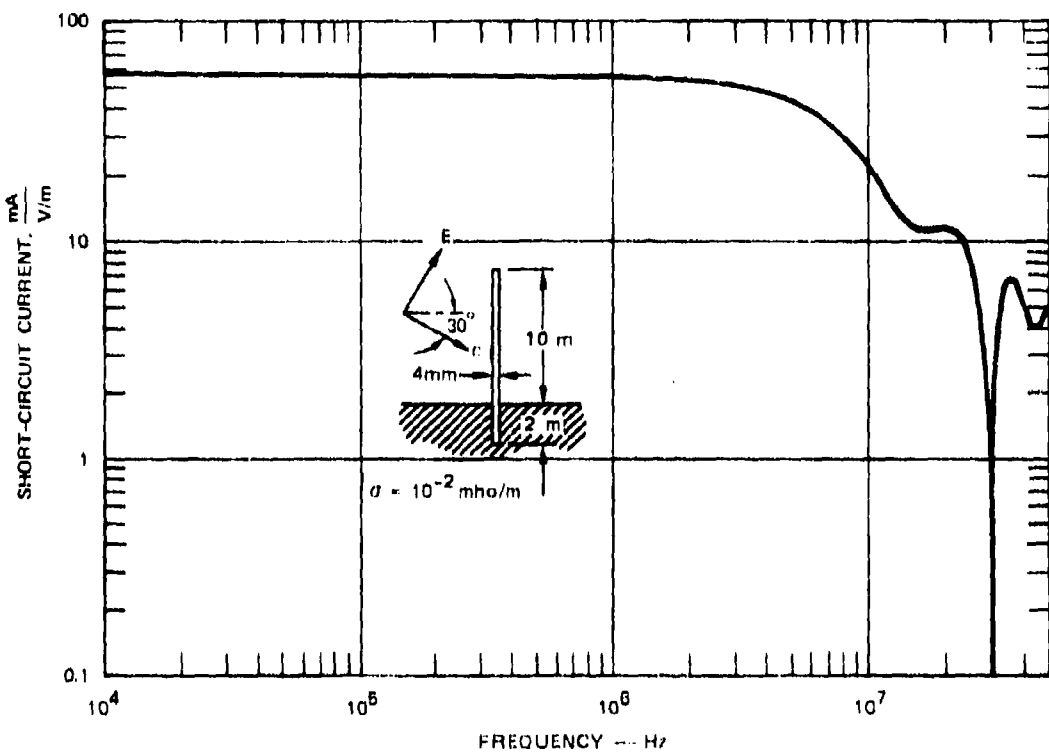


Figure 2-24 SHORT-CIRCUIT CURRENT AT TOP OF LOSSLESS VERTICAL ELEMENT TERMINATED IN SOIL AT THE BASE

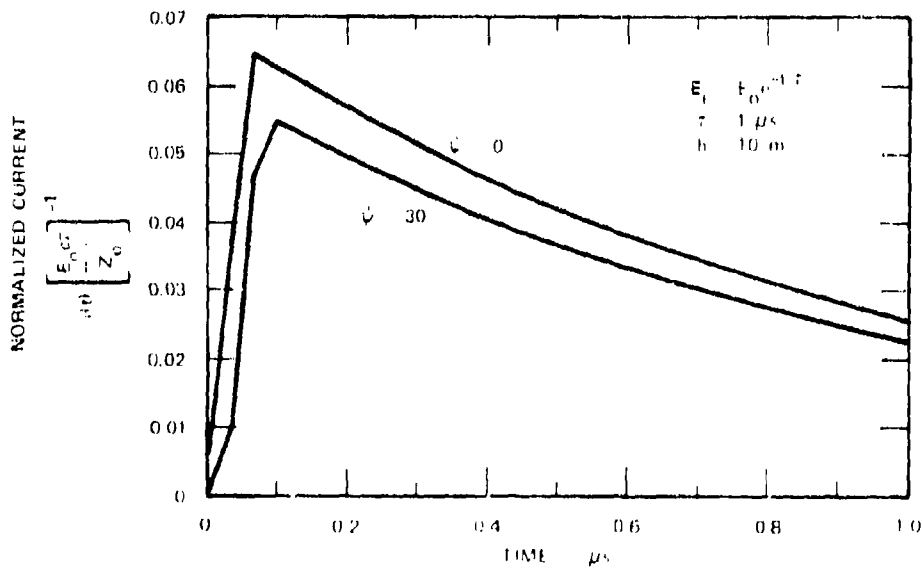


Figure 2-25 CURRENT DELIVERED TO A MATCHED LOAD AT THE TOP OF A VERTICAL RISER BY A VERTICALLY POLARIZED INCIDENT WAVE. Source: Ref. 7.

for sign. The direction of positive current in the vertical element is toward the top, while the direction of positive current assumed for the horizontal conductor in Section 2.2 is toward the terminals. Also note that the total source impedance at the top of the vertical element is the sum of the impedance of the vertical element and that of the horizontal line. Thus, for a semi-infinite horizontal line, the total source impedance is $Z_0 + Z(h)$ between terminals at the top of the vertical elements.

2.3.2 CURRENT AT BASE OF VERTICAL ELEMENT

The short-circuit current induced at the base of a vertical element by a vertically polarized wave incident at an elevation angle ψ is^{7,8}

$$I_{sc}(0, \omega) = \frac{E_0 c \cos \psi}{j\omega Z_0} e^{-j\omega t_0/2} \left[\frac{1 - e^{-j\omega(\frac{h}{c} - \frac{t_0}{2})}}{1 - \sin \psi} + \frac{1 - e^{-j\omega(\frac{h}{c} + \frac{t_0}{2})}}{1 + \sin \psi} \right] \times \left[\frac{1}{j\omega + 1/r} \right] \quad (2-39)$$

for an exponential pulse $E_0 e^{-t/\tau}$. In this expression, it is assumed that the ground behaves as a perfect conductor, the vertical element is terminated in its characteristic impedance at the top (a matched or semi-infinite horizontal line), and the attenuation of the vertical element is negligible. The meanings of the symbols are the same as in Eq. (2-32), and $t_0 = (2h \sin \psi)/c$.

The waveform of the short-circuit current at the base of the vertical element is

$$I_{sc}(0, t) = \frac{E_0 c \tau \cos \psi}{Z_0} \left\{ \left[\frac{1 - e^{-t'/\tau}}{1 - \sin \psi} + \frac{1 - e^{-t'/\tau}}{1 + \sin \psi} \right] t' > 0 \right. \\ \left. - \left[\frac{1 - e^{-(t' - t_1)/\tau}}{1 - \sin \psi} \right] t' > t_1 - \left[\frac{1 - e^{-(t' - t_2)/\tau}}{1 + \sin \psi} \right] t' > t_2 \right\} \quad (2-40)$$

where $t' = t - t_0/2 = t - (h \sin \psi)/c$, $t_1 = \frac{h}{c} - \frac{t_0}{2}$, and $t_2 = \frac{h}{c} + \frac{t_0}{2}$. Time and phase are referred to the top of the element, so that the time t and the phase in the frequency domain used here are consistent with those used for the horizontal lines in Section 2.2 and the vertical element in Section 2.3.1. Plots of the short-circuit current are shown in Figure 2-26 for an elevation angle of incidence $\psi = 30^\circ$ and $\psi = 0^\circ$ (grazing incidence).

The source impedance observed from the base of the element is the characteristic impedance Z_0 , and the open-circuit voltage at the base is $I_{sc}(0) Z_0$. It is noted that $I_{sc}(0)$ is the short-circuit current generated in the vertical element only; the component of current or voltage induced in the horizontal conductor as given in Section 2.2 must be added to these components from the vertical element to obtain the total current or voltage. It is also noted that the current in the vertical element is positive when it flows toward the top of the element (see Figure 2-23).

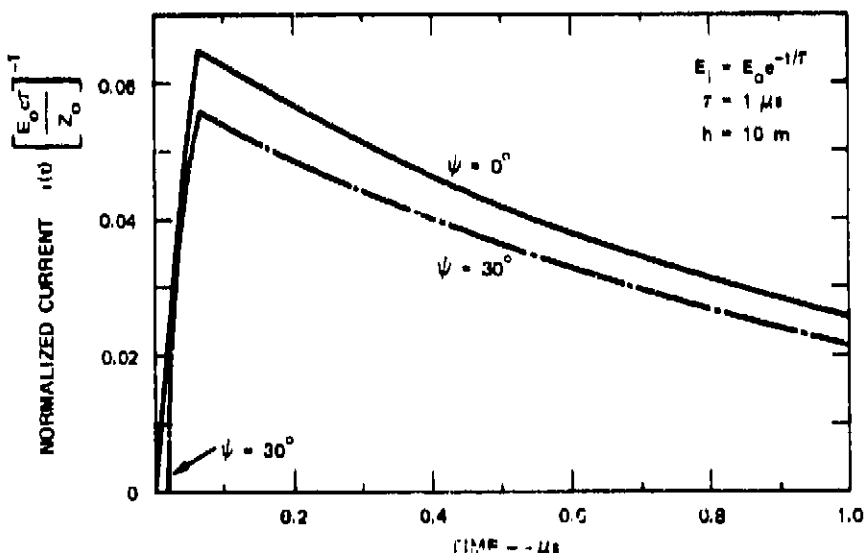


Figure 2-26 SHORT-CIRCUIT CURRENT INDUCED AT THE BASE OF A VERTICAL RISER BY A VERTICALLY POLARIZED INCIDENT WAVE

2.3.3 COMPARISON OF VOLTAGE IN VERTICAL AND HORIZONTAL ELEMENTS

To illustrate the relative magnitudes of the voltages induced in the horizontal line and the vertical element, the maximum open-circuit voltage induced in the semi-infinite horizontal line by a unit step incident field is

$$v_{oc}(t') = 4h \left(t' > \frac{h}{c} \right) \quad (\psi \rightarrow 0) \quad (2-41)$$

for a perfectly conducting ground and a vertically polarized wave incident at $\psi = \phi = 0^\circ$. The maximum open-circuit voltage induced at the base of the vertical element under these conditions is

$$\begin{aligned} v_{oc}(t) &= -2h \left(\frac{ct}{h} \right) \quad \left(0 \leq t \leq \frac{h}{c} \right) \\ &= -2h \quad \left(t > \frac{h}{c} \right) \end{aligned} \quad (2-42)$$

and it is of the opposite polarity.

The total voltage at the base of the vertical element is, therefore,

$$\begin{aligned} v_{oc}(t) &= -2h \left(\frac{ct}{h} \right) \quad \left(0 \leq t \leq \frac{h}{c} \right) \\ &= 2h \quad \left(t > \frac{h}{c} \right). \end{aligned} \quad (2-43)$$

The individual components and the total voltage waveforms are shown in Figure 2-27. The voltage induced in the vertical element causes a negative response for a time h/c and reduces the final value of the step-function response of the horizontal line by a factor of 2.0 when the soil is a perfect conductor. If the soil is a poor conductor, however, the peak voltage is much greater than $4h$ (see Figure 2-14) but the peak voltage induced in the vertical element is changed only slightly. Therefore for very long horizontal conductors over average or poorly conducting soil, the effect of the voltage induced in the vertical element is relatively less important.

2.3.4 GENERAL ANALYSIS OF VERTICAL ELEMENTS

The cases given in Sections 2.3.1 and 2.3.2 are generally of widest use in analyzing power systems. For certain special applications, however, more general formulas may be required. The general solutions for the current and voltage at any distance x from the base, from which Eqs. (2-32) and (2-39) were obtained, are

$$I(x) = [K_1 + P(x)] e^{-\gamma x} + [K_2 + Q(x)] e^{\gamma x} \quad (2-44a)$$

$$V(x) = Z_0 \{ [K_1 + P(x)] e^{-\gamma x} - [K_2 + Q(x)] e^{\gamma x} \} \quad (2-44b)$$

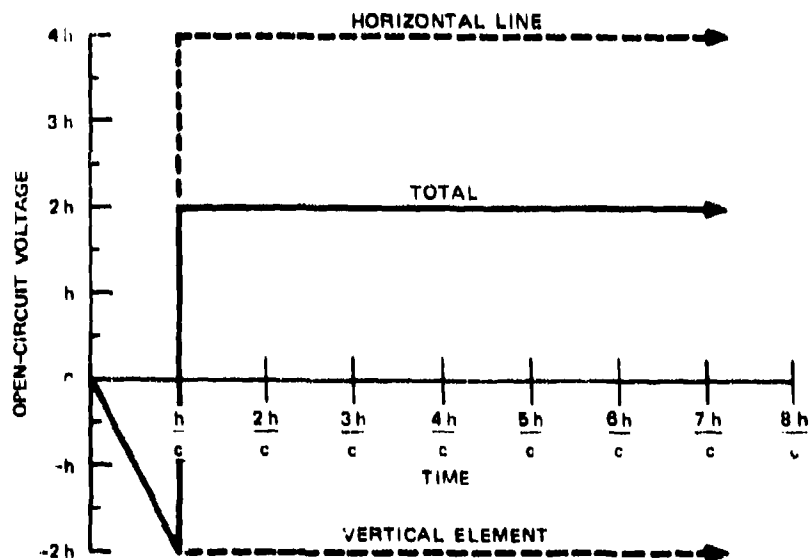
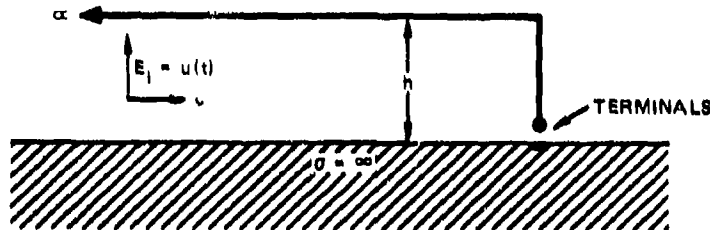


Figure 2-27 OPEN-CIRCUIT VOLTAGE INDUCED AT THE BASE OF VERTICAL ELEMENT BY A UNIT STEP INCIDENT WAVE

where

$$\gamma = \sqrt{ZY} \quad Z_0 = \sqrt{\frac{Z}{Y}} \quad (2-45a)$$

$$P(x) = \frac{1}{2Z_0} \int_0^x E_x(v) e^{\gamma v} dv$$

$$Q(x) = \frac{1}{2Z_0} \int_x^h E_x(v) e^{-\gamma v} dv \quad (2-45b)$$

$$K_1 = \rho_h \frac{\rho_h P(h) e^{-\gamma h} - Q(0) e^{\gamma h}}{e^{\gamma h} - \rho_o \rho_h e^{-\gamma h}} \quad (2-46a)$$

$$K_2 = \rho_h e^{-\gamma h} \frac{\rho_o Q(0) - P(h)}{e^{\gamma h} - \rho_o \rho_h e^{-\gamma h}} \quad (2-46b)$$

$$\rho_o = \frac{Z(0) - Z_0}{Z(0) + Z_0} \quad (2-47a)$$

$$\rho_h = \frac{Z(h) - Z_0}{Z(h) + Z_0} \quad (2-47b)$$

and where Z is the series impedance per unit length of the biconic transmission line, γ is its shunt admittance per unit length, $Z(0)$ is the terminating impedance at the base ($x = 0$), and $Z(h)$ is the terminating impedance at the top ($x = h$). Sufficient accuracy for many engineering applications is obtained by letting

$$Z_0 = \frac{\eta}{2\pi} \log \frac{2h}{a} = 60 \log \frac{2h}{a} \quad (2-48a)$$

$$\gamma = j\omega \sqrt{\mu_0 \epsilon_0} = j\frac{\omega}{c} \quad (2-48b)$$

where c is the speed of light (3×10^8 m/s) a is the radius of the vertical element, and h is its height. The current $I(x)$ is positive when it flows in the positive x -direction, and the voltage $V(x)$ is positive when the vertical element is positive with respect to the ground plane.

The formulas above can be used to calculate the current or voltage at any point $0 < x < h$ for arbitrary terminal impedances $Z(0)$ (see Section 2.3.5) at the base and $Z(h)$ at the top, and for arbitrary field $E_x(x)$ incident on the vertical element. For a uniform vertically polarized plane wave incident at an elevation angle ψ , the electric field is^{4,7,8}

$$E_x(x) = E_i \cos \psi (1 + R_v e^{-j2kx \sin \psi}) e^{-jk(h-x) \sin \psi} \quad (2-48)$$

where E_i is the magnitude of the incident electric field, $k = \omega \sqrt{\mu_0 \epsilon_0}$, and R_v is the reflection factor at the air/earth interface given by Eq. (2-8b).

2.3.5 IMPEDANCE OF A GROUND ROD

The surge impedance of a single, short ground rod of radius a driven into the ground a depth ℓ as illustrated in Figure 2-28 is⁴

$$Z(0) \approx \frac{1}{2\pi a \ell} \left[\log \frac{\sqrt{2\delta}}{\gamma_0 a} - j \frac{\pi}{4} \right] \quad \begin{matrix} (\sigma > \omega \epsilon) \\ (\ell \ll \delta) \\ (\ell \gg a) \end{matrix} \quad (2-50)$$

where σ is the soil conductivity, $\gamma_0 = 1.781 \dots$, and δ is the skin depth in the soil given by

$$\delta = \frac{1}{\sqrt{\pi f \mu_0 \sigma}} \quad (\mu_0 = 4\pi \times 10^{-7}) . \quad (2-51)$$

The log term in the expression for impedance is usually of the order of 10, as is illustrated in Figure 2-29, so that the surge impedance is predominantly resistive and relatively independent of frequency. This impedance formula is based on the transmission-line model of the buried conductor. This impedance may be used for $Z(0)$ in Section 2.3.4 for the terminating impedance at the base of a vertical element.

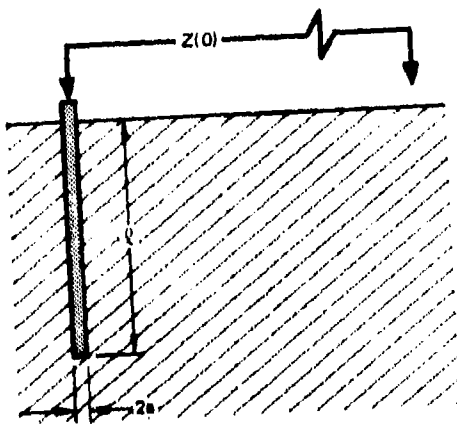


Figure 2-28 ILLUSTRATION OF A
VERTICAL GROUND ROD OF
CIRCULAR CROSS SECTION

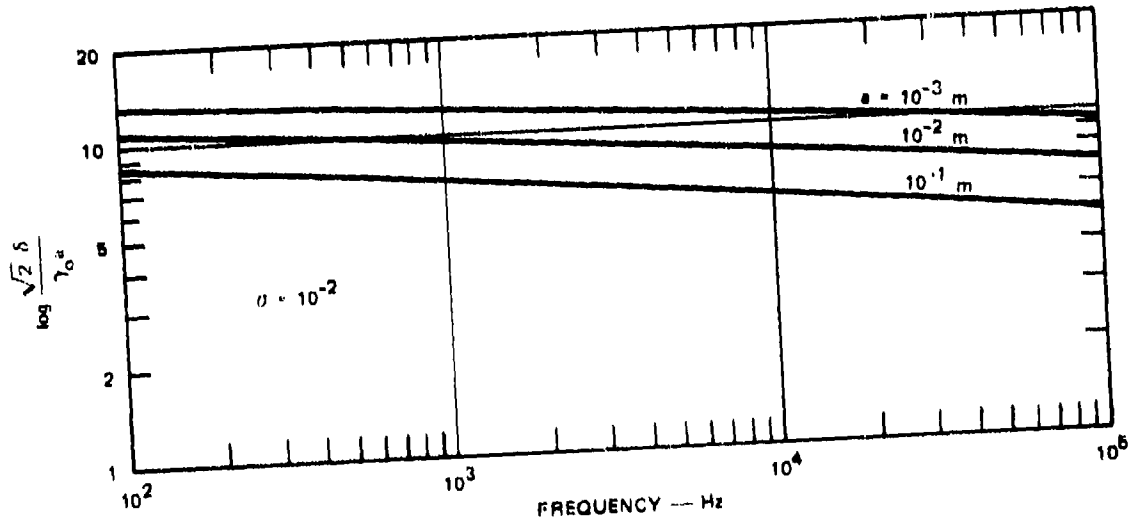


Figure 2-29 VARIATION OF LOG ($\sqrt{2\delta}/\gamma_0 a$) WITH FREQUENCY AND CONDUCTOR RADIUS.
(Note that a factor of 10 in conductor radius produces the same effect as a factor of 100 in soil conductivity.)

The dc resistance of a ground rod is²³

$$R = \frac{1}{2\pi\sigma l} \left[\log \frac{4l}{a} - 1 \right] \quad (l \gg a) \quad (2-52)$$

Plots of the dc resistance of a ground rod as a function of length are given in Figure 2-30.

2.3.6 RESPONSE OF HORIZONTAL CONDUCTOR WITH VERTICAL RISERS

The effect of the vertical elements (risers) on the finite-length horizontal conductor (see Figure 2-31) is to add additional length to the line at each end for either polarization, and to also add additional current to the system for vertical polarization. The frequency-domain solution is obtained by considering the risers as passive loads on the horizontal

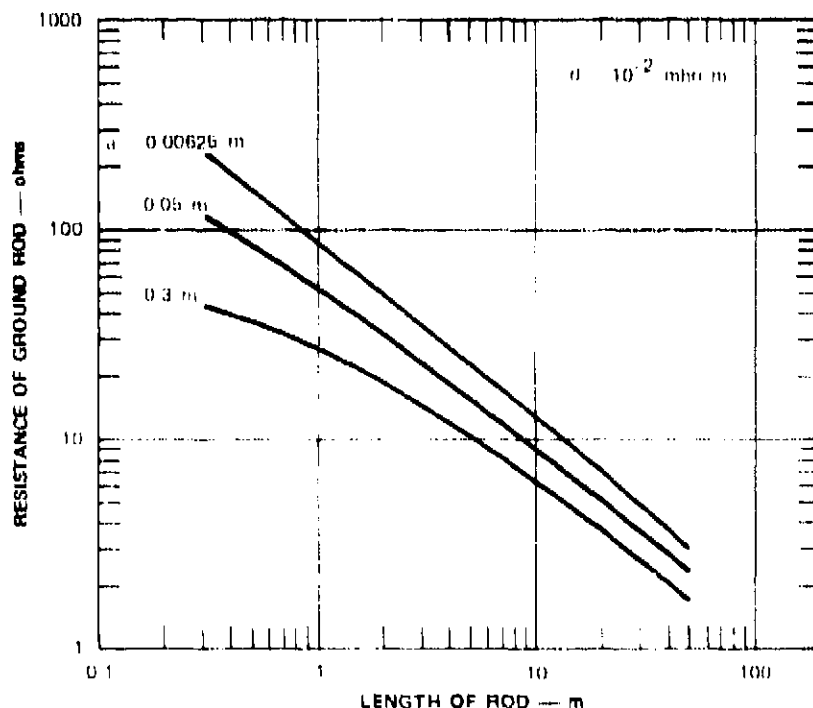


Figure 2-30 VARIATION OF dc RESISTANCE OF VERTICAL GROUND ROD WITH LENGTH Source: Ref. 23.

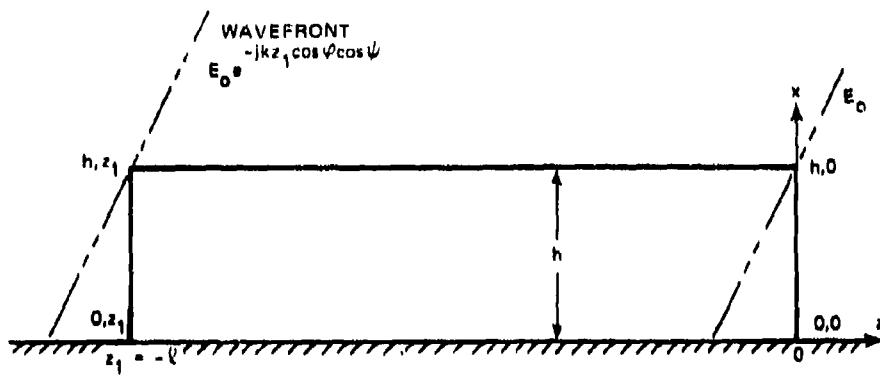


Figure 2-31 TRANSMISSION LINE TERMINATED WITH VERTICAL RISERS AT BOTH ENDS

conductor, with impedances Z_1 and Z_2 . For perfectly conducting ground, these impedances are:

$$Z_1 = Z_0 \left[\frac{1 + \rho'_1 e^{-2\gamma h}}{1 - \rho'_1 e^{-2\gamma h}} \right] \quad (2-53a)$$

and

$$Z_2 = Z_0 \left[\frac{1 + \rho'_2 e^{-2\gamma h}}{1 - \rho'_2 e^{-2\gamma h}} \right] \quad (2-53b)$$

where ρ'_1 and ρ'_2 are the reflection coefficients at the base of the risers. The reflection coefficients ρ_1 and ρ_2 in Eqs. (2-5) are then given by

$$\rho_1 = \rho'_1 e^{-2\gamma h} \quad (2-54a)$$

$$\rho_2 = \rho'_2 e^{-2\gamma h} . \quad (2-54b)$$

Thus, in Eqs. (2-5), the term $\mu_1\mu_2 e^{-2\gamma l}$ becomes $\mu'_1\mu'_2 e^{-2\gamma(l+2h)}$. When these quantities are substituted into Eq. (2-3a), the expression for the horizontal conductor with passive risers becomes:⁸

$$I(h,0) = \frac{E_i \sin \varphi (1 + R_h e^{-j2kh \sin \psi})}{2Z_0} (1 - \mu'_2 e^{-2\gamma h}) \\ \times \left[\frac{1 - e^{-(\gamma - jk \cos \psi \cos \varphi)l}}{\gamma - jk \cos \psi \cos \varphi} + \mu'_1 e^{-2\gamma(l+h)} \frac{1 - e^{(\gamma + jk \cos \psi \cos \varphi)l}}{\gamma + jk \cos \psi \cos \varphi} \right] \quad (2-55) \\ \times \left[1 + \mu'_1 \mu'_2 e^{-2\gamma(l+2h)} + (\mu'_1 \mu'_2)^2 e^{-4\gamma(l+2h)} + \dots \right].$$

Note that the effect of these substitutions has been to inject the $2\gamma h$ phase shifts at the proper point to account for the round-trip propagation times of the vertical risers.

For a vertically polarized incident wave the current induced in the risers by the vertical component of the electric field must be superimposed on that induced in the horizontal conductor by the horizontal component of the field. For an incident signal, the current at the top of the riser at $z = 0$ can be shown to be:

$$I_2(h,0) = \frac{E_i \cos \psi e^{-jkhs \sin \psi}}{2Z_0} \frac{1 - \mu'_1 e^{-2\gamma(h+l)}}{\gamma h [1 - \mu'_1 \mu'_2 e^{-2\gamma(2h+l)}]} \\ \times \left\{ \frac{e^{(\gamma + jk \sin \psi)h} - 1}{\gamma + jk \sin \psi} + R_v \frac{e^{(\gamma - jk \sin \psi)h} - 1}{\gamma - jk \sin \psi} \right. \quad (2-56) \\ \left. + \mu'_2 \left[\frac{e^{-(\gamma - jk \sin \psi)h} - 1}{\gamma - jk \sin \psi} + R_v \frac{e^{-(\gamma + jk \sin \psi)h} - 1}{\gamma + jk \sin \psi} \right] \right\}.$$

The form of the current $I_1(h,-l)$ at the top of the riser at $z = -l$ is the same as in Eq. (2-56), (with μ'_1 and μ'_2 interchanged), but it contains a phase factor $e^{jk k \cos \psi \cos \psi}$ to account for the phase difference between the wave at $(h,-l)$ and the wave at $(h,0)$. This current must be transferred to the other end of the horizontal conductor before it is

combined with $i_2(h,0)$ and $I(h,0)$, given by Eqs. (2-55) and (2-56), respectively. The current at $(h,0)$, induced in the riser at $z = -\ell$, will be

$$I_1(h,0) = \frac{E_0 \cos \psi e^{-jkhsin\psi}}{2Z_0} \frac{(1 - \rho'_2 e^{-2\gamma h})}{e^{\gamma(h+\ell)} [1 - \rho'_1 \rho'_2 e^{-2\gamma(2h+\ell)}]} \\ \times \left\{ \frac{e^{(\gamma+jksin\psi)h} - 1}{\gamma + jk \sin \psi} + R_v \frac{e^{(\gamma-jksin\psi)h} - 1}{\gamma - jk \sin \psi} \right. \\ \left. + \rho'_1 \left[\frac{e^{-(\gamma-jksin\psi)h} - 1}{\gamma - jk \sin \psi} + R_v \frac{e^{-(\gamma+jksin\psi)h} - 1}{\gamma + jk \sin \psi} \right] \right\} \quad (2-57)$$

The total current at $(h,0)$ from the horizontal conductor and the two risers is then

$$I_t(h,0) = I(h,0) + I_1(h,0) - i_2(h,0) \quad (2-58)$$

In which $i_2(h,0)$ carries a negative sign because of the convention for the direction of positive current in the risers. The current at $(h,0)$ produced by each element, and the total current caused by all three elements, are plotted in Figure 2-32 for an incident step function $E_0 u(t)$ that is vertically polarized. The earlier conditions that $\gamma \approx jk$, $\rho'_1 = \rho'_2 = -1$, $\varphi = \psi = 30^\circ$, $R_v = 1$, and $\ell = 2h$ are assumed, and only the first cycle of the response is plotted. From Figure 2-32 it is apparent that the current induced in the risers is considerably greater than that induced in the horizontal conductor, and even though the currents oppose each other, the net current is considerably larger than that induced in the horizontal conductor by the vertically polarized wave. Notice that the vertical scale in Figure 2-32(a) is twice as large as the scale used in Figures 2-32(b), (c), and (d).

2.3.7 PERIODICALLY GROUNDED LINE

Consider a periodically grounded line as shown in Figure 2-33(a) with a height h and a spacing between vertical ground leads of ℓ . The line extends to infinity at the left, and we will assume that γ and Z_0 are the same for the vertical leads and the horizontal conductors.

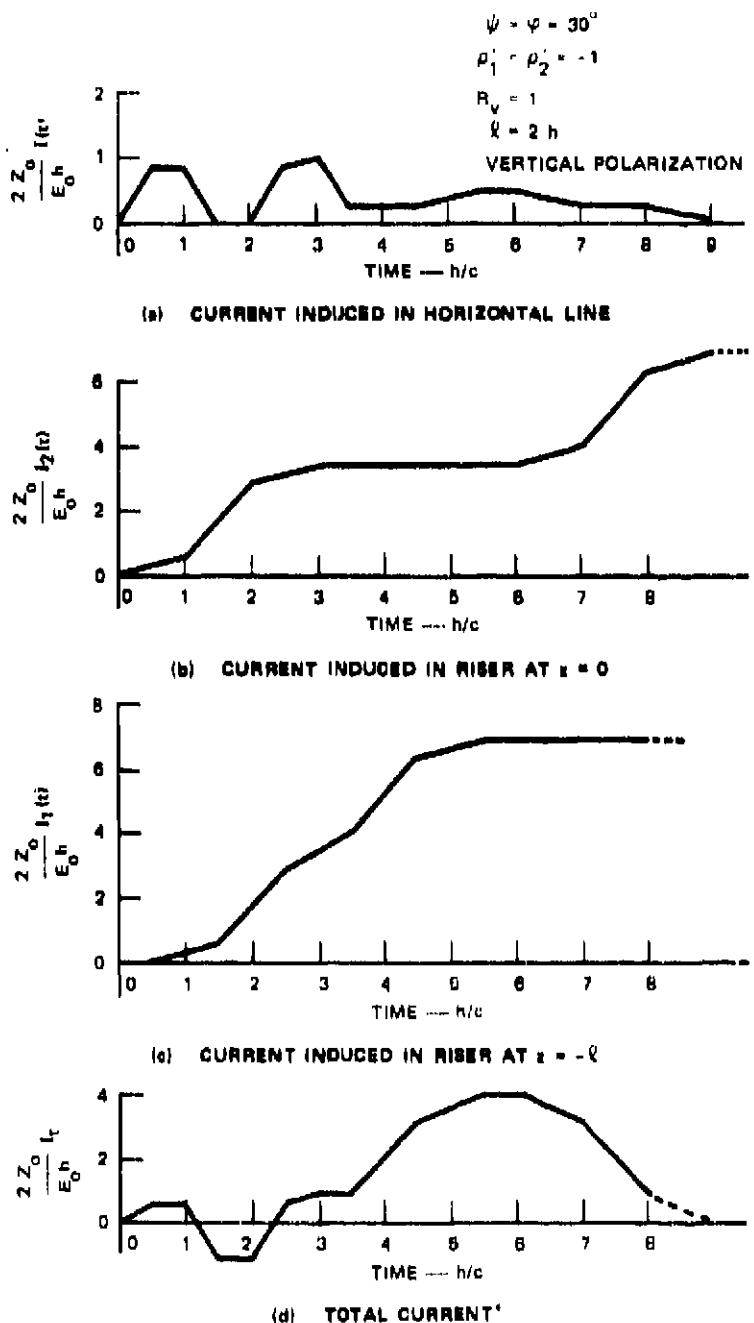


Figure 2-32 CURRENT COMPONENTS INDUCED ON HORIZONTAL LINE AND VERTICAL RISERS, AND TOTAL CURRENT AT $x = h$, $z = k$. Source: Ref. B.

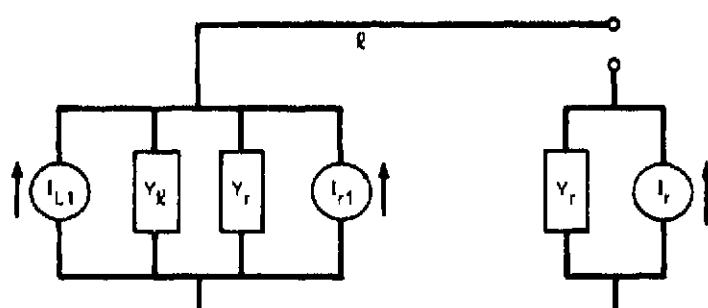
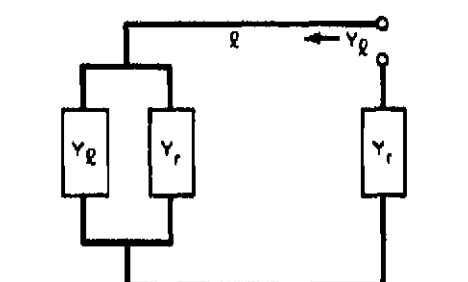
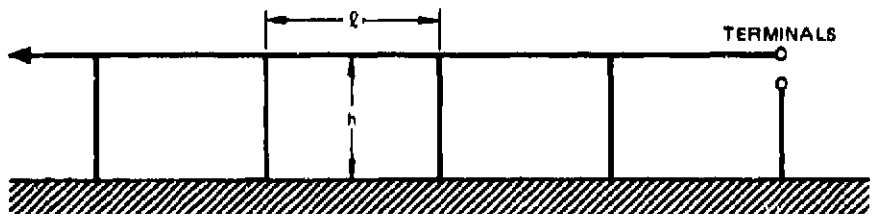


Figure 2-33 STEPS IN THE ANALYSIS OF A PERIODICALLY GROUNDED TRANSMISSION LINE

We wish to determine the Norton equivalent current source represented by the semi-infinite periodically grounded line to the left of the terminals.

In Figure 2-33(b) the right-hand loop formed by the last two ground leads and the horizontal conductor between them is redrawn, and in Figure 2-33(c) the pertinent admittance and transmission-line lengths required to obtain the source admittance are shown. The source admittance looking into the terminals in Figure 2-33(c) is Y_s in series with Y_L , where Y_r is the input admittance at the ground lead and Y_L is the input admittance of the transmission line of length l terminated in $Y_r + Y_L$. If $Y_0 = 1/Z_0$ is the characteristic admittance of the vertical and horizontal conductors (with ground as the second conductor in each case), the impedance Y_r of the ground lead is

$$Y_r = \frac{Y_r}{Y_0} = \frac{1 - \rho_g e^{-2\gamma h}}{1 + \rho_g e^{-2\gamma h}} \quad (2-59)$$

where ρ_g is the reflection coefficient at the base of the ground lead given by

$$\rho_g = \frac{Z_g - Z_0}{Z_g + Z_0} \quad (2-60)$$

where Z_g is the impedance of the ground connection at the base of the ground lead.

The admittance Y_L at the terminals is given by

$$Y_L = \frac{Y_L}{Y_0} = \frac{1 - \rho e^{-2\gamma l}}{1 + \rho e^{-2\gamma l}} \quad (2-61)$$

where ρ is the reflection coefficient at the left end of the circuit of Figure 2-33(c). It is given by

$$\rho = \frac{Y_0 - (Y_L + Y_r)}{Y_0 + (Y_L + Y_r)} = \frac{1 - (Y_L + Y_r)}{1 + (Y_L + Y_r)} . \quad (2-62)$$

Substituting this value into the expression for Y_L gives

$$Y_L = \frac{1 - e^{-2\gamma l} + (1 + e^{-2\gamma l}) (Y_L + Y_R)}{1 + e^{-2\gamma l} + (1 - e^{-2\gamma l}) (Y_L + Y_R)} \quad (2-63)$$

which can be solved for Y_L to give

$$Y_L = \frac{Y_R}{2} \left[-1 \mp \sqrt{1 + 4 \left(\frac{1}{Y_R^2} + \frac{1 + e^{-2\gamma l}}{Y_R (1 - e^{-2\gamma l})} \right)} \right] \quad (2-64)$$

The positive sign is evidently the correct choice if realizable admittances are to be obtained. The total source admittance at the terminals is then

$$Y_n = \frac{Y_L Y_R}{Y_L + Y_R} = \frac{Y}{Y_0} \quad (2-65)$$

Consider now the circuit of Figure 2-33(d) which shows the equivalent sources of the last two ground wires I_r and I_{r1} and of the transmission line to the left of the second ground wire $|L_1$. Suppose we replace the ground wire on the right by a perfect short circuit. Then the short-circuit current at the terminals will consist of the current delivered by the sources $|L_1$ and I_{r1} through the length l of line plus the short-circuit current I_l induced by the incident wave in the length l of horizontal line. The current delivered to the left end of the circuit by the sources $|L_1$ and I_{r1} is

$$I(-l) = (|L_1 + I_{r1}) \frac{Y_i}{Y_l + Y_r + Y_i} \quad (2-66)$$

where Y_i is the input admittance of the transmission line of length l that is short-circuited at its terminals. That is,

$$Y_i = Y_0 \frac{1 + e^{-2\gamma l}}{1 - e^{-2\gamma l}} \quad (2-67)$$

The short-circuit current I_L at the terminals is

$$I_L = I(-\ell) \frac{2e^{-\gamma\ell}}{1 + e^{-2\gamma\ell}} + I_\ell \quad (2-68)$$

which is obtained by transforming the current $I(-\ell)$ to the right end of the line and adding to it the current I_ℓ induced in the line by the incident wave. Now because the line is semi-infinite in length, the current I_L differs from the current I_{L1} only by the phase of the incident wave arriving at the terminals relative to its phase at the next-to-the-last ground wire. Similarly, I_r and I_{r1} differ only by this phase. Thus,

$$\begin{aligned} I_{r1} &= I_r e^{\gamma\ell'} = I_r e^{\gamma\ell} \cos \psi \cos \varphi \\ I_{L1} &= I_L e^{\gamma\ell'} \end{aligned} \quad (2-69)$$

and

$$I(-\ell) = (I_L + I_r) e^{\gamma\ell'} \frac{Y_1}{Y_L + Y_r + Y_1} \quad (2-70)$$

Substituting this value into the above expression for I_L gives

$$I_L = (I_L + I_r) \frac{Y_1}{Y_L + Y_r + Y_1} \frac{2e^{-\gamma(\ell - \ell')}}{1 + e^{-2\gamma\ell}} + I_\ell \quad (2-71)$$

which can be solved for I_L to obtain

$$I_L = \frac{I_\ell + I_r \frac{Y_1}{Y_L + Y_r + Y_1} \frac{2e^{-\gamma(\ell - \ell')}}{1 + e^{-2\gamma\ell}}}{1 - \frac{Y_1}{Y_L + Y_r + Y_1} \frac{2e^{-\gamma(\ell - \ell')}}{1 + e^{-2\gamma\ell}}} \quad (2-72)$$

If we now recall that the right-hand ground lead has finite admittance Y_r and a source I_r , we can combine these with I_L and its source admittance Y_L to obtain the short-circuit I_{sc} at the terminals:

$$I_{sc} = \frac{I_L Y_r - I_r Y_L}{Y_L + Y_r} . \quad (2-73)$$

The Norton equivalent source that replaces the periodically grounded line to the left of the terminals is then the current I_{sc} of Eq. (2-73) with a shunt admittance Y given by Eq. (2-65). The current sources I_L and I_r are obtained from the analysis of horizontal and vertical conductors of finite length. The current I_L is the short-circuit current induced in a horizontal line of length ℓ terminated in a short circuit at the right end ($z = 0$) and terminated in the impedance $1/(Y_L + Y_r)$ at its left end ($z = -\ell$). I_L can be obtained from Eq. (2-18) by multiplying $V_{oc}(\omega)$ by Y_L . The current I_r is the short-circuit current at the top of a vertical conductor of height h that is terminated in an impedance Z_g at its base ($x = 0$). The current I_r is given by Eqs. (2-38) and (2-32) when $Z(h) = 1/Y_r$. The impedance Z_g may be calculated from Eq. (2-50).

The magnitude of the open-circuit voltage induced in one horizontal segment is shown in Figure 2-34 for 1 V/m incident at 30° elevation and 0° azimuth angles. Note that at low frequencies, the open-circuit voltage is roughly $2E_0 h$, if E_0 is the magnitude of the incident field. Peaks and valleys associated with the resonant lengths and with the line height are also evident.

The short-circuit current and source admittance at the end of the semi-infinite, periodically grounded line are shown in Figure 2-35. Again the periodicities of the segment length and line height are evident, but these are commingled in such a way that it is more difficult to relate cause and effect. It is apparent, however, that the source admittance is between a few tenths of a mho and a few mhōs. Therefore, the periodically grounded line does have a low source impedance compared to the ungrounded line. In addition, a comparison of the magnitude of the short-circuit current with that of an ungrounded line (e.g., the open-circuit voltage of Figure 2-12 divided by a characteristic impedance of a few hundred ohms) indicates that the mean currents are of similar magnitudes to within a factor of 2 or 3. The peak short-circuit currents of the periodically grounded line are

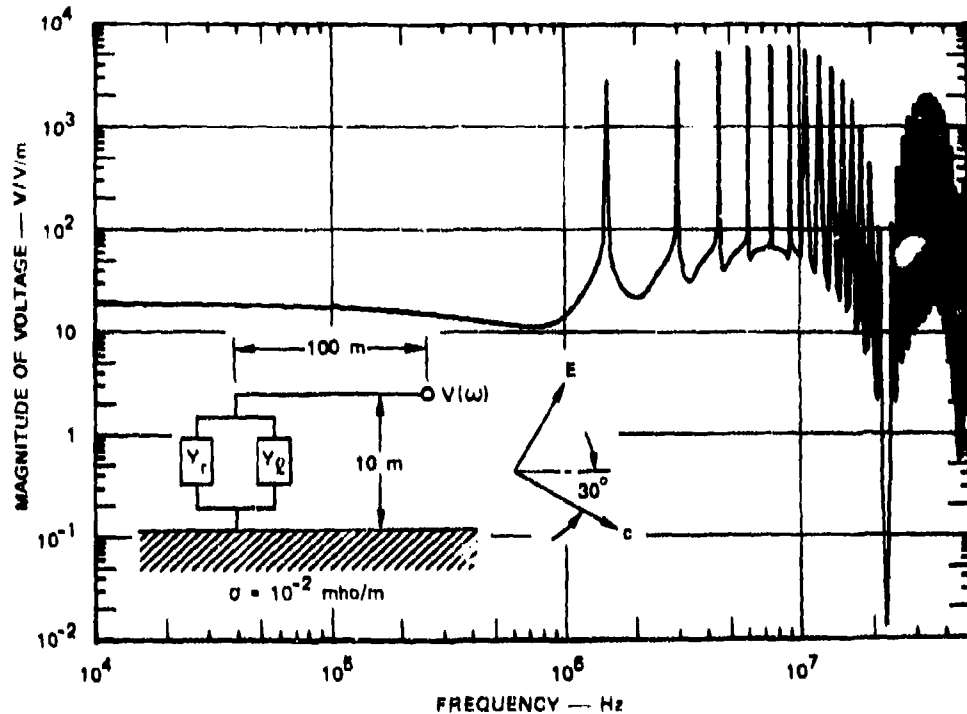


Figure 2-34 OPEN-CIRCUIT VOLTAGE AT TERMINALS OF FINITE HORIZONTAL TRANSMISSION LINE

considerably larger than the mean, however, so that selected frequencies in the pulse spectrum will be more strongly coupled to the periodically grounded line.

2.4 TRANSMISSION PROPERTIES OF POWER LINES

2.4.1 ATTENUATION AND PHASE CHARACTERISTICS

The propagation of a signal along a wire over earth of finite conductivity has been analyzed by Sunde.²³ The propagation constant γ is given by

$$\gamma = jk H(j\omega) = \alpha + j\beta \quad (2-74)$$

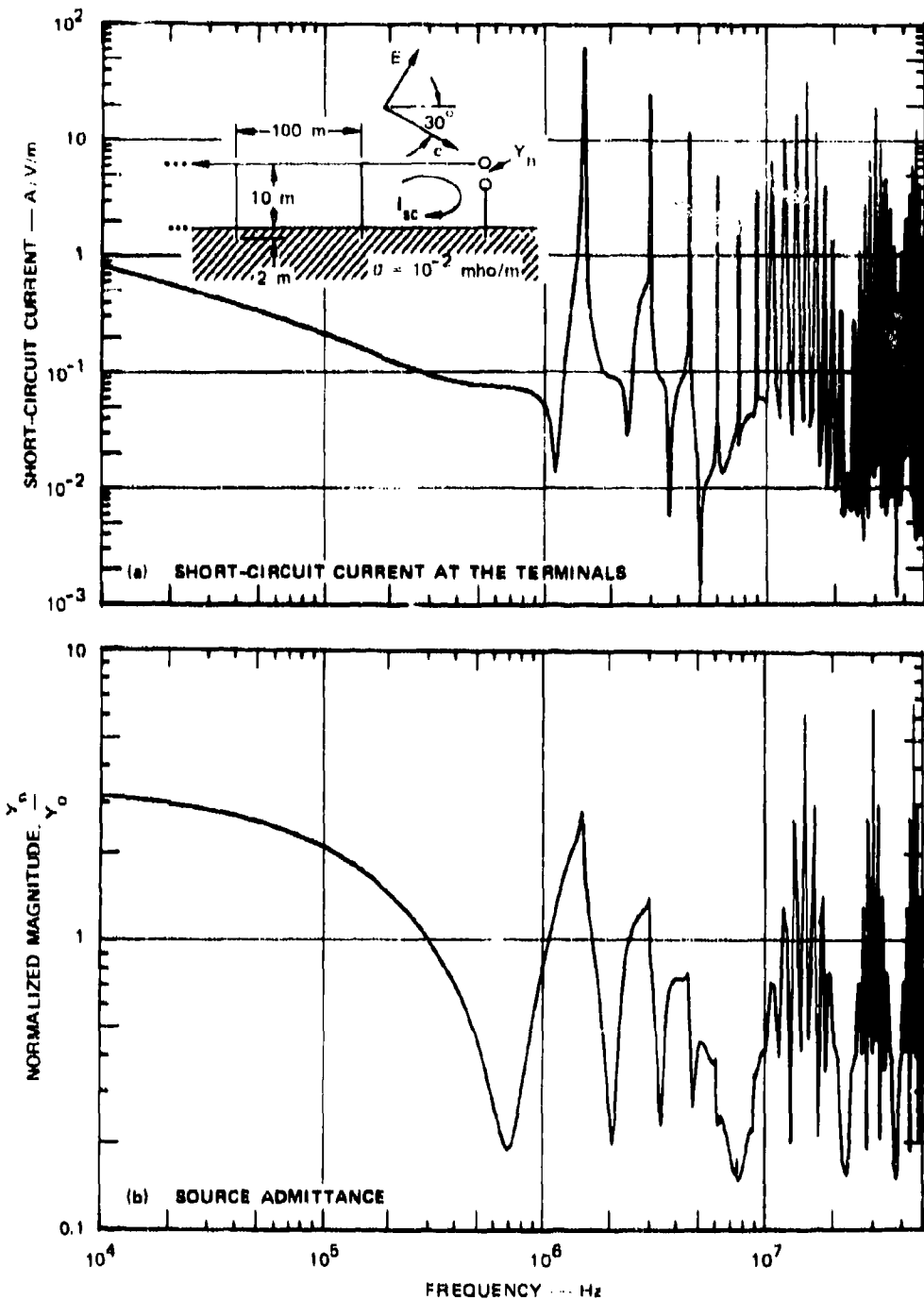


Figure 2-36 FREQUENCY-DOMAIN RESPONSE OF A PERIODICALLY GROUNDED LINE

where $k = \omega/c$ is the free-space propagation constant, c is the velocity of light in vacuum, and $H(j\omega)$ is a function that contains the earth and the line parameters. The function $H(j\omega)$ is given by

$$H(j\omega) = \left[1 + \left(\log \frac{2h}{a} \right)^{-1} \left(\log \frac{1 + (j\omega\tau_h)^{1/2}}{(j\omega\tau_h)^{1/2}} + \frac{1}{(j\omega\tau_a)^{1/2}} \right) \right]^{1/2}. \quad (2-75)$$

For most cases of interest the second term on the right is small compared to 1 so that

$$H(j\omega) \approx 1 + 1/2 \left(\log \frac{2h}{a} \right)^{-1} \left(\log \frac{1 + (j\omega\tau_h)^{1/2}}{(j\omega\tau_h)^{1/2}} + \frac{1}{(j\omega\tau_a)^{1/2}} \right) \quad (2-76)$$

where

$$\tau_h = \mu_0 h^2 \quad \tau_a = \mu_0 \sigma_1 a^2$$

and h is the line height over ground, a is the line radius, μ is the permeability, σ is the soil conductivity, and σ_1 is the wire conductivity. The terms $\sqrt{j\omega\tau_h}$ and $\sqrt{j\omega\tau_a}$ may be recognized as complex and related to the line height h and conductor radius a normalized to the appropriate skin depth, since

$$\sqrt{j\omega\tau_h} = \frac{h}{\delta} (1 + j), \quad \delta = \text{soil skin depth} = \left(\frac{\omega\mu\sigma}{2} \right)^{-1/2} \quad (2-77a)$$

$$\sqrt{j\omega\tau_a} = \frac{a}{\delta_1} (1 + j), \quad \delta_1 = \text{wire skin depth} = \left(\frac{\omega\mu\sigma_1}{2} \right)^{-1/2} \quad (2-77b)$$

The values of τ_h are plotted as a function of soil conductivity and line height in Figure 2-38.

If the complete expression for γ is manipulated to extract the attenuation and phase constants separately, rather simple expressions result when the wire loss is neglected:

$$\frac{\alpha}{k} \approx \frac{\left[\tan^{-1} \frac{1}{1 + 2h/\delta} \right]}{2 \log \frac{2h}{\delta}}$$

(2-78a)

$$\frac{\beta}{k} \approx 1 + \frac{\log \left[1 + \frac{1}{h/\delta} + \frac{1}{2(h/\delta)^2} \right]^{1/2}}{2 \log \frac{2h}{a}} \quad (2-78b)$$

The attenuation constant α calculated from Eq. (2-78a) is shown in Figure 2-37 as a function of frequency for various values of the time constant $\tau_h = \mu_0 \sigma h^2$, and the normalized attenuation constant and phase constant are shown in Figure 2-38. For a typical soil conductivity ($\sigma = 10^{-2}$ mho/m) and line height ($h = 10$ m) the value of τ_h is about 10^{-6} (see Figure 2-36), so that β/k and α/k are not strongly dependent on frequency.

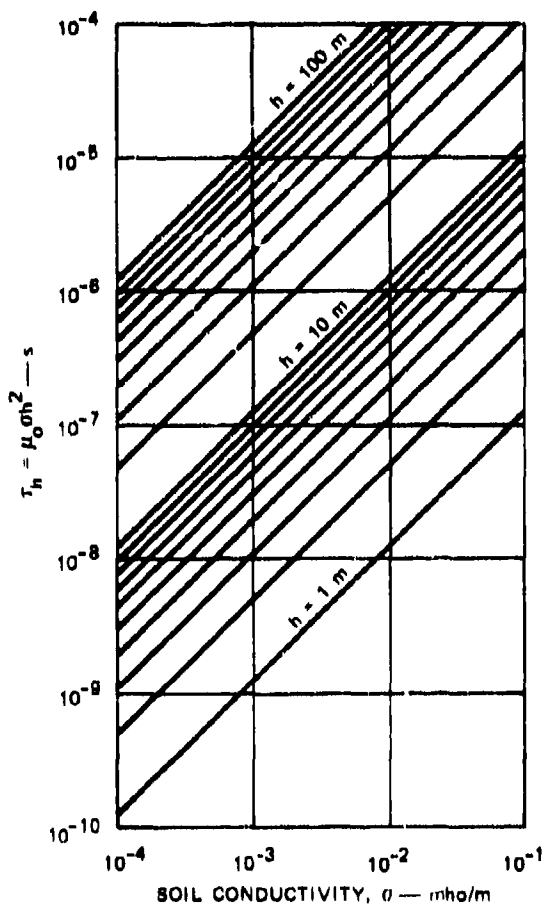


Figure 2-36 TIME CONSTANT τ_h AS A FUNCTION OF SOIL CONDUCTIVITY AND LINE HEIGHT h

The asymptotic behavior of α when h/δ is very small and very large compared to 1 illustrates how the line and soil parameters affect the early- and late-time solutions. When $h/\delta \ll 1$, the inverse tangent term reaches a constant value of $\pi/4$. Therefore

$$\alpha = \frac{k\pi}{8 \log \frac{2h}{a}} \quad (2-79)$$

for late times (low frequencies). For this condition, α is independent of σ and only weakly dependent on h through the $\log 2h/a$ term; α is linearly dependent on frequency.

When $h/\delta \gg 1$, the inverse tangent term reaches $1/(2h/\delta)$ so that

$$\alpha = \frac{k}{4h/\delta \log \frac{2h}{a}} \quad (2-80)$$

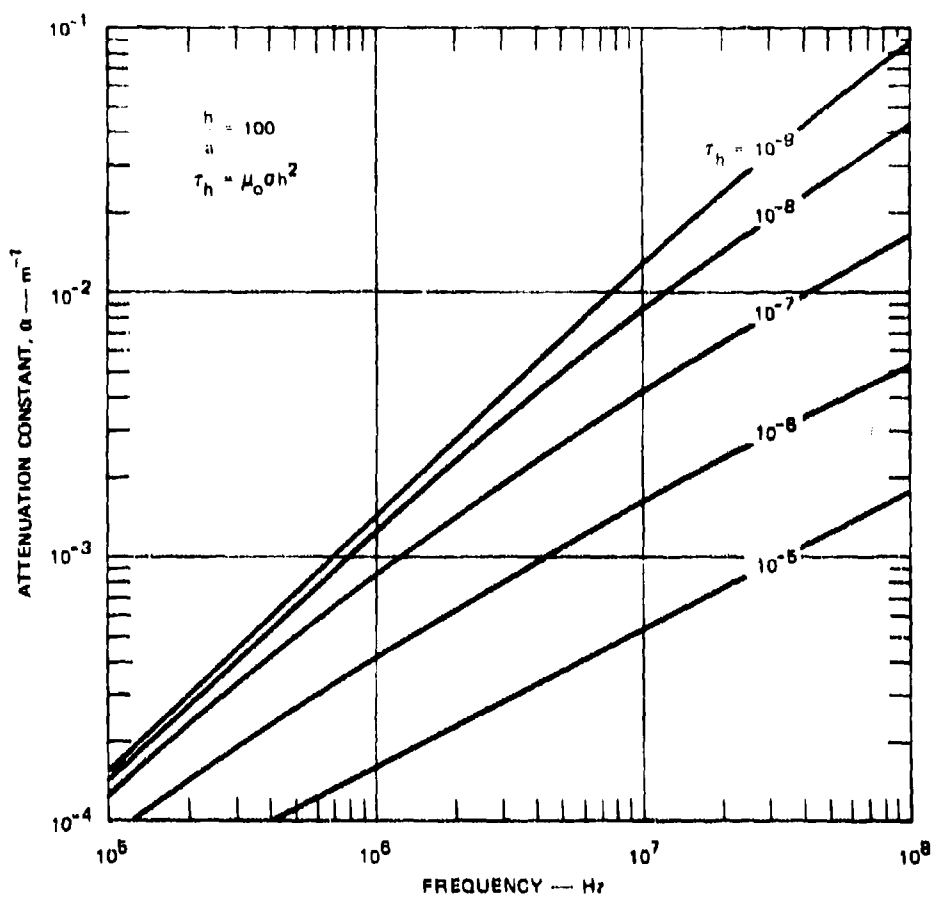


Figure 2-37 ATTENUATION CONSTANT α AS A FUNCTION OF FREQUENCY FOR VARIOUS LINE HEIGHTS AND SOIL CONDUCTIVITIES

for early times (high frequencies). Under these conditions α varies with $n^{-1/2}$ and with $f^{1/2}$. In addition, α is inversely proportional to h when the variation of $\log 2h/a$ is neglected.

A good analytic approximation for all frequencies is

$$\alpha = \frac{8.2 \times 10^{-9} f}{\log \frac{2h}{a} [1 + 1.47 h/\delta]} \text{ nepers/m.} \quad (2-81)$$

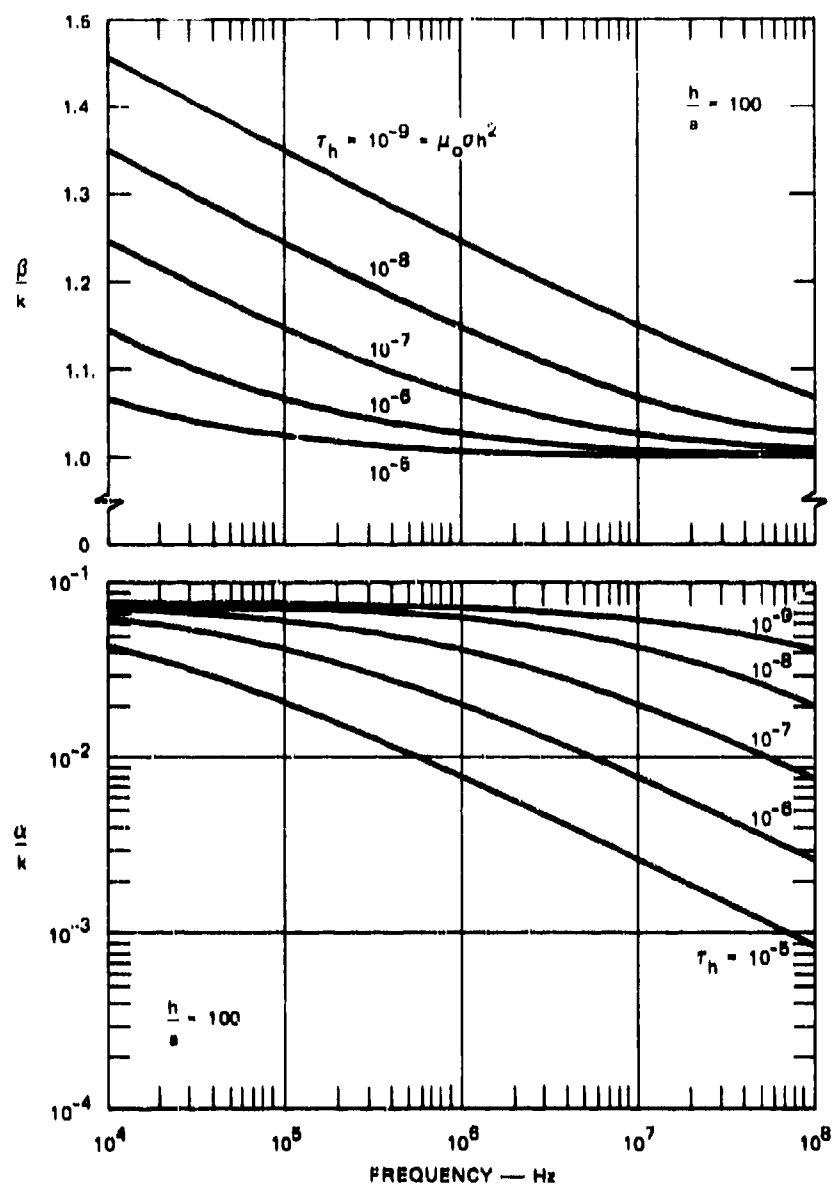


Figure 2-38 NORMALIZED ATTENUATION CONSTANT α/k AND PROPAGATION FACTOR β/k AS A FUNCTION OF FREQUENCY, LINE HEIGHT, AND SOIL CONDUCTIVITY

The step-function response of a line has also been calculated by Sunde. Although there is no closed-form solution for all times, an analytic solution may be found for both early times and late times, where the distinction between early and late times depends on the value of h/δ . If $h/\delta \gg 1$, the early-time solution is appropriate; if $h/\delta \ll 1$, the late-time solution is appropriate.

For early times, the current at a point z down the line normalized to the current at $z = 0$ is

$$\frac{I(z, \omega)}{I(0, \omega)} \approx \left[\exp\left(-\frac{j\omega z}{c}\right) \right] \cdot \exp\left[\sqrt{j\omega} z \left(2c\sqrt{\tau_1} \log \frac{2h}{a}\right)^{-1}\right] \quad (2-82)$$

where

$$\sqrt{\tau_1} = \frac{\sqrt{\tau_h \tau_a}}{\sqrt{\tau_h} + \sqrt{\tau_a}} .$$

For most cases, $\tau_a \gg \tau_h$ so that $\tau_1 \approx \tau_h$. The transform of this expression for current when a step function of current is introduced at $z = 0$ is

$$\frac{I(z, t)}{I(0, t_+)} \approx \operatorname{erfc} \left[z \left(4\sqrt{\tau_1} c t_z^{1/2} \log \frac{2h}{a} \right)^{-1} \right] \quad (2-83)$$

for early times, where $\operatorname{erfc}(z) = \text{complementary error function of } z$, and $t_z = t - z/c$.

For late times the normalized current in the frequency domain is

$$\frac{I(z, \omega)}{I(0, \omega)} \approx \exp -\frac{j\omega z}{c} \left[1 + \frac{j\omega z}{4c \log \frac{2h}{a}} \left(\log(j\omega \tau_h) - \frac{2}{\sqrt{j\omega \tau_a}} \right) \right] . \quad (2-84)$$

The time-domain solution with step-function input is

$$\frac{I(z,t)}{I(0,t_+)} \approx 1 - z \frac{\frac{1}{2} \left(\frac{t_2}{\pi r_a} \right)^{1/2}}{4c t_2 \log \frac{2h}{a}} \quad (2-85)$$

for late times.

For many cases $2(t_2/\pi r_a)^{1/2} \ll 1$, which further simplifies the solution. Note that for late times the response is independent of the value of soil conductivity and only weakly dependent on the height above ground through the logarithmic term in h/a . This contrasts with the early-time solution, which is a function of both σ and h .

Figure 2-39 shows the wave front of a unit step function after it has traveled a distance of 10 km (6.2 miles) along conductors of 1 mm and 1 cm radii, when the earth conductivity is 10^{-2} mho/m.

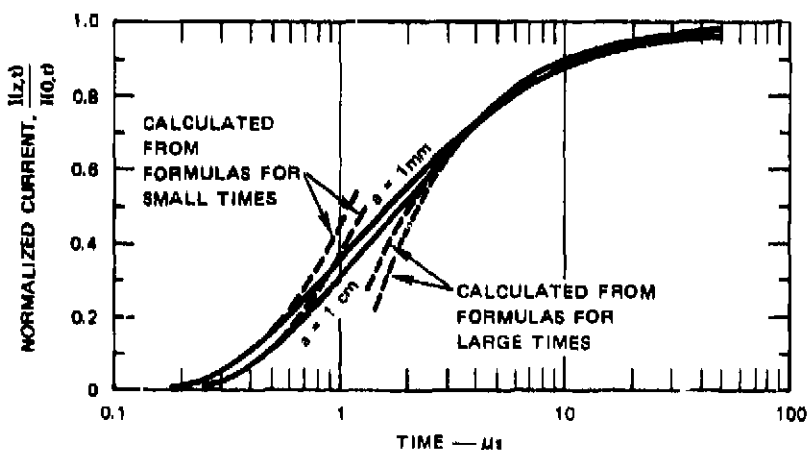


Figure 2-39 WAVE FRONT OF UNIT STEP CURRENT AFTER PROPAGATION FOR A DISTANCE OF 10 km (6.2 miles) ALONG COPPER CONDUCTORS OF 1 mm AND 1 cm RADIUS. Soil conductivity = 10^{-2} mho/m. Height on conductor, $h = 10$ m. Source: Ref. 23.

Figure 2-40 shows the wave front for various soil conductivities for a conductor of 1 mm radius. The curves show that, for perfectly conducting soil, the wave-front distortion due to the conductor resistance is small compared to that resulting from the finite conductivity of the soil.

2.4.2 JUNCTIONS IN TRANSMISSION LINES

When a transmission line branches into two lines or when a spur line is connected to a main line, an obvious discontinuity in high-frequency characteristics of the line is formed. The feed line and the two branches may be treated as transmission lines having individual characteristic impedances (which may be equal if the line heights and effective radii are the same) and propagation factors. Near the junction, however, there will be mutual coupling among the three lines. The treatment of transmission-line currents and voltages in the vicinity of branches or junctions has been analyzed for junctions forming tees and crosses by King²⁴ for the case where the line height is small compared to a wavelength. No theoretical analysis is available for the power-line EMP case where line height is greater than one wavelength; however, experimental determination of the reflection and transmission characteristics of symmetrical junctions have been made.⁷

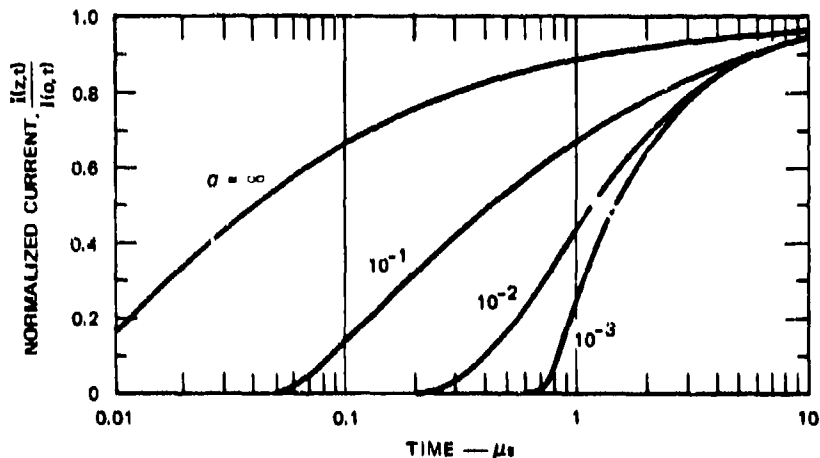


Figure 2-40 WAVE FRONT OF UNIT STEP CURRENT AFTER PROPAGATION FOR A DISTANCE OF 10 km (6.2 miles) ALONG A COPPER CONDUCTOR OF 1 mm RADIUS AT A HEIGHT OF 10 m, FOR VARIOUS SOIL CONDUCTIVITIES. Source: Ref. 23.

For a symmetrical wye junction, such as that illustrated in Figure 2-41, of a long feed line with two long branch lines, the branch lines can be considered as two loads of impedance Z_0 in parallel at the end of the feed line if mutual coupling is neglected. The current reflection coefficient and current transmission coefficient are then

$$\mu_i = \frac{I_{\text{ref}}}{I_{\text{inc}}} = \frac{Z_0 - Z_L}{Z_0 + Z_L} \quad (2-86a)$$

$$= \frac{1}{3} \quad (Z_L = Z_0/2)$$

$$\tau_i = \frac{I_{\text{trans}}}{I_{\text{inc}}} = \frac{2Z_0}{Z_0 + Z_L} \quad (2-86b)$$

$$= \frac{4}{3} \quad (Z_L = Z_0/2)$$

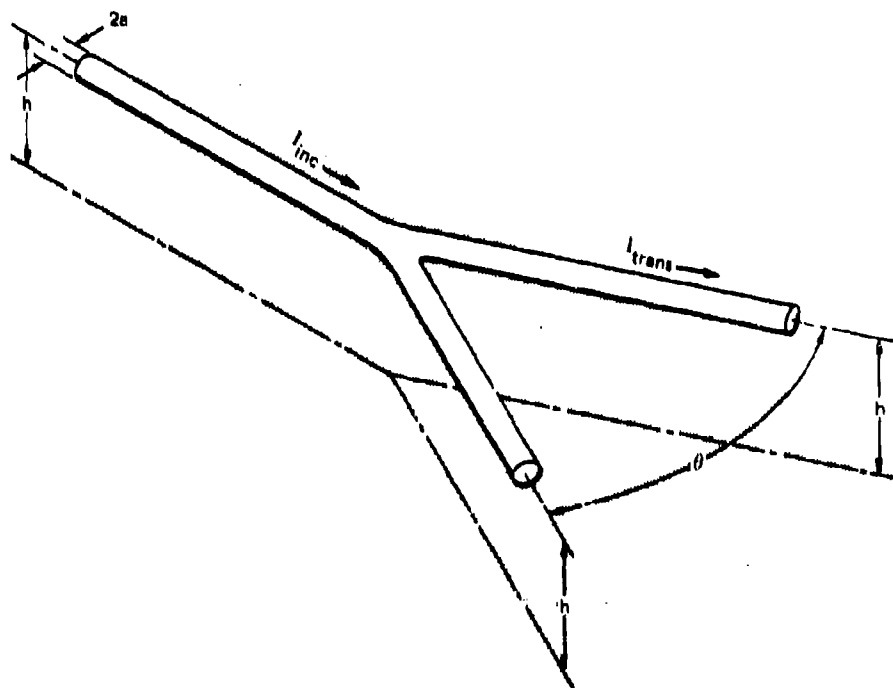


Figure 2-41 SYMMETRICAL JUNCTION IN A TRANSMISSION LINE

where τ_i indicates the total current transmitted to both branches. The characteristic impedance is, approximately,

$$Z_0 \approx \frac{\eta}{2\pi} \log \frac{2h}{a}$$

where h is the line height and a is the effective radius of the line for common-mode (zero sequence) propagation. The load impedance Z_L represented by the two branch lines in parallel is $Z_0/2$ if the lines are very long (in comparison to the pulselength $c\tau$) or are terminated in their characteristic impedance. For the symmetrical junction, therefore, 2/3 of the incident current is transmitted to each branch line. If h and a are different for each line, the load impedance will be $Z_L = Z_{01}Z_{02}/(Z_{01} + Z_{02})$, where Z_{01} and Z_{02} are the characteristic impedances of the individual branch lines, and the total transmitted current will be divided between the branch lines accordingly.

The effect of mutual coupling between the branch lines of a symmetrical wye junction can be estimated from the characteristic impedance of two wires over ground given by²¹

$$Z_0 = \frac{\eta}{4\pi} \log \left[\frac{2h}{a} \left(1 + \left(\frac{2h}{d} \right)^2 \right)^{1/2} \right] \quad (h \gg a) \quad (2-87)$$

where h is the height of the lines, a is their effective radius, and d is the spacing between conductors (see Figure 2-42). Note that when the lines are very far apart ($d \gg 2h$), the common-mode impedance of the two-wire line is half that of an isolated single-wire line, whereas when the lines are very close together ($d \approx a$), the common-mode impedance approaches that of isolated single-wire line.

The reflected and transmitted signals have been measured at symmetrical junctions on scale models.⁷ The line configuration and results are shown in Figure 2-43. The line height used was 40 ft, or six times the equivalent length of the rise time ($L_{eq} = c\tau_{rise}$).

If two lines forming a symmetrical junction are considered as two lines of characteristic impedance Z_0 in parallel and fed by a single input line of Z_0 , then the reflection coefficient would be 0.33 and the transmission coefficient would be 0.667 at the junction. These

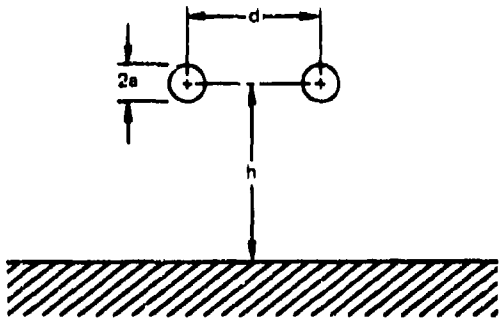


Figure 2-42 TWO-CONDUCTOR TRANSMISSION LINE OVER GROUND PLANE (common-mode excitation)

values are indicated in Figure 2-43. The experimental results show that this model accurately reflects the interaction at the junction when the junction angle is large. However, when the angle is small, the junction lines are more tightly coupled to each other, making the net impedance closer to Z_0 . This reduces the reflection and transmission coefficients. The reflection coefficient is shown in Figure 2-43 for early times (~ 20 ns) and for late times (~ 170 ns).

At early times the reflection coefficient is much lower than would be expected from the uncoupled branch lines of characteristic impedance Z_0 . In the limit as $\theta \rightarrow 0$, the value of Z_0 beyond the junction almost equals the value of Z_0 for the input line, resulting in only a very small reflection. This is shown as the dashed portion of the early-time curve from $\theta = 0^\circ$ to $\theta = 22.5^\circ$. It is apparent, however, that the assumption that the branch lines behave as independent isolated lines gives a good approximation to the reflected and transmitted currents if the branch angle is of the order of 90° or greater.

2.4.3 BENDS IN POWER LINES

The signals coupled to the power lines will not always propagate straight to the load. In this section, theoretical and experimental results for propagation of signals around bends are presented. Analysis is usually restricted to the case where the line height is small compared to the wavelength. However, experimental measurements have been made to see if significant deviations from theory could be found when the line height was comparable to the wavelength.

King has treated a simple bend in a two-wire line when $\beta h \ll 1$ using the geometry shown in Figure 2-44.²⁴ His analysis shows that the bend has the effect of lowering the

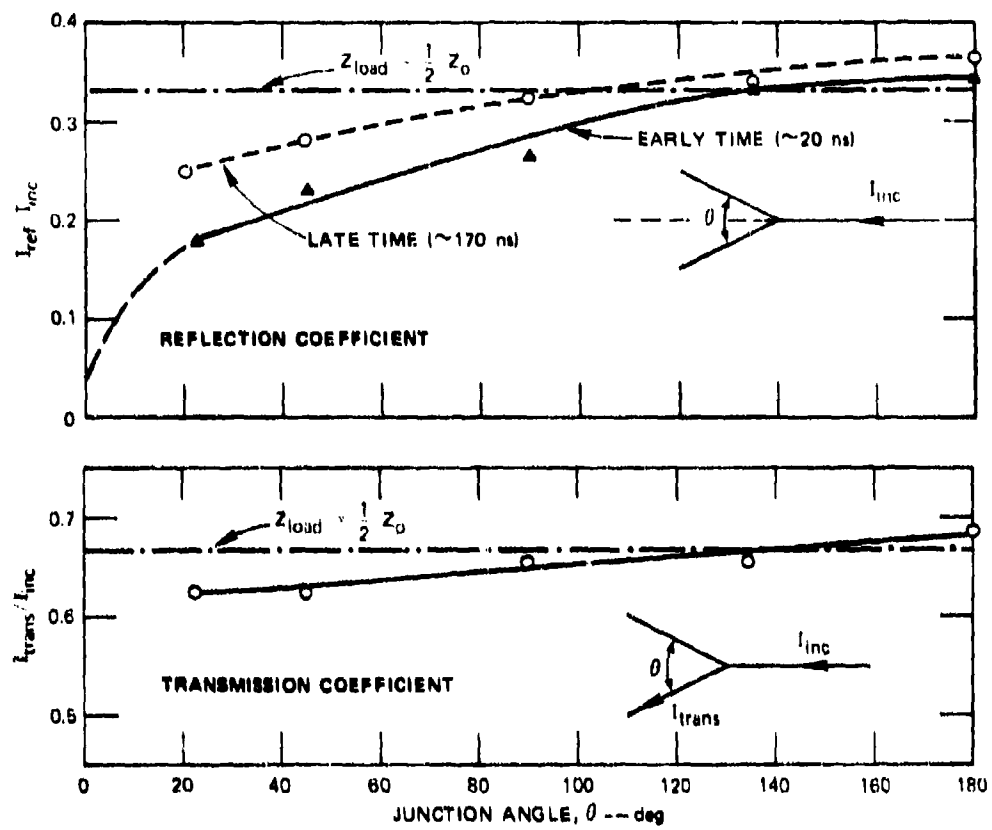


Figure 2-43 REFLECTION AND TRANSMISSION COEFFICIENT AT A SYMMETRICAL JUNCTION, WHERE $h = 40$ ft. Source: Ref. 7.

inductance $L(w)$ and capacitance $C(w)$ per unit length of line in the region around the bend. The values of $L(w)$ and $C(w)$ are

$$L(w) = \frac{\mu_0}{2\pi} (K - F_1(w) + F_2(w) \cos \theta) \quad (2-88a)$$

$$C(w) = \frac{2\pi\epsilon}{K - F_1(w) + F_2(w)} \quad (2-88b)$$

where

$$K = 2 \log \frac{2h}{a} \quad (2-89)$$

$$F_1(w) = \log \frac{w + \sqrt{w^2 + (2h)^2}}{w + \sqrt{w^2 + a^2}} \quad (2-90a)$$

$$F_2(w) = \log \frac{w \cos \theta + \sqrt{w^2 + (2h)^2}}{w \cos \theta + \sqrt{w^2 + a^2}} \quad (2-90b)$$

$(2a < 2h \ll c/f)$

and w is the distance from the bend.

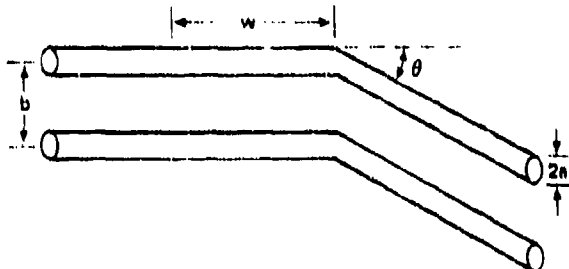


Figure 2-44 TWO-WIRE LINE WITH A BEND

Because the characteristic impedance $Z_0 = \sqrt{L(w)/C(w)}$ and the propagation factor $\gamma = \sqrt{L(w)/C(w)}$ depend on the inductance and capacitance per unit length, both are affected by the changes in L and C in the vicinity of a bend. Power lines do not meet the criterion that $2h \ll c/f$ for all frequencies of interest in the EMP spectrum; however, measurements were made of

the peak reflection coefficient using scale models of power-line configurations and scaled exponential pulses. The peak current reflection coefficient for a line 20 ft high and 0.2 inch in diameter with a 6-ns-rise-time pulse is shown in Figure 2-45 as a function of bend angles.⁷ The measured peak reflection coefficient computed using the low-frequency capacitance and inductance varies with bend angle in Figure 2-45. The experimental data indicate reflection coefficients slightly larger than those predicted using the static theory, but for bend angles less than 90° the reflection is small in either case.

The perturbation due to the bend is time-dependent. The values shown in Figure 2-45 are peak values. Generally the effect of bend has relaxed within a few tens of ns (or equivalently, a few line heights). This result is consistent with King's analysis, which shows that the effects on $L(w)$ and $C(w)$ are strong only near the junction. At later times — or longer wavelengths — the strong effects near the junction are smoothed, since perturbances that extend over only a small fraction of a wavelength cannot be resolved.

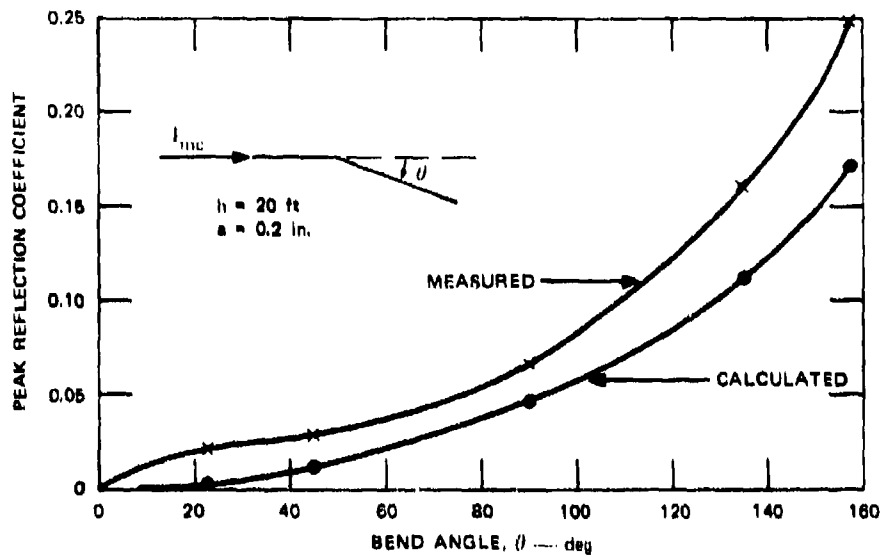


Figure 2-45 COMPARISON OF CALCULATED AND MEASURED REFLECTION COEFFICIENTS OF A BEND AS A FUNCTION OF BEND ANGLE. Source: Ref. 7.

Scale-model measurements have been made for a single wire line 20 ft and 40 ft above ground for a range of bend angles from 0° to 157.5° . A step-function signal with rise time of about 6 ns was fed onto the line. The reflection and transmission coefficients for these two line heights are shown in Figure 2-46, where it is apparent that the effect of line height is quite small.

The effect of radius of curvature on the reflection coefficient was also briefly investigated using scale models.⁷ The results are shown in Figure 2-47. The reflection coefficient decreases monotonically as the radius of curvature is increased.

2.4.4 OTHER EFFECTS

There are many deviations from the circular cylinder over a plane, uniformly conducting ground assumed in the analysis of coupling to, and propagation along,

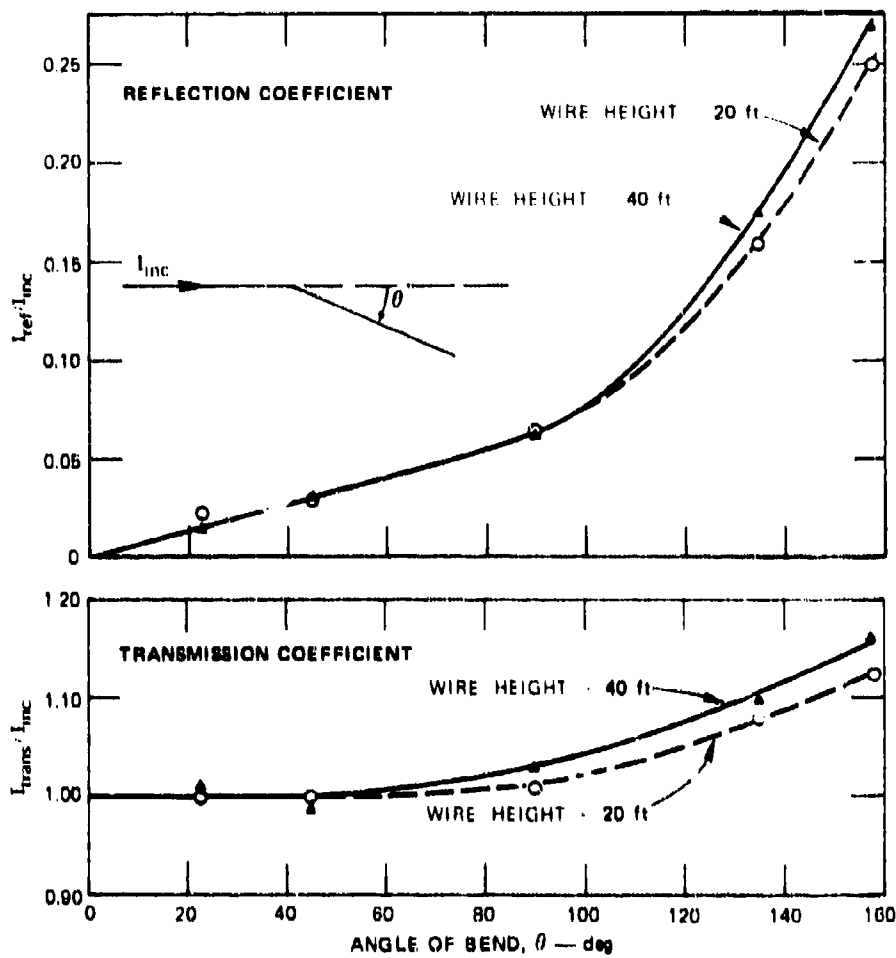


Figure 2-46 REFLECTION AND TRANSMISSION COEFFICIENT OF A BEND IN A SINGLE-WIRE LINE OVER GROUND AS A FUNCTION OF BEND ANGLE. Source: Ref. 7.

power lines. These deviations may be classified as scatterers or variations in line height:

(1) Scatterers

- Poles or towers
- Trees and other ground foliage
- Buildings, bridges, and other structures
- Cliffs, ravines, and mountains (with lines in shadows)

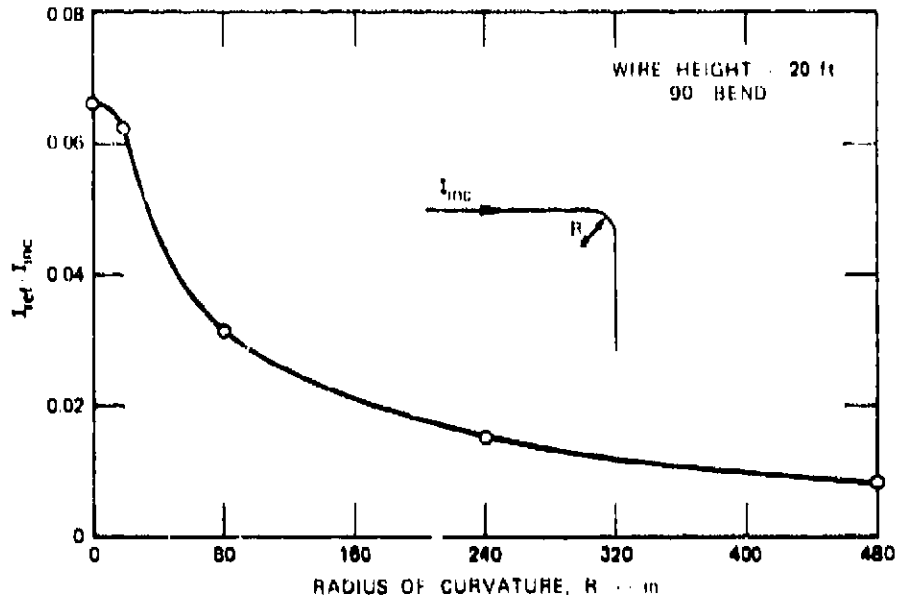


Figure 2-47 REFLECTION COEFFICIENT FOR A 90° BEND AS A FUNCTION OF RADIUS OF CURVATURE. Source: Ref. 7.

(2) Variations in line height

- Line sag between poles
- Undulating terrain
- Aerial ground wires
- Communications cables on shared poles.

The effect of such deviations from the abstract model is almost always to reduce the signal delivered to the power consumer's terminals. The scatterers reduce the excitation field at the power conductors, and the variation in line height produces multiple reflections of the current and voltage propagating along the line so that line losses are larger than those predicted for a uniform transmission line. One can conceive of resonances in the power line matching resonances in the consumer's low-voltage circuits to produce an enhanced overall EMP response; however, it is expected that the occurrence of such a situation in practice would be rather rare, particularly in view of the fact that resonances in wire-over-soil transmission lines tend to be rather weak.

An indication of the effect of variations in line height can be obtained from the variation in the characteristic impedance caused by line sag shown in Figure 2-48. For this example a line 10 m high at the crossarms sags to 5 m high midway between poles 100 m apart. The average height of the line is 6.56 m, at which height the characteristic impedance is 300 ohms. The characteristic impedance varies from 325 ohms at the poles to 284 ohms at the midpoint. The reflection coefficient associated with these extremes is only 0.07; therefore the effect of line height variations is relatively small unless the induced signal propagates over great distances.

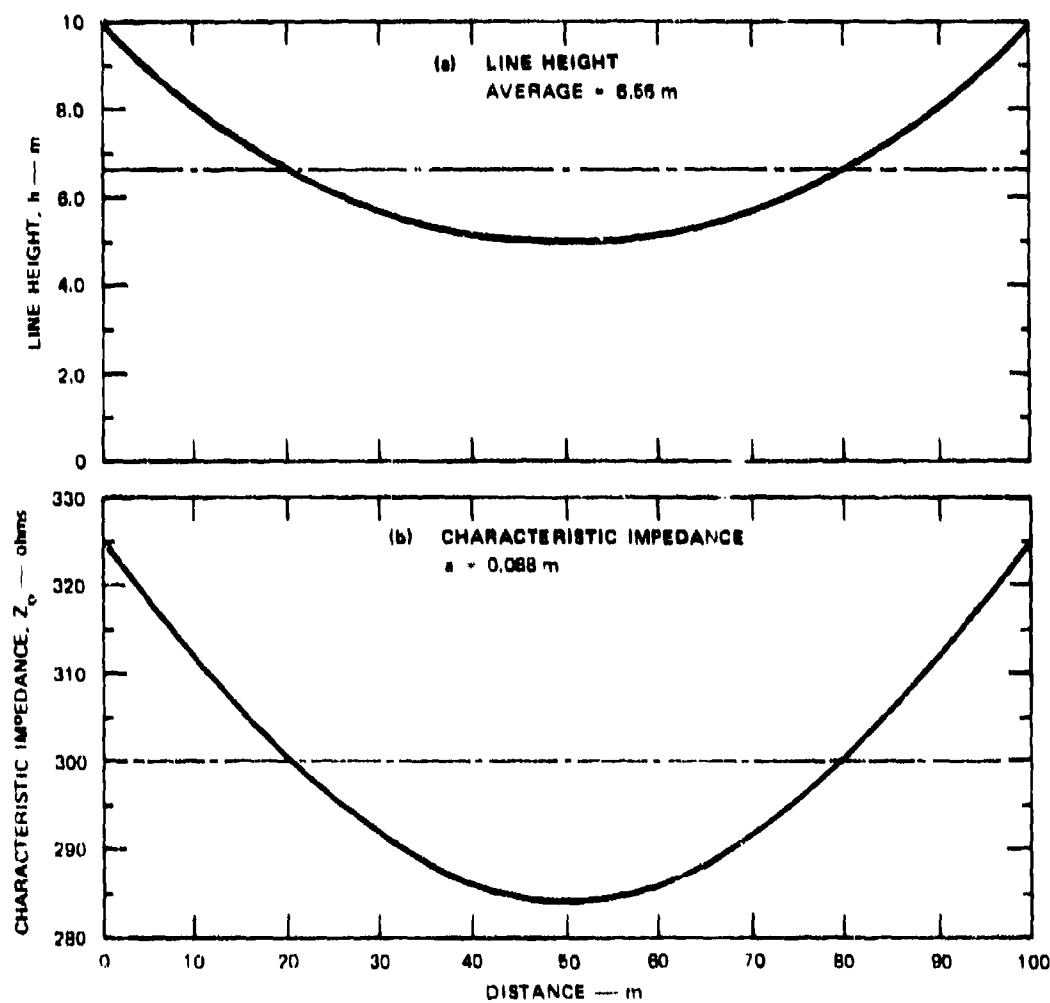


Figure 2-48 VARIATION IN CHARACTERISTIC IMPEDANCE CAUSED BY LINE SAG

2.5 DIFFERENTIAL COUPLING TO HORIZONTAL CONDUCTORS

2.5.1 WIRES IN A HORIZONTAL PLANE

For two conductors separated by a distance d and at a height h above ground as illustrated in Figure 2-49 the differential-mode current and voltage induced by a plane wave can be determined by an analysis very similar to that used for the common-mode current and voltage.²⁶ The differential equations of the current and voltage are

$$\frac{\partial V}{\partial z} + ZI = E_z^u(h,d,z) - E_z^u(h,0,z) + \frac{\partial V^u}{\partial z} \quad (2-91a)$$

$$\frac{\partial I}{\partial z} + YV = YV^u \quad (2-91b)$$

where $E_z^u(x,y,z)$ is the component of the resultant electric field parallel to the wire and at the wire location but in the absence of the wire. Z and Y are the impedance and admittance per unit length of the two-wire line, and V^u is given by

$$V^u = - \int_0^d E_y(h,y,z) dy . \quad (2-92)$$

The second-order differential equations are

$$\frac{d^2 I}{dz^2} - \gamma^2 I = -Y[E_z^u(h,d,z) - E_z^u(h,0,z)] \quad (2-93a)$$

$$\frac{d^2 V}{dz^2} - \gamma^2 V = -YZ_I V^u \quad (2-93b)$$

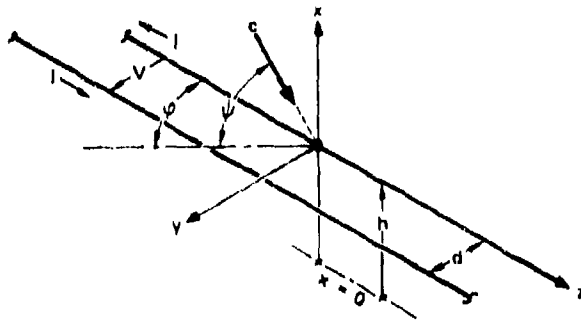


Figure 2-49 GEOMETRY OF TWO-WIRE TRANSMISSION LINE FOR DIFFERENTIAL-COUPLING ANALYSIS

where $\gamma = \sqrt{ZY}$ and Z_i is the internal impedance of the conductors (if finitely conducting wires are assumed). The form of the field $E_z^u(h,0,z)$ is identical to that given in Eq. (2-7) for the common-mode analysis. The field $E_z^u(h,d,z)$ differs from $E_z^u(h,0,z)$ by a phase term:

$$E_z^u(h,d,z) = E_z^u(h,0,z) e^{jkd'} \quad (2-94)$$

where $d' = d \sin \varphi \cos \psi$. The driving field in brackets in Eq. (2-93a) can thus be expressed as

$$E_z^u(h,d,z) - E_z^u(h,0,z) = E_i \left\{ \frac{\sin \varphi}{\cos \varphi} \right\} e^{-jkz'} (1 + R e^{-jk2h'}) (e^{jkd'} - 1) \quad (2-95)$$

where the upper trigonometric function ($\sin \varphi$) applies to horizontal polarization and the lower applies to vertical polarization. The primed quantities are $z' = z \cos \psi \cos \varphi$, $h' = h \sin \psi$, and $d' = d \sin \varphi \cos \psi$, and R is the appropriate reflection factor for horizontal or vertical polarization. The solutions for the differential current are, therefore, identical to those for the common-mode current given in Section 2.2.2 multiplied by the term $(e^{jkd'} - 1)$ if Z_0 and γ for the two-wire line are used instead of the corresponding quantities for the single wire over ground. If ground effects and losses in the wire are neglected, Z_0 and γ are

$$Z_0 \approx \frac{\eta}{\pi} \log \frac{d}{a} \quad \gamma \approx jk = j \frac{\omega}{c} \quad (2-96)$$

for the two-wire line.

Separating the current into the part that would exist for a perfectly reflecting ground and the part caused by a finitely conducting soil, the open-circuit voltage at the terminals of a semi-infinite line due to E_z^U is, in the frequency domain,

$$V_\infty(\omega) - V_\infty^U(\omega) = E_i c D(\psi, \varphi) \frac{1 - e^{-j\omega 2h'/c}}{j\omega} (e^{j\omega d'/c} - 1) \quad (\text{perfect ground}) \quad (2-97a)$$

$$\Delta(V - V^U) = E_i c D(\psi, \varphi) 2\sqrt{\tau_e} (\sin \psi)^{\pm 1} e^{-j\omega 2h'/c} (e^{j\omega d'/c} - 1) \quad (\text{ground effect only}) \quad (2-97b)$$

when all attenuation factors are negligible. The + exponent applies to horizontal polarization, the - to vertical polarization, and $D(\psi, \varphi)$ and τ_e are defined in Section 2.2.3. The spectral magnitudes shown in Figures 2-12 and 2-13 are thus applicable to the differential-mode voltages also if the spectra are multiplied by $e^{j\omega d'/c} - 1$, which can be written

$$e^{j\omega d'/c} - 1 = 2j e^{j\omega d'/2c} \sin \omega d'/2c = 2 \sin \omega d'/2c \sqrt{\omega d'/2c + \frac{\pi}{2}} . \quad (2-98)$$

The open-circuit voltage V^U caused by the y-component of the field is given by Eq. (2-92) with

$$E_y^U(h, y, z) = E_i \begin{cases} \cos \varphi \\ -\sin \psi \sin \varphi \end{cases} e^{-jkz'} (1 + Re^{-jk2h'}) e^{jky} \cos \psi \sin \varphi \quad (2-99)$$

where the upper trigonometric function applies to horizontal polarization and the lower applies to vertical polarization of the incident field. The open-circuit voltage $V^U(\omega)$ produced by the y-component of the field is then

$$V_\infty^U(\omega) = -E_i c D_U(\psi, \varphi) \frac{1 - e^{-j\omega 2h'/c}}{j\omega} (e^{j\omega d'/c} - 1) \quad (\text{perfect ground}) \quad (2-100a)$$

$$\Delta V^U(\omega) = -E_i c 2\sqrt{\tau_e} D_U(\psi, \varphi) (\sin \psi)^{\pm 1} \frac{e^{-j\omega 2h'/c}}{\sqrt{j\omega}} (e^{j\omega d'/c} - 1) \quad (\text{ground effect only}) \quad (2-100b)$$

where the + exponent applies to horizontal polarization, the - exponent applies to vertical polarization, and

$$D_U(\psi, \varphi) = \frac{\cos \varphi}{\cos \psi \sin \varphi} \quad (\text{horizontal polarization})$$

$$= - \frac{\sin \varphi \sin \psi}{\cos \psi \sin \varphi} \quad (\text{vertical polarization}) . \quad (2-101)$$

The apparent poles in $D_U(\psi, \varphi)$ at $\psi = \pi/2$ and $\varphi = 0$ do not affect the solution because

$$\lim_{\begin{array}{l} \psi \rightarrow \frac{\pi}{2} \\ \varphi \rightarrow 0 \end{array}} \frac{e^{j\omega d'/c} - 1}{\cos \psi \sin \varphi} = j\omega d/c . \quad (2-102)$$

Note that the form of $V^U(\omega)$ is the same as that of $V(\omega) - V^U(\omega)$ except for $D_U(\psi, \varphi)$, so that the spectra and waveforms for V^U and $V - V^U$ are similar.

Because $e^{j\omega d'/c}$ and 1 transform into time delays in the time domain, the time-domain responses are also similar to those obtained for the common-mode voltages. If $v_c(t)$ is the common-node voltage, the differential-mode voltage due to E_z^U is

$$v(t) - v^U(t) = v_c(t + d'/c) \quad (-d'/c \leq t \leq 0)$$

$$= v_c(t + d'/c) - v_c(t) \quad (t \geq 0) \quad (2-103)$$

and the total voltage caused by the z and y components of the incident field is

$$v(t) = (1 - D_U/D) v_c(t + d'/c) \quad (-d'/c \leq t \leq 0)$$

$$= (1 - D_U/D) [v_c(t + d'/c) - v_c(t)] \quad (t \geq 0) . \quad (2-104)$$

When $\alpha = 0$ and $\gamma = jk$, the coefficients $(1 - D_u/D)$ become

$$(1 - D_u/D) = \frac{\cos \psi - \cos \varphi}{\sin^2 \varphi \cos \psi} \quad (\text{horizontal polarization})$$

$$= \frac{1}{\cos \psi \cos \varphi} \quad (\text{vertical polarization}) . \quad (2-105)$$

Because the term $e^{j\omega d/c} - 1$ places a "window" on the leading edge of the voltage waveform $v_c(t)$, and because the voltage $v_c(t)$ continues to increase long after the ground-reflected wave arrives at the wires, the maximum differential voltage depends not only on the directivity function $(1 - D_u/D)$, but also on the width d'/c of the window. For linearly increasing voltage, which is a good approximation to the early-time behavior of the voltage and current, the maximum voltage will be obtained when $d'(1 - D_u/D)$ is maximum. This product is

$$d'(1 - D_u/D) = d \frac{\cos \psi - \cos \varphi}{\sin \varphi} \quad (\text{horizontal polarization})$$

$$= d \tan \varphi \quad (\text{vertical polarization}) . \quad (2-106)$$

The maximum open-circuit voltage will therefore occur when $\varphi \rightarrow 0$ for horizontal polarization and when $\varphi \rightarrow \pi/2$ for vertical polarization. (Attenuation of the line will prevent the product from going to infinity as $\varphi \rightarrow 0, \pi/2$).

A typical waveform for the open-circuit differential voltage at the end of a semi-infinite two-wire line 10 m high with 2-m spacing between the wires is shown in Figure 2-50. The waveform is shown for a horizontally polarized incident exponential pulse with perfectly conducting ground (dashed curve) and for ground of average conductivity (10^{-2} mho/m) (solid curve). From a comparison of the differential voltage waveform of Figure 2-50 with the common-mode waveform of Figure 2-14 (for $\sigma = 10^{-2}$, horizontal polarization) it is seen that the peak voltage in the differential mode is only about one-seventh the peak common-mode voltage, and the duration of differential-mode voltage pulse is only about 30 ns, compared with a duration of a few microseconds for the common-mode voltage.

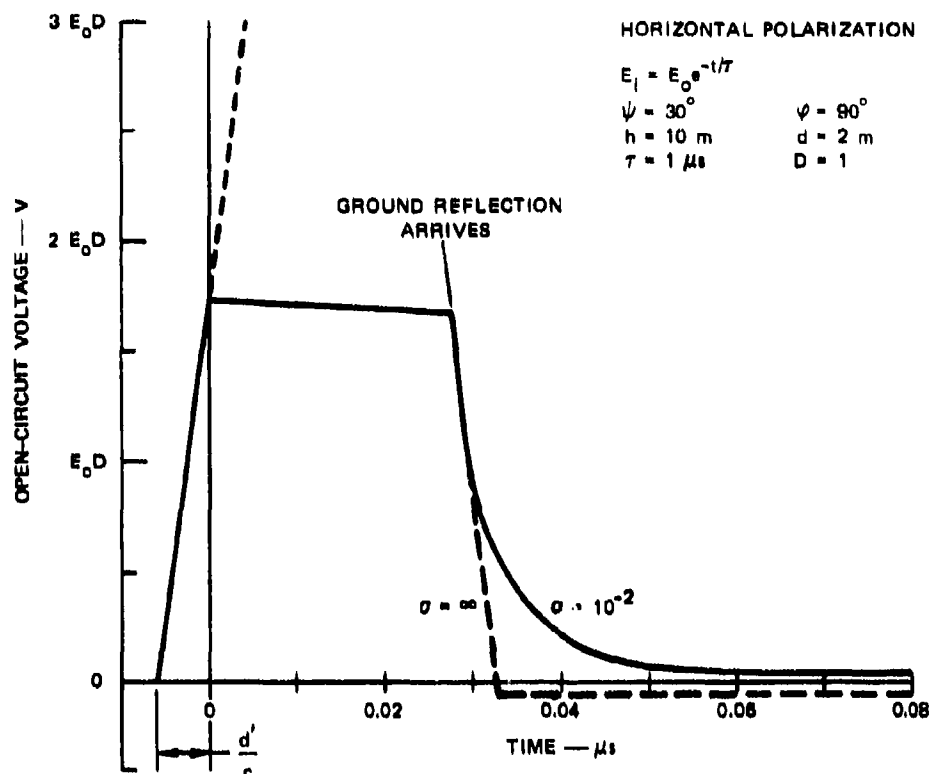


Figure 2-50 OPEN-CIRCUIT, DIFFERENTIAL VOLTAGE INDUCED IN A SEMI-INFINITE TWO-WIRE LINE BY AN EXPONENTIAL PULSE (wires in a horizontal plane)

For a three-wire line with the wires equally spaced in a horizontal plane, a similar voltage waveform would be obtained between the middle wire and the third wire at $y = -d$. This voltage would be of opposite polarity and shifted by d'/c to the right of $t = 0$, however. The voltage between the two outer lines would thus be approximately twice as large as the voltage between the middle wire and either outer wire, and the time to reach the peak value would be $2d'/c$.

2.5.2 WIRES IN A VERTICAL PLANE

If the two-wire line lies in a vertical plane as illustrated in Figure 2-51, the analysis is quite similar to that for the wires in a horizontal plane except that the form of V^u and E_z^u

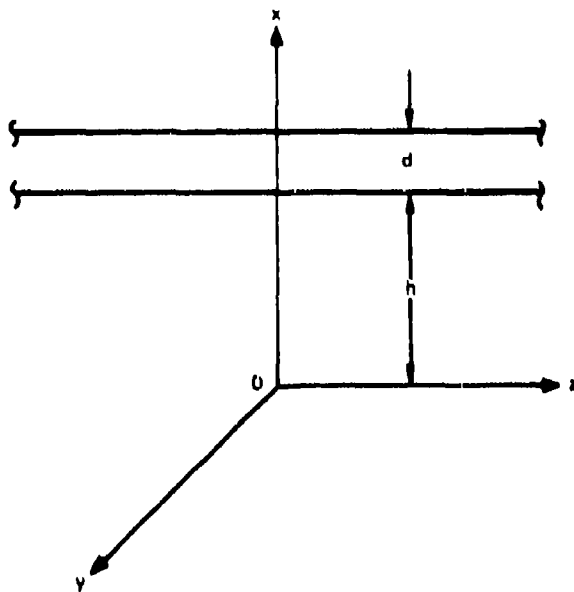


Figure 2-51 TWO-WIRE LINE LYING IN A VERTICAL PLANE

are different. The voltage V^u exists only for vertical polarization if the wires are in a vertical plane, and its value is.

$$V^u = - \int_h^{h+d} E_x(x, 0, z) dx \quad (2-107)$$

$$= -E_1 c \cot \psi \frac{(e^{j\omega d'/c} - 1) [1 + R_v e^{-j\omega(2h'+d')/c}]}{j\omega}$$

where $d' = d \sin \psi$ and $h' = h \sin \psi$.

The horizontal electric field terms on the right side of Eq. (2-95) are replaced by

$$E_z(h+d, 0, z) - E_z(h, 0, z) = E_1 \left\{ \begin{matrix} \sin \varphi \\ \cos \varphi \sin \psi \end{matrix} \right\} e^{-jkz'} (e^{jkd'} - 1) \quad (2-108)$$

$$\times [1 - R_v e^{-j\omega(2h'+d')}]$$

where the upper trigonometric function ($\sin \varphi$) applies to horizontal polarization and the lower function applies to vertical polarization. When this expression for the field is used and the solution to the differential equations is separated into that part obtained with a perfectly conducting ground and that part caused by the ground alone, the open-circuit differential voltage for a semi-infinite line is

$$V_{\infty}(\omega) - V_{\infty}^U(\omega) = E_0 c D(\psi, \varphi) \frac{1 + e^{-j\omega(2h'+d')/c}}{j\omega} \frac{(e^{j\omega d'/c} - 1)}{(e^{j\omega d'/c} + 1)}$$

(perfect
ground)
(2-109a)

$$\Delta(V - V^U) = -E_0 c D(\psi, \varphi) (1 + R) \frac{e^{-j\omega(2h'+d')/c}}{j\omega} \frac{(e^{j\omega d'/c} - 1)}{(e^{j\omega d'/c} + 1)}$$

(ground
effect
only)
(2-109b)

where

$$1 + R \approx \frac{2\sqrt{\omega\tau_0}}{\sin \psi} \quad (\text{vertical polarization})$$

$$\approx 2 \sin \psi \sqrt{\omega\tau_0} \quad (\text{horizontal polarization}) .$$

The expression for V^U for the differential voltage produced by the vertical component of the incident field can be similarly separated to give (for vertical polarization only)

$$V_{\infty}^U(\omega) = -E_0 c \cot \psi \frac{1 - e^{-j\omega(2h'+d')/c}}{j\omega} \frac{(e^{j\omega d'/c} - 1)}{(e^{j\omega d'/c} + 1)}$$

(perfect ground)
(2-110a)

$$\Delta V^U = -E_0 c \cot \psi (1 + R_V) \frac{e^{-j\omega(2h'+d')/c}}{j\omega} \frac{(e^{j\omega d'/c} - 1)}{(e^{j\omega d'/c} + 1)}$$

(ground
effect only)
(2-110b)

where $1 + R_V \approx 2$. In all of these expressions, the phase is referred to the phase of the incident wave at the end of the lower wire.

The combination of the voltages induced by E_z and E_x is somewhat more complicated for the case when the wires lie in the vertical plane because of the difference in sign of the term $\exp[-j\omega(2h'+d')/c]$ in the expressions for V_{∞}^U and $V_{\infty}(\omega) - V_{\infty}^U(\omega)$. This is a problem

for vertical polarization only, however, because $V^U = 0$ for horizontal polarization. Note that the term $\{1 + \exp[-j\omega(2h'+d')/c]\}$ in Eq. (2-109) transforms into the sum of two responses, one starting at $t = 0$ and the second starting at $t = (2h'+d')/c$. When the wires were in a horizontal plane, on the other hand, the negative sign of the exponential term made the second (delayed) response virtually cancel the late-time part of the first response.

The open-circuit differential voltage induced at the terminals of a semi-infinite two-wire line with one wire 2 m above the other is shown in Figure 2-52. With perfectly conducting ground and vertical polarization the voltage builds up in two steps (dashed curve) to a level similar to that shown in Figure 2-50 for horizontal polarization incident on wires in a horizontal plane. With finitely conducting ground, however, the ground effect reduces the level of the second step as illustrated by the solid curve of Figure 2-52. The late-time response also persists much longer for vertical polarization incident on wires in a vertical plane because of the lower reflection coefficient of the soil for vertical polarization. Comparison of the differential-mode voltage of Figure 2-52 with the common-mode voltage of Figure 2-14 indicates that the peak differential-mode voltage is a factor 10 or more smaller than the peak common-mode voltage.

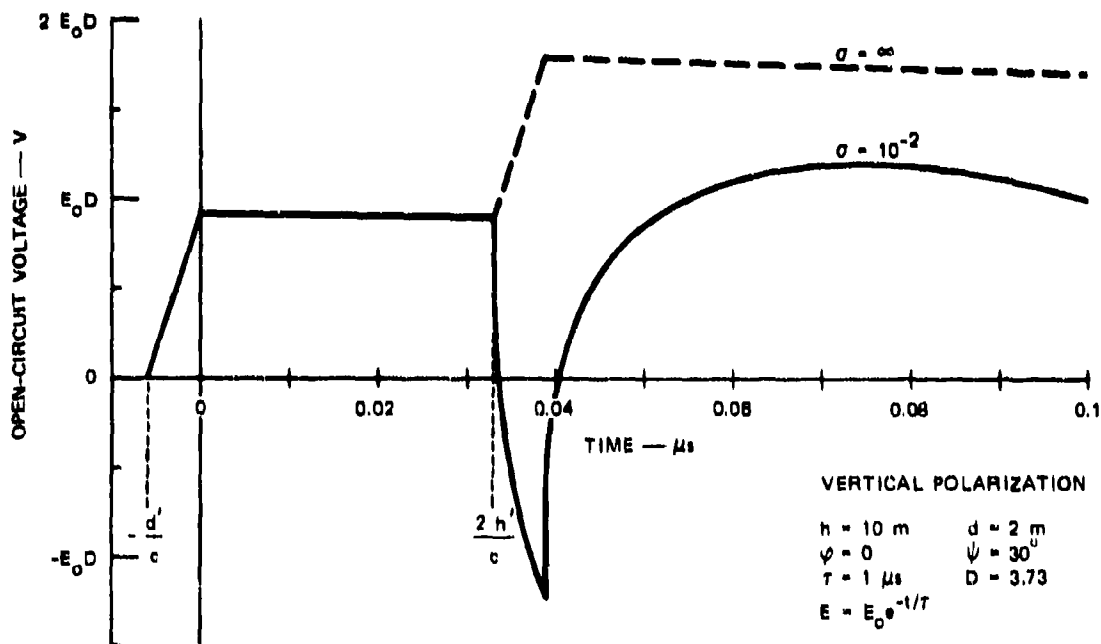


Figure 2-52 OPEN-CIRCUIT DIFFERENTIAL-VOLTAGE WAVEFORM INDUCED IN A SEMI-INFINITE, TWO-WIRE LINE BY AN EXPONENTIAL PULSE (wires in a vertical plane)

2.5.3 MODE CONVERSION AT THE LOAD

In addition to directly induced differential-mode currents in the power lines, differential-mode currents can be developed from the common-mode currents by unbalanced terminations. Consider, for example, a perfectly balanced four-wire transmission line with a common-mode voltage induced on it. As illustrated in Figure 2-53, the lines are represented by their Thevenin equivalent voltage source V_0 and equal characteristic impedances Z_0 , and mutual coupling between the lines will be neglected for simplicity. The unbalanced loads Z_i at the terminals cause unbalanced currents I_i to flow in the individual conductors. The relative magnitudes of the currents are

$$\frac{I_i}{I_4} = \frac{Z_0}{Z_0 + Z_i} \quad i = 1, 2, 3 \quad (2-111)$$

and for a balanced three-phase, 4-wire system in which $I_1 \approx I_2 \approx I_3$, the currents in the phase conductors would be approximately equal, while the current in the neutral might be significantly different from the phase-conductor currents. It is apparent that if Z_i is comparable to Z_0 , the differential current $3I_i - I_4 = I_4(3I_i/I_4 - 1)$ created by the asymmetrical load operating on the common-mode current can be significantly larger than the differential current induced directly by the incident wave.

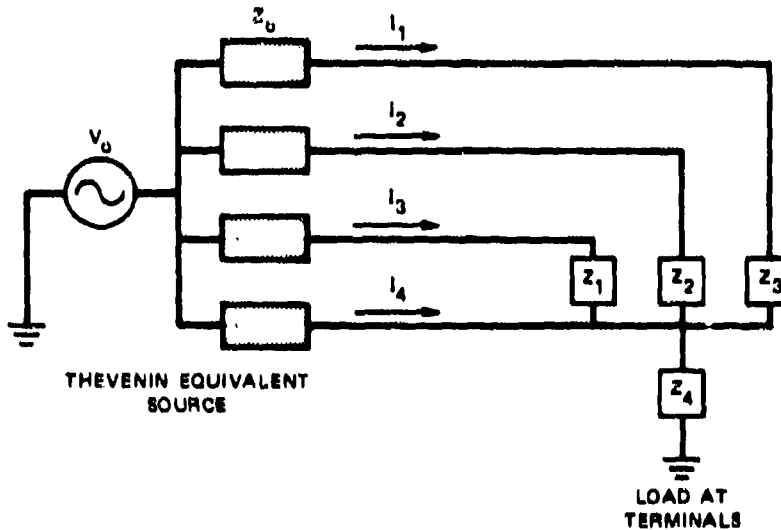


Figure 2-53 ASYMMETRICAL LOAD ON A FOUR-WIRE LINE WITH A COMMON-MODE VOLTAGE

2.6 HIGH-VOLTAGE PROPERTIES OF TRANSMISSION-LINE COMPONENTS

2.6.1 GENERAL

The analysis of interaction of the EMP with power lines indicates that very large voltages (several megavolts) may be induced between the line and ground. However, as indicated in Table 2-2, subtransmission and distribution lines are not designed to sustain such voltages. As a result, it can be expected that the EMP-induced voltages may be limited by insulation breakdown or flashover or cause activation of lightning arresters. Insulation breakdown, in the form of line insulator flashover or corona from the conductors may occur, but little is known about the behavior of these mechanisms for very large rates of rise of the conductor voltage. Fortunately, the very large voltages occur near the ends of the lines where protective devices such as lightning arresters may be installed. Limited data are available on the firing characteristic of distribution-type lightning arresters with large rates of rise. In this section, the high-voltage properties of line insulators, lightning arresters, and conductors are reviewed.

Table 2-2
TENTATIVE AIEE STANDARD ON INSULATION TESTS FOR OUTDOOR
AIR SWITCHES, INSULATOR UNITS, AND BUS SUPPORTS

Withstand Voltage (kV)			
Voltage Rating (kV)	Low Freq. 1 Min. (Dry)	Low Freq. 10 Sec. (Wet)	Impulse 1.5X40 Full Wave (Pos. or Neg.)
7.5	36	30	95
15	50	45	110
23	70	60	150
34.5	95	80	200
48	120	100	250
68	175	145	350
92	225	190	450
115	280	230	550
138	335	275	650
161	385	315	750
196	465	385	900
230	545	445	1050
287	680	555	1300
345	810	665	1550

Source: Ref. 1.

2.6.2 INSULATOR FLASHOVER CHARACTERISTICS

As implied in Table 2-2, insulators used in transmission and distribution systems can withstand an "impulse" voltage of 3 to 12 times the line voltage (with the higher multiples applying to the lower line-voltage ratings.) These ratings presumably apply to the "new-equipment" state, so that deterioration in service may reduce these insulation limits. Furthermore, the actual voltage the insulator can withstand depends on the polarity and the rate of rise or duration of the transient applied voltage. Because insulation flashover involves the formation of long (at least several inches) spark discharge channels, the arc formation time is significant in determining the magnitude and duration of the transient voltage that can be sustained without a high current discharge. In addition, because the spark formation in air is basically an electron avalanching process, in a nonuniform field, the breakdown conditions are quite different when the wire is positive from when it is negative.

The "impulse" flashover characteristics of some insulators in the 7.5-to-89 kV class are shown in Figure 2-54 for positive and negative voltage applied to the top of the insulator. These insulators display the typical characteristics of lower positive-voltage flashover thresholds and sharply increasing flashover voltage with increasing rate of rise of the voltage. These data are for the commonly used "impulse" that reaches its peak in 1.5 μ s and decays to half its peak value in 40 μ s. Flashover data are not available for applied voltage with rise times (or times to flashover) less than about 0.25 μ s.

Figure 2-55 shows similar data (plotted in a different form) for strings of suspension insulators.

Insulator flashover voltage also depends somewhat on altitude (or barometric pressure) and temperature, but the dependence on these parameters is relatively unimportant from an EMP point of view (the altitude dependence may be significant for lines in high mountainous regions, however). Contamination and adverse weather effects cause deviations from the flashover characteristics at standard air conditions shown in Figures 2-54 and 2-55. These deviations are likely to be more important and less predictable than those caused by variations in temperature or by normal fluctuations in surface barometric pressure.

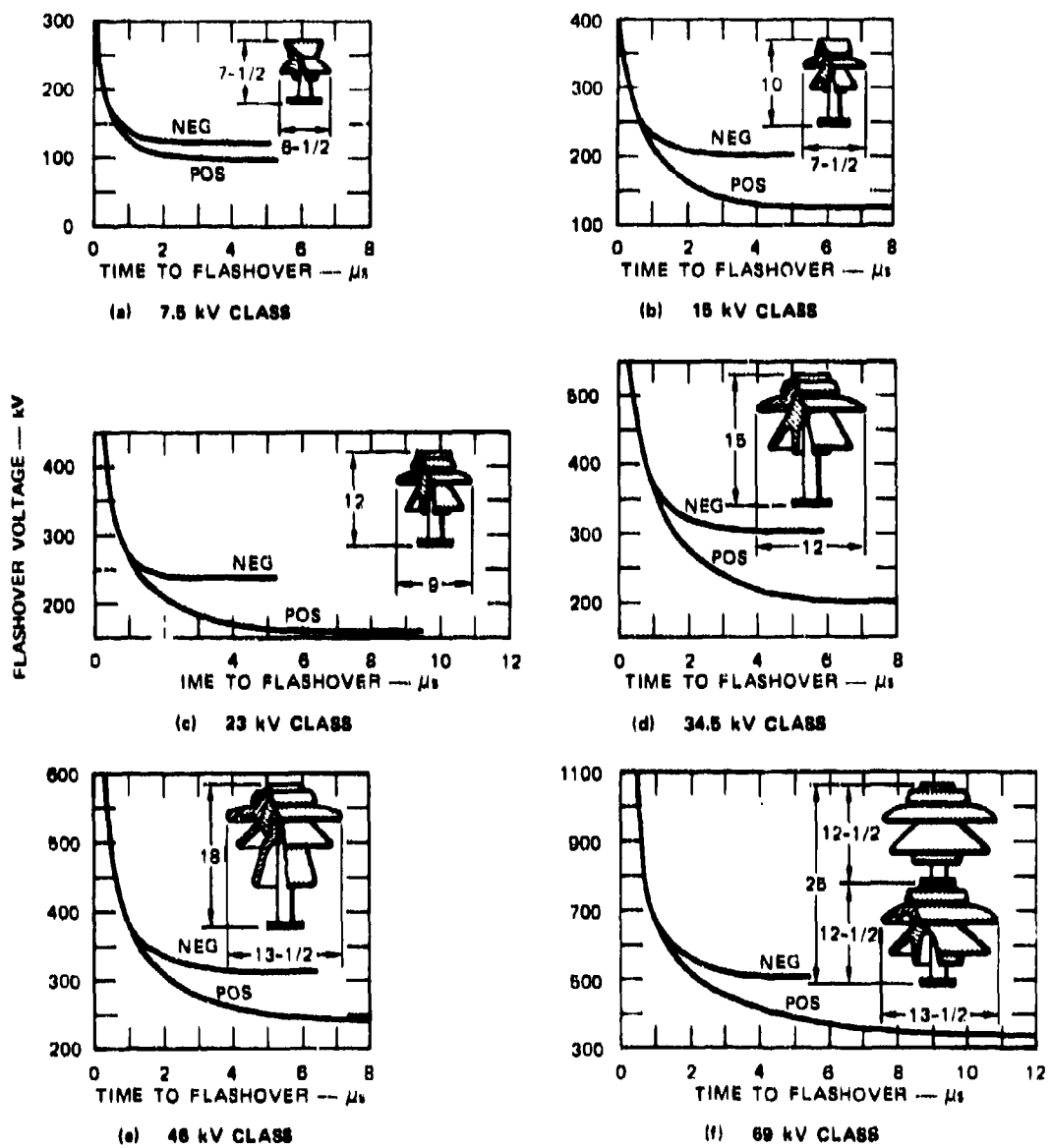


Figure 2-54 IMPULSE FLASHOVER CHARACTERISTICS OF PARTICULAR TYPES OF APPARATUS INSULATORS ON POSITIVE AND NEGATIVE 1-1/2 x 40 WAVES AT STANDARD AIR CONDITIONS. Source: Ref. 1.

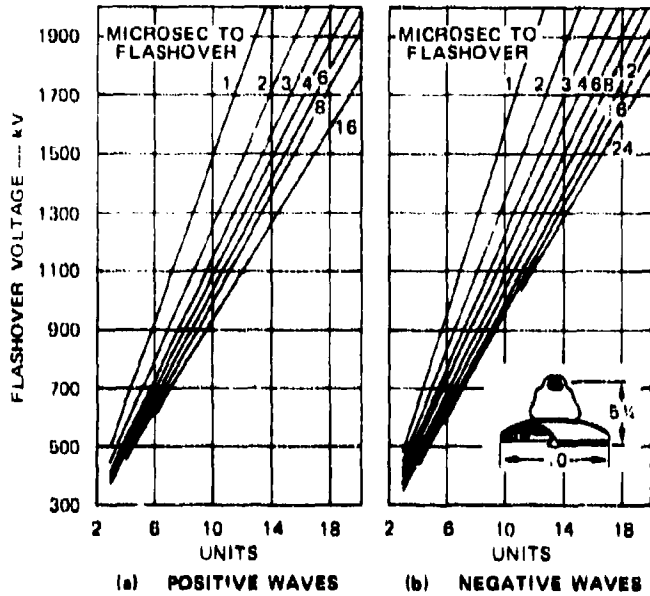
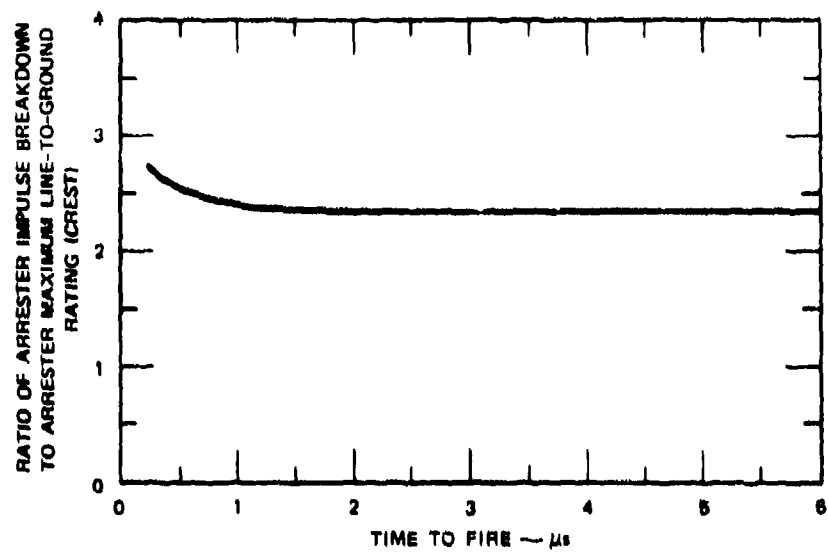


Figure 2-55 IMPULSE FLASHOVER CHARACTERISTICS OF SUSPENSION INSULATORS FOR 1-1/2 x 40 WAVES AT 77°F, 30-INCH BAROMETRIC AND 0.6085-INCH VAPOR PRESSURE. Relative air density = 1.0. Source: Ref. 1.

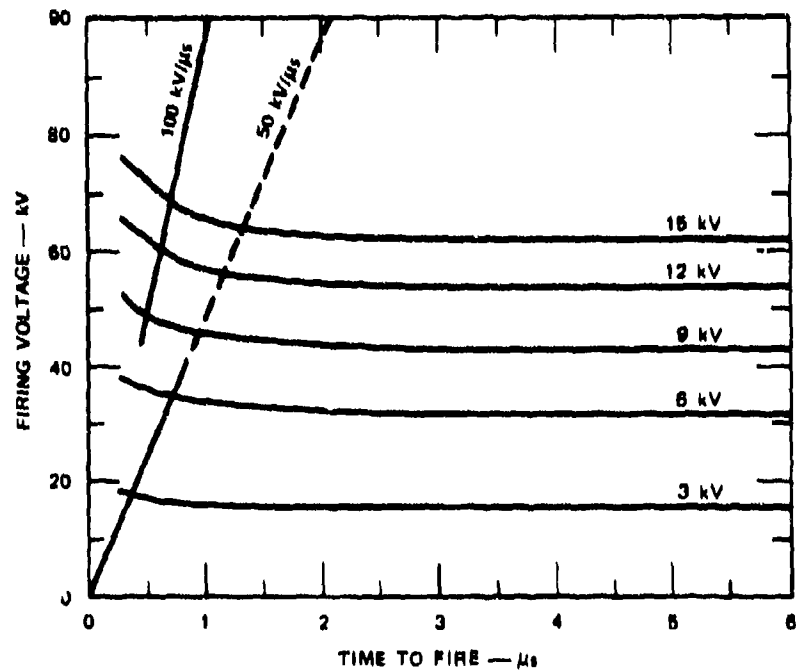
2.6.3 LIGHTNING-ARRESTER FIRING CHARACTERISTICS

The properties of commercial lightning arresters used in transmission and distribution systems are usually not specified for very-fast rising pulses, since the transients produced by lightning usually have rise times greater than 1 μ s. Typical firing characteristics of line and distribution lightning arresters are shown in Figure 2-56. These data indicate that the firing voltage increases 10% to 15% above the dc (slow pulse) firing voltage if the time to fire is shortened to 250 ns.^{1,3} Further reductions in time-to-fire will certainly be accompanied by further increases in firing voltage.

The time-to-fire and the firing voltage of the 9-kV distribution lightning arresters used to protect the transformers are plotted in Figure 2-57.²⁸ The maximum rate of rise of the voltage applied across the lightning arresters was 2.5 kV/ns, or about 25 times faster than that normally specified for 9-kV arresters. With this rate of rise (also plotted in Figure 2-56), the firing voltage was 100 kV, or about 2.5 times the static firing threshold, and the time-to-fire was only 40 ns.



(a) LINE-TYPE LIGHTNING ARRESTERS.



(b) DISTRIBUTION-TYPE LIGHTNING ARRESTERS

Figure 2-56 BREAKDOWN VOLTAGE AS A FUNCTION OF TIME-TO-FIRE FOR LIGHTNING ARRESTERS. Source: Ref. 5.

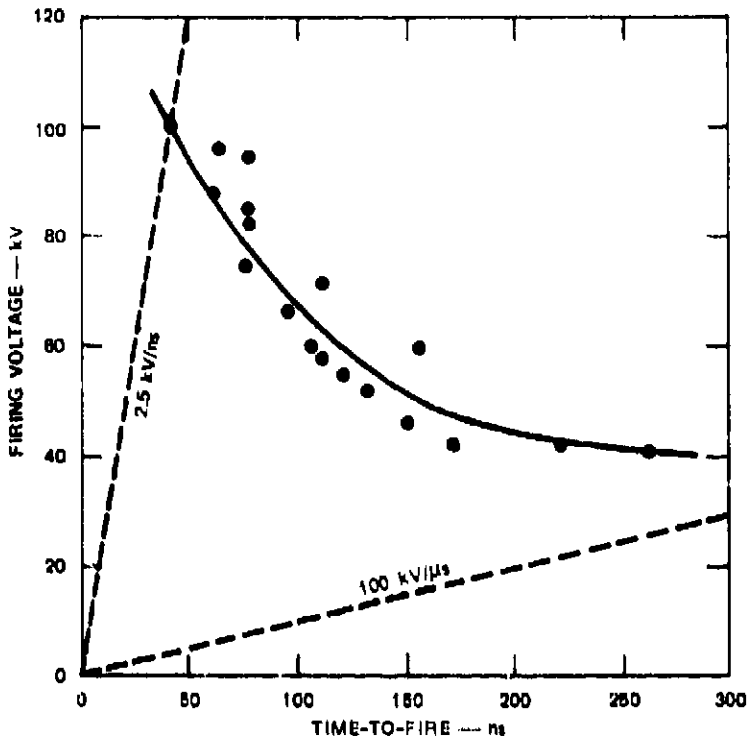


Figure 2-87 9-kV-DISTRIBUTION LIGHTNING-ARRESTER FIRING CHARACTERISTICS FOR FAST RATES OF RISE. Sources: Refs. 2 and 3.

The trend of increasing firing voltage with increasing rate of rise of the applied voltage is typical of spark-discharge devices and insulation flashover. Because lightning arrester firing and line insulator, transformer, or pothead bushing flashover involve similar air breakdown processes, it is expected that the lightning arrester that is designed to protect these components for slowly rising transients will also protect them for fast-rising transients. If solid or liquid insulation is protected by the lightning arrester, however, this generalization may not be valid because the temporal characteristics of solid or liquid breakdown may be different from those of air.

2.8.4 CORONA THRESHOLD OF CONDUCTORS

Even without lightning-arrester breakdown or insulation flashover, there is a high-voltage limit imposed by the dielectric strength of the air about the power conductors. When

the electric-field strength at the surface of the conductor exceeds 3×10^6 V/m, the air will break down and a corona discharge or arc leader will form. The field strength at the surface of a round wire at a height h , of radius a , and at a voltage V relative to ground is

$$E \approx \frac{V}{a \log \frac{2h}{a}} . \quad (2-112)$$

A plot of the static voltage V required to produce the corona-threshold field strength at the surface of the wire 10 m above the ground is plotted in Figure 2-58 as a function of wire radius. Since most distribution-line conductors are 1 cm or less in diameter, it is apparent from Figure 2-58 that the corona-threshold voltage of these conductors will be less than 250 kV.

If the transmission line is made up of three or more conductors, as is usually the case, the field strength at the surface of individual wires will be less, for a given potential, than for a single wire. This decrease in surface field strength or increase in corona-threshold voltage can, at the most, be in proportion to the number of wires, but it is usually considerably less. For three wires on a horizontal cross-arm, the corona-threshold potential of the two outer wires will be only slightly greater than the threshold potential of a single wire of the same size, but the threshold potential of the middle wire will be significantly higher because it is shielded by the outer wires. (Note that the surface field strength does not decrease in proportion to the increase in effective radius for a multiple-conductor system; the effective radius for the purposes of computing common-mode capacitance and inductance per unit length may increase by a factor of 100 if three conductors spaced a meter apart are used, but the conductor surface over which the charge is distributed has increased by only a factor of 3 over that of a single conductor.)

Corona losses on transmission lines have the effect of distorting the leading edge and limiting the peak of a transient voltage pulse.²⁷⁻²⁹ Therefore corona losses in combination with lightning arresters will limit the wire-to-ground potential difference of typical distribution lines to about 500 kV or less. Because these limiting actions are not equal for all of the conductors of the transmission line, however, sizable differential voltages may be generated on the transmission line. These differential-mode voltages, as well as the common-mode voltages, must pass through the distribution transformer to affect the customer equipment. A discussion of the behavior of the transformer is contained in Chapter Four.

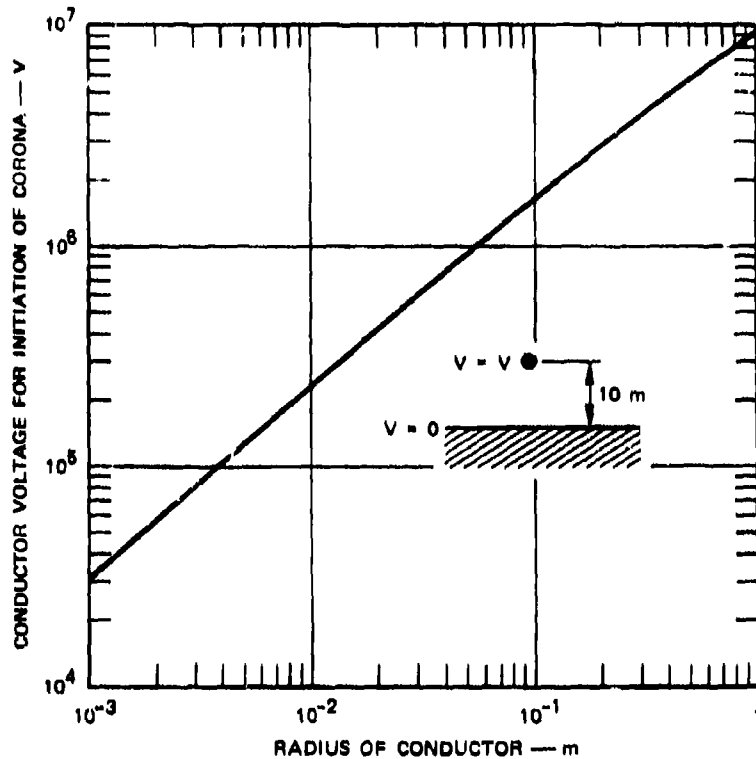


Figure 2-58 CORONA-THRESHOLD VOLTAGE OF A WIRE OVER GROUND WITH STANDARD AIR CONDITIONS. Source: Ref. 4.

2.7 CITED REFERENCES

1. *Electrical Transmission and Distribution Reference Book* (Westinghouse Electric Corporation, East Pittsburgh, Pennsylvania, 1964).
2. A. E. Knowlton, Ed., *Standard Handbook for Electrical Engineers* (McGraw-Hill Book Co., Inc., New York, N.Y., 1949).
3. W. W. Lewis, *The Protection of Transmission Systems Against Lightning* (John Wiley & Sons, Inc., New York, N.Y., 1950).
4. E. F. Vance and S. Dairiki, "Analysis of Coupling to the Commercial Power System," AFWL-TR-72-21, Contract F29601-69-C-0127, Air Force Weapons Laboratory, Kirtland Air Force Base, New Mexico (August 1972).
5. C. Flammer and H. E. Singhaus, "The Interaction of Electromagnetic Pulses with an Infinitely Long Conducting Cylinder Above a Perfectly Conducting Ground," Interaction Note 144, Contract F29601-69-C-0127, SRI Project 7995, Stanford Research Institute, Menlo Park, Calif. (July 1973, unpublished report).

6. C. Flammer, "On the Scattering of Electromagnetic Waves by a Perfectly Conducting Cylinder Over a Finitely Conducting Ground," Interaction Note 145, Contract F29601-69-C-0127, SRI Project 7995, Stanford Research Institute, Menlo Park, Calif. (August 1973, unpublished report).
7. W. E. Scharfman and E. F. Vance, "EMP Coupling and Propagation to Power Lines: Theory and Experiments," AFWL-TR-73-287, Contract F29601-69-C-0127, Air Force Weapons Laboratory, Kirtland Air Force Base, New Mexico (May 1973).
8. W. E. Scharfman, K. A. Graf and E. F. Vance, "Analysis of Coupling to Horizontal and Vertical Wires," Technical Memorandum 22, Contract F29601-69-C-0127, SRI Project 7995, Stanford Research Institute, Menlo Park, Calif. (January 1973, unpublished report).
9. S. Frankel, "Field Coupling Parameters for a Single Round Wire Close to a Ground Plane or Two Large Round Wires in Free Space," HDL-TM-72-14, MIPR 2.00518, Subtask EB-088, HDL Project E05E6, Harry Diamond Laboratories, Washington, D.C. (April 1972).
10. S. Frankel, "Externally Excited Transmission Line: Definition of Procedures for Determining Coupling Parameters," HDL-TM-72-11, AMCMF Code 5910.21.63387, HDL Project E05E3, Harry Diamond Laboratories, Washington, D.C. (May 1972).
11. J. A. Auxier, W. S. Snyder, and D. M. Davis, "Health Physics Division Annual Progress Report," Contract No. W-7405-eng-26, ORNL-4903, Oak Ridge National Laboratory, Tennessee (September 1973).
12. J. H. Marable, J. K. Baird, and D. B. Nelson, "Effects of Electromagnetic Pulse (EMP) on a Power System," Final Report, Interagency Agreement No. AEC 40-31-64 and OCD-PS-64-284, Work Unit 2213C, ORNL-4836, Oak Ridge National Laboratory, Oak Ridge, Tennessee (December 1972).
13. "Civil Defense Research Project Annual Progress Report," Contract No. W-7405-eng-26, ORNL-4784, Oak Ridge National Laboratory, Oak Ridge, Tennessee (December 1972).
14. "Civil Defense Research Project Annual Progress Report," Contract No. W-7405-eng-26, ORNL-4679, Oak Ridge National Laboratory, Oak Ridge, Tennessee (March 1972).
15. D. B. Nelson, "A Program to Counter the Effects of Nuclear Electromagnetic Pulse in Commercial Power Systems," ORNL-TM-3552, Part I, Oak Ridge National Laboratory, Oak Ridge, Tennessee (October 1972).
16. D. B. Nelson, "Effects of Nuclear EMP on AM Radio Broadcast Stations in the Emergency Broadcast System," ORNL-TM-2830, Oak Ridge National Laboratory, Oak Ridge, Tennessee (July 1971).

17. "EMP and Electric Power Systems," TR-61-D, Defense Civil Preparedness Agency, Washington, D.C. (December 1972).
18. E. C. Jordan, *Electromagnetic Waves and Radiating Systems* (Prentice-Hall, Inc., New York, N.Y., 1950).
19. S. A. Schelkunoff, *Antennas: Theory and Practice* (John Wiley & Sons, Inc., New York, N.Y., 1952).
20. S. Ramo and J. R. Whinnery, *Fields and Waves in Modern Radio* (John Wiley & Sons, Inc., New York, N.Y., 1953).
21. *Reference Data for Radio Engineers* 5th Ed. (Howard W. Sams & Co., Inc., A Subsidiary of ITT, New York, N.Y., 1969).
22. G. A. Korn, *Basic Tables in Electrical Engineering* (McGraw-Hill Book Co., New York, N.Y., 1965).
23. E. D. Sunde, *Earth Conduction Effects in Transmission Systems* D. Van Nostrand Co., Inc., New York, N.Y., 1949).
24. R. W. P. King, *Transmission-line Theory* (Dover Publications, Inc., New York, N.Y., 1955).
25. C. D. Taylor, R. S. Scatterwhite, and C. W. Harrison, Jr., "The Response of a Terminated Two-Wire Transmission Line Excited by a Nonuniform Electromagnetic Field," *Proc. IEEE*, Vol. AP-13, No. 6, pp. 987-989 (November 1965).
26. R. T. Bly, Jr. and E. F. Vance, "High-Voltage Transient Tests of Service Transformers, Lightning Arresters, and an Automatic Switching Unit," AFWL-TR-74-34, Contract F29601-69-C-0127, Air Force Weapons Laboratory, Kirtland Air Force Base, New Mexico (October 1973).
27. L. V. Bewley, *Traveling Waves on Transmission Systems* (Dover Publications, Inc., New York, N.Y., 1933).
28. R. Rudenberg, *Electrical Shock Waves in Power Systems* (Harvard University Press, Cambridge, Mass., 1968).
29. A. Greenwood, *Electrical Transients in Power Systems* (John Wiley & Sons, Inc., New York, N.Y., 1971).

Chapter Three

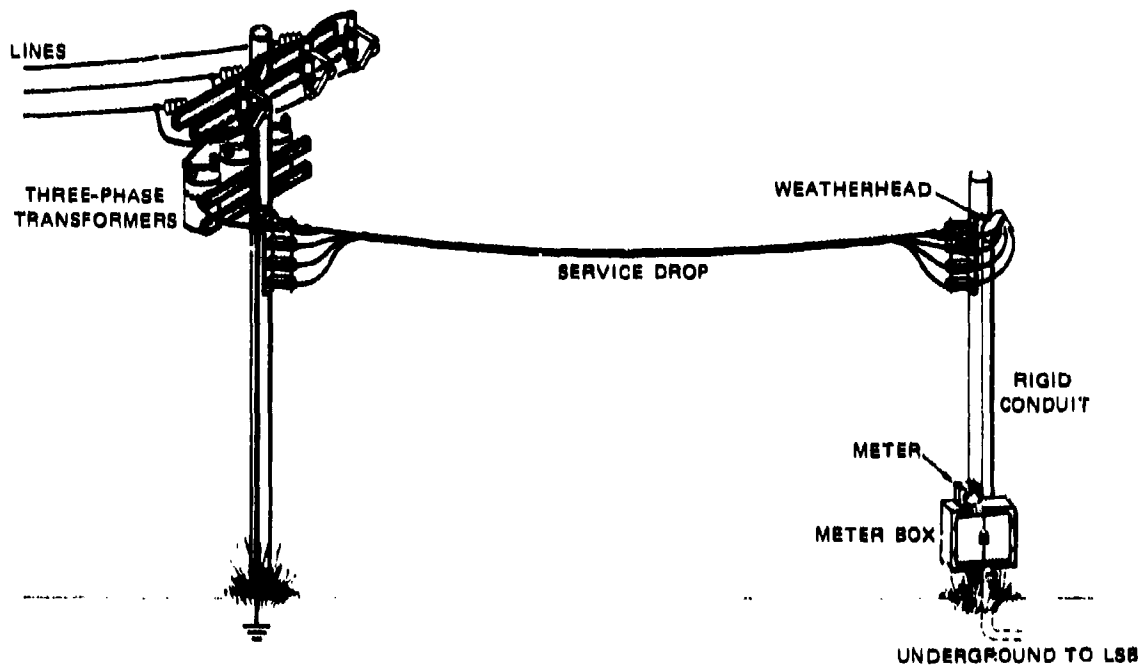
CONSUMER'S SERVICE ENTRANCE

3.1 INTRODUCTION

3.1.1 DESCRIPTION OF THE SERVICE ENTRANCE

At the consumer's end of a distribution line, the distribution voltage is reduced with transformers to the level required by the consumer (e.g., 120 V, 240 V, 480 V, etc.), metered, and wired to the consumer's main circuit-breaker and distribution panel. The properties of this equipment between the end of the aerial distribution line and the low-voltage circuit feeding the main circuit-breaker panel affect the coupling of the EMP-induced signal to the consumer's circuits. In this chapter, typical service-entrance properties and installation practices are described, and their effect on the EMP coupling is discussed. The distribution transformer, which is an important component of this terminal equipment, is discussed separately in Chapter Four.

For purposes of discussing their effects on EMP coupling, service entrance installations have been divided into two categories according to whether the service transformers are pole-mounted, as in Figure 3-1(a), or ground-based, as in Figure 3-1(b). For pole-mounted transformer installations, the transformers are usually installed on the last pole of the distribution line, and the low-voltage service drop is carried along a messenger cable to a service-entrance weatherhead, where the low-voltage conductors enter rigid steel conduit.



(a) SERVICE WITH POLE-MOUNTED TRANSFORMERS

Figure 3-1 TYPICAL POWER SERVICE ENTRANCES

The service entrance may be on a separate pole, as shown in Figure 3-1(a), it may be on the roof or exterior wall of a building, or it may be on the same pole as the transformers. There is some variation in the mounting of the transformers, also. For example, they may be mounted on a platform supported by four poles, rather than mounted directly on the final pole.

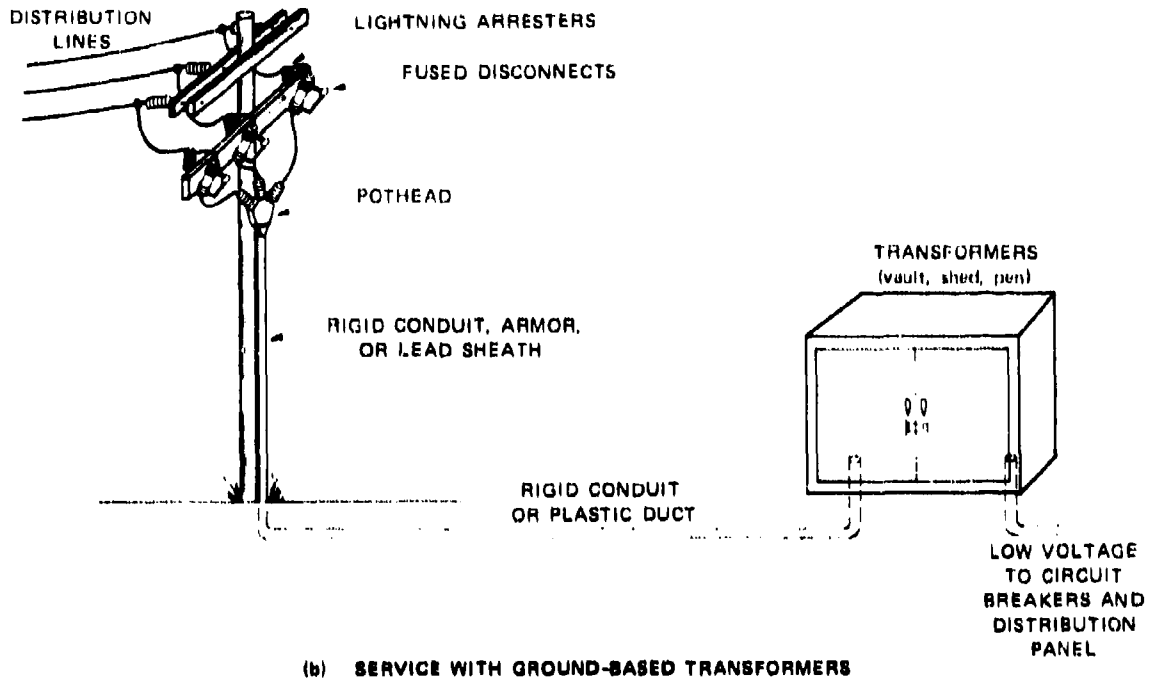


Figure 3-1 (Concluded)

3.1.2 GROUND-BASED TRANSFORMER INSTALLATIONS

Ground-based transformer installations are distinguished by the characteristic that the distribution voltage is carried underground from the last pole to the transformers. The transformers may be located in a shed or fenced-in area near the consumer's buildings, or they may be in a vault within the consumer's building. Shielded cables are used to transmit power from the pothead near the top of the last pole to the transformers. These cables are usually routed through rigid steel conduit or plastic or fiber duct for mechanical protection underground and on the pole.

The principal components of the ground-based transformer installations that affect the EMP coupling and voltage-limiting are the potheads, the shielded cable, and the steel or fiber duct. (Transformer characteristics are also important; they are discussed in Chapter Four.) The pothead is a weatherproof interface between the aerial distribution line and the

shielded cable used for the underground service entrance. Typical potheads for use with single- and three-conductor lines are shown in Figure 3-2. Basically, they consist of insulated high-voltage bushings, to which the aerial conductors are connected, and a controlled-gradient termination for the shields and/or lead sheath of the underground cables. The lower cavity of the pothead is usually filled with an asphalt-based compound to weatherproof and seal the cable termination. The dielectric strength of the pothead should be commensurate with the basic insulation level required for the distribution voltage (see Table 3-1). To prevent damage to the pothead and cable insulation, the pothead is usually protected with lightning arrestors.

Cables for use at distribution voltages are stranded copper or aluminum insulated with cross-linked polyethylene and shielded (for gradient control) with spiral-wound copper tape. An overall lead sheath or vinyl jacket is sometimes provided for mechanical protection. The construction of typical one- and three-conductor cables is shown in Figure 3-3. Semiconducting tape and semiconducting polyethylene are sometimes used adjacent to the inner and outer conductors for electric gradient control. A concentric wrap of solid copper strands may also be provided over the shield tape if the shield carries appreciable current (the shield tape is usually only a few mils thick and is used for gradient control rather than to carry return or neutral currents). In some older installations, paper-insulated cable may be found.¹

Rigid steel conduit is almost always used at the ends of the conduit run (i.e., at the pole and at the transformer) but plastic (styrene) or fiber conduit is often used along the buried portion of the run. The plastic or fiber duct may be of the rigid, direct-burial type (Type II), or of the concrete-encasement type (Type I) that is partially encased in concrete after it is installed in the trench. This encasement is normally accomplished by laying the conduits on a bed of sand so that they are less than one-third embedded in sand, then pouring concrete over the conduits until the trench is filled to a few inches above the top of the conduits. The remainder of the trench is then backfilled to grade level with local soil. From an EMP coupling standpoint, the rigid steel conduit can provide excellent shielding for the cables and it provides a uniform return conductor for the common-mode current on the cables. Plastic and fiber conduits provide no shielding and no return path for the common-mode current.

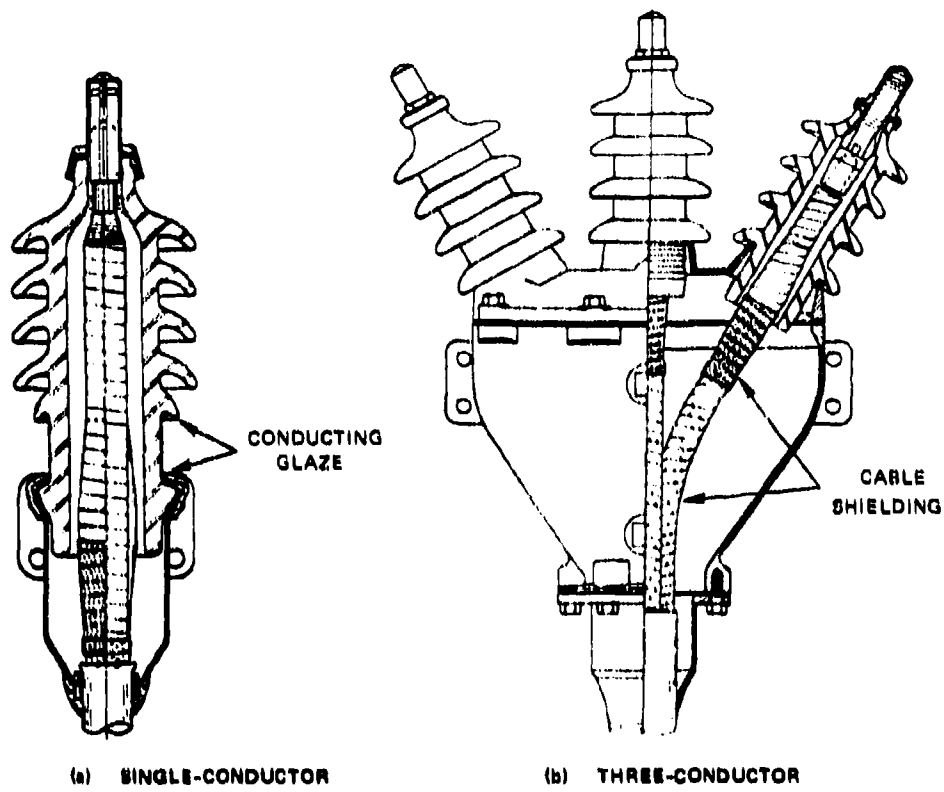


Figure 3-2 POTHEADS FOR SINGLE- AND THREE-CONDUCTOR CABLES

3.1.3 POLE-MOUNTED TRANSFORMER INSTALLATIONS

For installations with pole-mounted transformers, the low-voltage conductors may be exposed to the EMP fields between the transformer and the service entrance. Because the components in the low-voltage system are not specifically designed to withstand high voltages, this portion of the installation may be vulnerable to large induced voltages (even if the transformer does not pass extremely large common-mode voltages). Vinyl- or neoprene-insulated cables are normally used for the low-voltage service. These cables are typically loosely spiraled about a steel messenger cable (which may also serve as a ground or neutral conductor) between the transformer and the service entrance. The service-entrance weatherhead is a hooded conduit fitting that permits the cables to be brought into the conduit without permitting varmints or excessive rainwater to enter the building through the conduits. The service-entrance weatherhead contains an insulating spacer for the cables so

Table 3-1

**SUGGESTED WITHSTAND IMPULSE VOLTAGES
FOR CABLES WITH METALLIC COVERING***

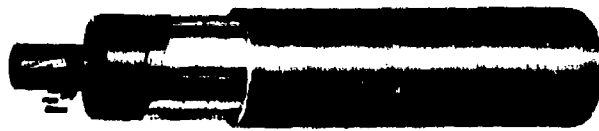
Rated Voltage (kV)	Basic Impulse Insulation Level for Equipment (kV)	Solid-Paper Insulation		Oil-Filled-Paper Insulation	
		Insulation Thickness (mils)	Withstand Voltage (kV)	Insulation Thickness (mils)	Withstand Voltage (kV)
1.2	30	78	94	—	—
2.5	45	78	94	—	—
5.0	60	94	113	—	—
8.7	75	141	189	—	—
15	110	203	244	110	132
23	150	266	319	145	174
34.5	200	375	450	190	228
46	250	489	563	225	270
69	350	688	825	315	378
115	550	—	—	480	576
138	650	—	—	580	672
161	750	—	—	648	780
230	1050	—	—	925	1110

*Source: Ref. 1.

that they are separated from each other and from the rough edges of the metal hood. A typical service entrance is shown in Figure 3-4.

Although the cable and weatherhead insulation are not designed for high-voltage applications, insulation breakdown in the low-voltage cable system seldom occurs in the conduit or weatherhead unless the cable is old and deteriorated. Breakdown usually occurs where the insulation has been removed or compromised, such as in the metering cabinet where the cable insulation has been removed to make the meter voltage taps, or at the main circuit-breaker panel where the insulation is removed to make the connection to the circuit breaker terminals.

It is also noteworthy that although large voltages may be induced in the low-voltage service drop, there is some voltage-limiting built into the secondary terminals of the transformer, which normally has a voltage-limiting spark gap built into the hardware associated with at least one of the secondary bushings. In addition, when long, exposed service drops are used, it is not uncommon to install secondary lightning arresters in the low-voltage circuit at the transformer, service entrance, or main circuit-breaker panel (or all three).



(a) SINGLE-CONDUCTOR SOLID, COMPACT-ROUND CONDUCTOR



(b) THREE-CONDUCTOR SHIELDED, COMPACT-SECTOR CONDUCTORS

Figure 3-3 SHIELDED CABLES FOR SERVICE ENTRANCE

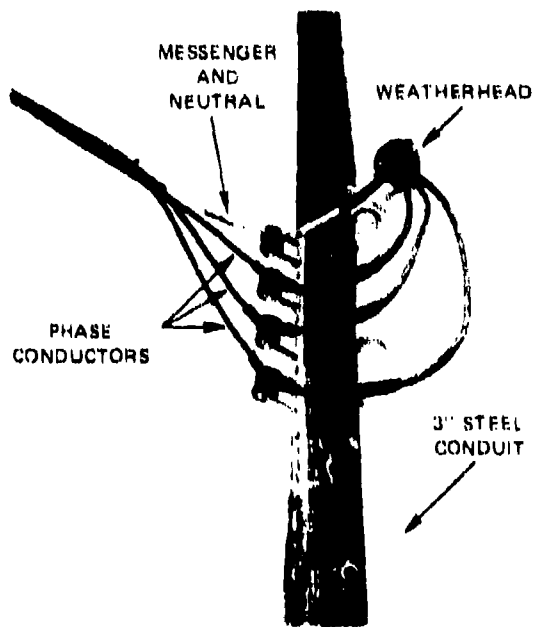


Figure 3-4 POLE-MOUNTED SERVICE ENTRANCE

3.1.4 EFFECT OF SERVICE ENTRANCE ON EMP COUPLING²

The consumer service entrance is an important part of the power system for EMP coupling considerations because it is closer to the consumer's equipment than the remainder of the system, and because of the following:

- (1) The service transformer behaves as a bandpass filter (see Chapter Four).
- (2) The low-voltage entrance-conduit circuits or shielded service-entrance cables have much lower characteristic (surge) impedances than the aerial distribution lines.
- (3) Additional EMP coupling can occur along the unshielded low-voltage service drop or along service-entrance cables in buried plastic or fiber ducts.
- (4) Voltage limiting may occur at lightning arresters and in low-voltage circuits.

The difference in characteristic impedance between the aerial transmission lines and the shielded service-entrance cables used in ground-based transformer installations causes a large mismatch between these transmission lines. For times less than the round-trip propagation time from the pothead to the transformer, the common-mode load impedance on the aerial transmission line is the parallel combination of the characteristic impedances of the shielded service-entrance cables. Since the source impedance of the aerial transmission lines is several hundred ohms and the characteristic impedance of the shielded cables (in parallel) is of the order of ten ohms, only a small fraction of the large open-circuit voltage induced in the aerial transmission line is transmitted through the shielded cables; the remainder is reflected back down the aerial line.

At times greater than the round-trip propagation time on the shielded cables, the transformer and the loads on its secondary winding affect the input impedance at the pothead seen by the aerial line. In the frequency domain, however, the shielded cables may behave as matching transformers that provide maximum coupling between the aerial transmission line and the transformer for a band (or several bands) of frequencies in the pulse spectrum. Because of the narrow bandwidth of the matching-transformer effect, this effect is usually not important in terms of transformer insulation breakdown, but it is important

In determining the spectral content of the signal delivered to the consumer's low-voltage circuits.

Similar considerations apply to the low-voltage conduit circuit between the service-entrance and the main circuit-breaker panel in pole-mounted transformer installations. The principal differences in this case are: (1) the signal induced in the aerial transmission line is filtered by the transformers before it gets to the service-entrance weatherhead, and (2) the common-mode characteristic impedance of the conductors in conduit is somewhat larger than that of the shielded service-entrance cables.

In the case of pole-mounted transformers with long, low-voltage service drops, significant voltage can be induced in the service drop by the EMP in much the same way as it is induced in the aerial distribution line. This voltage will enter the conduit circuit before the voltage induced in the transmission line behind the transformer, and it may be larger than that passing through the transformer (particularly if the transformer is protected with lightning arresters). Similarly, current may be induced in the shields of the buried shielded cables between the potheads and ground-based transformer when these cables are in plastic ducts, but if the cable shields are effective, the voltage induced between the conductor and the shield by this means is a major concern only if the cables are quite long (several hundred feet). If steel conduit is used for the entire run instead of plastic conduit, the voltage induced in the buried cables will usually be relatively small (compared to that delivered by the aerial transmission line) unless the run is several thousand feet long.

Intentional voltage-limiting occurs in the terminal installation because of distribution lightning arresters protecting the transformer or pothead bushings and secondary lightning arresters (if present) at the weatherhead and main circuit-breaker panels. Unintentional voltage limiting may occur because of low-voltage insulation breakdown at metering taps, circuit-breaker terminals, and similar points where the insulation is weak. Voltage breakdown in the low-voltage system may have deleterious effects such as damage to the watt-hour meter and damage to power-monitoring relays and control circuits.

3.2 TRANSMISSION THROUGH CONDUITS AND CABLES

3.2.1 TRANSFER FUNCTIONS FOR CONDUITS AND SHIELDED CABLES

The conduit and conductors between the service-entrance weatherhead and the main distribution panel, and the shielded cables between the potheads and the transformers can be analyzed as transmission-line segments between the source (aerial transmission lines) and the load (low-voltage circuits or transformer primary). The equivalent circuit for this part of the system is illustrated in Figure 3-5 where the source is represented by an open-circuit voltage V_0 and a source impedance Z_1 and the load is represented by Z_L . The transmission line has a characteristic impedance Z_0 and is of length ℓ . For a long(semi-infinite) aerial distribution line connected to shielded cables for transformer service, the source voltage V_0 and impedance Z_1 are the open-circuit voltage induced in the semi-infinite line and its characteristic impedance. The load impedance Z_L is the input impedance of the primary terminals of the transformer, including any lead inductance and bushing capacitance.

The reflection coefficient at the load end of the transmission line is defined by³

$$\rho = \frac{Z_L - Z_0}{Z_L + Z_0} \quad (3-1)$$

and the propagation factor for the line is $\gamma = \alpha + j\beta$. The ratio of the voltage $V(\ell)$ across the load to the source voltage V_0 is

$$\frac{V(\ell)}{V_0} = \frac{(1 + \rho)e^{-\gamma\ell}}{\frac{Z_1}{Z_0} (1 - \rho e^{-2\gamma\ell}) + (1 + \rho e^{-2\gamma\ell})} \quad (3-2)$$

Plots of the magnitude of this transfer function are shown in Figure 3-6 for Z_L resistive, Figure 3-7 for Z_L inductive, and Figure 3-8 for Z_L capacitive. These results are for a lossless air-insulated transmission line ($\gamma = jk = j\omega/c$) 30 m long and a source impedance of 300 ohms (typical of an aerial distribution line). A characteristic impedance of 10 ohms is assumed for the transmission line. However, these data can be applied to any similar circuit with

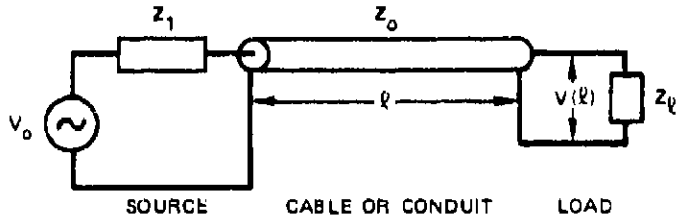


Figure 3-5 APPROXIMATE EQUIVALENT CIRCUIT FOR ANALYSIS OF TRANSMISSION THROUGH SHIELDED CABLE OR CONDUIT FEEDER CIRCUITS

$Z_1/Z_0 = 30$ for which the values of R/Z_0 , Lc/lZ_0 , or cZ_0C/R shown are applicable, if the upper normalized-frequency ($k\ell$) scale is used. (The speed of light, c , may be replaced by the propagation velocity $v = c/\sqrt{\epsilon_r}$ if insulation other than air is used.)

Note that for all load impedances except the matched resistive load ($Z_L = R + Z_0$), the transfer function is frequency-selective and tends to pass certain frequencies more readily than others. Because the first few passbands lie in the range $0.1 < k\ell < 10$, power-system responses are often characterized by fundamental oscillations in this frequency range.

Time-domain responses of the circuit of Figure 3-5 have been obtained experimentally using RF transmission line to simulate the conduit or shielded cable. This line is not lossless, and the load elements are not pure resistances or reactances, so that the waveforms obtained with the analog circuit are somewhat more representative of those that might be observed in a power system. The waveforms for a step voltage V_o with source impedance such that $Z_1/Z_0 = 30$ are shown in Figure 3-9 for resistive loads. It is seen in Figure 3-9(a) that the voltage $V(\ell)$ across the load resistance is a stair-step rising toward $R/(R + Z_1)$ when $R > Z_0$. The length of the steps is $2\ell/c$, and the "smoothed" stair-step for $R > Z_0$ approaches an exponential function $V_1[1 - \exp(-t/\tau)]$ where

$$\tau = \frac{RZ_1C}{R + Z_1} \quad (3-3)$$

$$V_1 = \frac{R}{R + Z_1} V_o \quad (3-4)$$

and C is the total capacitance of the transmission line ($C = l/cZ_0$). When $R < Z_0$, as in Figure 3-9(b), a damped square wave of initial amplitude $2RZ_0/(R + Z_0)(Z_1 + Z_0)$ oscillating

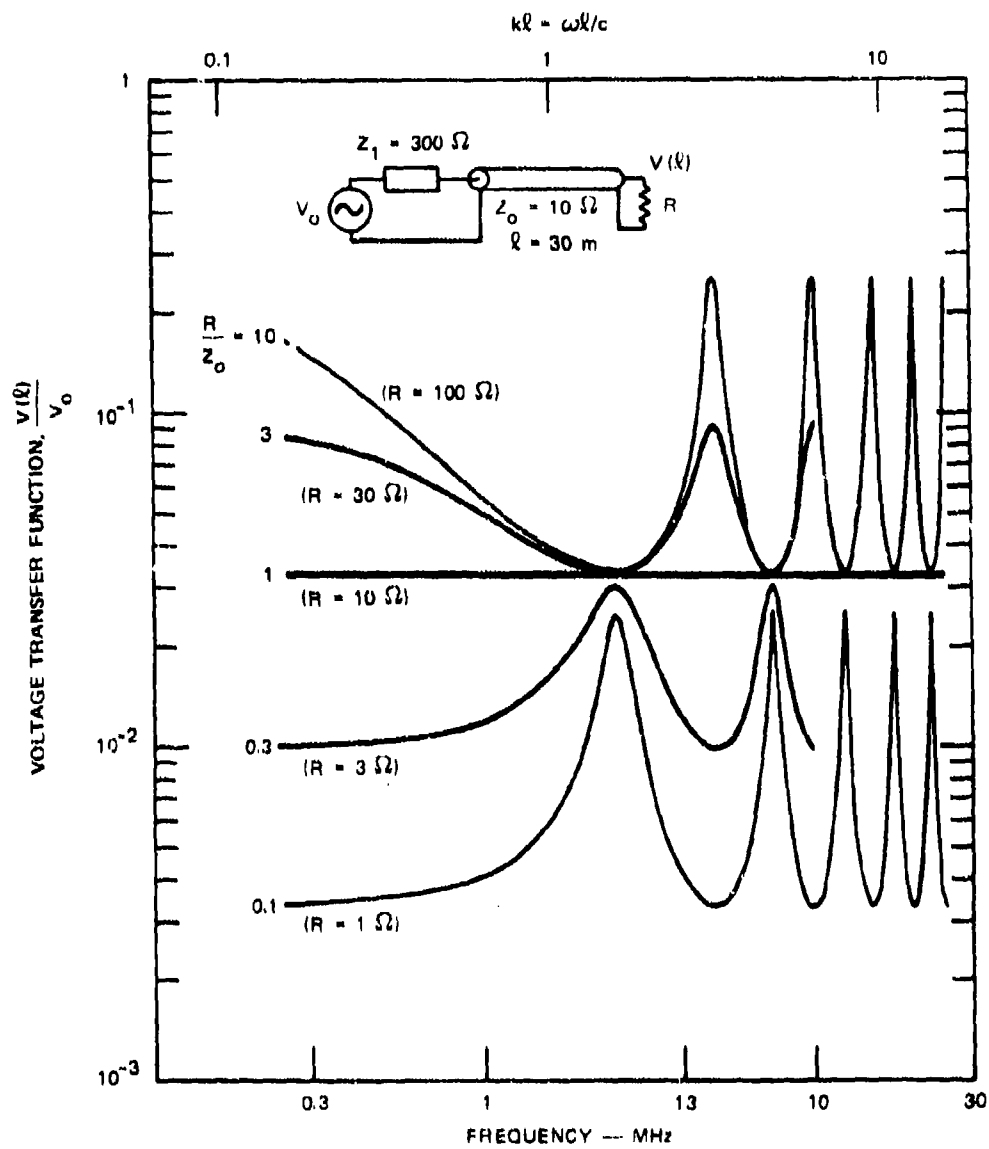


Figure 3-6 FEEDER TRANSFER FUNCTIONS FOR RESISTIVE LOADS

about the value $R/(Z_1 + R)$ is obtained. For a load $R = Z_o$, the voltage $V(\ell)$ would be a step of magnitude $R/(R + Z_1)$.

The response with an inductive load is of more interest in practice because of the large lead inductance associated with power circuits near transformer or circuit-breaker terminals. The load voltage $V(\ell)$ for three values of inductance is shown in Figure 3-10 for the step-voltage source with $Z_1/Z_o = 30$. In Figure 3-10(a), the time constant L/Z_o of

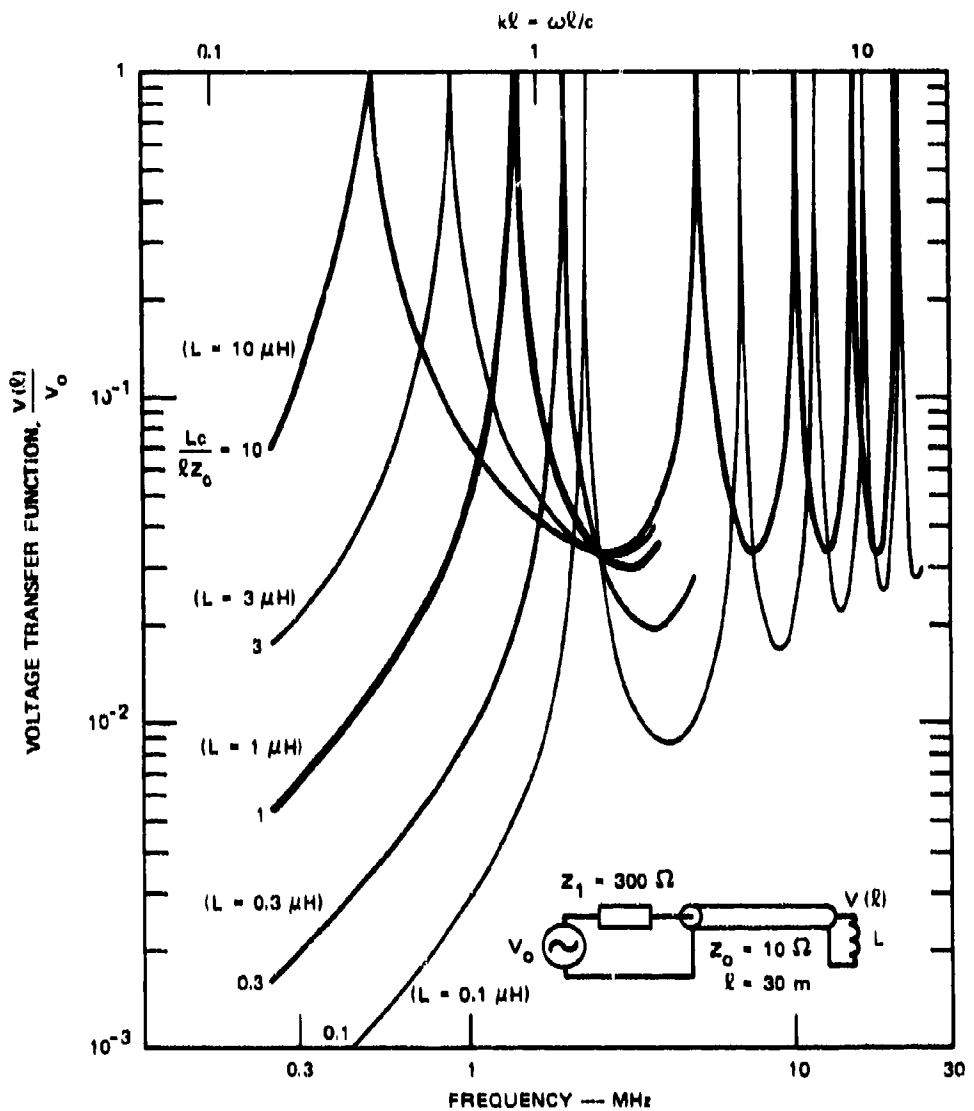


Figure 3-7 FEEDER TRANSFER FUNCTIONS FOR INDUCTIVE LOADS

the inductive load is smaller than the round-trip transient time $2l/c$ of the line. During the first $2l/c$ of the response, therefore, the response voltage is a decaying exponential with time-constant L/Z_0 , but beyond $2l/c$ the response becomes very complicated because of the convolution of the exponential response with multiple reflections from the inductive load and the resistive source impedance. The waveform of Figure 3-10(a) is quite representative of the complexity of the power-system response waveforms that are observed in practice, however.

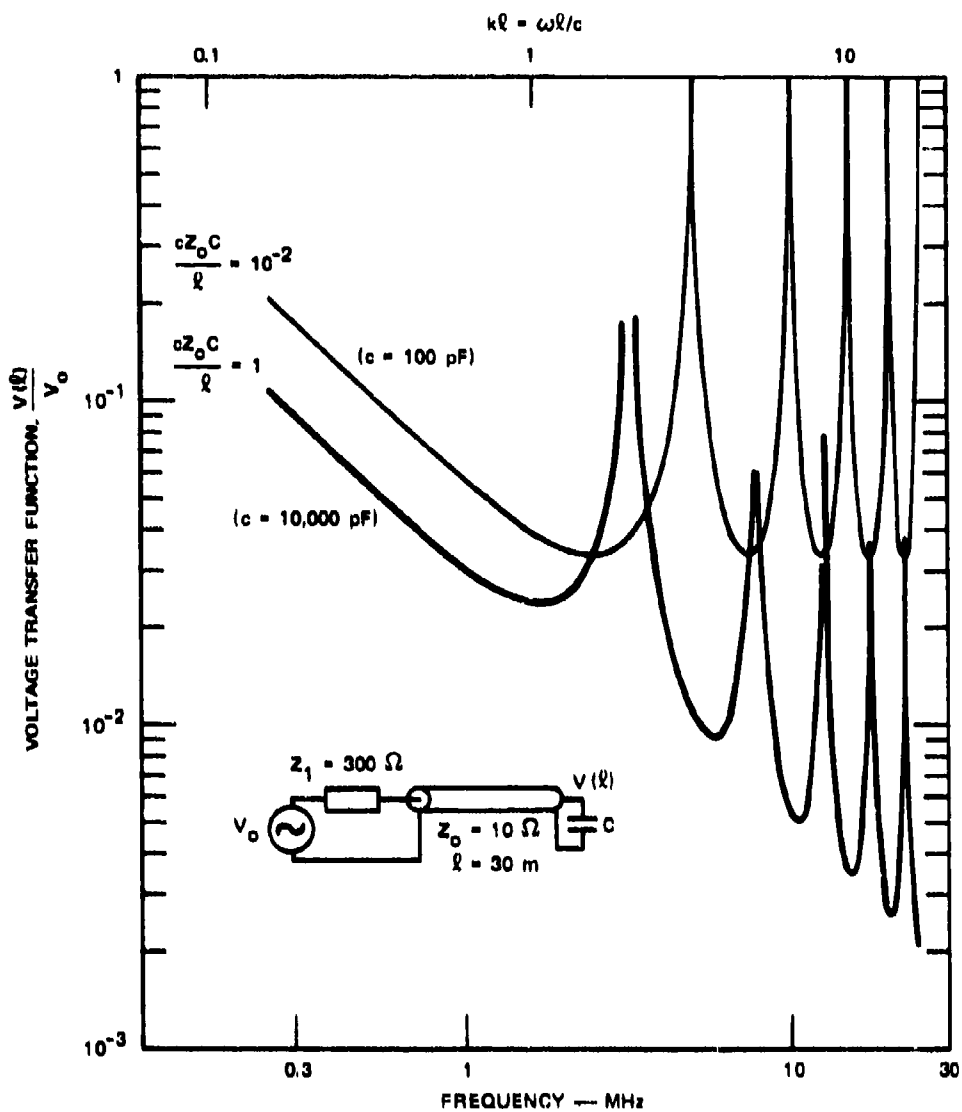


Figure 3-8 FEEDER TRANSFER FUNCTIONS FOR CAPACITIVE LOADS

Note that, although it is masked by the fine structure of the reflections, the response contains a fundamental oscillation with a period of $2\pi\sqrt{\ell L/cZ_0}$, about three cycles of which can be seen in Figure 3-10(a).

The responses shown in Figure 3-10(b) and (c) are for larger inductances. In Figure 3-10(b), the time constant L/Z_0 of the inductance is about equal to the round-trip transit time $2\ell/c$, so that the exponential decay of the voltage across the inductance is easily

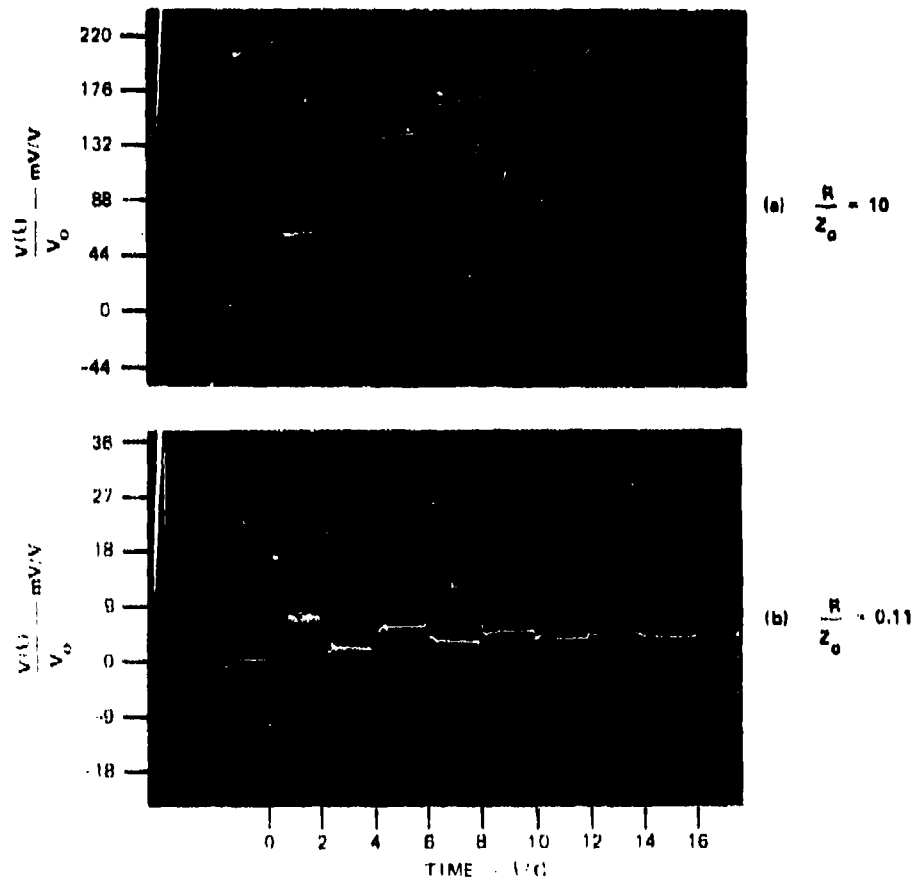


Figure 3-9 VOLTAGE ACROSS A RESISTIVE LOAD PRODUCED BY A UNIT STEP SOURCE
 $(Z_1/Z_0 = 30$, circuit of Figure 3-5)

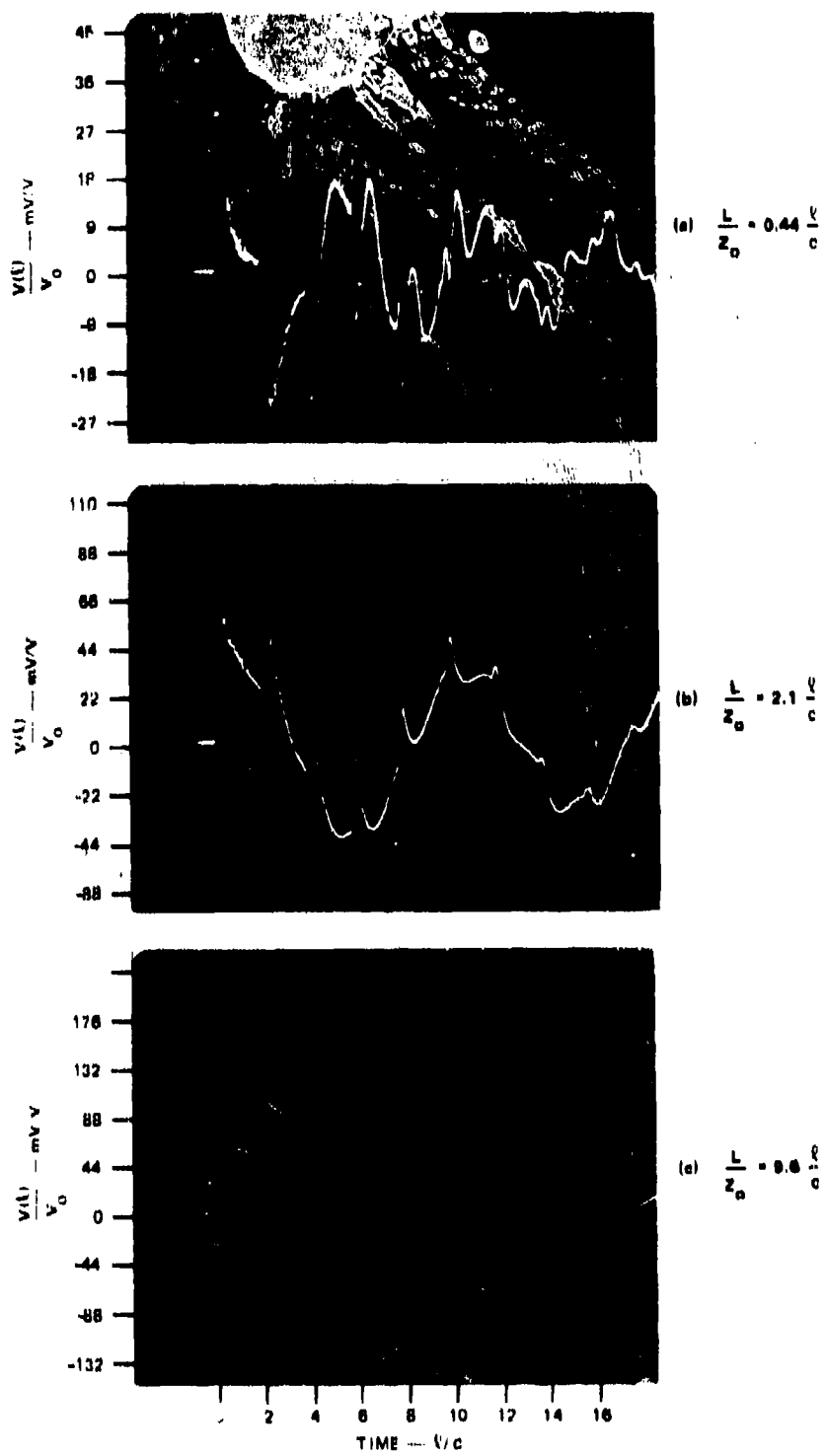


Figure 3-10 VOLTAGE ACROSS AN INDUCTIVE LOAD PRODUCED BY A UNIT STEP SOURCE ($Z_1/Z_0 = 30$, circuit of Figure 3-5)

identified even after several reflections. The fundamental oscillation with a period of $2\pi/\ell L/cZ_0$, upon which these exponential responses ride is also easily recognizable. In Figure 3-10(c), where $L/Z_0 > 2\ell/c$, the multiply reflected exponential responses appear as a saw-tooth wave superimposed on the fundamental oscillation.

The voltage developed across a capacitive load by a step voltage V_0 with source impedance $Z_1 = 30Z_0$ is shown in Figure 3-11 for a capacitance whose time constant Z_0C is small compared to the transit time $2\ell/c$. The early-time voltage across the capacitor behaves as

$$v(\ell) = \frac{Z_0}{Z_1 + Z_0} (1 - e^{-t/\tau_c}) \quad (0 \leq t \leq 2\ell/c) \quad (3-5)$$

where $\tau_c = Z_0C$. After the first reflection returns, the waveform is more complicated, but generally increases along an "average" curve given by

$$v(\ell) \approx 1 - e^{-t/Z_1C} \quad (3-6)$$

when Z_1 is resistive. Therefore, if the capacitance is increased, both the "average" time constant Z_1C and the short-term time constant Z_0C increase so that the size of the ripples is reduced and the average rate of rise is reduced. Waveforms such as that shown in Figure 3-11 are seldom observed in power systems because the capacitances in power circuits are usually distributed capacitances associated with machine or component windings, so that they behave as transmission lines rather than lumped capacitors.

3.2.2 THEVENIN-EQUIVALENT SOURCE

The Thevenin-equivalent source voltage at the load end of the conduit or shielded cable may be obtained from Eq. (3-2) by letting $Z_L \rightarrow \infty$ so that $\rho = 1$, resulting in

$$V'_o = \frac{2e^{-\gamma l} V_o}{\frac{Z_1}{Z_0} (1 - e^{-2\gamma l}) + (1 + e^{-2\gamma l})} \quad (3-7)$$

The source impedance associated with this open-circuit voltage is³

$$Z'_1 = Z_0 \frac{1 + \rho' e^{-2\gamma l}}{1 - \rho' e^{-2\gamma l}} \quad (3-8)$$

where

$$\rho' = \frac{Z_1 - Z_0}{Z_1 + Z_0} \quad (3-9)$$

A Thevenin-equivalent source of voltage V'_o and impedance Z'_1 at the load end of the conduit can then be used to replace the source V_o , its impedance Z_1 , and the transmission line as illustrated in Figure 3-12.

3.2.3 CHARACTERISTIC IMPEDANCE OF CONDUCTORS IN A CONDUIT

Formulas for the common-mode characteristic impedance of two- and four-conductor shielded cables have been derived by Kaden.⁴ These formulas are exact for perfect conductors and uniform dielectric between the inner conductors and the shield. The cable

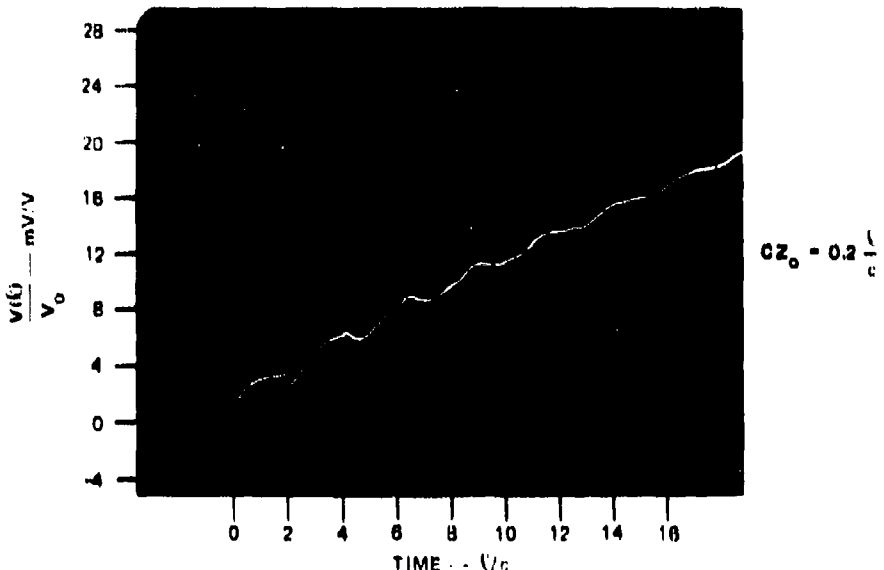
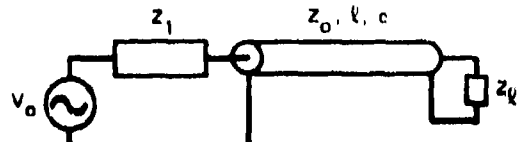


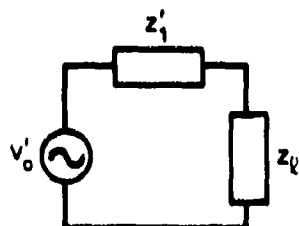
Figure 3-11 VOLTAGE ACROSS A CAPACITIVE LOAD PRODUCED BY A UNIT STEP SOURCE ($Z_1/Z_0 = 30$, circuit of Figure 3-8)

configuration and appropriate formulas for the common-mode characteristic impedance are shown in Figure 3-13(a) and (b). The formulas also assume a uniformly spaced, symmetrical array of conductors as illustrated. The effects of eccentricity of the cable bundle in the conduit can be estimated from the behavior of the characteristic impedance of the eccentric "coaxial" cable shown in Figure 3-13(c).⁵ If a , in Figure 3-13(c), is the effective radius of the bundle of conductors, the common-mode characteristic impedance of the bundle with an offset from the center of the conduit can be estimated using the formula given in Figure 3-13(c). A plot of this variation with offset is shown in Figure 3-14, where it is apparent that the bundle can be off-centered up to 50% with less than 20% reduction in characteristic impedance.

As an illustration of a typical four-conductor circuit in a conduit, the common-mode characteristic impedance of four 300-MCM conductors in a 3-inch conduit is shown in Table 3-2 for an arrangement like that shown in Figure 3-13(b). Air was assumed for the dielectric, but the maximum and minimum spacings between conductors ("compact" and "loose" in Table 3-2) were obtained assuming insulation of 0.933 inch diameter over the conductors. The "mean" spacing is the geometric mean of the maximum and minimum spacings. As is apparent in the table, the characteristic impedance changes by a factor of a little more than



(a) ORIGINAL CIRCUIT



(b) NEW THEVENIN EQUIVALENT

Figure 3-12 FEEDER SOURCE TRANSLATED
TO THE LOAD TERMINALS

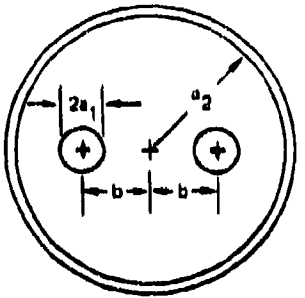
2 as the spacing varies from the maximum to the minimum permitted by the insulation. If allowance is made for the dielectric constant of the insulation, all of the characteristic impedances shown in the table will be reduced somewhat.

Table 3-2

COMMON-MODE CHARACTERISTIC IMPEDANCE OF FOUR 300-MCM
INSULATED CONDUCTORS IN A THREE-INCH-DIAMETER CONDUIT

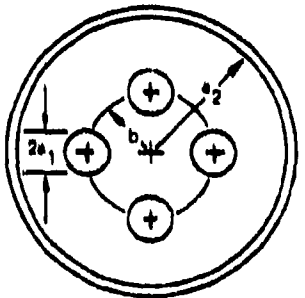
Wire Spacing, <i>b</i> (inches)	Characteristic Impedance, Z_0 (ohms)	Comments
0.680	33.3	compact
0.840	25.0	Mean
1.068	14.6	Loose

Notes: O.D. of insulation: 0.933 inch
 O.D. of conductor: 0.629 inch
 I.D. of conduit: 3.068 inch



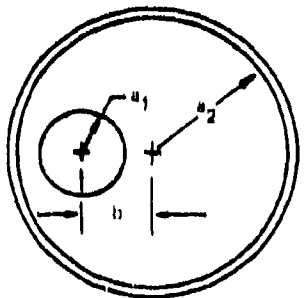
$$Z_0 = \frac{\eta}{4\pi} \left\{ \log \left(\frac{1 - B^4}{2AB^2} \right) + \left[1 + \frac{4B^4}{1 - B^4} \right]^2 \left(\frac{A}{2} \right)^2 \right\}; \quad B = \frac{b}{d_2}, \quad A = \frac{d_1}{b}$$

(a) SHIELDED PAIR



$$Z_0 = \frac{\eta}{8\pi} \left\{ \log \left(\frac{1 - B^8}{4AB^4} \right) + \left[3 + \frac{8B^8}{1 - B^8} \right]^2 \left(\frac{A}{2} \right)^2 \right\}; \quad B = \frac{b}{d_2}, \quad A = \frac{d_1}{b}$$

(b) SHIELDED QUAD



$$Z_0 = \frac{\eta}{2\pi} \cosh^{-1} \left[\frac{d_1^2 + d_2^2 - b^2}{2d_1d_2} \right]; \quad \text{WHEN } b = 0, \quad Z_0 = \frac{\eta}{2\pi} \log \frac{d_2}{d_1}$$

(c) ECCENTRIC CENTER CONDUCTOR

Figure 3-13 CHARACTERISTIC IMPEDANCE OF CONDUCTORS IN A METAL CONDUIT.
Source: Refs. 4 and 5.

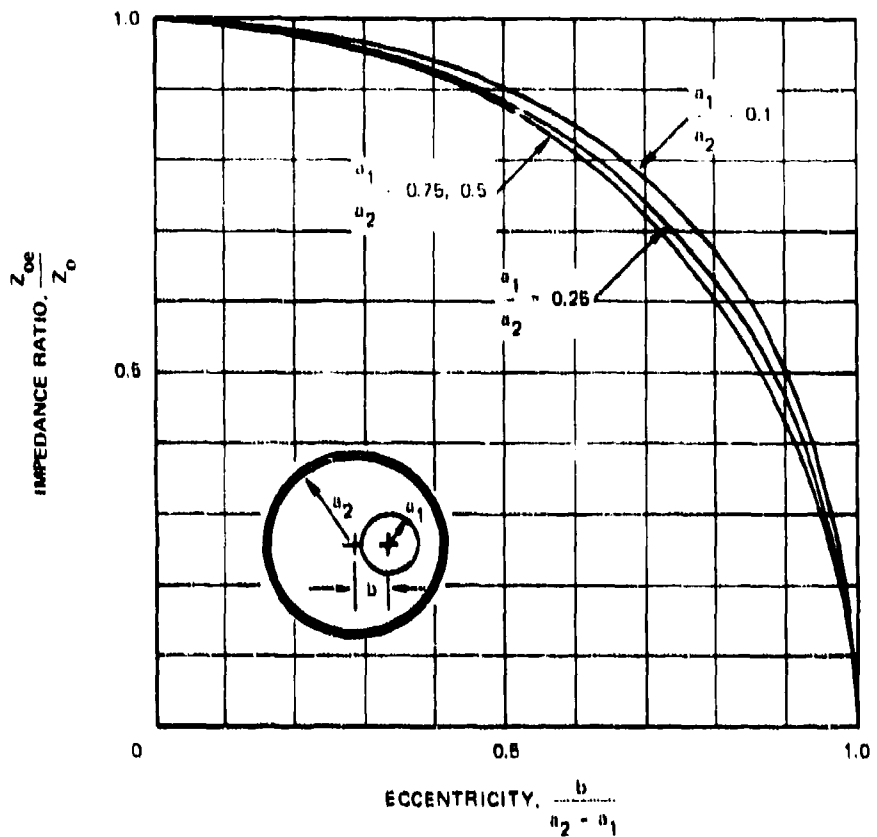


Figure 3-14 VARIATION OF CHARACTERISTIC IMPEDANCE OF ECCENTRIC COAXIAL CABLE

3.2.4 CHARACTERISTIC IMPEDANCE OF SHIELDED CABLES

The high-frequency characteristic (surge) impedance of shielded cables can be obtained from manufacturers' capacitive reactance data. The characteristic impedance is

$$Z_0 = \frac{\sqrt{\epsilon_r}}{cC} \quad (3-10)$$

where c is the speed of light, C is the capacitance per unit length, and ϵ_r is the dielectric constant of the insulation. The capacitive reactance of cables is often tabulated in ohms/mile at 60 Hz. In terms of the reactance per mile, X_c , the characteristic impedance in ohms is

$$Z_0 = 2.02 \times 10^{-3} \sqrt{\epsilon_r X_c} . \quad (3-11)$$

A table of values of characteristic impedance for various sizes and voltage ratings of single, paper-insulated shielded cables is given in Table 3-3. These values were deduced from the reactance-per-mile data given in Ref. 1.

Modern shielded cables are commonly insulated with cross-linked polyethylene, although some paper insulation is still in use. Polyethylene-insulated cables tend to have similar characteristic impedances because the dielectric constant of polyethylene is smaller than that of paper, but the extruded insulation is slightly thinner than paper insulation for the same voltage rating.

3.3 COUPLING THROUGH STEEL CONDUIT WALLS

3.3.1 GENERAL CONSIDERATIONS

Buried steel conduits, such as those between the service-entrance weatherhead and the main circuit-breaker panel, may have current induced in them by the electromagnetic field in the soil. The current induced in the conduit will, in turn, induce a current in the conductors inside the conduit. This current is superimposed on the current injected at the end of the conduit by the exposed aerial conductors. A similar situation exists for the shielded cables between the potheads and the transformers, although if these cables are routed through rigid steel conduit, the conductors are shielded by both the conduit and the cable shields.

Table 3-3

CHARACTERISTIC IMPEDANCES OF PAPER-INSULATED
SHIELDED POWER CABLES

Size (AWG or MCM)	Voltage Rating						
	1 kV	3 kV	5 kV	8 kV	15 kV	23 kV	36 kV
	Characteristic Impedance (ohms)						
6	16	19	26	30	--	--	--
4	13	16	22	26	33	--	--
2	11	13	18	21	28	35	--
1	9.7	12	16	19	26	31	--
0	8.7	10	14	17	23	28	36
00	7.9	9.5	12	15	20	26	33
000	7.1	8.6	11	13	18	23	30
0000	6.4	7.8	9.6	12	16	21	27
250	5.9	7.2	8.5	11	15	19	25
350	5.0	6.2	7.3	9	13	17	22
500	4.2	5.2	6.2	7.8	11	14	19
750	3.4	4.1	5.2	6.5	9.4	12	17
1000	3.1	3.8	4.4	5.7	8.7	11	15
1500	2.5	3.1	3.7	4.7	6.9	9.1	12
2000	2.2	2.7	3.2	4.1	6.1	8.0	11

Based on capacitive reactance values given in Ref. 1. Dielectric constant is 3.7.

The usual approach to calculating the current or voltage on the conductors inside the conduit consists of (1) determining the electric field in the soil parallel to the conduit, (2) calculating the current in the conduit, (3) calculating the transfer impedance and saturation characteristics of the conduit as a tubular shield, and (4) analyzing the conductors and conduit as a coaxial transmission line with a distributed driving source.⁶⁻¹⁰ In the case of shielded cables in plastic conduit, Steps 2, 3, and 4 are applied to the cable shields rather than to the conduits. In the case of shielded cables inside steel conduit, Step 3 will include calculating transfer impedance of the cable shield, and in Step 4 the coaxial transmission line analyzed will be that formed by the cable conductor and its shield.

A rigorous analysis of the signals induced on conductors inside steel conduits is apparently very difficult.⁶ However, there are several properties of the conduit and of typical installations that may be used to simplify the problem and obtain good estimates of the conductor voltage and current. First, it is noted that rigid steel conduit is a very effective shield, particularly at high frequencies, so that very little of the external electromagnetic field penetrates through the conduit walls to the conductors inside. Thus, unless the conduit is very long (of the order of 10^5 ft or more), the signal induced through the walls of a continuous steel conduit with tight couplings is usually negligible compared to that injected on the conduit conductors by the aerial conductors at the entrance end. Even for long conduit runs, the rise time of the current and voltage transient induced on the internal conductors is very long (of the order of 1 ms if the steel is unsaturated), so that ordinary voltage limiting and filtering techniques can be applied.

Second, since only the low-frequency spectrum can penetrate the steel conduit walls, only the low-frequency current in the conduit and the low-frequency fields in the soil need be analyzed.^{4, 10, 11} Because only the low-frequency spectrum is of interest, the conduit can be considered electrically short (i.e., short compared to a wavelength of the highest frequency of interest).

Finally, the depth of burial of conduits is ordinarily only a few meters, so that in the low-frequency spectrum of interest in the analysis of the internal conductors, the fields in the soil at the depth of burial are approximately equal to those at the surface of the ground. One can therefore often neglect the $\exp(-d/\delta)$ dependence of the field strength on depth d and skin depth $\delta = (\pi f \mu_0 \sigma)^{-1/2}$ in the soil.

The simplifications noted above are valid only for conductors in effectively continuous rigid steel conduits (i.e., steel conduit with tight couplings for the entire run). If the conductors are routed through plastic (or other nonmetallic) conduit for all or part of the run, the above simplifications do not apply, because these assumptions are all contingent on the high-frequency shielding characteristics of the rigid steel conduit. Even shielded cables in plastic conduit may require special consideration because the electrostatic shields on these cables may not be particularly effective at high frequencies (see Section 3.4).

3.3.2 BULK CURRENTS INDUCED IN BURIED CONDUITS

3.3.2.1 General

This section presents formulas for calculating the total current induced in a buried conduit by an incident uniform plane wave, for bare or thinly insulated conduits. The incident electromagnetic pulse is assumed to have an exponential waveform $E_0 \exp(-t/\tau)$. The wave arrives on the surface of the earth from a direction defined by an elevation angle ψ and an azimuth angle φ as illustrated in Figure 3-15. The depth of burial of the conduit is small compared to a skin depth in the soil, so that the fields at the conduit depth are essentially the same as those at the surface. It is assumed that the conduit is a single, isolated conduit with no other conductors in its vicinity.

In all the bulk-current formulas, the soil is considered to be a good conductor, as defined by $\sigma \gg \omega\epsilon$. The wave-propagation factor in the soil, and the propagation factor for bare conductors, is thus³

$$\gamma = \sqrt{j\omega\mu_0(\sigma + j\omega\epsilon)} \approx \sqrt{j\omega\mu_0\sigma} = \frac{1 + j}{\delta} \quad (3-12)$$

where δ is the skin depth in the soil, σ is the soil conductivity, and μ_0 and ϵ are the permeability and permittivity of the soil, respectively. A plot of the skin depth as a function of frequency and soil conductivity is given in Figure 3-16. The dashed line along the right-hand side of Figure 3-16 indicates the limit of validity of the approximation $\gamma \approx (1 + j)/\delta$. Although this limit falls between a few hundred kHz and a few MHz for typical soil conductivities, steel conduit walls have very large attenuation at frequencies above 100 kHz, so that the bulk-current spectrum at these frequencies is usually of secondary interest.

3.3.2.2 Current Far from the Ends of a Long Conduit

The conduit-current formulas presented here apply to points far (several skin depths in soil) from the ends of long buried conduits that have no insulation, or have insulation that is thin compared to the conduit radius. The results are presented for an incident exponential pulse that propagates as a plane wave that is uniform (constant

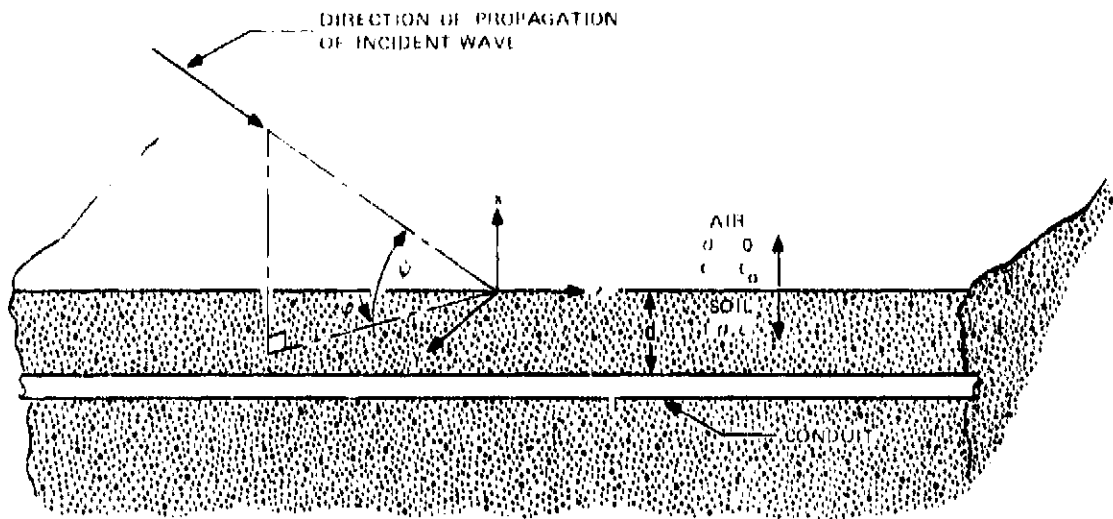


Figure 3-16 ILLUSTRATION OF COORDINATES FOR CONDUIT AND ANGLE OF ARRIVAL OF TRANSIENT WAVE

magnitude) over several soil skin depths along the conduit (the skin depth δ in the soil is plotted in Figure 3-16). The decay time constant τ of the exponential pulse is large compared to the soil time constant $\tau_0 = \epsilon_0/\sigma$. The small resistance of the cable is neglected, and it is assumed that the depth of burial is small compared to the soil skin depth at the highest frequencies of interest.

The total current induced far from the ends of a long conduit by an incident field $E_0 e^{-t/\tau}$ is given by¹⁰

$$I(\omega) \approx I_0 \frac{1}{\sqrt{j\omega\tau(j\omega + 1/\tau)}} \quad (3-13)$$

in the frequency domain, or

$$I(t) = I_0 e^{-t/\tau} \frac{2}{\sqrt{\pi}} \int_0^{\sqrt{t/\tau}} e^{-u^2} du \quad (3-14)$$

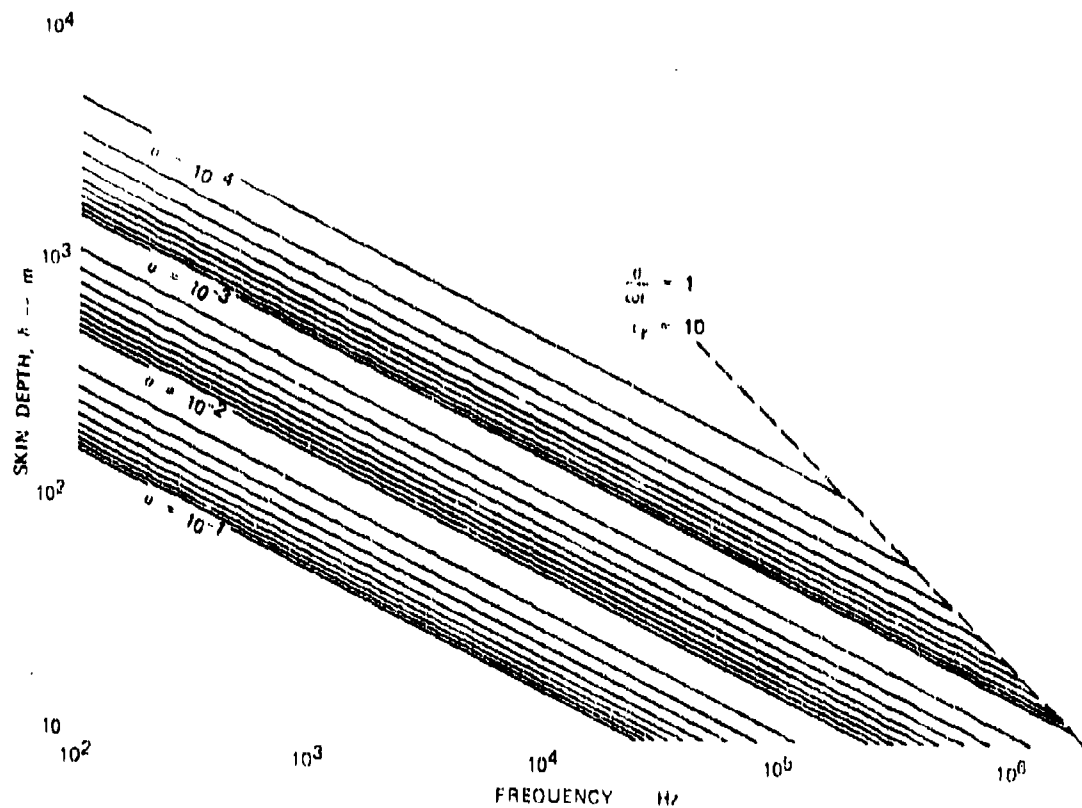


Figure 3-18 SKIN DEPTH δ IN SOIL AS A FUNCTION OF FREQUENCY AND SOIL CONDUCTIVITY σ

In the time domain, where

- $$I_0 \approx 10^9 \sqrt{\tau_e \tau} E_0 D(\psi, \varphi) \text{ (ampere seconds)}$$
- $$\tau_e = \frac{C_0}{\sigma} = \frac{8.85 \times 10^{-12}}{\sigma} \text{ Time constant of soil (s)}$$
- τ = Decay time constant of incident pulse (s)
- E_0 = Peak electric-field strength of incident pulse (V/m)
- $D(\psi, \varphi)$ = $\cos \varphi$ for vertically polarized wave
= $\sin \psi \sin \varphi$ for horizontally polarized wave.

The waveform for $i(t)$ and the incident exponential pulse are shown in Figure 3-17 as a function of time in incident-pulse-decay time constant.

The peak current induced in the conduit is¹⁰

$$I_{pk} = I_0 \left[e^{-t/\tau} \frac{2}{\sqrt{\pi}} \int_0^{\sqrt{t/\tau}} e^{u^2} du \right]_{max} = 0.61 I_0 \quad (3-15)$$

and the peak current occurs at

$$t_{pk} = 0.85 \tau. \quad (3-16)$$

The variation of the peak current with azimuth angle of incidence φ and elevation angle of incidence ψ is shown in Figure 3-18. The magnitude of the peak current for maximum coupling [$D(\psi, \varphi) = 1$] is plotted in Figure 3-19 as a function of soil conductivity for various incident-field time constants. The plots are truncated in the lower left-hand part of the graph where $\tau = \tau_e$. The responses given in this section are valid only if $\tau > \tau_e$. Where the approximations used here are valid, the peak current is inversely proportional to the square root of the soil conductivity (i.e., $\sqrt{\sigma} I_0 = \text{constant}$).

Useful insight into the physics of the coupling process can be obtained from the frequency form of the current in the conduit given by⁸

$$I(z, \omega) \approx \frac{\sigma E_z \pi \delta^2}{j \log \frac{\sqrt{2\delta}}{\gamma_0 a}} \quad (3-17)$$

where E_z is the component of the electric field (in the soil) parallel to the conduit, a is the radius of the conduit, and $\gamma_0 \approx 1.781$. The current density in the soil is σE_z (in the absence of the conduit), and $\pi \delta^2$ is the area of a circle one skin-depth in radius in the soil. Thus the total current induced in the conduit is approximately proportional to the current that would flow in a circular cylinder of soil one skin depth in radius if the cable were not present. Because $E_z \propto E_0 / \sqrt{\sigma}$ through $(1 + R)E_0$ [see Eqs. (2-9)], the conduit current is also proportional to $E_0 / \sqrt{\sigma}$. The approximation $\log (\sqrt{2\delta}/\gamma_0 a) \approx 10$ is valid (within a factor of 2) for a wide range of soil conductivities, conductor radii, and frequencies as can be seen in Figure 3-20. This approximation has been used in deriving I_0 in Eqs. (3-13) and (3-14).

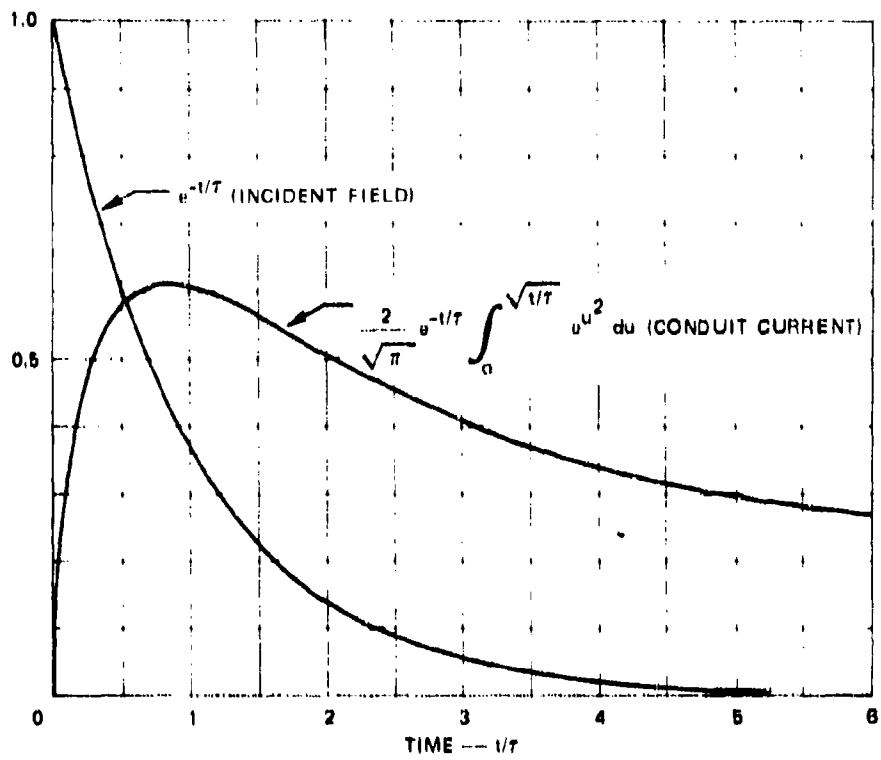


Figure 3-17 WAVEFORMS OF INCIDENT FIELD, CABLE CURRENT, AND OPEN-CIRCUIT VOLTAGE BETWEEN THE SHIELDS

3.3.2.3 Current Near the End of a Long Bare Conduit

The conduit current formulas presented here are for points near the end of a long (semi-infinite) conduit. The bulk current in the conduit is based on the assumption that the conduit is in contact with the soil and that the end of the conduit is terminated in a very low impedance (short circuit) or a very high impedance (open circuit) compared to the characteristic impedance. The short-circuit case might be representative of a conduit that is terminated in a large counterpoise or similar low-impedance structure. The open-circuit case is representative of a conduit that is dead-ended or insulated at the end of the run. The assumptions that $\omega > \omega_c$ and $a < \delta$ used for the long conduit above apply to these cases as well. The results are presented for an exponential pulse with decay time constant τ that is large compared to the soil time constant $\tau_s = \epsilon_0/a$. The electromagnetic pulse is incident from a direction defined by an elevation angle ψ measured from horizontal and an azimuth angle φ measured from the axis of the conduit (see Figure 3-15).

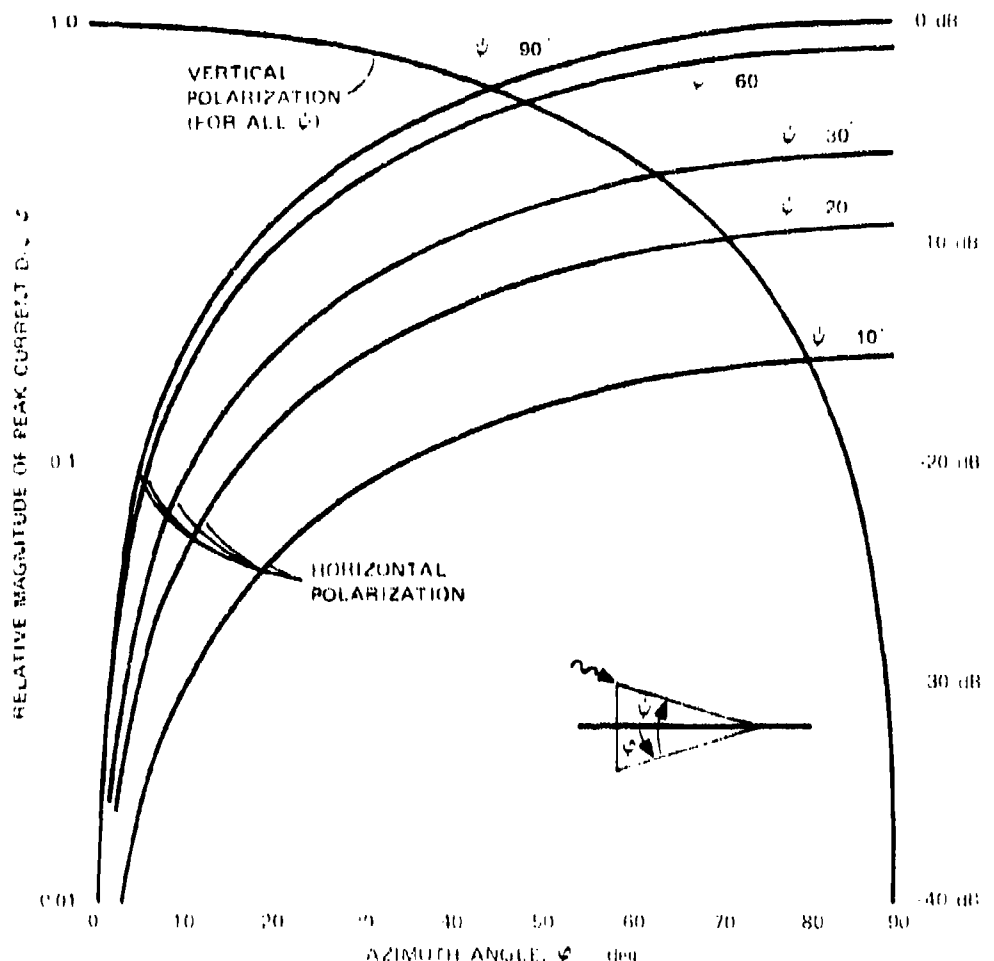


Figure 3-18 VARIATION OF PEAK CONDUIT CURRENT AS AZIMUTH (ϕ) AND ELEVATION (ψ) ANGLES OF INCIDENCE CHANGE [$D(\psi, \phi)$]

The total current induced near the end of a long conduit that is *short-circuited* is identical to the current far from the ends and is given by Eqs. (3-13) and (3-14), and has the waveform shown in Figure 3-17.

The total current induced near the end of a long conduit that is *open-circuited* at the end by an incident exponential pulse $E_0 e^{-j\omega t}$ is given by¹⁰

$$I(z, \omega) \approx I_0 \frac{1 - e^{-\sqrt{\omega/\tau_0} z/k}}{\sqrt{j\omega\tau} (j\omega + j/\tau)} \quad (3-18)$$

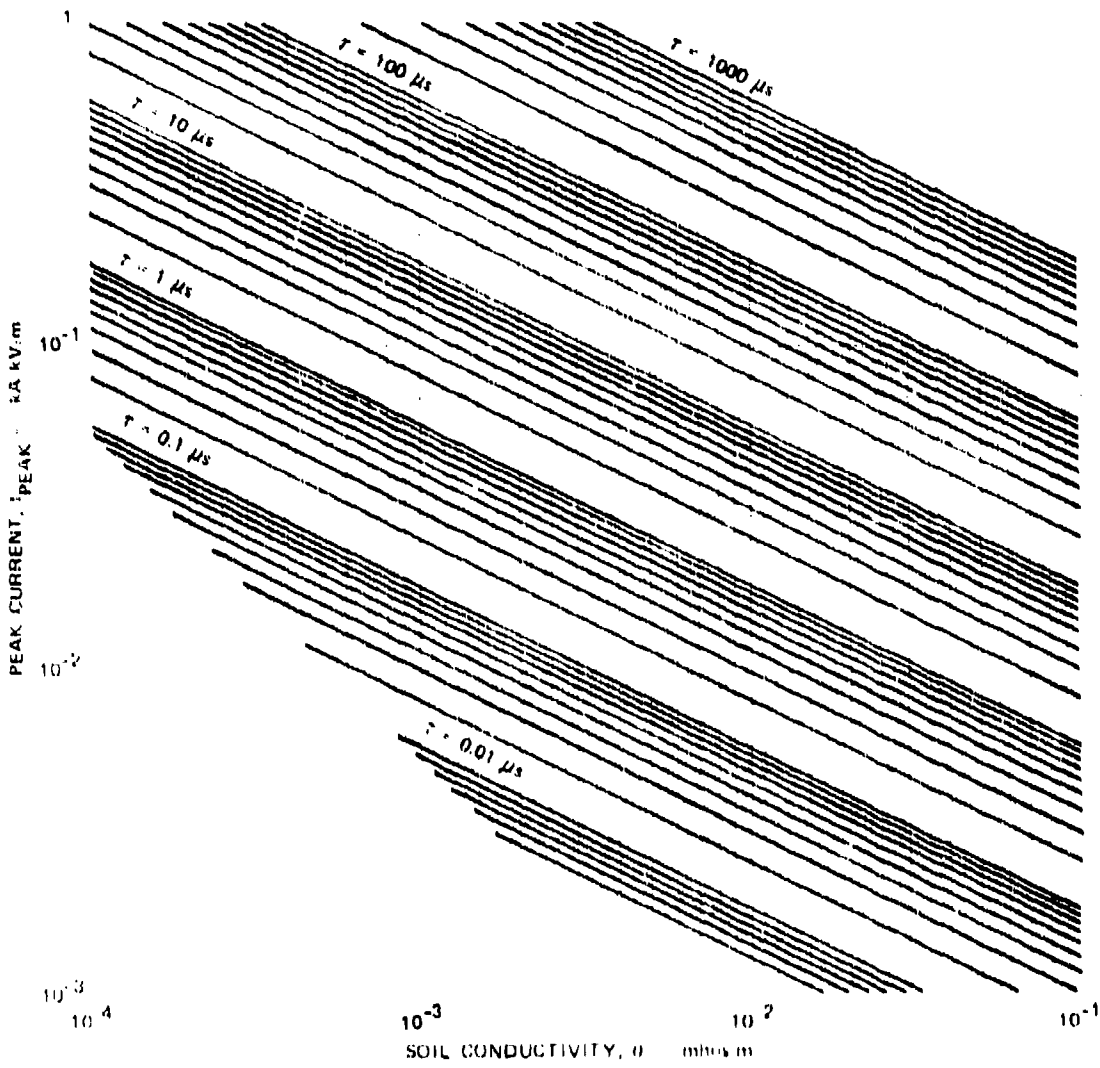


Figure 3-19 PEAK CONDUIT CURRENT AS A FUNCTION OF SOIL CONDUCTIVITY AND INCIDENT EXPONENTIAL PULSE-DECAY TIME CONSTANT $\tau[D(\psi,\phi) = 1]$

in the frequency domain, and by

$$i(z,t) \approx I_0 e^{-t/\tau} \frac{2}{\sqrt{\pi}} \int_0^{\sqrt{t/\tau}} \left(1 - e^{-u^2}\right) e^{-p/u^2} du \quad (3-19)$$

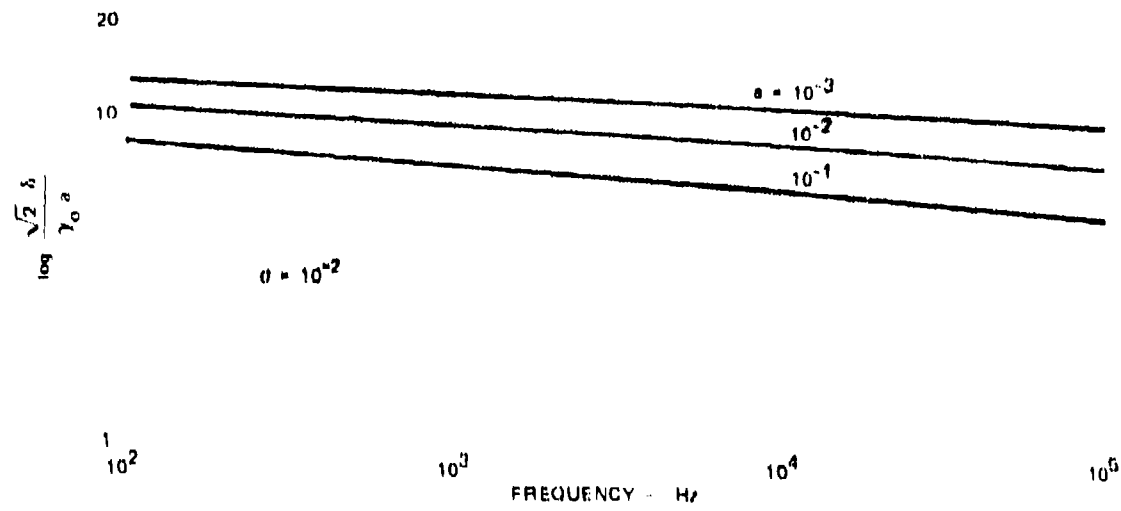


Figure 3-20 VARIATION OF LOG ($\sqrt{2h/\gamma_0 a}$) WITH FREQUENCY AND CONDUCTOR RADIUS. (Note that a factor of 10 in conductor radius produces the same effect as a factor of 100 in soil conductivity.)

In the time domain, where

$$I_0 = 10^6 \sqrt{\tau_0 \tau} E_0 D(\psi, \varphi) \text{ (ampere-seconds)}$$

$$\tau_0 = \frac{r_0}{a} = \text{Time constant of soil (s)}$$

τ = Decay time constant of incident pulse (s)

E_0 = Peak electric-field strength of incident pulse (V/m)

$D(\psi, \varphi)$ = $\cos \varphi$ for vertical polarization

$D(\psi, \varphi)$ = $\sin \psi \sin \varphi$ for horizontal polarization

z = Distance from end of cable (m)

$c = 1/\sqrt{\mu_0 \epsilon_0}$ = Speed of light in free space

$$D = \left(\frac{z}{c} \right)^2 \frac{1}{4\tau \tau_0} .$$

This current is zero (very small) at the end ($z = 0$) and approaches the value given by Eq. (3-14) at large distances from the end. Plots of the waveform at distances of 3.16, 10, and 31.6 m from the end of the cable are shown in Figure 3-21 for a soil conductivity of 10^{-2} mho/m.

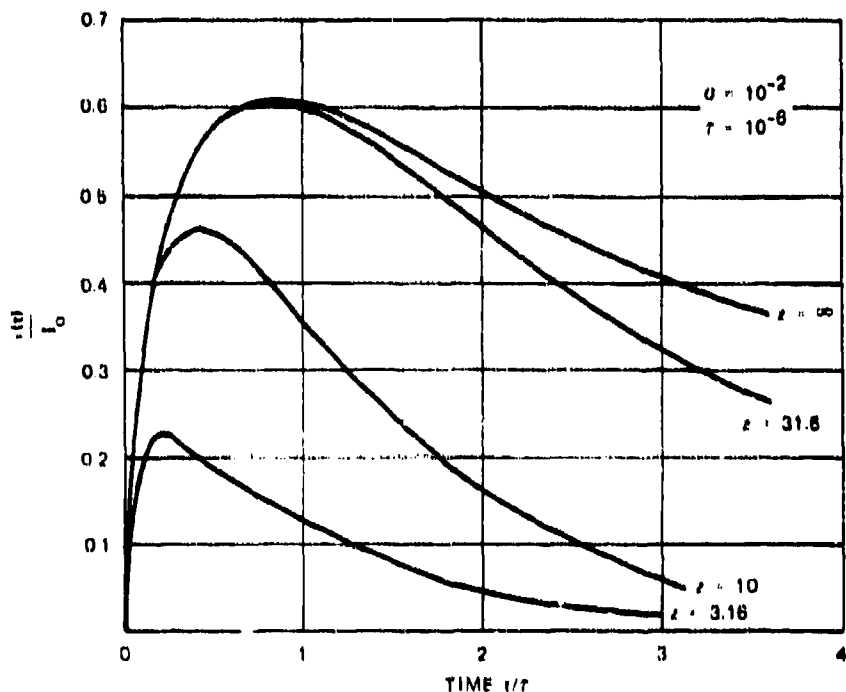


Figure 3-21 WAVEFORM OF THE CONDUIT CURRENT NEAR THE END WHEN CONDUIT END IS OPEN-CIRCUIT

Since the waveform is determined by $\frac{1}{\tau_e} (z/c)^2 = \sigma z^2 / \epsilon_0 c^2$, the waveforms shown in Figure 3-21 will represent different distances from the end of the cable if the soil conductivity differs from 10^{-2} mho/m. The magnitude of the current remains inversely proportional to the square root of the soil conductivity ($\sqrt{\sigma} I_o \approx \text{constant}$). Again, the approximation $\log \frac{\sqrt{2\delta}}{\gamma_0 \delta} \approx 10$ is used in deriving I_o .

3.3.2.4 Current in an Electrically Short Conduit

The conduit may be considered electrically short if its length is short compared to a skin depth in the soil of all frequencies of interest. From the analysis of conduit shielding properties in Section 3.3.3, it is apparent that even if the steel in the conduit is saturated, the frequencies penetrating the conduit walls lie principally in the spectrum below 6 kHz, and from Figure 3-16 the skin depth in average ($\sigma = 10^{-2}$) soil is about 60 m and in poorly conducting ($\sigma = 10^{-3}$) soil it is about 200 m. Thus, conduits a few tens of meters long in soil of poor to average conductivity may be considered electrically short at the frequencies penetrating to the interior of the conduits.

The conduit may then be analyzed as an electrically short dipole in a finitely conducting medium. The current at the center of a conduit of length ℓ is then

$$I \approx \frac{E_z \ell Y}{2} \quad (3-20)$$

where E_z is the field strength in the soil and Y is admittance of a center-fed dipole of length ℓ and radius a in the conductive medium. Neglecting the capacitive susceptance (since $\sigma \gg \omega \epsilon$), the admittance Y is

$$Y \approx G \approx \frac{\pi \sigma \ell}{2 \log \ell/a} \quad (3-21)$$

where σ is the soil conductivity and a is the radius of the conduit. The current at the center is thus

$$I \approx -\frac{\pi \sigma E_z \ell^2}{4 \log \ell/a} \quad (3-22)$$

The z-component of the electric field in the soil, from Eqs. (2-7) and (2-9) with $h = 0$ and the phase $kz \cos \psi \cos \varphi$ neglected, is

$$E_z \approx 2 E_i \sqrt{\tau_0} \left\{ \frac{\sin \varphi \sin \psi}{\cos \varphi} \right\} \sqrt{j\omega} \quad (3-23)$$

where $\tau_0 = \epsilon_0/a$, E_i is the incident field strength, and the upper and lower trigonometric functions apply to horizontal and vertical polarization, respectively. For an exponential pulse of the incident field $E_0 e^{-t/\tau}$,

$$E_z \approx 2 E_0 \sqrt{\tau_0} \left\{ \frac{\sin \varphi \sin \psi}{\cos \varphi} \right\} \frac{\sqrt{j\omega}}{j\omega + \frac{1}{\tau}} \quad (3-24)$$

The midpoint current in the short conduit is thus

$$I = \frac{\pi a E_0 l^2}{2 \log k/a} \sqrt{\tau_0} \left\{ \frac{\sin \varphi \sin \psi}{\cos \varphi} \right\} \frac{\sqrt{j\omega}}{j\omega + \frac{1}{\tau}} \quad (3-25)$$

for the exponential pulse of incident field (upper trigonometric functions for horizontal polarization; lower for vertical polarization). The ratio of this current to the current in an infinitely long conduit is

$$\frac{I_{\text{short}}}{I_{\infty}} = \frac{5 \log \frac{\sqrt{2\delta}}{\gamma_0 a}}{8 \log k/a} j\omega \tau_q \quad (3-26)$$

where $\tau_q = \mu_0 a l^2$, and the log term in the numerator is plotted in Figure 3-20. The ratio is thus of the order of $j\omega \tau_q$. By definition of electrical shortness, $\omega \tau_q \ll 1$; therefore the magnitude of the current at the midpoint of a short conduit is always smaller than the current in an infinitely long conduit (or far from the ends of a long conduit). Observe also that because multiplication by $j\omega$ in the frequency domain corresponds to differentiation with respect to time in the time domain, the waveforms of the current in the time domain

will correspond to the derivative of the waveform shown in Figure 3-17. This waveform of the current at the center of the conduit is thus¹²

$$i(t) \approx I_0 \left[\frac{1}{\sqrt{\pi \tau}} - e^{-t/\tau} - \frac{2}{\sqrt{\pi}} \int_0^{\sqrt{t/\tau}} e^{-u^2} du \right] (t > \tau_e) \quad (3-27)$$

where

$$I_0 = \frac{\pi \sigma E_0 l^2}{2 \log \ell/a} \sqrt{\tau_{eff}} D(\psi, \varphi)$$

$$\tau_e = \epsilon_0 / \sigma$$

- $D(\psi, \varphi) = \sin \varphi \sin \psi$ (horizontal polarization)
- $= \cos \varphi$ (vertical polarization)
- τ = Time constant of incident exponential field pulse.

This waveform is infinite at $t = 0$, but the solution is not valid for times less than τ_e , because for such times the soil does not behave as a good conductor.

Equations (3-26) and (3-27) give the current at the center of the short conduit. Since the maximum current occurs at the center, the current anywhere else on the conduit is less than the values given by these formulas. The variation of the current with position along the conduit is frequency-dependent (or time-dependent) also, so that a transformable current distribution or average current that can be used in the calculation of internal conductor voltages and currents is not readily available. To within a factor of about 2 for these calculations, however, it may be assumed that the current in the conduit is uniform at the midpoint value.

3.3.3 CURRENT AND VOLTAGE INDUCED ON INTERNAL CONDUCTORS

3.3.3.1 Transfer Impedance of Steel Conduit

The voltage and current induced on conductors inside a steel conduit by current flowing on the conduit can be obtained from the transfer impedance of the conduit. The transfer impedance of a cylindrical shield is the ratio of the voltage per unit length developed between the internal conductors and the shield to the current flowing in the shield. In its general form, the transfer impedance Z_T is defined by

$$Z_T = \frac{1}{I} \frac{dV}{dz} \quad (3-28)$$

where V is the conductor-to-shield voltage, I is the shield current, and z is the distance along the conduit.

For thin-walled tubular shields of uniform cross section that contain no holes or cracks, the transfer impedance is^{4,9-11}

$$Z_T \approx R_0 \frac{(1+j) T/\delta}{\sinh(1+j) T/\delta} \quad (3-29)$$

where R_0 is the dc resistance per unit length of the shield given by

$$R_0 \approx \frac{1}{2\pi a T_0} \quad (3-30)$$

and T is the wall thickness of the shield, a is the mean radius of the shield, σ is the conductivity of the shield, and δ is the skin depth in the shield given by

$$\delta = \frac{1}{\sqrt{\pi f \mu_0}} \quad (3-31)$$

For ferrornagnetic shields such as steel conduit, the permeability, μ , is an important factor.

Since

$$(1 + j) \frac{T}{\delta} = \sqrt{\omega \tau_s} = (1 + j) \sqrt{\frac{f}{f_\delta}} \quad (3-32)$$

where

$$\tau_s = \mu \sigma T^2$$

$$f_\delta = \frac{1}{\pi \mu \sigma T^2} = \frac{1}{\pi \tau_s}$$

the transfer impedance may also be expressed in terms of the diffusion time-constant τ_s or the frequency f_δ at which the wall thickness is one skin depth. The dimensions of standard steel conduit are given in Table 3-4. A plot of the magnitude of the transfer impedance as a function of frequency is shown in Figure 3-22 in a normalized form that can be applied to

Table 3-4

PROPERTIES OF STANDARD GALVANIZED OR ENAMELED
RIGID STEEL CONDUIT

Size (inches)	Diameter (inches)		Thickness (inches)	Threads per inch	Weight per 100 Feet (lbs)
	External	Internal			
1/2	0.840	0.622	0.109	14	79
5/8	1.050	0.824	0.113	14	105
1	1.315	1.049	0.133	11½	153
1 1/4	1.660	1.380	0.140	11½	201
1 1/2	1.900	1.610	0.145	11½	249
2	2.375	2.067	0.154	11½	332
2 1/2	2.875	2.469	0.203	8	527
3	3.500	3.069	0.216	8	682
3 1/2	4.000	3.548	0.226	8	831
4	4.500	4.026	0.237	8	972
5	5.563	5.047	0.258	8	1314
6	6.625	6.065	0.280	8	1745

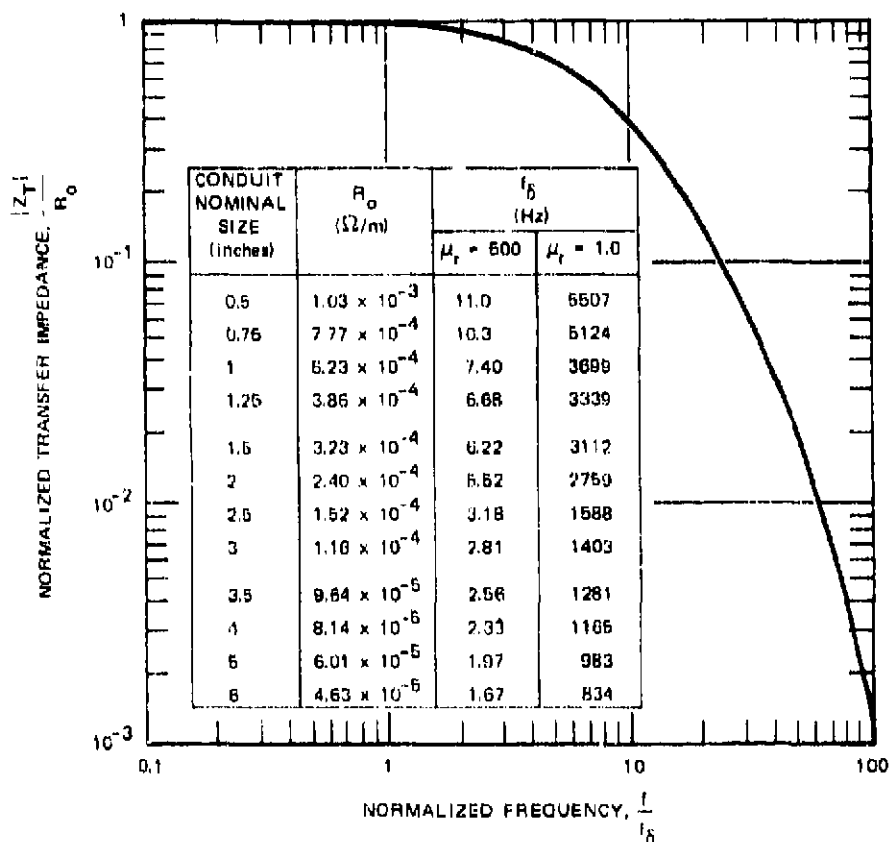


Figure 3-22 MAGNITUDE OF THE TRANSFER IMPEDANCE OF RIGID STEEL CONDUIT ($\mu_r = 6 \times 10^6$ mho/m)

any tubular shield. The normalization values of R_0 and f_h for standard rigid steel conduits are shown in the table inset in Figure 3-22.

Note that for frequencies significantly above f_h , the transfer impedance is quite small, so that only the frequencies below f_h are effective in inducing current and voltage on the conductors inside the conduit. Even if the conduit steel is saturated, the cutoff frequency f_h is less than 6 kHz, so that the conduit run may be considered electrically short (for the analysis of internal current and voltage) if its length is

$$L \ll \frac{c}{f_h} \gg 50 \text{ km}$$

Since most feeder conduits are only a few hundred feet long, they may usually be considered electrically short for purposes of analyzing coupling through the conduit walls.

3.3.3.2 Internal Voltage Induced in an Electrically Short Conduit-Uniform Exponential Current

For an electrically short conduit of length ℓ with a uniform current I induced by external fields, the total induced internal voltage will be

$$V(\omega) = IZ_T\ell \quad (3-33)$$

where Z_T is the transfer impedance of the conduit. If the internal conductors are open-circuited with respect to the conduit at both ends, half of this voltage will appear between the conductors and the conduit at each end.

When the current I is that derived from an exponential pulse $I_0 e^{-t/\tau}$ and the transfer impedance from Eq. (3-29) is used, the open-circuit voltage at one end of conductors that are open-circuited at both ends is¹⁰

$$V(\omega) = \frac{I_0 R_0 \ell}{2} \frac{\sqrt{j\omega\tau_s}}{\left(j\omega + \frac{1}{\tau}\right) \sinh \sqrt{j\omega\tau_s}} \quad (3-34)$$

where

$$R_0 = (2\pi\mu_0 T)^{-1} = \text{dc resistance per meter of the conduit}$$

$$\tau_s = \mu_0 T^2 = \text{Diffusion time constant for the conduit}$$

$$\tau = \text{Decay time constant of the exponential pulse of conduit current.}$$

The quantities a , σ , μ , and T are the radius, conductivity, permeability, and wall thickness of the conduit, respectively. The voltage waveform is

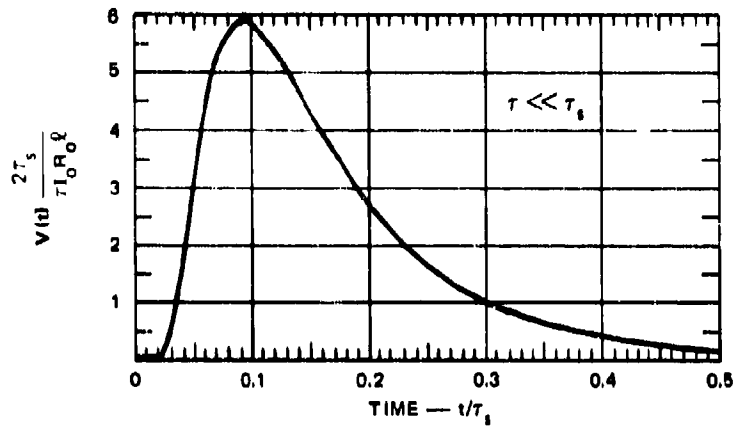
$$v(t) = \frac{I_0 R_0 \ell}{2} \left(\frac{\tau}{\tau_s} \right) \frac{1}{\sqrt{\pi}} \left(\frac{\tau_s}{t} \right)^{3/2} \sum_{n=1}^{\infty} \left[\frac{(2n-1)^2 \tau_s}{2t} - 1 \right] \exp \left[-(2n-1)^2 \frac{\tau_s}{4t} \right] \quad (\tau \ll \tau_s) \quad (3-35)$$

$$v(t) = \frac{I_0 R_0 \ell}{2} \frac{2}{\sqrt{\pi}} \left(\frac{\tau_s}{t} \right)^{1/2} \sum_{n=1}^{\infty} \exp \left[-(2n-1)^2 \frac{\tau_s}{4t} \right] \quad (\tau \gg \tau_s) \quad (3-36)$$

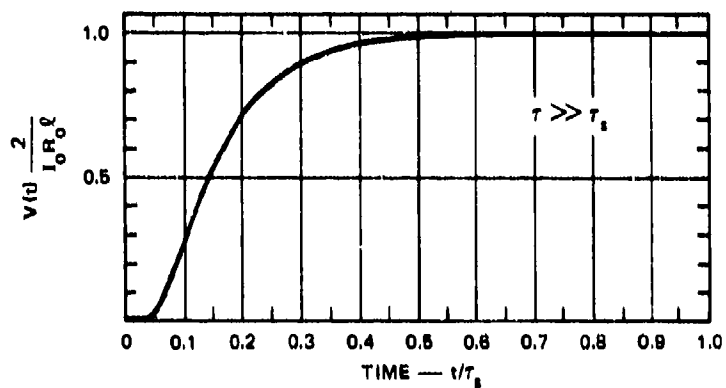
The waveform for $\tau \ll \tau_s$ is τ times the impulse response of the conductors, and the waveform for $\tau \gg \tau_s$ is the step-function response of the conductors. Plots of these waveforms and the response when $\tau = \tau_s$ are shown in Figure 3-23 normalized to $I_0 R_0 \ell / 2$ in magnitude and to τ_s in time.

The peak open-circuit voltages are

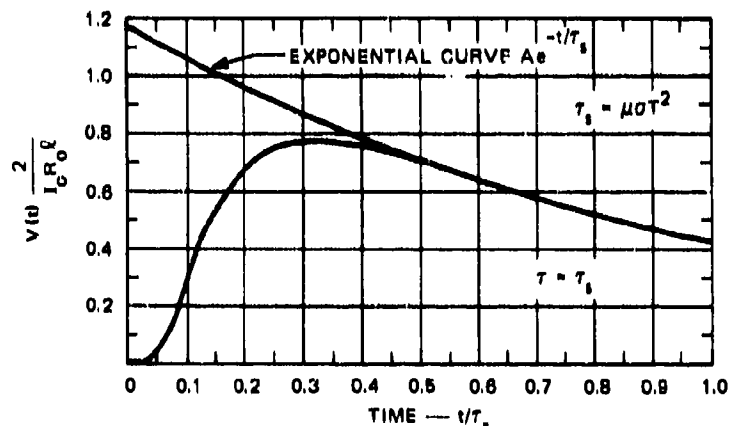
$$\begin{aligned} v(t)_{\text{peak}} &= \frac{I_0 R_0 \ell}{2} \quad (\tau \gg \tau_s) \\ &= 5.9 \frac{\tau}{\tau_s} \left(\frac{I_0 R_0 \ell}{2} \right) \quad (\tau \ll \tau_s) \\ &= 0.77 \left(\frac{I_0 R_0 \ell}{2} \right) \quad (\tau = \tau_s) \end{aligned} \quad (3-37)$$



(a) IMPULSE RESPONSE



(b) STEP FUNCTION RESPONSE



(c) EXPONENTIAL RESPONSE

Figure 3-23 VOLTAGE WAVEFORMS PRODUCED BY AN EXPONENTIAL PULSE $I_0 e^{-t/\tau}$ OF CURRENT IN THE SHIELD (normalized to $V_0/Z_0 = I_0 R_0 \Omega^2$)

if the conductors are open-circuited (relative to the conduit) at both ends. The 10-to-90% rise time for the voltage is

$$\begin{aligned}
 t_{10-90} &= 0.236 \tau_s & (\tau \gg \tau_s) \\
 &= 0.038 \tau_s & (\tau \ll \tau_s) \quad (3-38) \\
 &= 0.15 \tau_s & (\tau = \tau_s)
 \end{aligned}$$

Plots of the asymptotic values of the peak voltage and rise time against τ/τ_s are shown in Figure 3-24 as solid lines, and an estimate of their behavior between asymptotes is shown as a dashed curve. Values of τ_s and R_o for rigid steel conduit are given in Table 3-5.

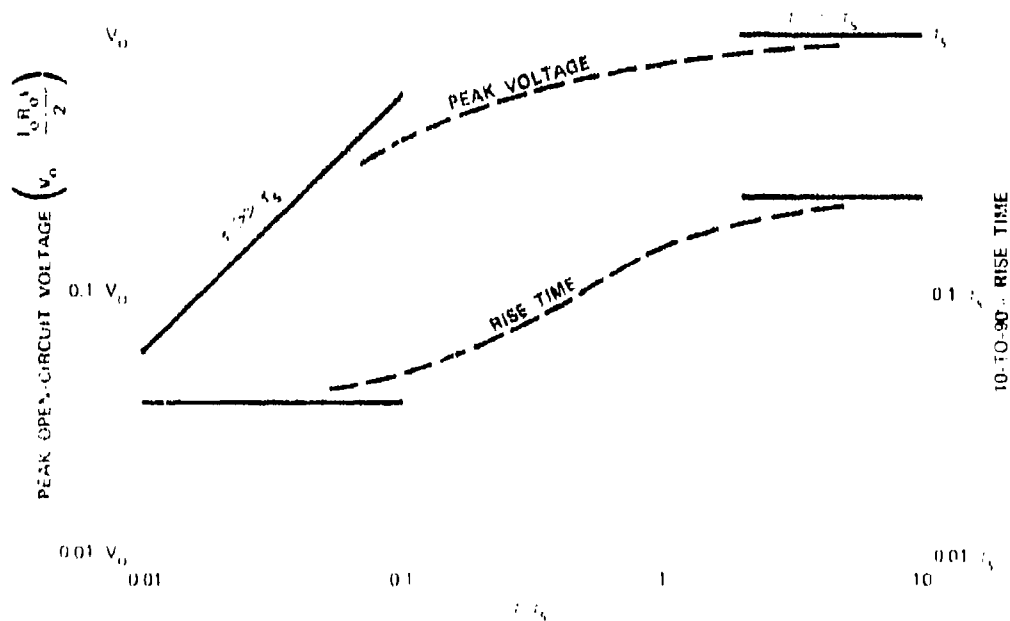


Figure 3-24 VARIATION OF PEAK OPEN-CIRCUIT VOLTAGE AND RISE TIME OF CONDUCTOR VOLTAGE AS A FUNCTION OF EXPONENTIAL CONDUIT-CURRENT-DECAY TIME CONSTANT τ (normalized to diffusion constant τ_s)

Table 3-5
SHIELDING PARAMETERS FOR RIGID STEEL CONDUIT

Nominal Conduit Size (inches)	R_o (ohms/m)	T_s		Q_s (A-s)
		$\mu_r = 500$ (ms)	$\mu_r = 1.0$ (μ s)	
½	1.03×10^{-3}	28.9	57.8	2.1
¾	7.77×10^{-4}	31.1	62.1	2.9
1	5.23	43.0	86.0	5.2
1¼	3.86	47.7	95.3	7.4
1½	3.23	51.1	102	9.1
2	2.40	57.7	115	13
2½	1.52	100	200	27
3	1.16	113	227	38
3½	9.64×10^{-5}	124	248	48
4	8.14	137	273	59
5	6.01	162	324	87
6	4.63	191	381	120

The voltage has the same magnitude and shape at both ends of the conduit; however, the polarity at one end is opposite to the polarity at the other end. If the conductors are shorted to the conduit at one end, the open-circuit voltage at the opposite end will have the same waveform but it will double in magnitude.

The current through matched terminations Z_0 at the ends of the conductors will be

$$I(\omega) = V(\omega)/Z_0 \quad . \quad (3-39)$$

3.3.3.3 Internal Voltage from Incident Field

The results presented here give the voltage between the conductors and the conduit induced by an exponential plane-wave pulse incident on the surface of the ground. The results apply to buried conduits that are short compared to the shortest wave-length penetrating the wall (see Figure 3-22) but long compared to a skin depth in soil. The results are obtained from the convolution of the conduit current obtained in Section 3.3.2.2 with the impulse response of the conduit obtained in Section 3.3.3.2.

The open-circuit voltage induced between the conductor and the conduit by an incident exponential pulse $E_0 e^{-t/\tau}$ is given by¹⁰

$$V(\omega) = \frac{I_0 R_0 \ell}{2} \sqrt{\frac{\tau_s}{\tau}} \frac{1}{(|\omega + 1/\tau| \sinh \sqrt{|\omega \tau_s}} \quad (3-40)$$

where

$$I_0 = 10^8 \sqrt{\tau \tau_s} E_0 D(\psi, \varphi) \quad (\text{see Eq. (3-14)})$$

$\tau_s = \mu_0 T^2$ is the diffusion constant for the tubular shield.

The open-circuit voltage waveform is

$$v(t) = \frac{I_0 R_0 \ell}{2 \sqrt{\pi}} \sqrt{\frac{\tau_s}{\tau}} e^{-t/\tau} \int_0^{t/\tau_s} \left\{ e^{-(\tau_s/\tau)y} \sum_{n=1}^{\infty} \frac{n}{y^{3/2}} \right. \\ \times \exp \left[-\left(\frac{(2n-1)^2}{2} \frac{1}{y} \right) \right] dy \quad (3-41)$$

This waveform, normalized to $\frac{I_0 R_0 t}{2\sqrt{\pi}}$, is plotted in Figure 3-25 for several values of τ_s/τ .

In deriving Eqs. (3-40) and (3-41), it has been assumed that the conductors are open-circuited with respect to the conduit at both ends, and that the conduit run is long enough that the conduit current may be considered uniform throughout the length of the conduit (i.e., end effects such as those described in Section 3.3.2.3 are negligible).

3.3.3.4 Saturation of Steel Conduit

Much of the shielding effectiveness of steel conduit is caused by the large relative permeability of steel. When very large currents flow in the conduit, however, the magnetic

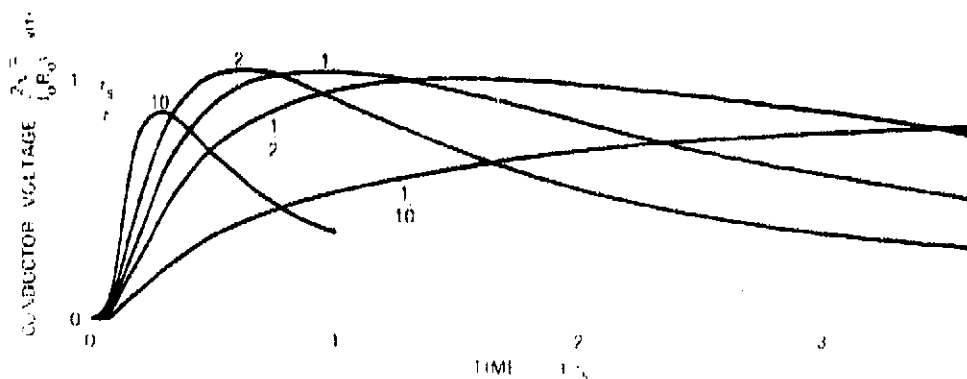


Figure 3-25 CORE-TO-SHIELD VOLTAGE WAVEFORMS INDUCED IN CONDUCTORS IN A BURIED CONDUIT BY AN INCIDENT PLANE-WAVE EXPONENTIAL PULSE $e^{-t/\tau}$

flux density in the steel may become large enough to saturate the steel and drastically reduce its permeability. It has been demonstrated that most ferromagnetic materials do not become completely saturated instantaneously.¹³ As saturation begins, the surface impedance of the saturated outer layer is much lower than the surface impedance of the interior unsaturated region, so that most of the current flows in the saturated layer. If the current is of sufficient magnitude and duration, it will eventually saturate the entire conduit wall. For transient

currents of short duration, however, the entire thickness of the wall may never saturate, so that the ferromagnetic shielding properties may be maintained even if partial saturation occurs.

Based on an analysis that assumes that the shield material is either completely saturated ($\mu_r = 1.0$) or completely unsaturated, the depth of saturation is found to be dependent on the charge transferred by the shield. For complete saturation of a tubular shield by a single transient, the saturation depth must approach the thickness, T , of the shield at some time $t \leq \infty$, giving

$$Q_s = \int_0^t I dt = \pi a \sigma B_s T^2 \quad (3-42)$$

where B_s is the flux density at saturation, a is the radius of the shield, and σ is the conductivity of the shield. The charge Q_s is the total charge that must flow along the shield to saturate the shield material completely. For a current step function, Q_s is therefore a measure of the time required to saturate all the way through the shield, since

$$Q_s = I_0 t_{sat} = \pi a \sigma B_s T \quad (3-43)$$

Any value of I_0 greater than that required to begin saturation will eventually saturate the shield all the way through, but the smaller the value of I_0 , the longer it will take to saturate the shield completely. For a rectangular pulse of width τ and amplitude I_0 , we have

$$I_0 \tau = \pi a \sigma B_s T^2 \quad (3-44)$$

and the current I_0 required to saturate the shield completely increases as the pulselength decreases. Similar relations can be obtained for other pulse shapes. For an exponential current $I_0 e^{-t/T}$, for example,

$$I_0 \tau = \pi a \sigma B_s T^2 \quad (3-45)$$

The values of Q_s are tabulated in Table 3-5 for rigid steel conduit with $\sigma = 6 \times 10^6$ mho/m and $B_s = 1.6 \text{ w/m}^2$ (16 kilogauss). Note that for pulse durations of about $1 \mu\text{s}$, peak currents of tens of megamperes are required to completely saturate 2-inch and larger conduits. Therefore, complete saturation of rigid steel conduits by the induced current from the high-altitude EMP is unlikely.

3.4 CABLES IN NON-METALLIC CONDUIT

3.4.1 GENERAL CONSIDERATIONS

As pointed out in Section 3.3, nonmetallic conduit offers no shielding to the conductors inside the conduit. Therefore the electric field in the soil induces current and voltage directly on the conductors in the conduit, and the high-frequency as well as the low-frequency spectra are important. The current induced on the cables may, in fact, be comparable to that induced on the metallic conduits discussed in Section 3.3. The current differs from that induced in the metal conduit only because the conductors are not in direct contact with the soil. Thus the coupling to the conductors is through the capacitance between the conductor and the soil and through the terminating impedances at the ends of the cable.

Because the cables are insulated from the soil by the conduit and by the air and cable insulation inside the conduit, the attenuation of induced currents is somewhat less (particularly at low frequencies) than it is for conductors in direct contact with the soil. For conductors in direct contact with the soil (such as metallic conduits), the current is attenuated as $\exp(-z/\delta)$, where δ is the skin depth in the soil, and z is the distance along the conductor. At low frequencies such that

$$\frac{\omega e}{\sigma} \frac{\log r_1/a}{\sqrt{2}\delta} \ll 1 \quad (3-46)$$

$$\log \frac{r_1}{\gamma_0 \delta}$$

where r_1 is the radius to the outside of the conduit and a is the effective radius of the conductors, the admittance per unit length between the conductor and the soil is dominated by the capacitance of the insulation, and the attenuation constant is much smaller than $1/\delta$. At high frequencies where the admittance per unit length is dominated by the admittance of the soil, however, the buried insulated conductor behaves in approximately the same manner as the buried bare conductor. Because of the lower attenuation at low frequencies, the conductors in nonmetallic conduits several hundred feet long may support current resonances at frequencies of several hundred kilohertz (see Section 2.2.1).

When shielded cables are used in nonmetallic conduit, the cable shield provides some protection for the conductor inside. The shields on power cables are usually designed primarily for electrostatic gradient control, however, rather than electromagnetic shielding. These shields are often fabricated of thin copper tape spiraled around the conductor insulation (with some overlap) to form a smooth outer conductor at low frequencies. Because the contact resistance of the overlapped tape is large compared to the resistance of the copper, the current in the shield tends to flow in the direction of the tape rather than parallel to the axis of the cable. Thus the tape-wound shield behaves as a solenoid, and at high frequencies the $j\omega L$ drop along this solenoid can be quite large (large enough to cause arcing between the turns of the tape). This $j\omega L$ drop drives the conductor inside the shield, and because of the ω dependence, the shield tends to readily pass the high-frequency spectrum (in contrast to the steel conduit, which almost completely eliminates the high-frequency spectrum).

3.4.2 CURRENT INDUCED ON CABLES

The current induced in buried insulated cables can be calculated in the same way as the current in the aerial transmission lines described in Chapter Two, except the excitation field is that at the surface (or just below the surface) of the ground and the characteristic impedance Z_0 and propagation factor γ of the buried conductor are used to replace those

of the aerial transmission line. Consider the buried, insulated conductor shown in Figure 3-26. If the conductor extends from $z = -\ell$ to $z = 0$, the current at the end $z = 0$ is

$$I(0) = I_{sc} \cdot \frac{1 - \mu_0}{2} \left\{ 1 - e^{-(1 - jk')\ell} + \frac{1 - jk'/\gamma}{1 + jk'/\gamma} \mu_0 e^{-2\gamma\ell} \right. \\ \times \left[1 - e^{(1 + jk')\ell} \right] \left\{ \frac{1}{1 - \mu_0 \mu_0 e^{-2\gamma\ell}} \right. \quad (3-47)$$

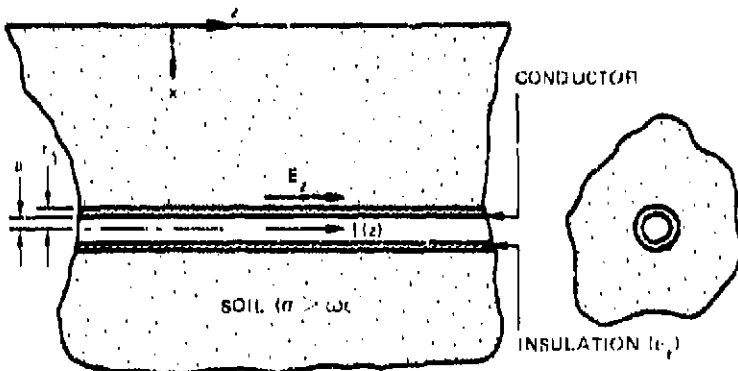


Figure 3-26 BURIED INSULATED CONDUCTOR

where

γ = Propagation factor for the cable/earth line

k' = $\frac{\omega}{c} \cos \psi \sin \psi$

Z_L = Terminal impedance at $z = -\ell$

Z_0 = Terminal impedance at $z = 0$

$$\rho_{\ell} = \frac{Z_{\ell} - Z_0}{Z_{\ell} + Z_0} \quad (3-48a)$$

$$\rho_0 = \frac{Z_0 - Z_0}{Z_0 + Z_0} \quad (3-48b)$$

The current $I_{sc\infty}$ is the short-circuit current at the end $z = 0$ of a semi-infinite buried conductor extending from $z = -\infty$ to $z = 0$. This short-circuit current is given by

$$I_{sc\infty} = \frac{2E_i}{Z_0\gamma} \left| \frac{\cos \varphi}{\sin \psi \sin \varphi} \right| \frac{\sqrt{j\omega r_0}}{1 - jk'/\gamma} \quad (3-49)$$

where $r_0 = \epsilon_0/a$ (a is the soil conductivity), and the upper trigonometric function applies to vertical polarization and the lower applies to horizontal polarization of the incident field E_i (see Figure 3-15 for spherical coordinate system).

The propagation factor γ and the characteristic impedance Z_0 are obtained from the impedance per unit length Z and the admittance per unit length Y with

$$Z_0 = \sqrt{Z/Y} \quad \gamma = \sqrt{ZY} \quad (3-50)$$

For low frequencies ($f \ll a/2\pi c$), the impedance per unit length is

$$Z = \frac{\omega\mu_0}{8} + j\omega \frac{\mu_0}{2\pi} \log \frac{\sqrt{2\delta}}{\gamma_0 a} \quad (3-51)$$

where μ_0 is the permeability of free space (and the soil), δ is the skin depth in the soil, a is the effective radius of the conductors, and $\gamma_0 = 1.781 \dots$

The admittance per unit length is

$$Y = j\omega C_l \frac{1}{1 + \frac{j\omega C_l}{Y_s}} \quad (3-52)$$

where C_l is the capacitance per unit length between the conductor and the soil, and Y_s is the admittance per unit length of the soil. The capacitance is

$$C_l = \frac{2\pi\epsilon}{\log r_1/a} \quad (3-53)$$

where r_1 is the radius to the outside of the conduit. The admittance per unit length Y_s of the soil is given by

$$Y_s = \frac{j\omega\mu_0\sigma}{\frac{\omega\mu_0}{8} + j\omega \frac{\mu_0}{2\pi} \log \frac{\sqrt{2\delta}}{\gamma_0 r_1}} + \frac{2\pi\sigma}{\log \frac{\sqrt{2\delta}}{\gamma_0 r_1}} \quad (3-54)$$

Since $\omega C_l/Y_s \ll 1$ when

$$\frac{\omega e}{\sigma} \frac{\log \frac{\sqrt{2\delta}}{\gamma_0 r_1}}{\log \frac{r_1}{a}} \ll 1$$

it follows that

$$Y = j\omega C_l \left(1 - \frac{\omega e}{\sigma} \frac{\log \frac{\sqrt{2\delta}}{\gamma_0 r_1}}{\log \frac{r_1}{a}} \right) \quad (3-55)$$

at low frequencies. The impedance per unit length Z is, therefore, primarily inductive reactance with a small resistive component $R = \omega\mu_0/8$, and the admittance per unit length Y is primarily capacitive susceptance $j\omega C$; with a small conductive component

$$G = \frac{\omega^2 \epsilon^2}{\sigma} \frac{2\pi \log \frac{\sqrt{2}\delta}{\gamma_0 r_1}}{\left(\log \frac{r_1}{a}\right)^2} \quad (3-56)$$

The attenuation constant α is,

$$\alpha \approx \operatorname{Re}(\gamma) \approx \frac{R}{2Z_0} + \frac{GZ_0}{2} \quad (3-57)$$

where R and G are given by the real part of Eq. (3-51) and Eq. (3-56), respectively. The characteristic impedance is

$$Z_0 \approx \frac{\eta_0}{2\pi} \sqrt{\epsilon_r \log \frac{\sqrt{2}\delta}{\gamma_0 a} \log \frac{r_1}{a}} \quad (3-58)$$

where $\eta_0 = \sqrt{\mu_0/\epsilon_0} = 120\pi$. The phase factor β is approximately

$$\beta = \operatorname{Im}[\gamma] \approx \frac{\omega}{c} \sqrt{\frac{\epsilon_r \log \frac{\sqrt{2}\delta}{\gamma_0 a}}{\log r_1/a}} \quad (3-59)$$

The quantities α , β/k , and $|Z_0|$ are plotted in Figures 3-27 and 3-28 for a typical 4-inch conduit in average soil. It is apparent that $|Z_0|$ is fairly independent of frequency, β/k is moderately independent of frequency and of the order of 3, and α is strongly dependent on frequency but so small that attenuation in propagating a few hundred feet is negligible at frequencies below 1 MHz.

The values of Z and Y can be substituted into Eqs. (3-50), (3-49), and (3-47) to evaluate the current in the conductors for frequencies $f < \frac{a}{2\pi\epsilon}$. Numerical techniques can be used to obtain the inverse transform of Eq. (3-47). Some approximations can be made that permit estimates of the current to be obtained without extensive machine computations. In Eq. (3-49), for example, the term $Z_0\gamma$ can be approximated by

$$Z_0\gamma = Z \approx j\omega \frac{\mu_0}{2\pi} \log \frac{\sqrt{2\delta}}{\gamma_0 a} \approx j\omega \frac{10\mu_0}{2\pi} \quad (3-60)$$

and the quantity jk'/γ is

$$\frac{jk'}{\gamma} \approx \frac{k \cos \psi \cos \varphi}{\beta} = \frac{k'}{\beta} \quad (3-61)$$

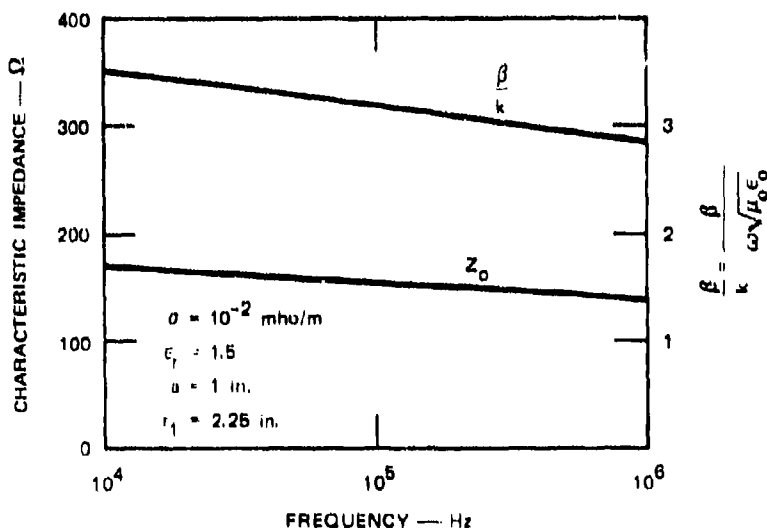


Figure 3-27 CHARACTERISTIC IMPEDANCE Z_0 AND PROPAGATION FACTOR β FOR CONDUCTORS IN A BURIED NONMETALLIC CONDUIT

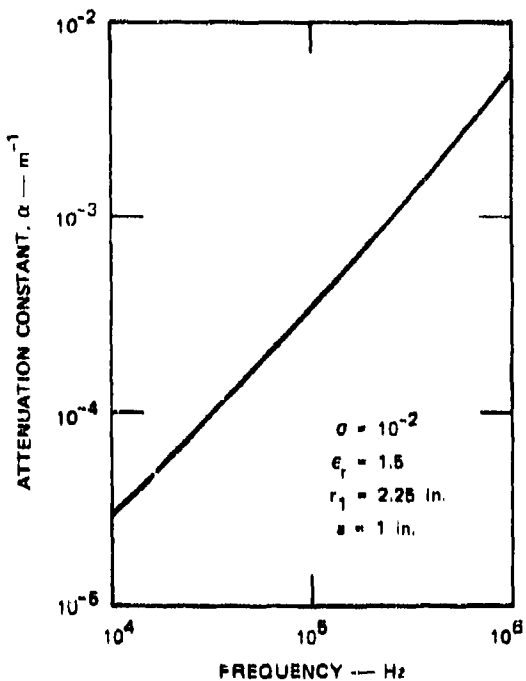


Figure 3-28 ATTENUATION CONSTANT α FOR CONDUCTORS IN A BURIED NON-METALLIC CONDUIT

so that Eq. (3-49) becomes

$$I_{sc\infty} \approx 10^6 \frac{E_0 \sqrt{\epsilon_r}}{1 - k'/\beta} \left\{ \frac{\cos \varphi}{\sin \psi \sin \varphi} \right\} \frac{1}{\sqrt{j\omega}} . \quad (3-62)$$

The terms $1 \pm jk'/\gamma$ in Eq. (3-47) have been replaced by $1 \pm k'/\beta$.

For an exponential pulse $E_0 e^{-t/\tau}$ whose transform is $E_0/(j\omega + 1/\tau)$, the short-circuit current $I_{sc\infty}$ above is the same as that given by Eq. (3-13) for a long, bare conduit. The waveform of this current is shown in Figure 3-17 and its amplitude can be obtained from Figures 3-18 and 3-19. For the finite length of conduit, this waveform is modified by the exponential terms in Eq. (3-47), which in the time domain represent combinations of the basic waveform of Figure 3-17 with delay and attenuation.

A plot of the induced current waveform for an incident exponential pulse of decay time constant $\tau = 0.5 \mu\text{s}$ is shown in Figure 3-29 for a 100-ft-long cable short-circuited at both ends. For comparison, the short-circuit current I_{sc} induced in a semi-infinite cable is also shown as a dashed curve in Figure 3-29. The short-circuit current is normalized to the quantity

$$I_0 = \frac{2E_0 \sqrt{\tau_e \tau} v}{Z_0 \left(1 - \frac{k}{\beta}\right)} \begin{Bmatrix} \cos \varphi \\ \sin \varphi \sin \psi \end{Bmatrix} \quad (3-63)$$

where $v = \omega/\beta$. The upper trigonometric function applies to vertical polarization, and the lower applies to horizontal polarization. For the waveform of Figure 3-29 the attenuation α was neglected, and the phase factor β was assumed to have a constant value of $3k$ (see Figure 3-27). It is observed that the peak short-circuit current induced in the 100-ft-long cables is almost as large as that induced in the semi-infinite cable, but it has more "fine structure" because of the end effects associated with the finite length. It is also observed that the value of I_0 given above is the same as that given in Eq. (3-14) for a long buried conductor if $v = c$, $k/\beta \ll 1$, and the approximation of Eq. (3-60) is used for $Z_0/v = Z_0 \gamma / j\omega$.

The source impedance of the Norton equivalent source associated with the short-circuit current is

$$Z(0) = Z_0 \frac{1 + \rho_\ell e^{-2\gamma l}}{1 - \rho_\ell e^{-2\gamma l}} \quad (3-64)$$

where ρ_ℓ is given by Eq. (3-48). The open-circuit voltage at the end $z = 0$, when the other end has a reflection coefficient ρ_ℓ is, therefore,

$$V_{oc}(0) = I_{sc}(0) Z(0) \quad (3-65)$$

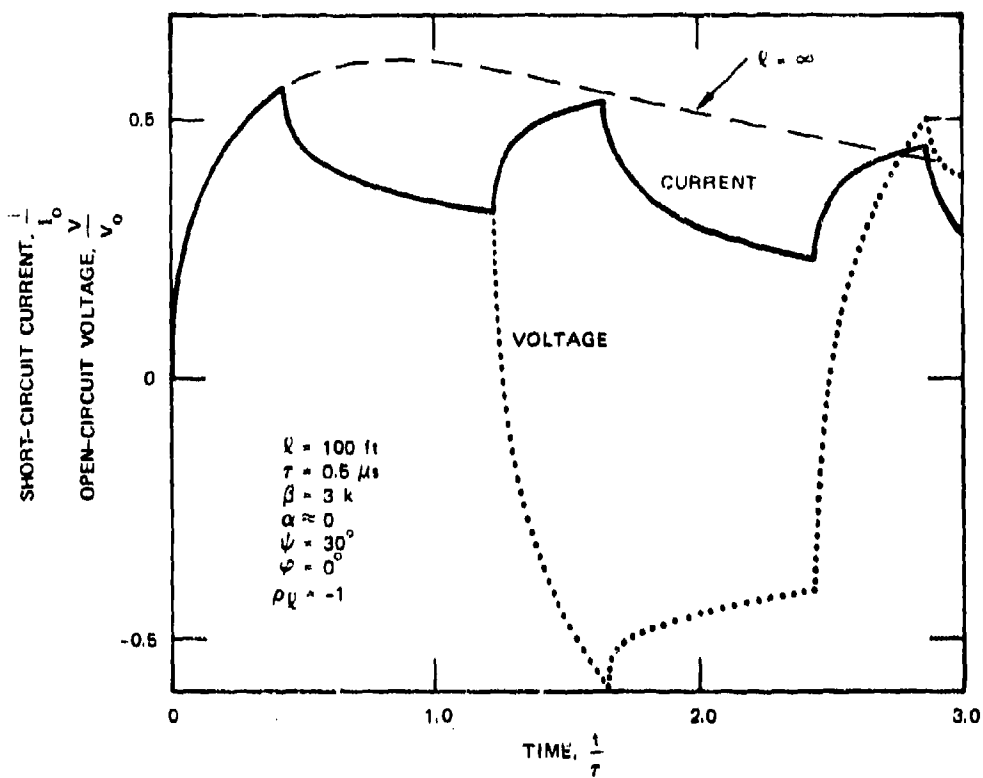


Figure 3-29 SHORT-CIRCUIT CURRENT AND OPEN-CIRCUIT VOLTAGE INDUCED IN CONDUCTORS IN A BURIED, NONMETALLIC CONDUIT

where $I_{sc}(t)$ is given by Eq. (3-47) when $\rho_0 = -1$. The voltage waveform is thus similar to the current waveform except that the reflected waves alternate in polarity. This can be seen by examining the last term (outside the braces) in Eq. (3-47):

$$\frac{1}{1 - \rho_L \rho_0 e^{-2\gamma t}} = \sum_{n=0}^{\infty} [\rho_L \rho_0 e^{-2\gamma t}]^n \quad (3-66)$$

When $\rho_0 = -1$, as is the case for the short-circuit current at $z = 0$,

$$\frac{1}{1 + \rho_\ell e^{-2\gamma\ell}} = \sum_{n=0}^{\infty} [-\rho_\ell e^{-2\gamma\ell}]^n, \text{ (short-circuit current)} \quad (3-67)$$

and when this is multiplied by $Z(0)$ to obtain the open-circuit voltage,

$$Z(0) \frac{1}{1 + \rho_\ell e^{-2\gamma\ell}} = \frac{Z_0}{1 - \rho_\ell e^{-2\gamma\ell}} = Z_0 \sum_{n=0}^{\infty} [\rho_\ell e^{-2\gamma\ell}]^n \quad \text{(open circuit voltage).} \quad (3-68)$$

The odd terms in the voltage series are thus opposite in sign to the corresponding terms in the current series when $\rho_\ell = -1$.

The open-circuit voltage waveform is also plotted in Figure 3-29 (dotted curve) for the 100-ft-long cable with the end $z = -l$ short-circuited. The voltage is normalized to $V_0 = I_0 Z_0$. For the conditions assumed here and in Figures 3-27 and 3-28, a 50-kV/m exponential pulse with a 0.5- μ s decay time constant would induce a short-circuit current of 600 A or an open-circuit voltage of 90 kV at the end of the 100-ft-long cables in non-metallic conduit.

3.4.3 TRANSFER IMPEDANCE OF CABLE SHIELDS

When the cables in the nonmetallic conduit are shielded cables, as is generally the case for cables used between the potheads and ground-based transformers, the currents discussed in the preceding section are induced in the cable shields. As indicated in Section 3.4.1 the shields for these cables are often spiral-wound copper tape and the tape or spiral-wound shield tends to behave as a solenoid wound about the internal conductors. There is, therefore, strong coupling between the shield current and internal conductors. For large $dI/dt (j\omega l)$, the voltage developed per turn can become large enough to produce arcing between turns. (When this occurs, the shield actually improves, because the coupling is reduced).

For a tape-wound shield in which the turns are not overlapped and have no contact between turns,* the geometry of the shield can be defined by the radius, a , of the shield and the width, w , of the tape as illustrated in Figure 3-30. This geometry may also be defined in terms of the spiral angle θ or the turns per unit length N , which are related through

$$\cos \alpha = \frac{w}{2\pi a}, N = \frac{\sin \theta}{w} \quad (3-69)$$

and

$$2\pi a N = \tan \theta.$$

The shield current I has the same pitch as the tape and is assumed to be uniformly distributed across the tape width, w .

The transfer impedance of the tape-wound shield is⁴

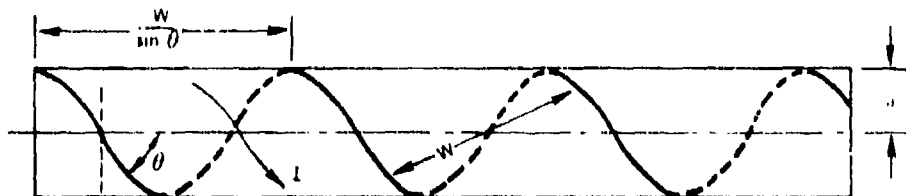
$$Z_T = \frac{1}{I} \frac{dV}{dz} = Z_{TO} + \left(Z_i + \frac{j\omega\mu_0}{4\pi} \right) \tan^2 \theta \quad (3-70)$$

where $Z_{TO} = R_o \frac{\gamma T}{\sinh \gamma T}$ and $Z_i = R_o \gamma T \coth \gamma T$, T is the tape thickness and $\gamma = (1+j)/\delta$

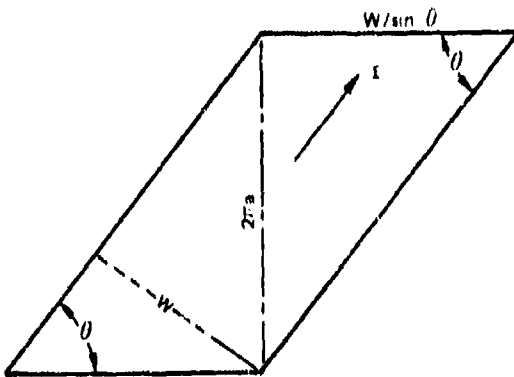
(δ is the skin depth in the tape). The magnitude of the transfer impedance Z_T , normalized to the low-frequency transfer impedance R_o of a cylindrical tube of the same wall thickness, is shown in Figure 3-31 for various spiral angles θ . The low-frequency transfer impedance R_o is the dc resistance per unit length of a tubular shield of radius a and thickness T . Under this normalization we obtain

$$\frac{Z_T}{R_o} = \frac{\gamma T}{\sinh \gamma T} + \left[\gamma T \coth \gamma T + j \left(\frac{T}{\delta_o} \right)^2 \frac{a}{T} \tan^2 \theta \right] \quad (3-71)$$

*That is, the contact resistance is large compared to the resistance of one turn of tape.



(a) TAPE-WOUND SHIELD



(b) ONE TURN DEVELOPED ON A PLANE

Figure 3-30 ILLUSTRATION OF PARAMETERS FOR A SINGLE-LAYER TAPE-WOUND SHIELD

where δ_0 is the skin depth for a nonferrous shield ($\mu = \mu_0$), whether or not the material is ferrous, with a conductivity σ . In Figure 3-31, $a/T = 10$.

From Figure 3-31 it is apparent that for low frequencies ($T/\delta_0 \ll 1$) the transfer impedance increases with increasing spiral angle θ . This follows from the fact that a larger spiral angle θ is accompanied by a narrower tape (smaller w) and more turns per unit length (larger N). Thus the tape required to wind a unit length of shield is longer and narrower, and has a large resistance, for large spiral angles.

At high frequencies ($T/\delta_0 \gg 1$) the transfer impedance is dominated by the inductance term, which is proportional to $(T/\delta_0)^2$. The magnitude of the transfer impedance again increases as the spiral angle θ increases, because the number of turns per unit length and the inductance per unit length increase.

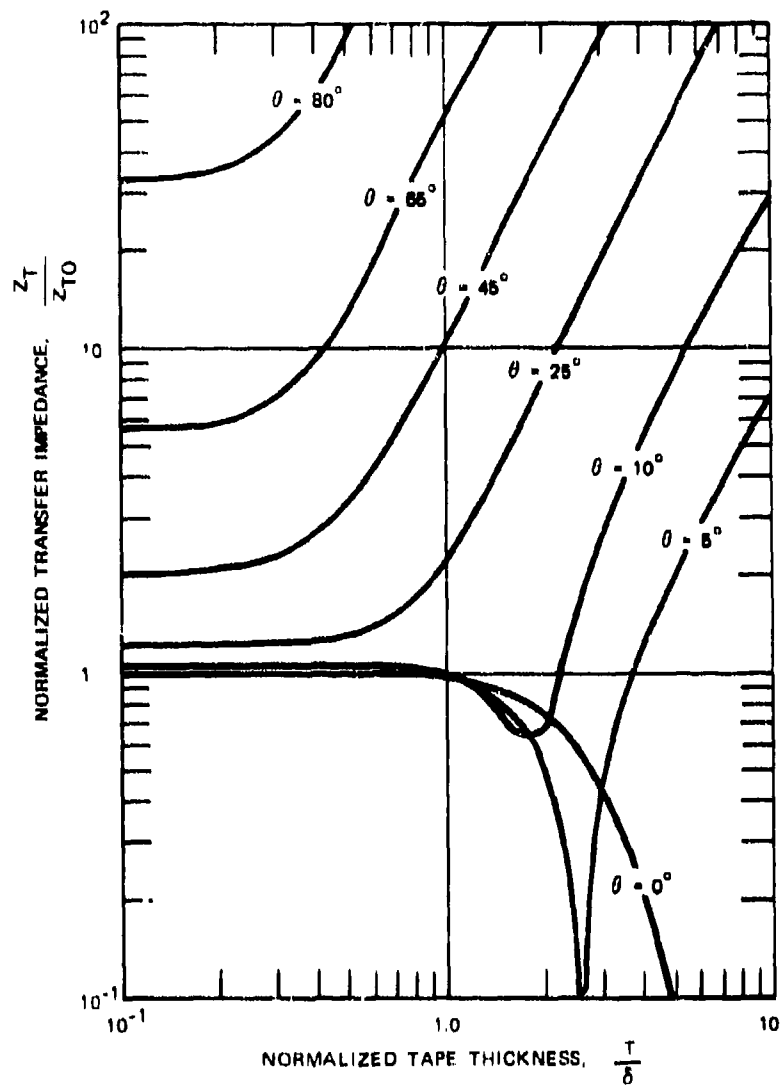


Figure 3-31 MAGNITUDE OF THE TRANSFER IMPEDANCE COMPUTED FOR A TAPE-WOUND SHIELD

Similar expressions have not been developed for the overlapped tape-wound shields, but the high-frequency characteristics of a single-layer-overlapped shield with tape width w and overlap width w_0 can be obtained by substituting $w - w_0$ for w in Eq. (3-69). At low frequencies ($T/\delta \ll 1$) the transfer impedance obtained with this substitution will be too large by a factor $w/(w - w_0)$, however, and at very high frequencies, the capacitance

between the overlapped turns will begin to short out the inductance so that the magnitude of the transfer impedance will reach a maximum and then begin to decrease.

Between the low-frequency (resistive) region and the high-frequency (capacitive) region, the tape-wound shield behaves as a solenoid of inductance per unit length

$$L = \frac{\mu_0}{4\pi} \tan^2 \theta \quad (3-72)$$

which, for a winding angle $\theta = 45^\circ$, is $0.1 \mu\text{H/m}$. For current rates of rise of tens of kiloamperes per microsecond that might be induced in the cable shield by a 50-kV/m incident exponential field, the voltage induced between the conductor and the shield would be

$$V = L \frac{di}{dt} \approx 10^{-7} \times 10^{10} = 10^3 \text{ V/m}. \quad (3-73)$$

Thus, several kilovolts per meter would be induced on the conductors inside the tape-wound shield, compared to less than 1 V/m for conductors inside steel conduit. Typical service-entrance cables cannot be considered electrically short at the frequencies penetrating the tape-wound shield. For this reason, a transmission-line solution such as that described in Eqs. (2-3 through 2-5), in which $E_z = iZ_T$, is required to obtain the waveform of the induced voltage.

Shields formed with a longitudinal overlapping seam ($\theta = 0$) and multilayer spiral-wound shields with alternating winding directions for alternate layers display a much smaller inductive coupling effect (typically less than 1 nH/m). Even these shields are much poorer than rigid steel conduit, however, because they are thin (usually a few mils) and non-ferrous (copper or aluminum). For example, a 5-mil-thick longitudinal copper-tape shield on a $3/4$ -inch-diameter cable has a dc resistance of $2.3 \times 10^{-3} \text{ ohm/m}$ and a cutoff frequency (at which $T = \delta$) of $2.7 \times 10^5 \text{ Hz}$, while a 4-inch rigid steel conduit has a dc resistance of only $8.1 \times 10^{-5} \text{ ohm/m}$ and a cutoff frequency of only 2.3 Hz . Thus the gain-bandwidth product ($R_0 f_\delta$) for the thin copper shield is about 3×10^6 times greater than that of the steel conduit. As a result, one can usually neglect the effect of the cable shields on shielded

cables routed through continuous steel conduit. When the cable shield is the only shield protecting the conductors from the fields in the soil, however, its shielding properties are important in the analysis of the current and voltage induced on the conductors.

3.5 CITED REFERENCES

1. *Electrical Transmission and Distribution Book*, 4th Ed. (5th printing) (Westinghouse Electric Corporation, East Pittsburgh, Penn., 1964).
2. E. F. Vance and S. Dairiki, "Analysis of Coupling to the Commercial Power System," Technical Report AFWL-TR-72-21, Contract F29601-69-C-0127, Air Force Weapons Laboratory, Kirtland Air Force Base, New Mexico (August 1972).
3. S. Ramo and J. R. Whinnery, *Fields and Waves in Modern Radio*, 2nd Ed., (John Wiley & Sons, New York, N.Y., 1963).
4. H. Kaden, *Wirbelströme und Schirmung in der Nachrichtentechnik* (Springer-Verlag, Berlin, 1959).
5. W. R. Smythe, *Static and Dynamic Electricity*, 3rd Ed., pp. 77, 78, (McGraw-Hill Book Co., New York, N.Y., 1968).
6. E. D. Sunde, *Earth Conduction Effects in Transmission Systems*, (Dover Publications, Inc., New York, N.Y., 1968).
7. *DASA EMP (Electromagnetic Pulse) Handbook*, DASA 2114-1, Chap. 11, (DASA Information and Analysis Center, Santa Barbara, Calif., September 1968).
8. A. L. Whitson and E. F. Vance, "Measurement of Fields Near a Vertical Monopole," Sensor and Simulation Note 152, Stanford Research Institute, Menlo Park, Calif. (September 1965, unpublished report).
9. E. F. Vance, "Internal Voltages and Currents in Complex Cables," EMP Interaction Note VIII, Stanford Research Institute, Menlo Park, Calif. (June 1967, unpublished report).
10. E. F. Vance, "Prediction of Transients in Buried Shielded Cables," Interim Technical Report, Contract DAEA18-71-1-0204, SRI Project 2182, Stanford Research Institute, Menlo Park, Calif. (March 1973).

11. S. A. Schelkunoff, "The Electromagnetic Theory of Coaxial Transmission Lines and Cylindrical Shields," *Bell System Tech. J.*, Vol. 13, pp. 532-579 (October 1934).
12. G. A. Korn, *Basic Tables in Electrical Engineering* (McGraw-Hill Book Co., New York, N.Y., 1965).
13. R. R. Ferber and F. J. Young, "Enhancement of EMP Shielding by Ferromagnetic Saturation," *IEEE Trans. on Nuclear Science*, Vol. NS-17, No. 6, pp. 354-359 (December 1970). Also see *Proc. IEEE*, Vol. 61, pp. 404-413 (April 1973).

Chapter Four

PROPERTIES OF DISTRIBUTION TRANSFORMERS

4.1 INTRODUCTION

4.1.1 EFFECTS OF TRANSFORMERS AND LIGHTNING ARRESTERS

The commercial electric power for operating ground-based facilities is typically supplied from three-phase distribution lines with a three-phase ground-based or pole-mounted transformer bank at the facility to reduce the voltage to 120, 240, or 480 V. Three single-phase transformers are usually used for the three-phase system. The low-voltage leads from the transformers are carried into the facility in plastic or rigid steel conduit. If the power system is subjected to the EMP of a nuclear detonation, extremely large voltages will be induced in the long, above-ground transmission lines supplying the primary side of the transformer. Part of this induced voltage will be passed by the transformers and will enter the facility on the low-voltage power conductors. In addition, the induced voltages can be large enough to fire the lightning arresters installed between the primary terminals of the transformer and ground. However, because of the fast rise time (tens of nanoseconds) of the induced voltage, the lightning arresters fire at much

higher voltages under the EMP excitation than they do with the more slowly rising lightning transients.

Single-frequency, or continuous-wave (CW), measurements of transformer transfer characteristics indicate that distribution transformers of different manufacturers and winding design are quite similar to each other. All transformers display a bandpass-filter characteristic for common-mode excitation, with the frequencies below a few hundred kilohertz suppressed by the interwinding capacitance and frequencies above about 10 MHz suppressed by the bushing inductance. Generally, the type of winding, the manufacturer, and even the kVA rating have no major effect on the transfer characteristics, although each transformer has its own fine structure — for example, in the voltage transfer functions.

The results of transient tests of the transformers at excitation levels below the lightning-arrester firing threshold show that the rise times of the primary current and the secondary voltages are stretched by the transformer bushing inductance, and the late-time response of the secondary voltage is suppressed by the interwinding capacitance. Thus, a fast-rising, wide-excitation pulse applied to the primary terminals produces a narrow pulse with a slower rise time at the secondary terminals. The peak secondary-terminal voltage for a 1-V common-mode step excitation of the primary terminals is 0.2 to 0.3V, with a time-to-peak of about 70 ns and a principal response duration of about 200 to 400 ns.

At an excitation level of about four times their rated voltage, distribution lightning arresters fire and limit the primary voltage. Near the threshold, 150 to 200 ns are required, after application of primary excitation, for the lightning-arrester spark gaps to ionize and become conducting. As the excitation level is increased, this time lag is decreased, but fast-rising excitation voltages may reach very large values before the lightning arresters fire. Because of the inductively limited rate of rise of the primary current, however, it is theorized that most of the initial applied voltage appears across the bushing inductance, rather than across the winding insulation. The shortest time-to-fire that has been observed experimentally was 40 ns, at a firing voltage of about ten times the rated voltage (2.5 times the static firing voltage). It has been observed, however, that in spite of the large peak voltages that can be attained before the lightning arrester fires, the lightning arrester always fires before any of the transformer insulation (e.g., bushings, winding insulation) fails. Thus,

the lightning arresters appear to be effective protective devices for the fast-rising EMP transients as well as the slower-rising lightning transients.

The effect of the lightning-arrester firing on the secondary voltage waveform has also been examined. At excitation levels only slightly greater than the firing threshold, the lightning-arrester firing has very little effect on the peak secondary voltage, because the firing time-lag is about as wide as the main secondary response (about 200 ns). At greater excitation levels, where the firing time-lag is significantly less than 200 ns, the peak secondary voltage ceases to increase linearly with the excitation level. At still greater excitation levels, where time-to-fire is equal to or less than the time-to-peak of the secondary voltage (in the absence of the lightning arrester), the peak secondary voltage becomes virtually independent of the excitation level. For the 7.2/12.5-kV transformer exhibiting the strongest common-mode coupling, this saturation level was about 30 kV at the secondary terminals. The lightning arresters at the primary terminals are therefore effective in limiting the EMP-induced throughput of the transformers as well as in protecting the transformer from damage.

4.1.2 TRANSFORMER CONSTRUCTION

Power transformers are available in a variety of shapes and sizes; the discussion here is limited to a presentation of the major characteristics of the oil-insulated distribution transformers of the type commonly used for single-customer service. In these transformers, the transformer core and windings are submerged in a metal tank of insulating oil that circulates by natural or forced convection. Glazed porcelain feedthrough bushings provide access to the transformer windings; the larger primary bushings are commonly mounted on the tank lid, while the smaller secondary bushings are usually arranged along one side of the tank (above the internal oil level). Figure 4-1 shows a photograph of two pole-mounting transformers.

The internal construction of a typical transformer is illustrated in Figure 4-2 with the photographs of a 25-kVA G.E. unit taken from the primary and secondary sides when the core and windings were removed from the housing for a final damage inspection. The

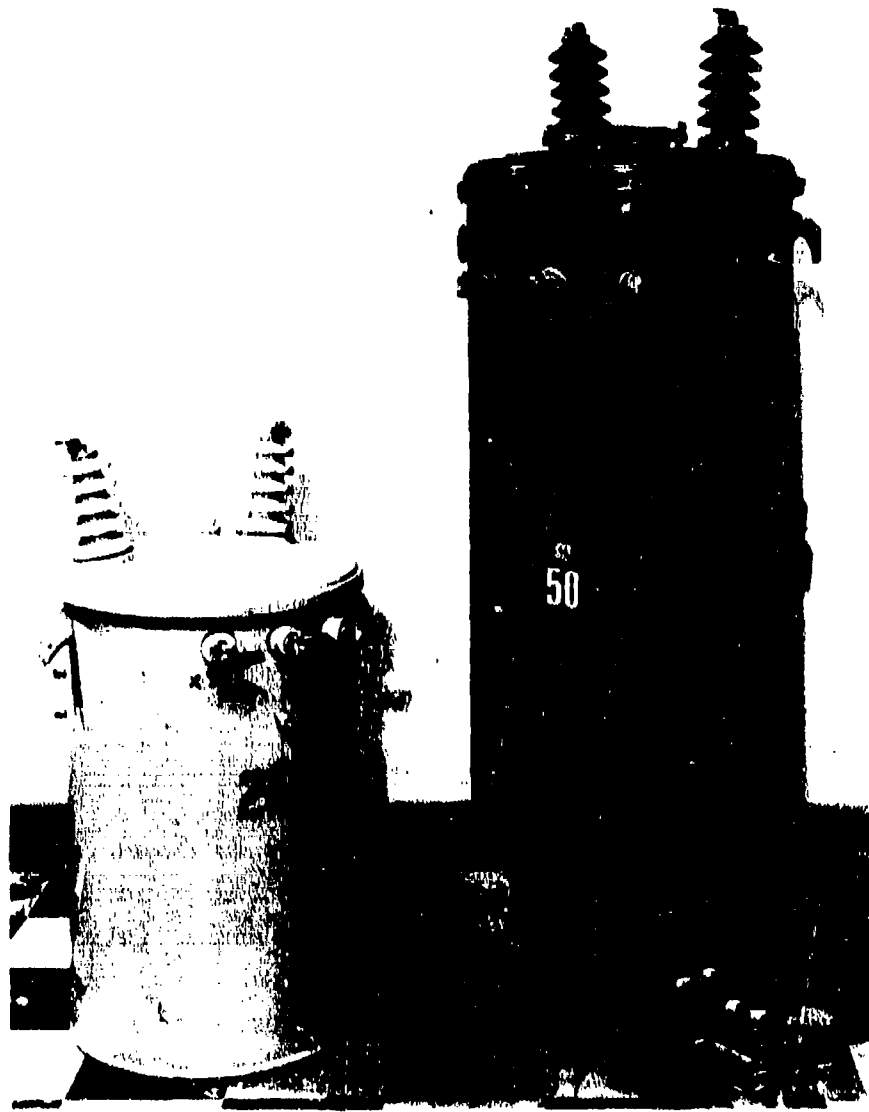


Figure 4-1 TYPICAL POWER-DISTRIBUTION TRANSFORMERS

switch and knob visible in the photographs are part of the primary-side tap changer. The single primary winding is actually split in the center and several taps are made on each side; this permits the number of primary turns to be varied somewhat to compensate for slight undervoltages (the adjustment range is +0, -10% in 2.5% steps). The types of windings and insulation used in the transformer depend on the time of manufacture of the transformer.

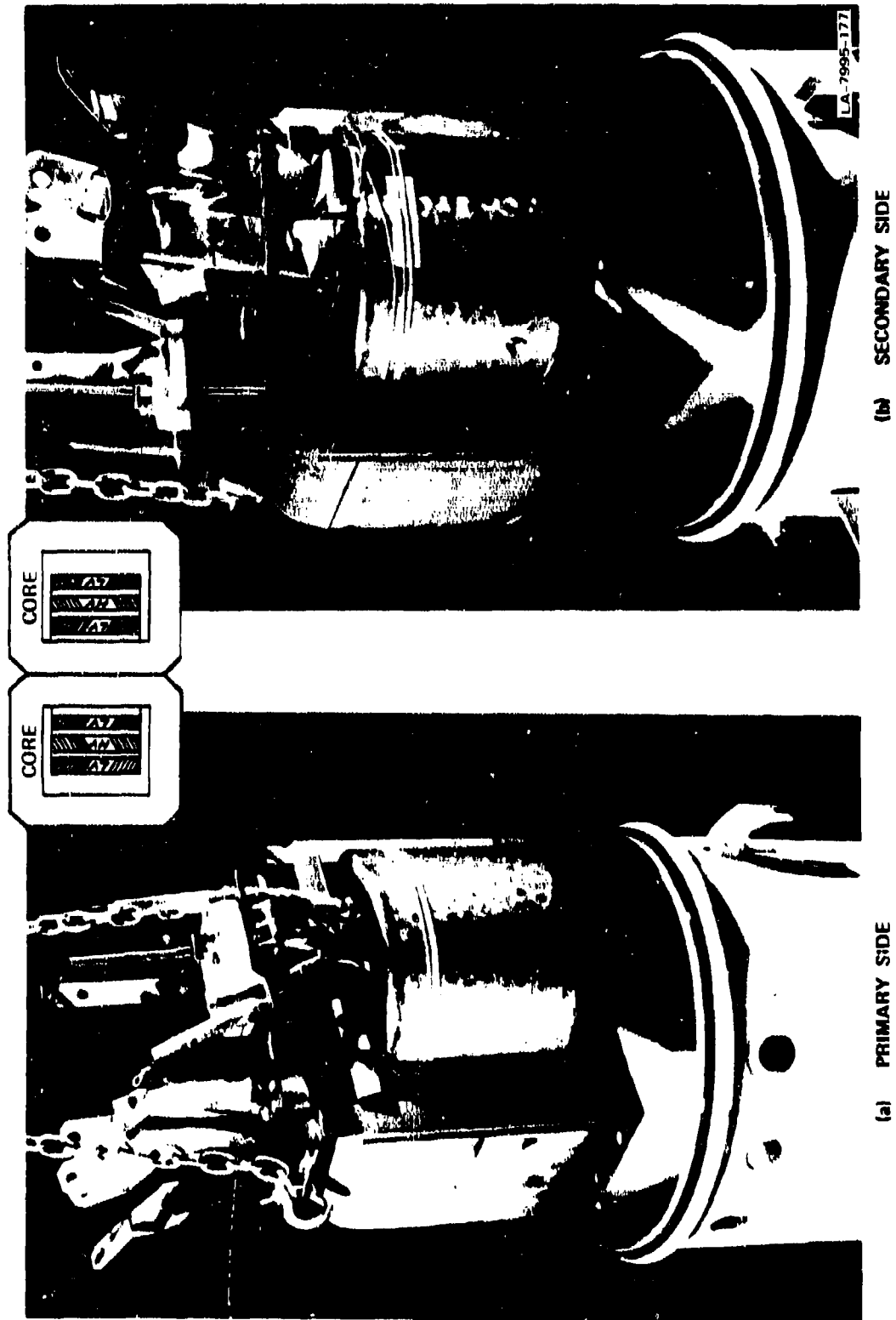


Figure 4-2 PHOTOGRAPHS OF THE WINDINGS AND CORE OF THE 25-kVA GE TRANSFORMER (insert shows shell-type core construction)

Older transformers are wound with round or rectangular copper wire with paper or carnbric insulation (in addition to oil) between layers. At the time of this writing, however, common practice is to use aluminum strip for the secondary windings. Because economic factors dictate the design of power transformers, the relative costs of copper and aluminum and the cost of manufacturing processes at the time of manufacture have strong influences on transformer construction.

In shell-type transformer construction (illustrated in the inset in Figure 4-2) the transformer core commonly consists of two roughly square cores butted together along one side, with the windings linking each hollow square. The windings of the transformers consist of concentrically layered primary and secondary windings with the primary (high-voltage) winding sandwiched between the secondary windings. This construction contributes to asymmetry in the coupling between the primary and the secondary windings. A simple rectangular core with windings on two legs of the core is also used in some power transformer designs.

Basic types of cooling used for distribution transformers are referred to by the following designations:¹

- **OA** – Oil-Immersed Self-Cooled. In this type of transformer the insulating oil circulates by natural convection within the tank (see Figures 4-1 and 4-2).
- **OA/FA** – Oil-Immersed Self-Cooled/Forced-Air Cooled. This type of transformer is basically an OA unit with the addition of fans to increase the rate of heat transfer from the cooling surfaces.
- **OA/FOA/FOA** – Oil-Immersed Self-Cooled/Forced-Oil Forced-Air Cooled/Forced-Oil Forced-Air Cooled. OA rating increased by the addition of some combination of fans and oil pumps.
- **FOA** – Oil-Immersed Forced-Oil-Cooled with Forced-Air Cooler.
- **OW** – Oil-Immersed Water-Cooled. In this type of water-cooled transformer, the cooling water runs through coils of pipe that are in contact with the insulating oil of the transformer.

- **FOW** – Oil-Immersed Forced-Oil Cooled with Forced-Water Cooler. External oil-to-water heat exchangers are used in this type to transfer heat from oil to cooling water.
- **AA** – Dry-Type Self-Cooled. Dry-type transformers, available at voltage ratings of 15 kV and below, contain no oil or other liquid to perform insulating and cooling functions.
- **AFA** – Dry-Type Forced-Air Cooled. This type of transformer has a single rating, based on forced circulation of air by fans or blowers.
- **AA/FA** – Dry-Type Self-Cooled/Forced-Air Cooled. This design has one rating based on natural convection and a second rating based on forced circulation of air by fans or blowers.

Standard impulse tests are conducted on distribution transformers to ensure that the bushings and winding insulation meet the basic insulation level (BIL) specified for their type, power, and voltage class. Transformers in a given BIL class are tested to the levels given in Table 4-1. The three basic insulation tests specified by the American Standards Association are:

- (1) The full-wave test with an impulse that reaches its crest in 1.5 μ s and decays to half its crest voltage in 40 μ s.
- (2) The chopped-wave test in which the impulse is truncated by an air-gap firing after the specified minimum time-to-flashover has elapsed. Only the leading edge of the impulse is applied to the transformer, since the air gap chops the tail off the impulse after the specified minimum time.
- (3) The low-frequency test in which about twice the rated voltage at about twice the rated frequency is applied for no longer than 1 minute.

The transformer high-voltage bushings and windings must be capable of withstanding these tests when applied between the two high-voltage terminals and when applied between either

Table 4-1

STANDARD INSULATION CLASSES AND DIELECTRIC TESTS FOR DISTRIBUTION AND POWER TRANSFORMERS

Rated Voltage (kV)	Rated Voltage Between Terminals of Power-Transformers ^(a)			Low-Frequency Tests		Impulse Tests Oil-Immersed Transformers 500 kVA or Less		
	Single-Phase		3-Phase	Oil-Immersed Type (kV rms)	Dry Type ^(b) (kV rms)	Chopped Wave		Full Wave ^(e)
	For Y-Connection on 3-Phase System ^(c) (kV rms)	For Delta-Connection on 3-Phase System (kV rms)	Delta or Y-Connected ^(d) (kV rms)			Crest (kV)	Minimum Time to Flash-over(μs)	Crest (kV)
1.2	0.69	0.69 ^(d)	1.2	10	4	36	1.0	30
2.5	—	—	2.5	15	10	54	1.25	45
5.0	2.89	2.89 ^(d)	5.0	19	12	69	1.5	60
8.86	5.0	5.00 ^(d)	8.86	26	19	88	1.6	75
15	8.66	15.0	15.0	34	31	110	1.8	95
25.0	14.4	25.0	25.0	50	—	175	3.0	150
34.5	19.9	34.5	34.5	70	—	230	3.0	200
46.0	26.6	46.0	46.0	95	—	290	3.0	250
69.0	39.8	69.0	69.0	140	—	400	3.0	350
92	53.1	92	92	185	—	620	3.0	450
115	66.4	115	115	230	—	830	3.0	550
138	79.7	138	138	275	—	750	3.0	650
161	93.0	161	161	325	—	865	3.0	750
196	113	196	196	395	—	1035	3.0	900
230	133	230	230	460	—	1210	3.0	1050
287	166	287	287	575	—	1500	3.0	1300
345	199	345	690	690	—	1785	3.0	1550

Notes: (a) Intermediate voltage ratings are placed in the next higher insulation class unless otherwise specified.

(b) Standard impulse tests have not been established for dry-type distribution and power transformers. Present-day values for impulse tests of such apparatus are as follows:

1.2-kV class, 10-kV; 2.5-kV class, 20 kV; 5.0-kV class, 25 kV; 8.86-kV class, 35 kV; 15-kV class, 50 kV. These values apply to both chopped-wave and full-wave tests.

(c) Y-connected transformers for operation with neutral solidly grounded or grounded through an impedance may have reduced insulation at the neutral. When this reduced insulation is below the level required for delta operation, transformers cannot be operated delta-connected.

(d) These transformers are insulated for the test voltages corresponding to the Y connection, so that a single line of apparatus serves for the Y and delta applications. The test voltages for such delta-connected single-phase transformers are therefore one step higher than needed for their voltage rating.

(e) 1.5 × 40-μs wave.

Source: Ref. 1.

terminal and the case. The impulse tests are to be conducted with normal 60-Hz energization, and timed to ensure that the impulse is applied within 30° of the 60-Hz crest.

4.1.3 LIGHTNING-ARRESTER CONSTRUCTION

The valve-type lightning arrester is a series combination of a spark-gap assembly and a nonlinear resistance element. The non-linear resistance element is voltage-sensitive; its resistance decreases exponentially with the voltage across it. The valve elements are non-linear resistors made of silicon-carbide crystals.

The spark-gap assembly is designed to minimize the time from overvoltage onset to firing and to minimize the time duration of any 60 Hz current flow. The first objective is frequently accomplished by use of a "preionizer." The latter objective is accomplished by extending the arc's path length and/or by breaking the arc up into a number of parallel, series, or rotating arcs. This tends to cool (deionize) the arc and help ensure that the arc is extinguished at or before the end of the half-cycle in which the surge or overvoltage occurs. The gap and valve assemblies of a lightning arrester are generally hermetically sealed in a glazed porcelain body and provided with an external, open-air spark-gap in series with the arrester. Figure 4-3 shows the internal construction of a typical valve-type lightning arrester. Lightning arresters may be designed as a part of another unit, such as a fuse or a cutout switch. Figure 4-4 shows three arresters; two are combination units that include open-link fused cutout switches.

Lightning arresters are installed with the gap side of the arrester connected to the line and the opposite end grounded. In the absence of a voltage surge, all of the line voltage appears across the open gap and none is impressed on the valve element (which typically has a maximum resistance of a few thousand ohms). If the arrester is subjected to an overvoltage with a magnitude sufficient to arc across the gap assembly, the resistance of the gap assembly is reduced to a negligible value, subjecting the valve element to the entire surge voltage. This causes the valve-element resistance to undergo a rapid decrease, thereby forming a low-resistance path to ground through which the surge can be dissipated.

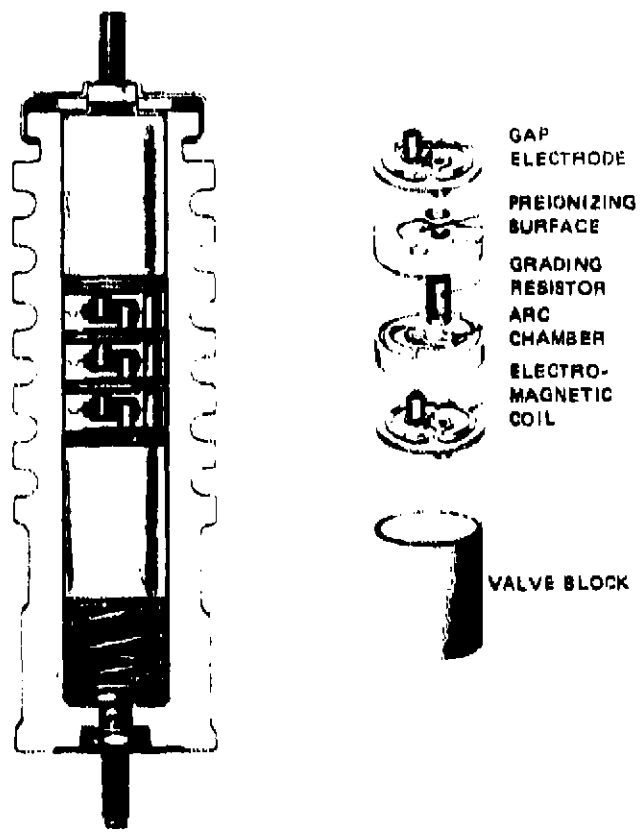
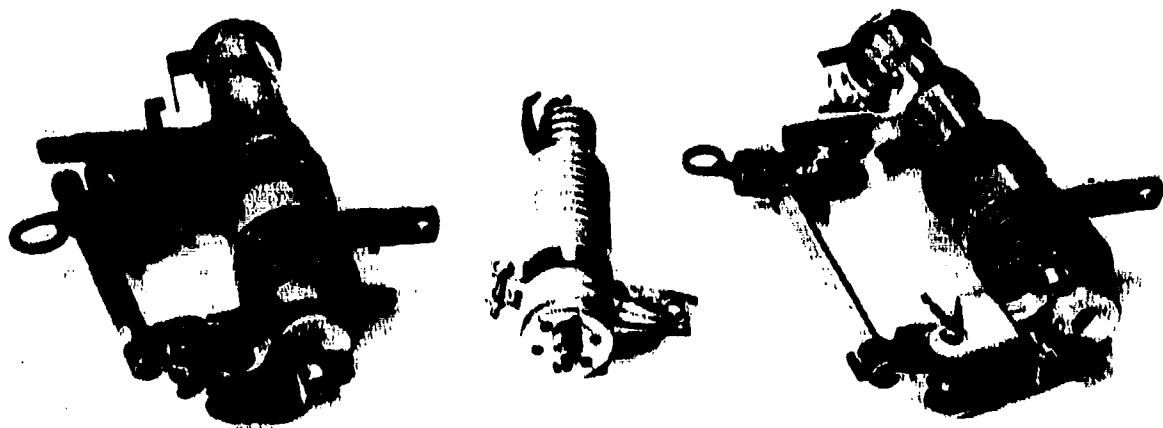


Figure 4-3 INTERNAL CONSTRUCTION OF A VALVE-TYPE LIGHTNING ARRESTER

After discharge of the surge voltage, the voltage across the arrester drops back to the normal line voltage. This voltage is not high enough to initially fire the arrester's gap assembly, but it would be adequate to maintain the external arc initiated by the overvoltage if it were not that (1) the line voltage is insufficient to maintain the low resistance of the valve element (which therefore returns to a high value) and (2) the internal gap assemblies are designed to extinguish the lower current permitted by the high resistance of the valve element.

The rapid increase in the valve element's resistance causes a substantial reduction in the 60-cycle power current; older-style arresters relied on this to reduce the current flow to a value low enough that the gap assembly could act to extinguish the arc at or before the next system voltage zero. This subjects the valve element to considerable currents for a



(a) MCGRAW EDISON
AF 8G1 8 KV
TYPE UC

(b) GENERAL ELECTRIC
MODEL 9L24BCX009

(c) A. B. CHANCE
C70J-202500

Figure 4-4 LIGHTNING-ARRESTER STYLES USED IN CONJUNCTION WITH THE TRANSFORMER HV TRANSIENT TESTS

potentially extended period of time; modern arresters are designed to transfer much of this responsibility for 60 Hz current-limiting to the arrester gap assembly itself. The major benefit of this design is that the valve elements can have lower discharge resistances, which decrease the arrester's IR drop. This IR drop is the voltage applied to the devices or circuitry that the arrester is intended to protect during an overvoltage surge.^{1,2}

Typical firing characteristics of distribution-type lightning arresters are shown in Section 2.6.3.

4.2 LINEAR CHARACTERISTICS OF TRANSFORMERS

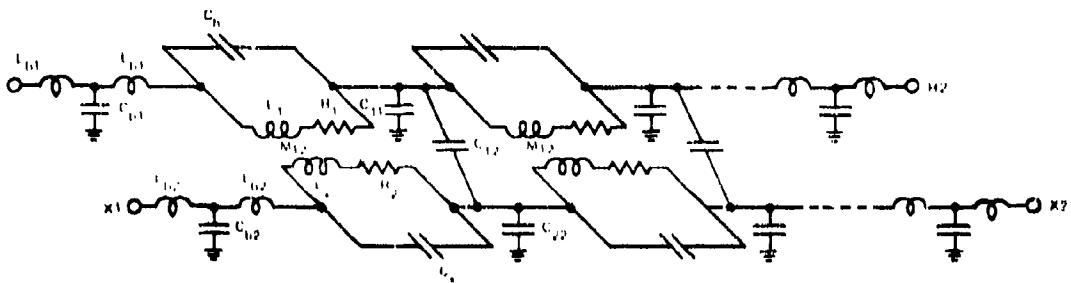
4.2.1 ANALYSIS OF TRANSFORMER COUPLING CHARACTERISTICS

The linear, high-frequency behavior of power transformers has been studied in connection with their response to lightning transients and their effect on the power-line carrier

communication systems.^{3,4,5} Unfortunately, the analytical treatments of the transformer, in order to be tractable, tend to be highly idealized; the models obtained therefrom must be accepted with due regard for these idealizations. Two areas in which the models fail to adequately describe the transformer are in the primary bushing impedance (which is probably not significant for lightning transients, but is for EMP), and in the symmetry of the windings. In addition, most of the models seem to imply that a common-mode primary excitation produces no differential-mode secondary response because both the primary and secondary windings are assumed to be symmetrical with respect to the core and with respect to each other. In practice these windings are far from symmetrical in either respect, so that coupling in the above mode is significant.

The linear response of power transformers can be analyzed by treating the primary and secondary windings of the transformer as coupled transmission lines.^{3,4,5} The windings are characterized as illustrated in Figure 4-5 by (1) inductances L_1 and L_2 and resistances R_1 and R_2 per unit length shunted by the turn-to-turn capacitances per unit length, C_x and C_h ; (2) capacitances per unit length C_{11} and C_{22} between the winding and the core or housing; and (3) a capacitance per unit length C_{12} between the primary and secondary windings and a mutual inductance M between the primary and secondary turns. Coupling between the primary and secondary at low frequencies (e.g., power frequencies) is primarily through the mutual inductance M , but at high frequencies the capacitances C_x and C_h carry most of the current between the terminals, and the coupling between primary and secondary windings is primarily through the interwinding capacitance C_{12} . The manner in which one divides all frequencies into low and high frequencies is dependent on the power and voltage rating of the transformer, since the turn-to-turn capacitances C_x and C_h and the primary-to-secondary capacitance C_{12} are dependent on number of turns, size of wire, and compactness of windings. For example, measurements on a 9.5-kV/220-V service transformer have shown that the primary turn-to-turn capacitance C_h is dominant above 2.4 kHz, but the secondary turn-to-turn capacitance C_x is not dominant until frequencies well above 23 kHz are reached.

Thus, a complete and accurate analysis of the linear, transient behavior of a transformer at higher frequencies must take into account the interwinding capacitances, as well as the self and mutual inductances of the winding. Furthermore, as is pointed out in Refs. 3 and 4, an important difference exists between the transmission-line model of the transformer windings and the conventional transmission line, regarding the self and mutual



MUTUAL

M_{12} = mutual inductance between primary and secondary

C_{12} = capacitance between primary and secondary windings

PRIMARY (H1-H2)

- C_h = turn-to-turn capacitance
- L_1 = self inductance of winding
- R_1 = winding resistance
- C_{11} = winding-to-frame capacitance
- L_{b1} = inductance of bushing
- C_{bt} = capacitance of bushing

SECONDARY (X1-X2)

- C_x = turn-to-turn capacitance
- L_2 = self inductance of winding
- R_2 = winding resistance
- C_{22} = winding-to-frame capacitance
- L_{b2} = inductance of bushing
- C_{h2} = capacitance of bushing

Figure 4-5. TRANSMISSION-LINE MODEL FOR COUPLED TRANSFORMER WINDINGS

Inductance per unit length. This difference is related to the fact that the inductance (self or mutual) of a turn is a function of the position of the turn in the whole winding. For example, a turn in the center of the winding is coupled to other turns on either side of it, while a turn at the end of the winding is coupled to other turns on only one side. Reference 3 proposes a parabolic variation of magnetic flux partially linking the turns, with a maximum partial flux linkage at the center of the winding and the flux linkage decreasing toward the ends of the winding and reaching zero at some point beyond the end of the winding. This variation in flux linkage leads to self and mutual inductances that are functions of position.

The result is a set of two coupled fourth-order differential equations relating the mutual and self-inductance voltages of the primary and secondary windings — i.e.,

$$\frac{\partial^4 V_1}{\partial x^4} + j\omega \frac{\partial}{\partial x} [L_1 I_{L1} + M I_{L2}] = 0 \quad (4-1)$$

$$\frac{\partial^4 V_2}{\partial x^4} + j\omega \frac{\partial}{\partial x} [L_2 I_{L2} + M I_{L1}] = 0 \quad (4-2)$$

Where V_1 is the voltage on the high-voltage winding and V_2 is the voltage on the low-voltage winding (both referred to the transformer core and frame), and L_1 , L_2 , and M are the self and mutual inductances.

A detailed solution of Eqs. (4-1) and (4-2) appears in Refs. 3 through 5. The results are

$$\left\{ p^8 - p^6 s^2 (L_1 C_h + L_2 C_x) + p^4 s^2 [L_1 C_{11} + L_2 C_{22} + C_{12} (L_1 + L_2 - 2M)] + p^4 s^4 (L_1 L_2 - M^2) C_h C_x + p^2 s^4 (M^2 - L_1 L_2) (C_x C_{11} + C_x C_{12} + C_h C_{12} + C_h C_{22}) + s^4 (L_1 L_2 - M^2) (C_{11} C_{22} + C_{11} C_{12} + C_{22} C_{12}) \right\} V = 0 \quad (4-3)$$

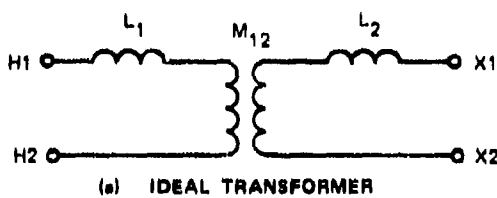
where

$$p^n = \partial^n / \partial x^n \text{ and } s^n = ((j\omega)^n \text{ or } \partial^n / \partial t^n).$$

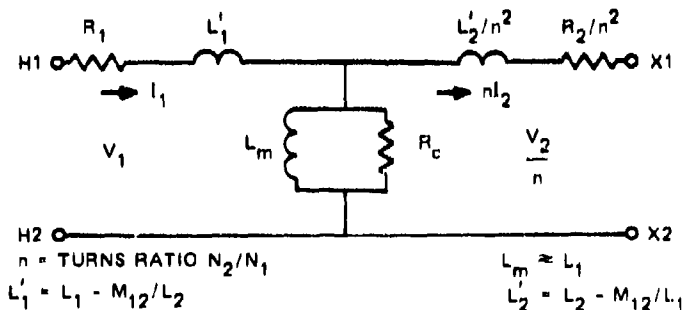
The solution to this eighth-order differential equation depends on access to a great deal of information not normally available and not readily determined from measurements made at the transformer's terminals. In addition, the winding resistances R_1 and R_2 have not been included in the voltage equations. Finally, for distribution-type power transformers, the lumped bushing capacitance C_b and inductance L_b in Figure 4-5 play an important role in determining the coupling between the primary and secondary windings, since they behave as L-section filters between the transformer terminals and the windings at high frequencies.^{6,7}

It is informative to examine the behavior of the transformer at the extremes of the frequency range. As ω approaches zero, for example, all capacitive susceptances become small and we are left with only the self- and mutual-inductance terms in the equivalent circuit of Figure 4-5 (the winding resistances have been neglected). In addition, because the windings are short compared to a wavelength at low frequencies, the distributed self and mutual inductances can be adequately represented by lumped self and mutual inductances as illustrated in Figure 4-6(a), where the equivalent circuit of an ideal transformer is shown. The practical equivalent circuit containing copper losses (winding resistances) R_1 and R_2 , and core loss R_c , is shown in Figure 4-6(b) with all impedances referred to primary side.

At the high-frequency extreme, ω approaches infinity and the capacitive reactances carry all of the current, leaving none to flow through the self and mutual inductances of



(a) IDEAL TRANSFORMER



(b) PRACTICAL EQUIVALENT CIRCUIT

Figure 4-6 LOW-FREQUENCY EQUIVALENT CIRCUITS FOR
A TRANSFORMER

Figure 4-5 (except the bushing inductances). The differential equation for the voltage in either winding becomes

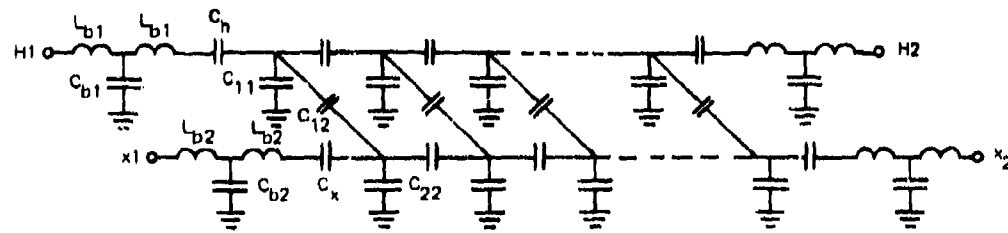
$$\frac{d^4V}{dx^4} - \frac{C_x C_{11} + C_x C_{12} + C_h C_{12} + C_h C_{22}}{C_h C_x} \frac{d^2V}{dx^2} - \frac{C_{11} C_{22} + C_{11} C_{12} + C_{22} C_{12}}{C_h C_x} V = 0 \quad (4-4)$$

and the high-frequency equivalent circuit becomes that illustrated in Figure 4-7. The stray inductance and capacitance associated with the bushings has been retained in Figure 4-7(a) because these small inductances are significant in the high-frequency response, and they are not bypassed by capacitances as are the winding inductances. Notice that the distributed capacitances C_h , C_x , C_{11} , C_{22} , and C_{12} form a capacitive network that couples:

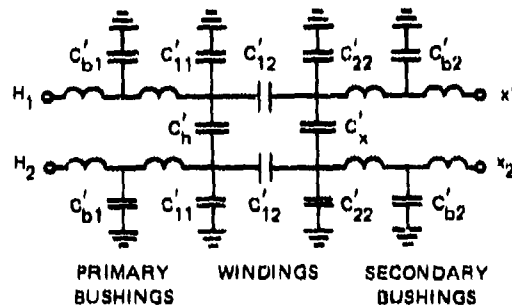
- (1) The primary terminals to each other and to the case or core
- (2) The secondary terminals to each other and to the case or core
- (3) Each primary terminal to each secondary terminal.

A rough lumped-element equivalent circuit is shown in Figure 4-7(b) in which the distributed winding capacitances have been replaced by lumped capacitances between windings, between terminals, and between terminals and ground (case or core). Even with this simplification, the relation between primary and secondary currents and voltages is not simple, but the coupling paths are more obvious and the bandpass nature of terminal-to-terminal coupling caused by the bushing inductances and the bushing and winding capacitances is apparent.

The analytic model of Figure 4-5 is probably a good representation of a bifilar-wound 1:1 transformer, but for typical power transformers that have separate primary and secondary windings the analytic model is only a crude approximation at high frequencies. It is nevertheless a useful aid in interpreting the transient behavior of practical power transformers. It is also significant that, because the primary windings of transformers are dominated by the turn-to-turn capacitance above a few kilohertz, the high-frequency equivalent circuit may be applicable throughout the 10-kHz-to-100-MHz frequency range of interest here.



(a) IDEAL TRANSFORMER WITH BUSHINGS



(b) APPROXIMATE LUMPED-ELEMENT CIRCUIT

Figure 4-7 HIGH-FREQUENCY EQUIVALENT CIRCUITS FOR A TRANSFORMER

4.2.2 DISTRIBUTION OF VOLTAGE ALONG THE WINDINGS

The distribution of a transient voltage along a transformer winding can be estimated from the distributed-parameter circuit model of Figure 4-5. The results of calculation with such a model (without bushings) predict that when a fast-rising voltage reaches a terminal of one winding of a two-winding transformer, the voltage is initially distributed nonuniformly in both windings due to the effect of the turn-to-turn capacitance, the capacitance-to-ground of each winding, and the mutual capacitance between the windings. Following this initial capacitively coupled transient, both windings go into oscillation due to the interaction of their inductances and capacitances.

Figures 4-8, 4-9, and 4-10 show plots of calculated voltages in the windings of a single-phase transformer when stressed at the high-voltage terminal with a fast-rising voltage. The neutral of the primary winding and both of the terminals of the secondary winding of the transformer are assumed to rise to a peak of 330 kV in 10 ns.

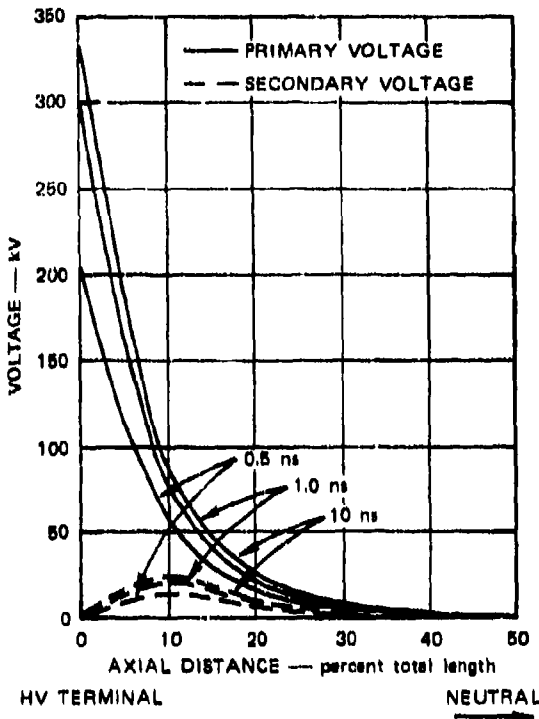


Figure 4-8 SPATIAL DISTRIBUTION OF WINDING VOLTAGE AT EARLY TIMES.

Source: Ref. 8.

peak applied voltage of 330 kV is impressed upon the insulation of these first turns alone and, depending upon the insulation strength, could cause breakdown. From Figure 4-8 it is also apparent that the voltages in the secondary winding due to the various winding capacitances are much less than those in the primary.

After the initial transients shown in Figure 4-8, which propagate through the windings by means of the turn-to-turn capacitance, the capacitance to ground, and the mutual capacitance, oscillations are set up due to the combined effect of the winding inductances and capacitances. This behavior is shown in Figures 4-9 and 4-10. The oscillations become apparent only for times of the order of or greater than the first natural period of the windings, which lies in the range of a few microseconds for the secondary winding. By these times, the voltage at the high-voltage terminal of the primary is also beginning to decay, but because the natural frequency of the primary winding is much lower than that of the secondary, only the beginnings of an oscillation are apparent in the primary voltage distribution.

Figure 4-8 shows the spatial distribution of the voltage inside the primary and secondary winding for early times during which only the winding capacitances are playing a role. The spatial coordinate is the distance along the axis of the winding, which is assumed to be cylindrical in shape. The zero of the spatial coordinate is assumed to be at the high-voltage terminal of the winding, with 100% of the winding having been traversed upon reaching the neutral. It is clear from Figure 4-8 that for times of the order at the rise time of the pulse, the voltage applied to the high-voltage terminal does not distribute itself uniformly over the entire winding but tends to pile up across the first 40% of the turns nearest the high-voltage terminal. Hence, the

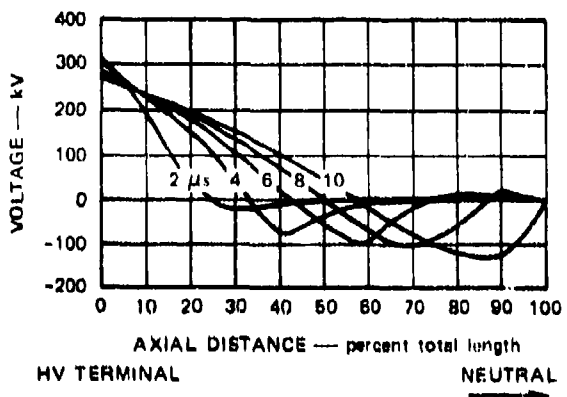


Figure 4-9 VOLTAGE DISTRIBUTION ALONG PRIMARY WINDING AT LATE TIMES. Source: Ref. 8.

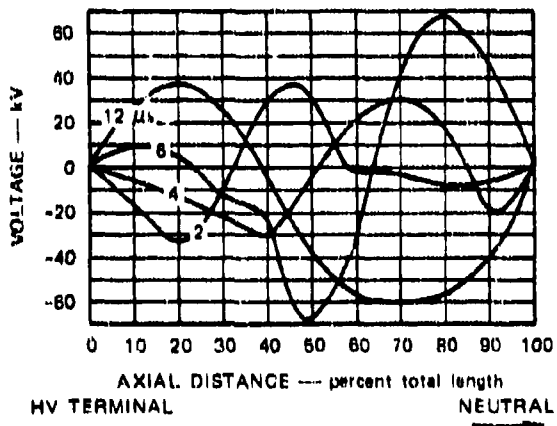


Figure 4-10 VOLTAGE DISTRIBUTION ALONG SECONDARY WINDING AT LATE TIMES. Source: Ref. 8.

The results shown in Figures 4-8 through 4-10 are indicative only of the qualitative behavior of a station transformer stressed by EMP, because of the waveform assumed and because the circuit constants for the transformer can be estimated only crudely. In addition, because the inductance and capacitance of the bushings are neglected in the calculation of the voltage distributions shown in Figures 4-8, 4-9, and 4-10, the assumed rate of rise (33 kV/ns) is considerably greater than that actually applied to the winding by an EMP-induced voltage. For example, a 300-ohm line feeding a 100-pF bushing has a rise time-constant of 30 ns, so that even a step-fronted wave would have its rise slowed to about 60 ns upon entering the transformer.

4.2.3 CW MEASUREMENTS OF TRANSFORMER CHARACTERISTICS

Viewed as a multiterminal network, the typical distribution transformer of the types discussed here must be considered a 7-terminal device, because there are two primary terminals, four secondary terminals (two for each winding), and a ground or case terminal. A large number of measurements are required to specify the equivalent impedances between the terminals of a 7-terminal device, and even with these impedances specified,

considerable complex algebra is required to apply the equivalent circuit to a practical transformer coupling problem. To avoid this complexity, the complete definition of the equivalent network has been compromised in favor of obtaining readily usable equivalent circuits that are representative of those encountered in typical transformer installations.⁷ Thus, instead of defining a 5- or 7-terminal network, we have defined the four 3-terminal networks illustrated in Figure 4-11.

Low-level CW measurements of the voltages and currents necessary to specify the elements of the T-networks of Figure 4-11 have been made over the frequency range from 10 kHz to 50 MHz for each of four transformers⁷ (see Table 4-2). To illustrate the similarity of the transfer characteristics of the transformer and to illustrate the dominant features of the coupling analysis discussed above, the ratio of the voltage delivered to a 100-ohm load across the undriven terminals to the driving voltage has been computed for each transformer for each of the four configurations of Figure 4-11.

Table 4-2
PROPERTIES OF CLASS OA TRANSFORMERS USED IN CW AND
TRANSIENT MEASUREMENTS

Unit No.	Power Rating (kVA)	Voltage Rating (V)	Manufacturer	Secondary Winding
1	25	7200/12470 Y - 120/240	General Electric (new)	Aluminum strip
2	25/28	13200 - 120/240	Allis-Chalmers (used)	Copper wire
3	25	7200/12470 Y - 120/240	Westinghouse (new)	Aluminum strip
4	50	7200/12470 Y - 120/240	Allis-Chalmers (new)	Aluminum strip

The voltage transfer function for the common-mode configuration of Figure 4-11(d) is shown in Figure 4-12 for each of the four transformers. The average transfer characteristic for all four transformers is also shown in Figure 4-12. It is apparent from Figure 4-12 that the coupling to the 100-ohm load is dominated by the interwinding capacitance in the low-frequency range between 10 kHz and about 1 MHz. The average interwinding capacitance from Figure 4-12 is about 1000 pF in this configuration. Also apparent is the effect of the bushing capacitance and the lead inductance associated with the primary bushings and the leads to the secondary bushings in reducing the voltage transfer function above about 10 MHz. In spite of the fact that two different power ratings, two different winding types,

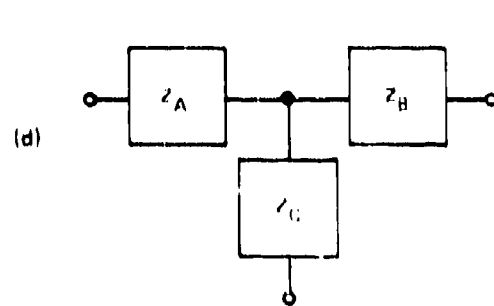
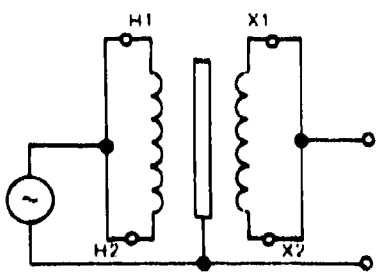
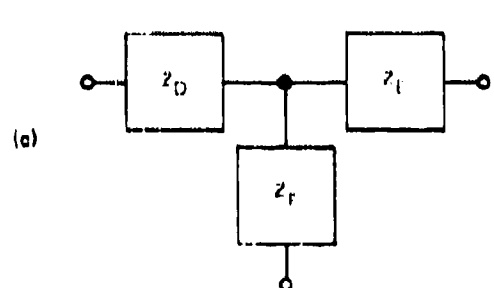
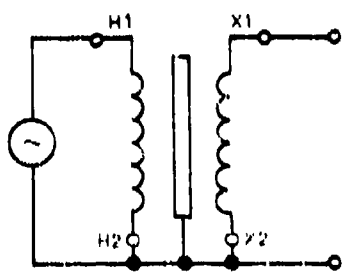
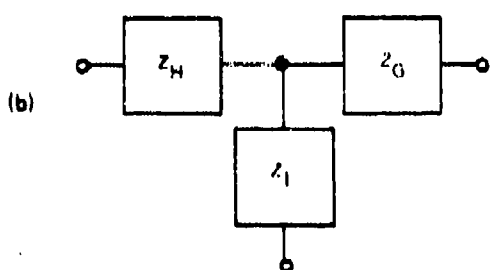
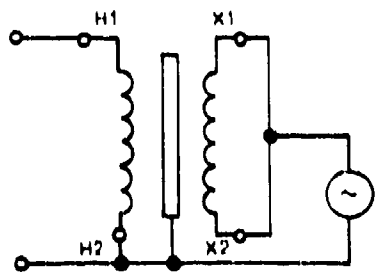
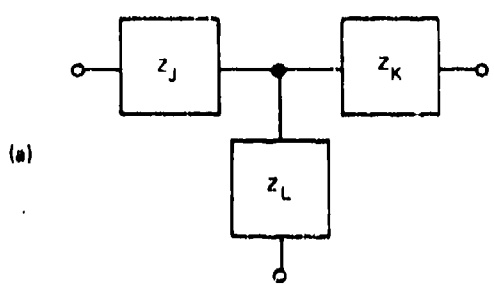
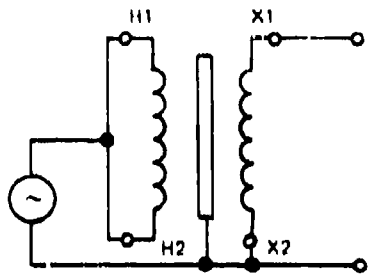


Figure 4-11 POWER-TRANSFORMER CONFIGURATIONS AND EQUIVALENT T-NETWORKS USED TO OBTAIN CW TRANSFER-FUNCTION DATA

and three different manufacturers are represented by the four transformers, their common-mode voltage transfer characteristics are remarkably similar.

Similar results for the common-mode excitation and differential-mode output of Figure 4-11 (a) are shown in Figure 4-13. Although the four transformers are similar in this mode also, the deviations of the individual transformers from the mean is greater. As can be seen in the approximate equivalent circuit of Figure 4-7, the coupling for common-mode excitation (H_1 and H_2 driven against ground) and differential-mode loading (X_2 grounded and 100 ohms between X_1 and ground) is achieved through the asymmetry of the windings (the asymmetry occurring naturally due to the construction of the transformer as well as that introduced by grounding the terminal X_2). This voltage transfer function is thus more dependent on the winding-to-case capacitance and the turn-to-turn capacitance than are the common-mode transfer functions of Figure 4-12. Thus the type and form of the secondary winding are probably responsible for the greater variation among the transformers in Figure 4-13. In spite of this, however, the similarity of the four transformers is quite striking. It is noteworthy that in this coupling mode also, the transformer displays a likeness to a bandpass filter.

Figure 4-14 illustrates the voltage transfer characteristics for the common-mode secondary excitation and differential-mode primary loading of Figure 4-11 (b). The coupling mechanism for this configuration is similar to that in the preceding example, except that the forced unbalance (caused by grounding H_2) is now in the primary winding. Because there is only one primary winding and it is, in all four cases, placed between the secondary windings, coupling in this mode is undoubtedly more strongly dependent on the interwinding capacitance than on the primary-winding-to-ground capacitance. The observed similarity among the transfer characteristics in Figure 4-14 is quite striking, and again the bandpass-filter characteristics are apparent.

The voltage transfer characteristics for differential-mode excitation and differential-mode loading [see Figure 4-11 (c)] are shown in Figure 4-15. For this configuration, as for the other configuration involving a differential-mode secondary, there is considerable variation from transformer to transformer, although there is significant overall similarity. It appears that below about 100 kHz the transfer function is relatively independent of frequency. If H_2 and X_2 in Figure 4-7 are grounded, the coupling between H_1 and X_1 is through the capacitive divider formed by the interwinding (C_{12}) and winding-to-ground

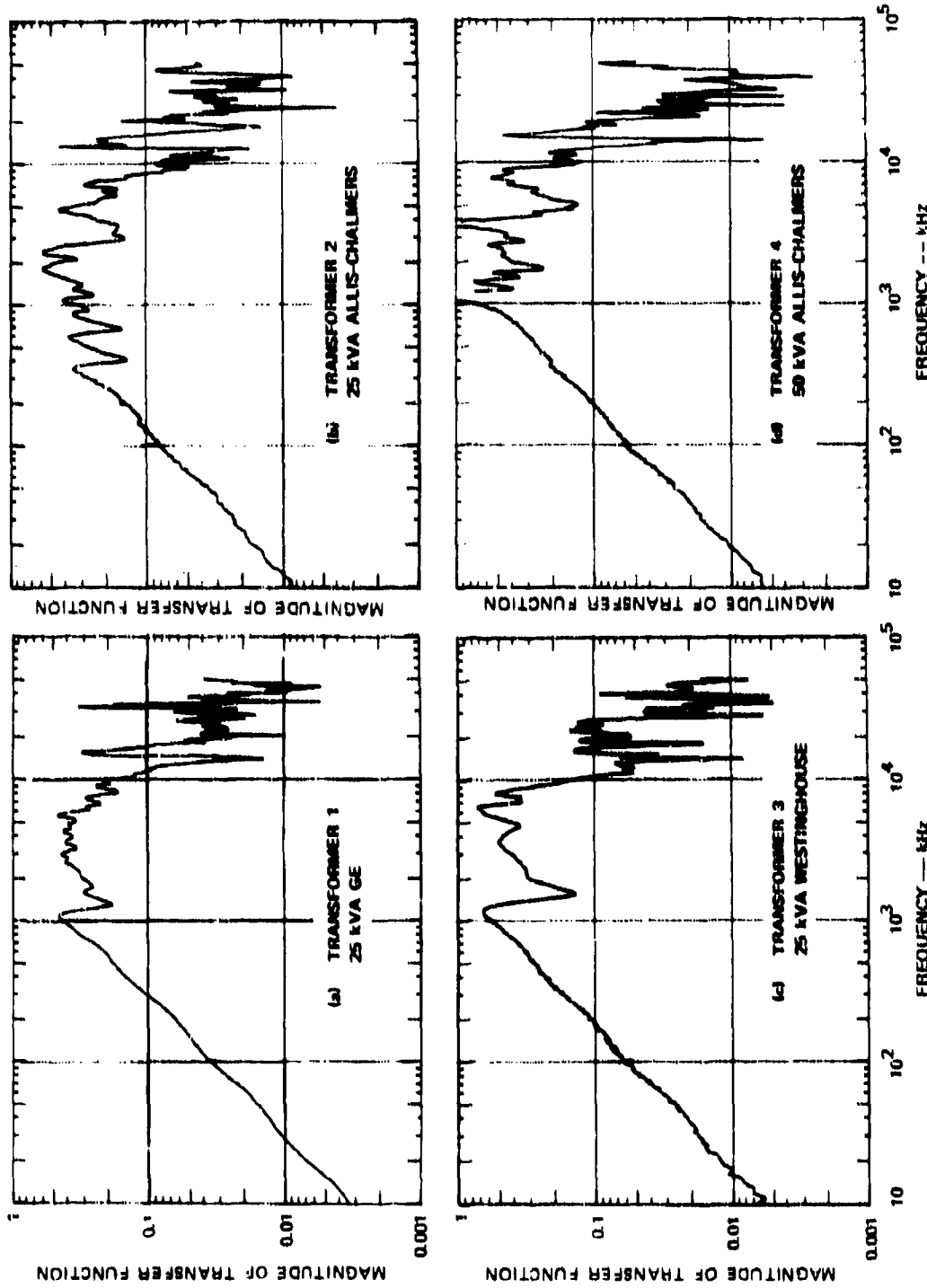
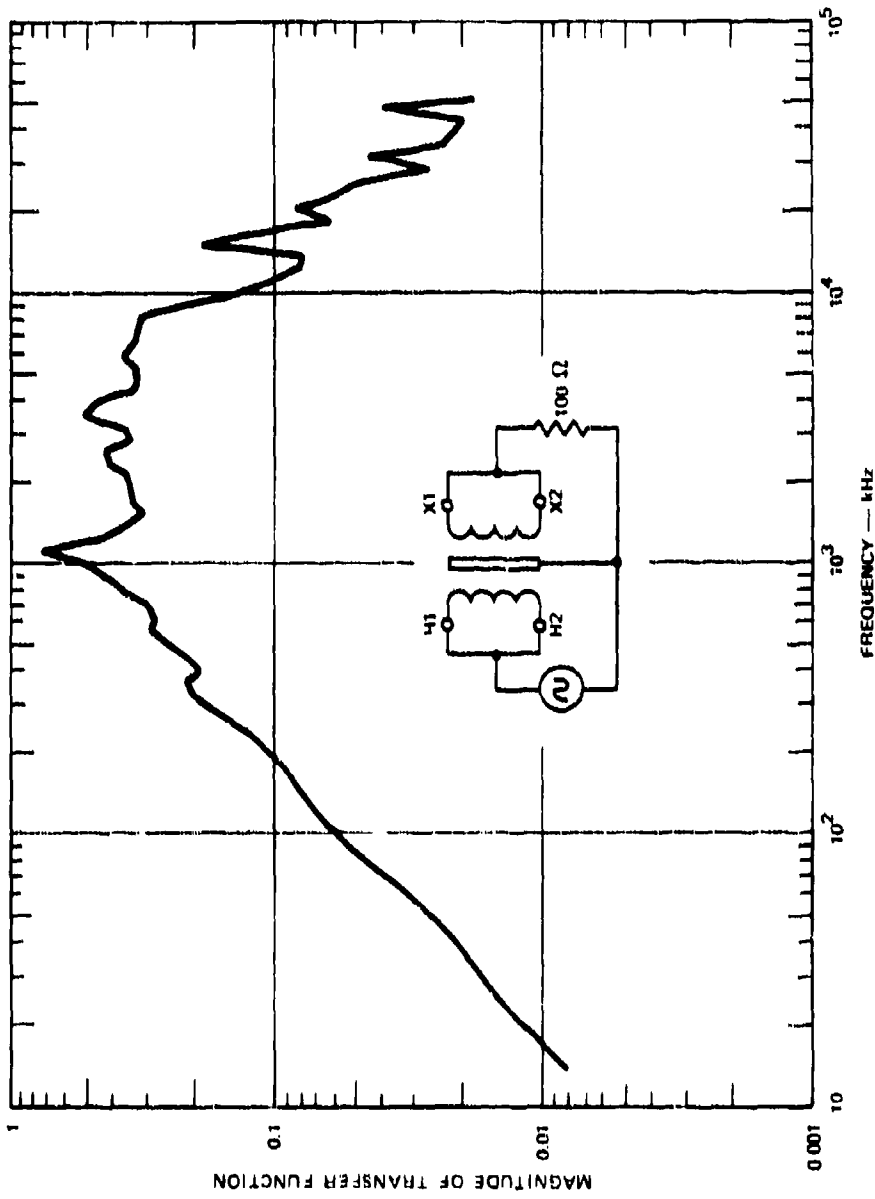


Figure 4-12 MAGNITUDE OF TRANSFER FUNCTION RELATING COMMON-MODE PRIMARY VOLTAGE TO COMMON-MODE SECONDARY VOLTAGE ACROSS A 100-ohm LOAD FOR THE TEST TRANSFORMERS



(d) SMOOTHED AVERAGE (integrated from ten frequency averages of Transformers 1, 2, 3, and 5)

Figure 4-12 (Concluded)

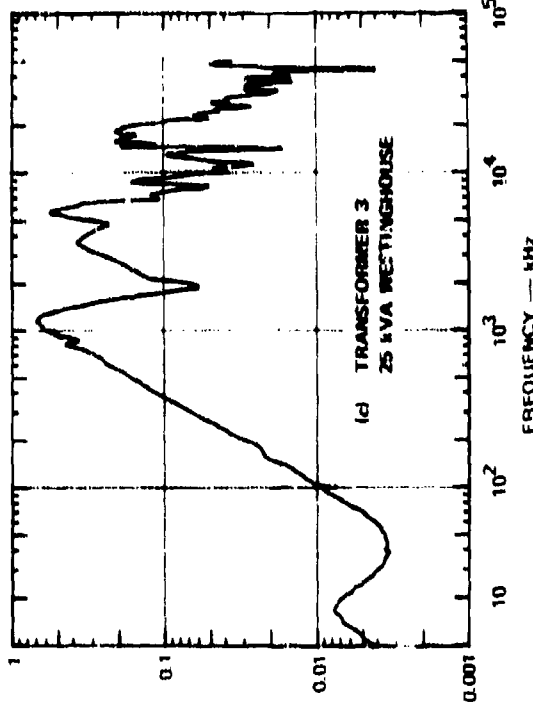
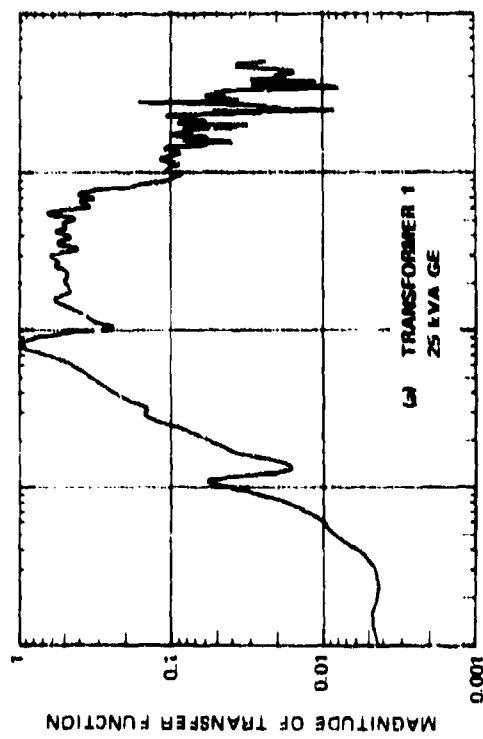
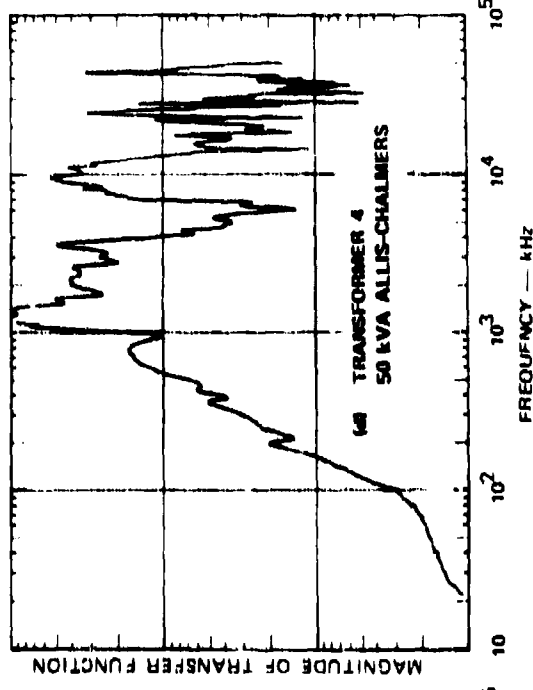
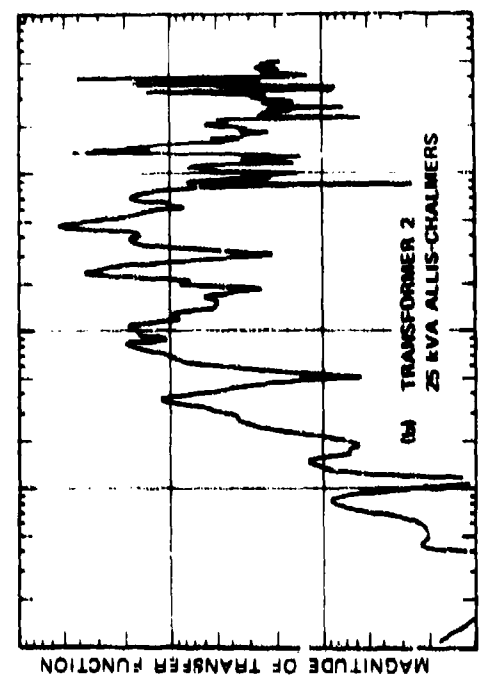
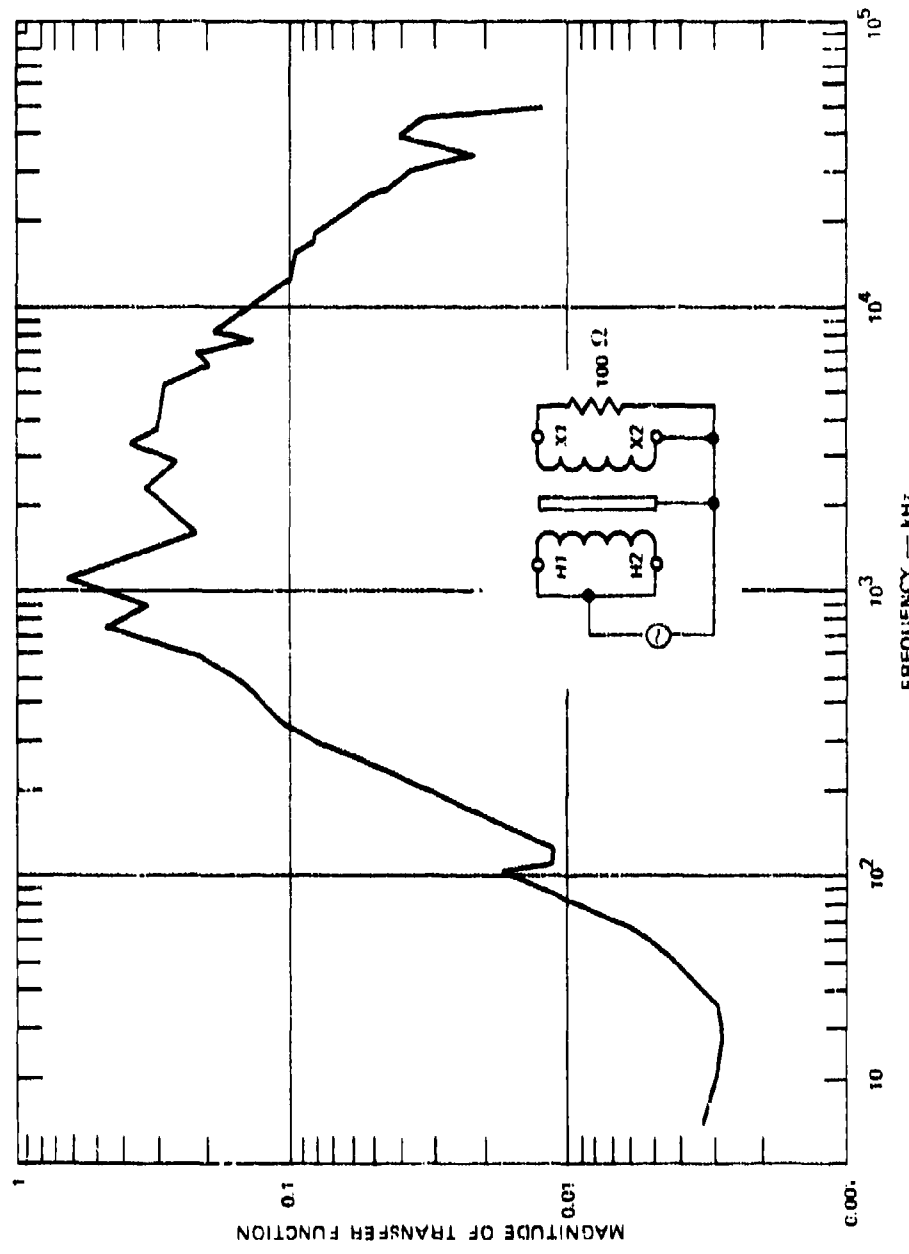


Figure 4-13 MAGNITUDE OF TRANSFER FUNCTION RELATING COMMON-MODE PRIMARY VOLTAGE TO DIFFERENTIAL-MODE SECONDARY VOLTAGE ACROSS A 100-ohm LOAD FOR THE TEST TRANSFORMERS



(e) SMOOTHED AVERAGE (generated from ten frequency averages of Transformers 1, 2, 3, and 5)

Figure 4-13 (Concluded)

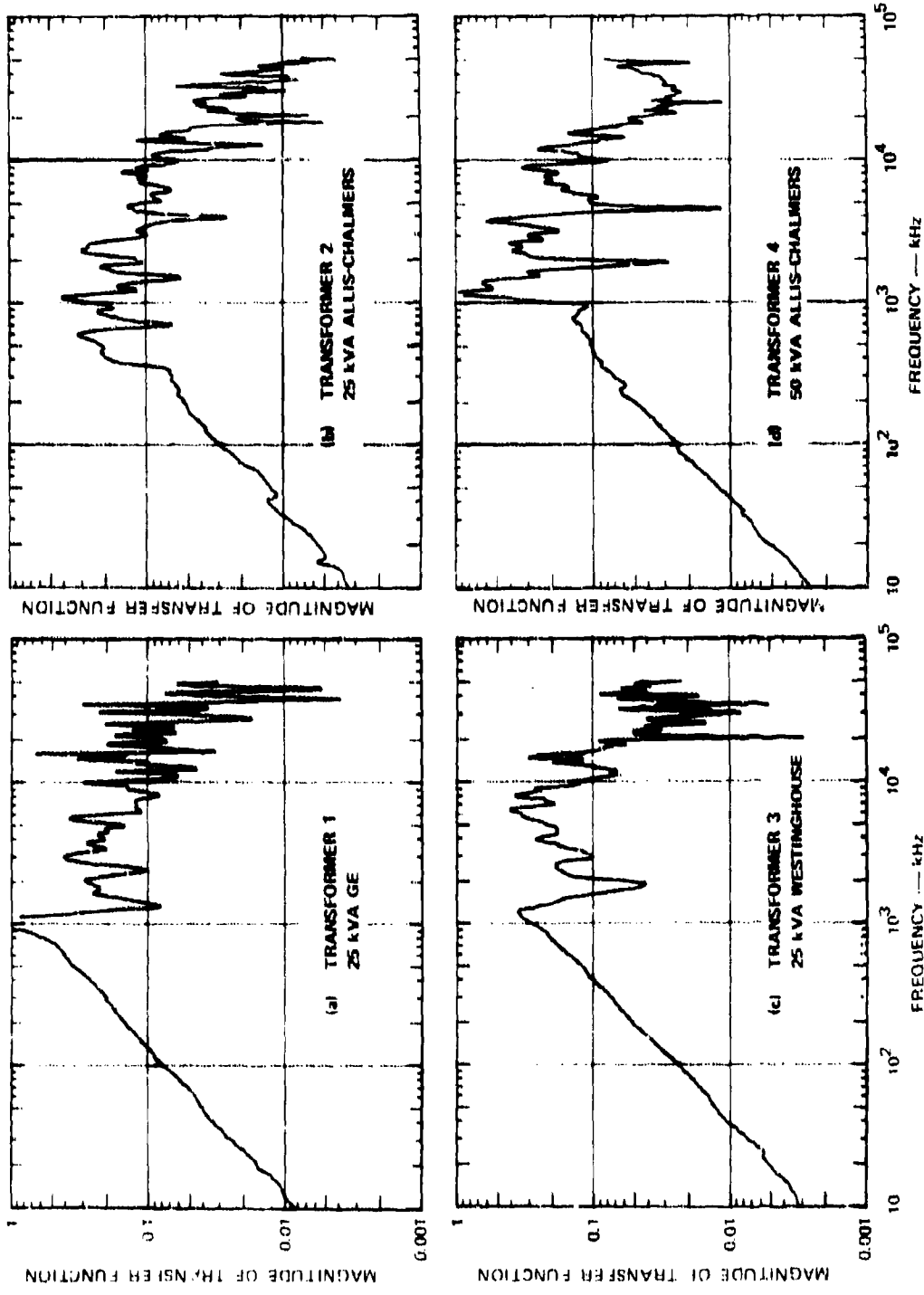
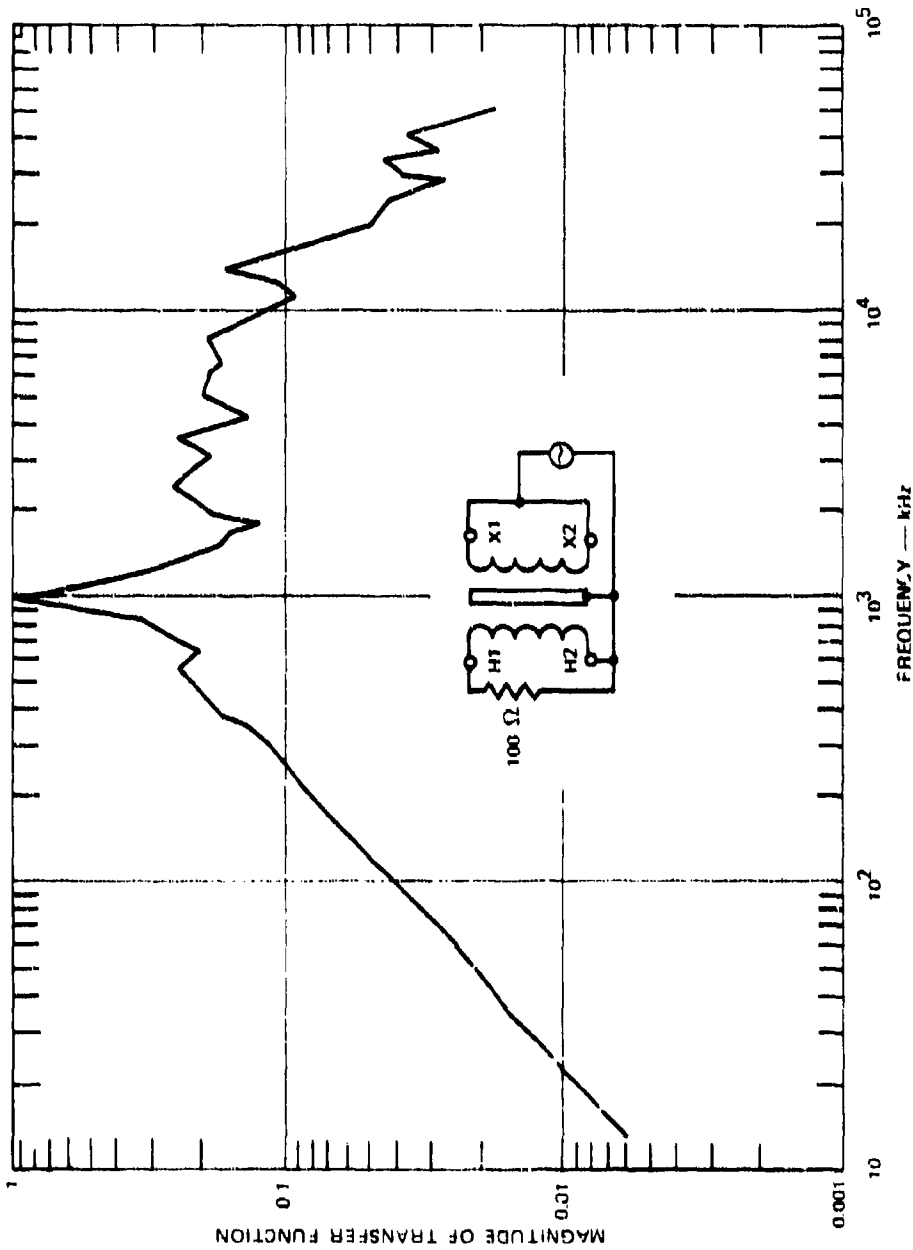


Figure 4-14 MAGNITUDE OF TRANSFER FUNCTION RELATING DIFFERENTIAL-MODE PRIMARY VOLTAGE TO COMMON-MODE SECONDARY VOLTAGE ACROSS A 100- Ω LOAD FOR THE TEST TRANSFORMERS



1a SMOOTHED AVERAGE (generated from ten frequency averages of Transformers 1, 2, 3, and 5)

Figure 4-14 (Concluded)

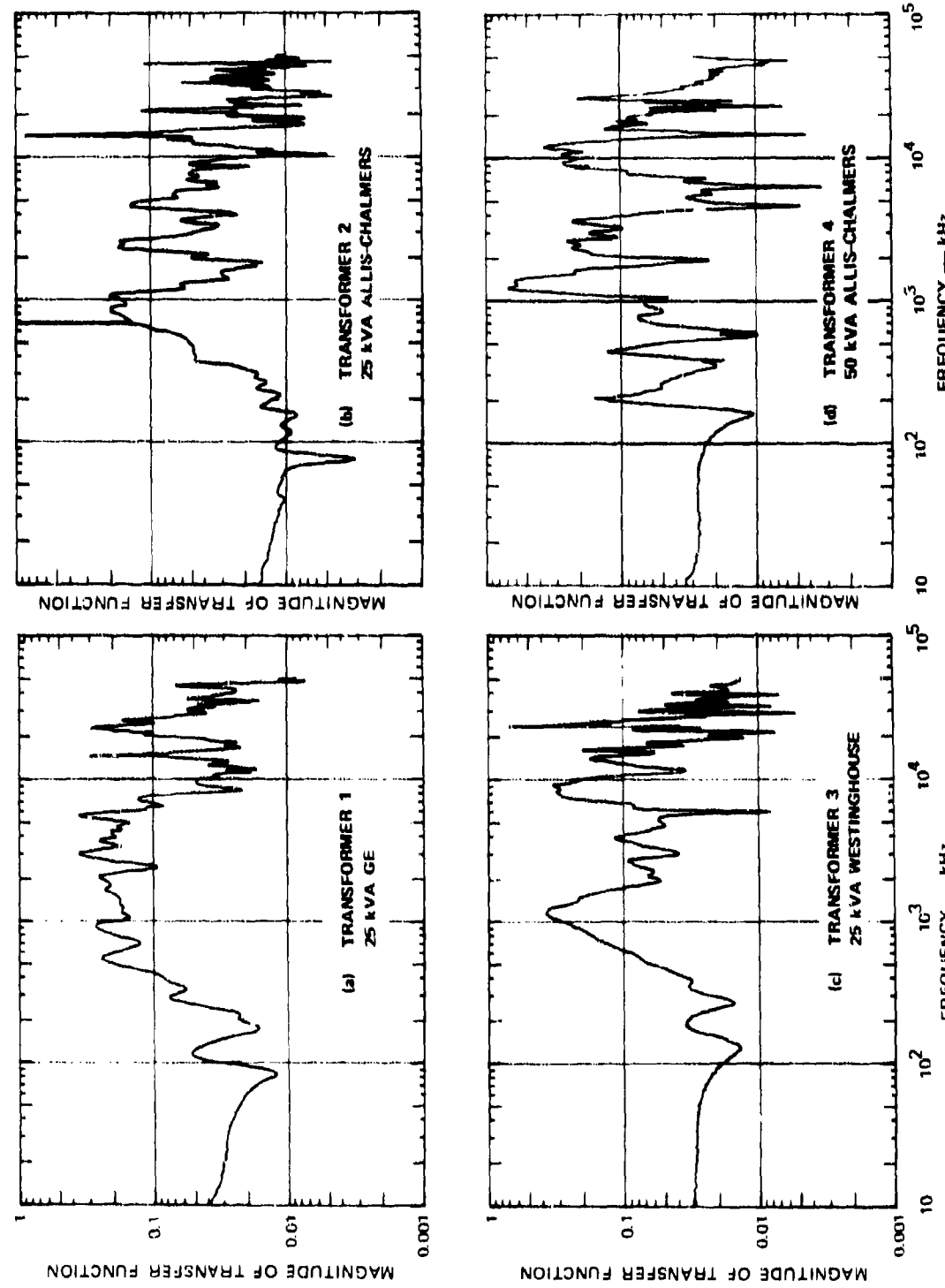
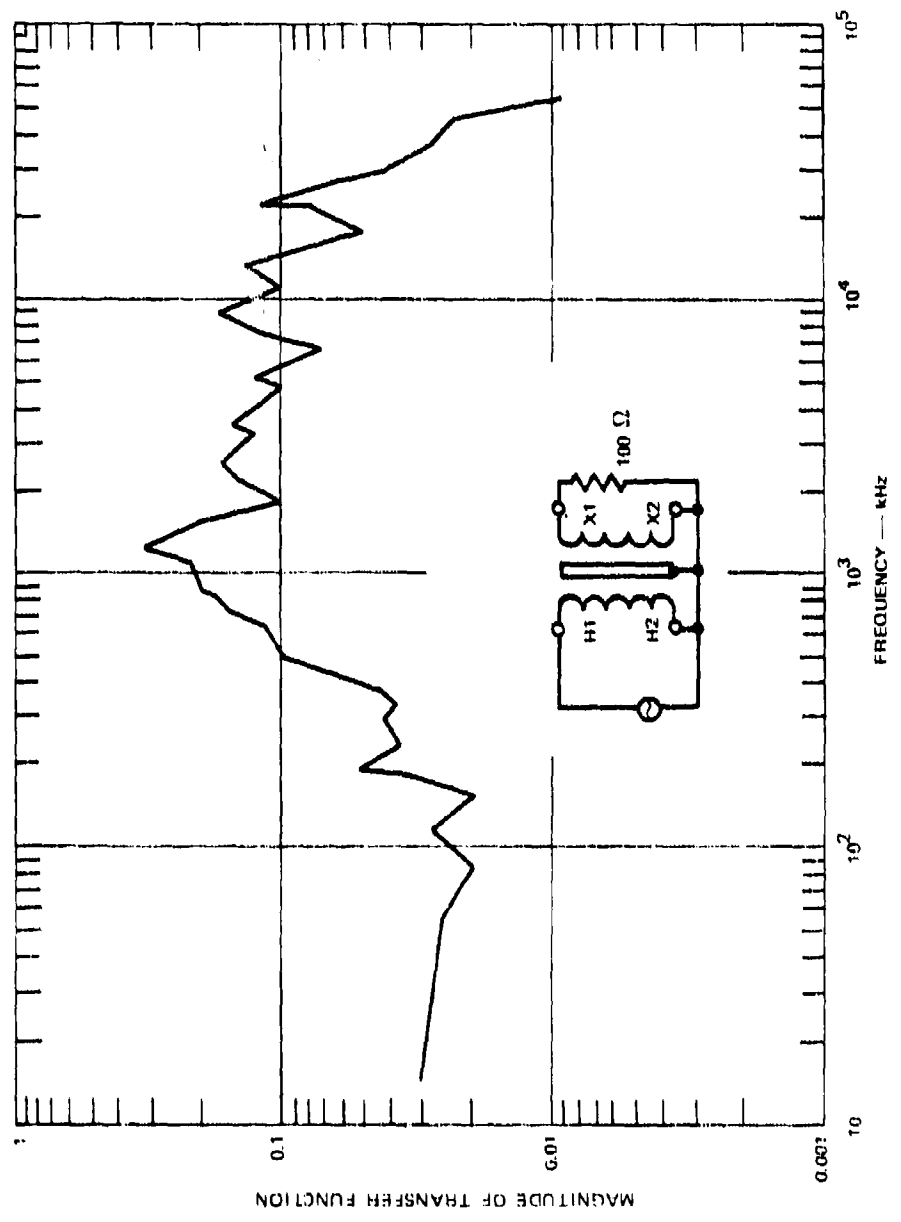


Figure 4-15 MAGNITUDE OF TRANSFER FUNCTION RELATING DIFFERENTIAL-MODE PRIMARY VOLTAGE TO DIFFERENTIAL-MODE SECONDARY VOLTAGE ACROSS A 100- Ω LOAD FOR THE TEST TRANSFORMERS



[e] SMOOTHED AVERAGE (generated from ten frequency averages of Transformers 1, 2, 3, and 5)

Figure 4-15 (Concluded)

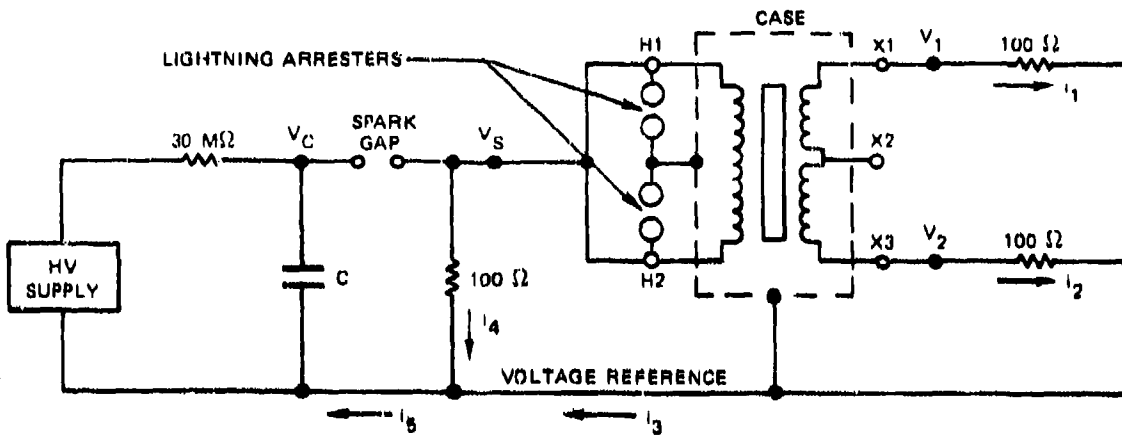
(C'_{11} , C'_{22}) capacitances. In addition, the transformer, in this configuration, is behaving somewhat as a step-down transformer even though the primary current is being shunted by the turn-to-turn capacitance (the primary resonance occurs below 10 kHz). In either event, winding resonances that are unique to the individual transformers occur above 100 kHz.

When the average characteristics of the four configurations are compared, it is apparent that the voltage transfer function for a 100-ohm load is greatest for the common-mode-to-common-mode configuration (Figure 4-12), slightly less for the common-mode-primary-to-differential-mode-secondary (Figure 4-13), and slightly less yet for the differential-mode-secondary-to-common-mode-primary (Figure 4-14). The smallest high-frequency coupling occurs for the differential-mode-to-differential-mode configuration, but in this configuration the low frequencies are not cut off as strongly as they are in the other configurations.

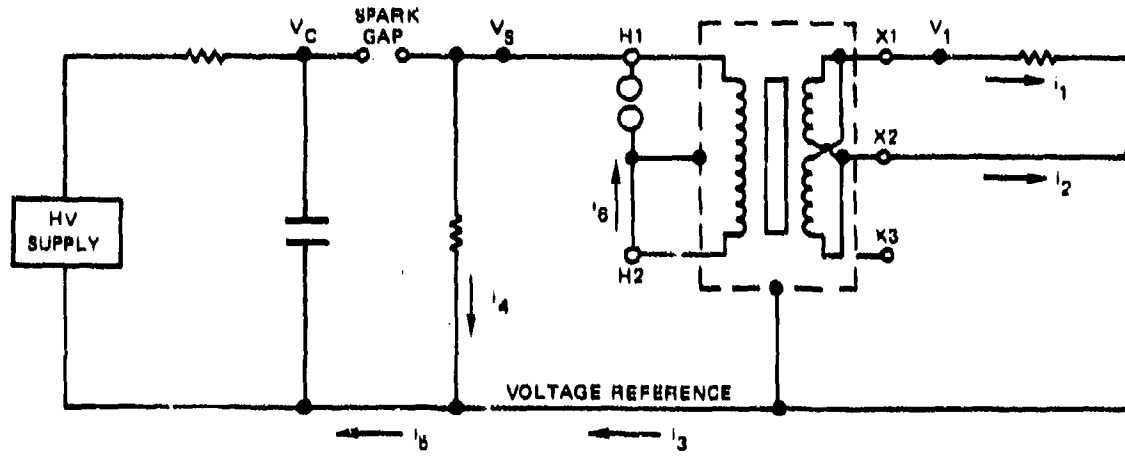
4.2.4 LINEAR TRANSIENT TEST RESULTS

Transient tests of the four transformers of Table 4-2 have also been conducted at a low level to obtain the linear response characteristics of the transformers.⁷ The driving level used for these tests ranged from about 8 kV to about 40 kV (the lightning arresters fired at about 42 kV). At driving levels below the threshold for lightning-arrester firing, the transformer behaves as a linear device, and the transient responses can be related to the frequency-domain characteristics. The circuits of Figure 4-16 were used for these tests.

For the low-level tests, the 0.075- μ F switched capacitor was used as the driving source, so that the source-voltage waveform across the 100-ohm resistor at the pulser output terminals (see Figure 4-16) was an exponential pulse with a 10-to-90% rise time of about 20 ns and a decay time constant of about 7.5 μ s. The voltage waveform appearing at the terminals of the transformer is shown in Figure 4-17. A slight oscillation during the first 400 ns caused by the winding reactance is apparent in Figure 4-17. Also of interest is the waveform of the current entering the transformer, shown in Figure 4-18. (Figure 4-18



(a) COMMON-MODE DRIVE AND COMMON-MODE OUTPUT CONFIGURATIONS
(shown with transformer secondary windings connected in series)



(b) DIFFERENTIAL-MODE DRIVE AND DIFFERENTIAL-MODE OUTPUT CONFIGURATIONS
(shown with transformer secondary windings connected in parallel)

Figure 4-16 SCHEMATIC DIAGRAM OF TRANSFORMER TEST CIRCUITS (subscripts on V and I indicate test measurement points)

shows the total capacitor current, which includes about 300 A through the 100-ohm load.) It is observed that the rise time of the current is significantly longer than that of the driving voltage. This observation is consistent with the contention that significant series inductance is associated with the primary bushings. It is also observed that the duration of the current,

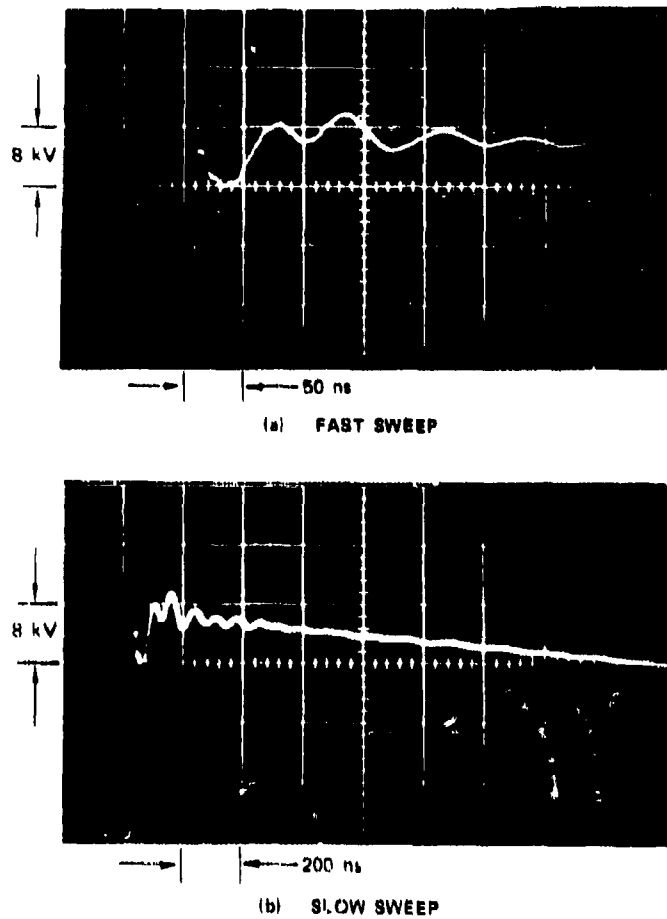


Figure 4-17 WAVEFORM OF EXCITATION VOLTAGE APPLIED TO TRANSFORMER

when the load-resistor current is neglected, is much shorter than the duration of the impressed voltage. The primary current is mainly that required to charge the capacitances associated with the windings and bushings, and once these are charged, no more current, other than that associated with the oscillations triggered by the transients, can flow. The waveforms shown in Figures 4-17 and 4-18 were obtained with the 25-kVA G.E. transformer in the common-mode drive configuration, but they are quite representative of the general characteristics of all the transformers tested.

The waveforms of the voltage across the 100-ohm load on the secondary terminal X1 are shown in Figure 4-19 for the four transformers tested in the configuration of

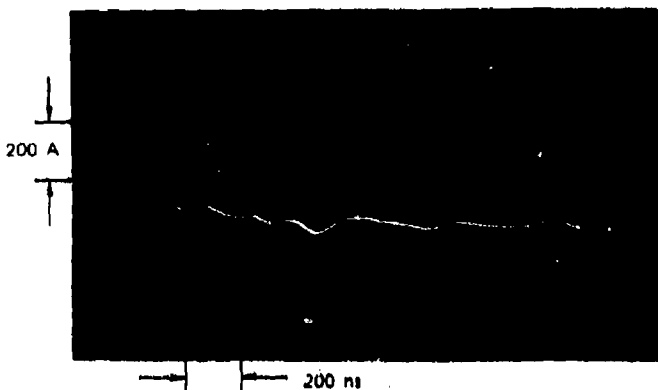


Figure 4-18 WAVEFORM OF PULSER CAPACITOR DISCHARGE CURRENT (which includes the current through the 100-ohm pulser load)

Figure 4-16. From the fast oscillograms of Figure 4-19 it is apparent that the rise times of the secondary voltage are of the order of 50 ns although the primary-voltage rise time was only 20 ns. Thus the rise time stretching caused by the primary bushing inductances is observable in the secondary voltages as well as in the primary current.¹ From the slower oscillograms of Figure 4-19 it is also apparent that the late-time voltage present in the driver has been suppressed, so that only about 200 ns of high-level response is observed at the secondary terminal. The stretching of the rise time in the time-domain corresponds to the high-frequency suppression observed in the frequency domain, and the suppression of the late-time response corresponds to the low-frequency roll-off observed in the frequency domain. Thus the transient waveforms are quite consistent with the frequency-domain data for voltage transfer functions.

These basic features of the secondary voltages — the stretching of the rise time and the suppression of the late-time response — were common to all four transformers, and were consistent with their frequency-domain transfer characteristics. There are obvious differences in the fine structure of the waveforms, but these appear to be of secondary importance, as are the size and location of the peaks and valleys of the frequency-domain transfer functions. The peak output voltage at Terminal X1 for one-volt peak at the primary is also quite similar for all four transformers, as is apparent in Table 4-3.

¹ The bushing inductance was responsible for the slow rise time of the current in the tests with a low source impedance; when source impedances of a few hundred ohms are used, the rise time of the terminal voltage is similarly slowed by the bushing capacitance.

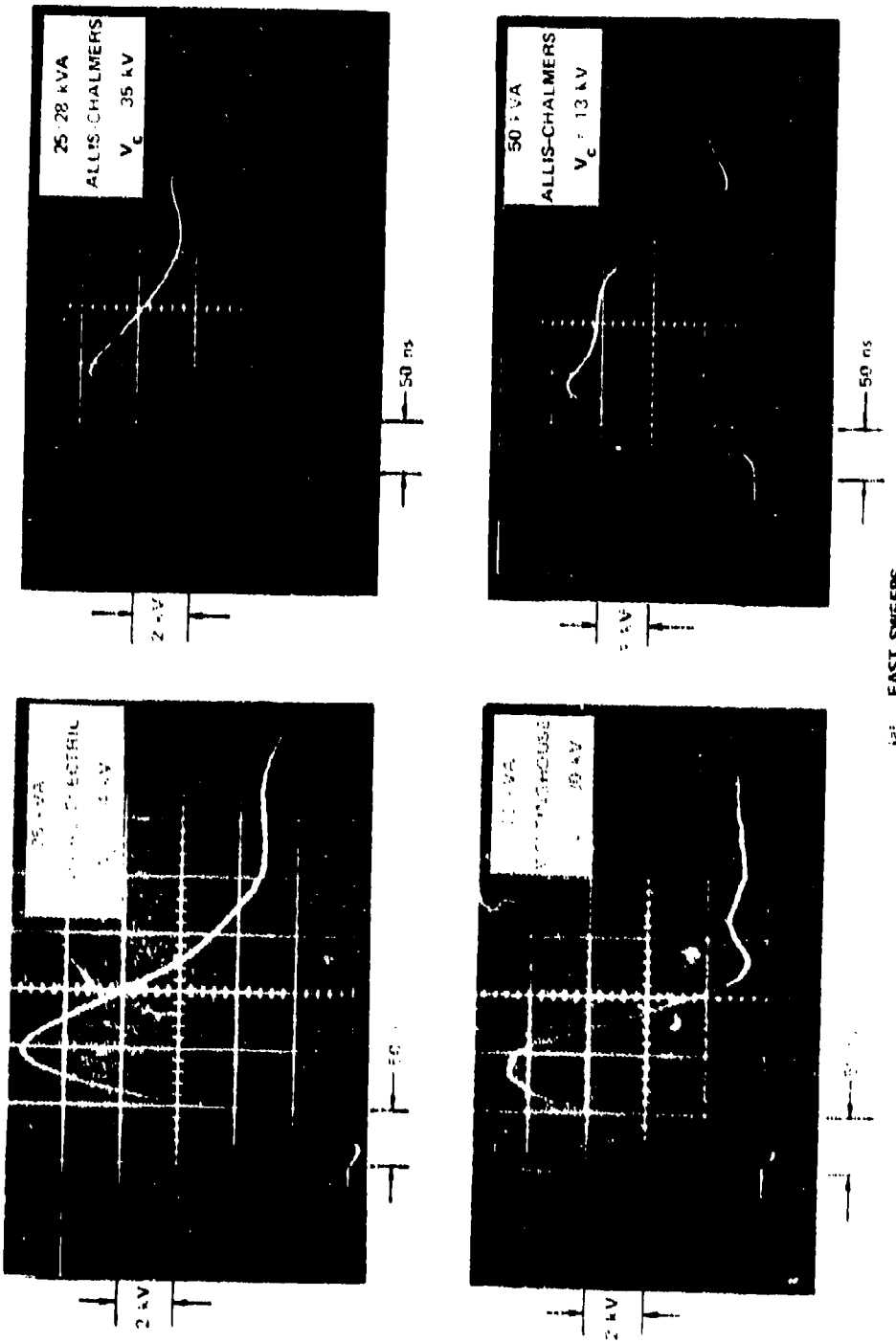


Figure 4-19 SECUNDARY INPUT-GROUND VOLTAGE OBSERVED AT X1 FOR COMMON-MODE EXCITATION AND LOADING $\epsilon_1 = \epsilon_2 = 10^3$ OF THE TRANSFORMERS RECORDINGS IN SERIES Note: V_C = peak excitation voltage.

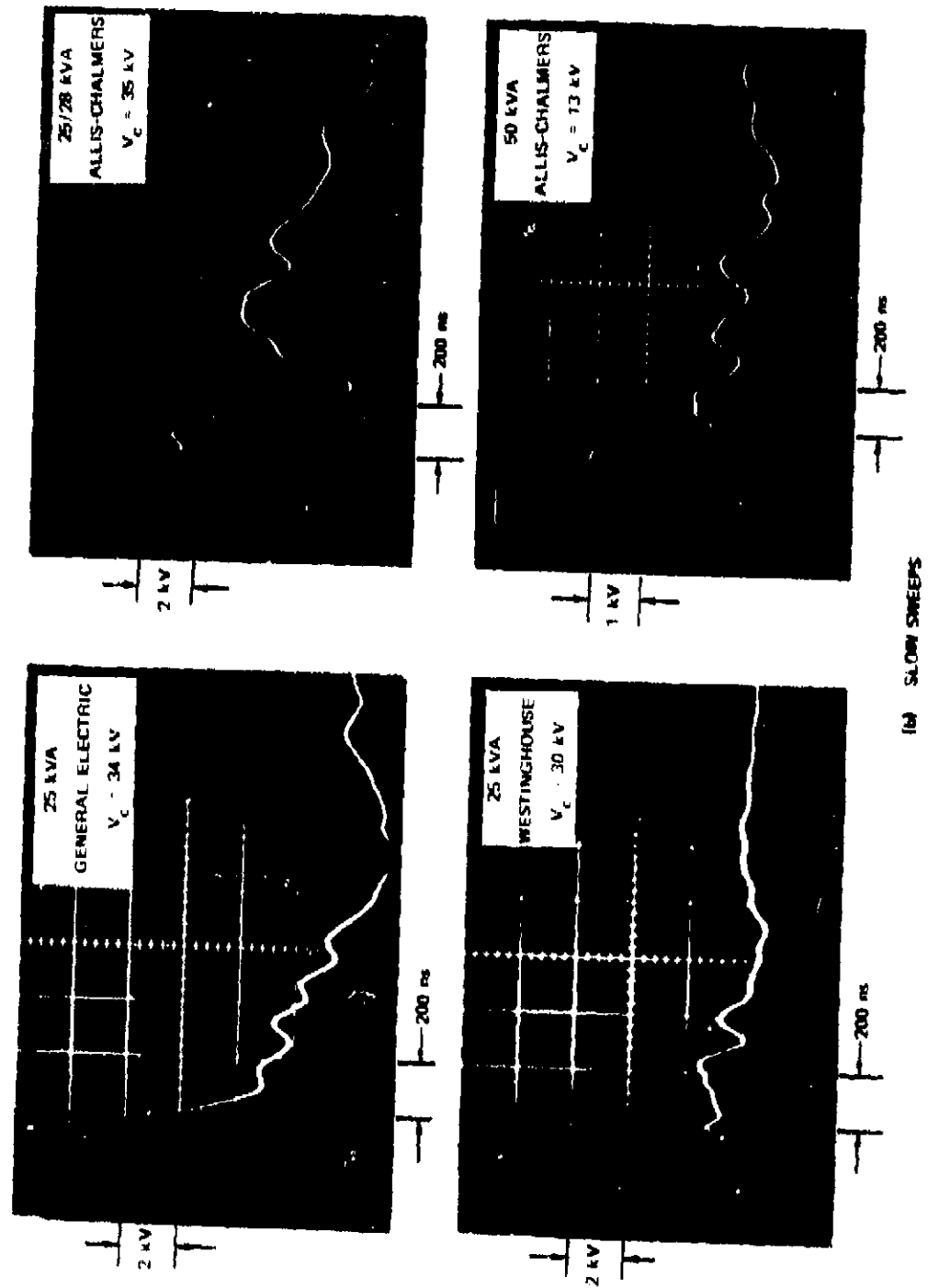


Figure 4-19 (Concluded)

Table 4-3

**COMPARISON OF PEAK VOLTAGE AT SECONDARY TERMINAL X1
FOR A ONE-VOLT, 7.5- μ s EXPONENTIAL PULSE
APPLIED TO THE PRIMARY**

Transformer Number	Transformer Type	Peak Voltage at X2 (V)
1	25-kVA G.E.	0.33
2	25-kVA Allis Chalmers	0.22
3	25-kVA Westinghouse	0.29
4	50-kVA Allis Chalmers	0.28

A comparison of the transient responses of the secondary to common-mode and differential-mode excitations at the primary can be made from the oscillograms of Figure 4-20, which show the voltage waveforms at secondary terminal X3 of the 25-kVA Westinghouse transformer for these two excitation modes. Although the responses are generally similar in shape, it is apparent that the differential-mode excitation at the primary produces only a little over half the peak secondary voltage produced by the common-mode excitation. This relationship is significant, because the common-mode excitation of the primary by the transmission lines is usually much greater than the differential-mode excitation; hence, if the weaker differential-mode signal is further reduced in passing through the transformer, its importance may be greatly reduced.

The oscillograms of Figure 4-19 and Figure 4-20 also permit the voltages at Terminals X1 and X3 to be compared for Transformer No. 1, for the configuration of Figure 4-10. It is apparent that the peak voltage at Terminal X1 is somewhat larger than that at Terminal X3 for the common-mode primary excitation. This difference is produced primarily by the asymmetry or unbalance in the windings; in a symmetrical bifilar-wound transformer these two voltages should be identical. This differential secondary voltage is shown in Figure 4-21 for the two excitation modes.

All of the waveforms in Figures 4-19, 4-20, and 4-21 were obtained with a common-mode output configuration. Figure 4-22 shows the voltage waveforms obtained at the secondary terminal X1 for a differential-mode output configuration such as that shown in

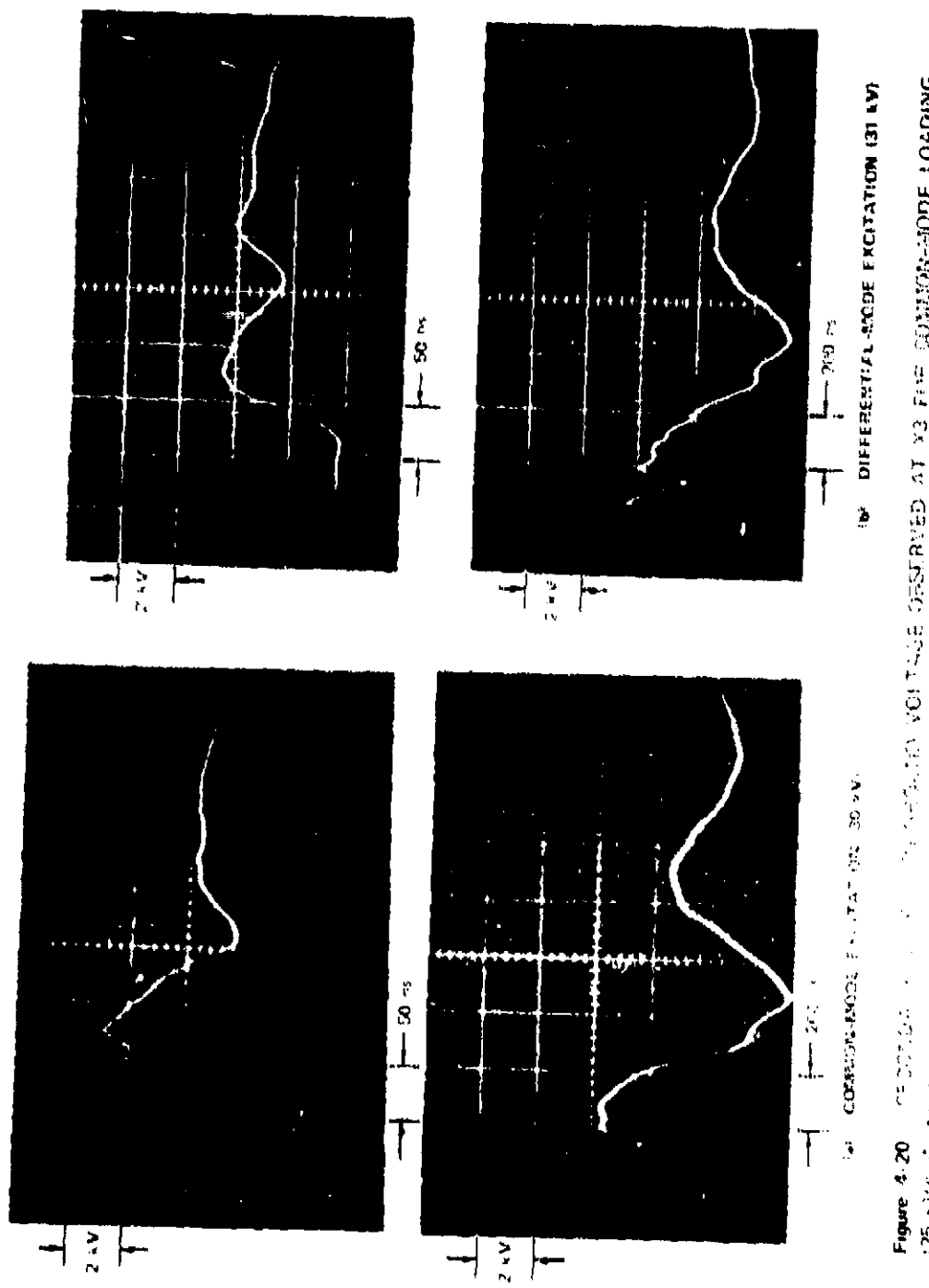


Figure 4-20. COMMON- and DIFFERENTIAL-MODE CURRENT-VOLTAGE CHARACTERISTICS OF THE 25-kV AND 30-kV VGT'S TESTED AT X2 FIVE MINUTE-BLOCK LOADING

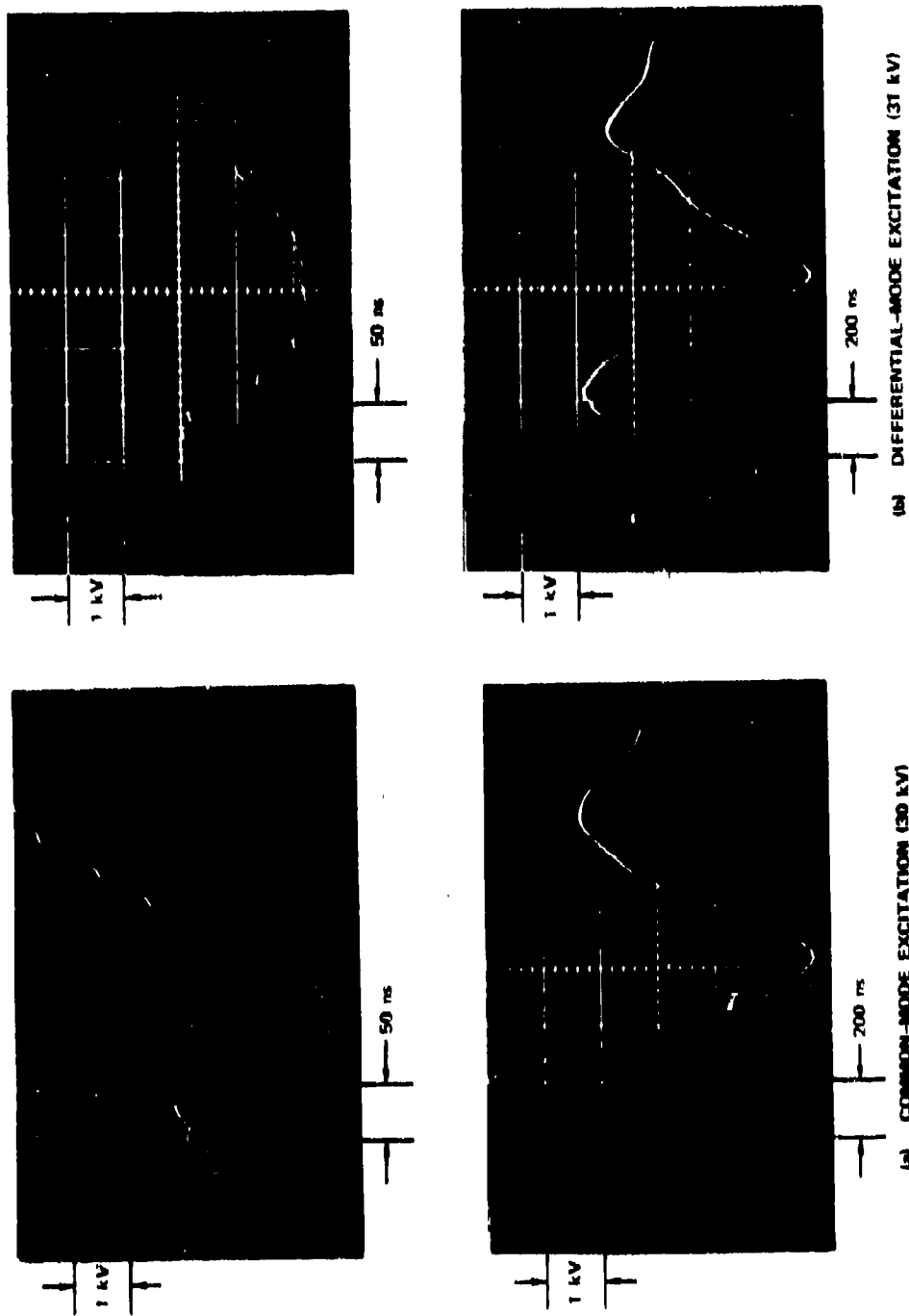


Figure 4-21 DIFFERENTIAL VOLTAGE APPEARING BETWEEN SECONDARY TERMINALS X₁ AND X₃ FOR COMMON-MODE LOADING (25-kVA GE unit: secondaries in series)

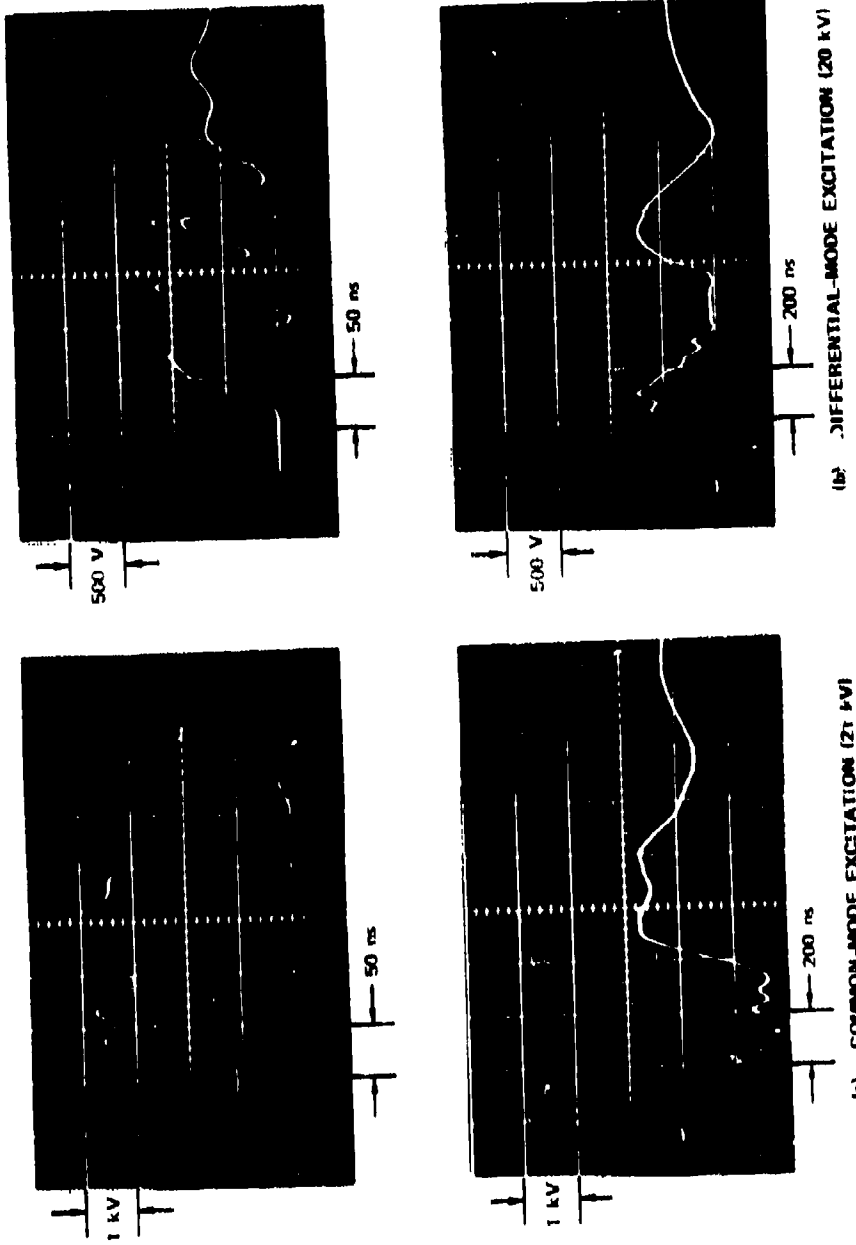


Figure 4-22 SECONDARY OUTPUT-TO-GROUND VOLTAGE OBSERVED AT X1 FOR DIFFERENTIAL-MODE LOADING
(25-kVA Westinghouse unit; secondaries in parallel)

Figure 4-16(b). The peak secondary voltage produced by the common-mode primary excitation with this secondary connection is larger than the peak secondary voltage produced by the differential-mode primary excitation. A comparison of Figure 4-22 with Figure 4-19, however, shows that the peak secondary voltage for the differential-mode output configuration is only about half as large as it is for the common-mode output configuration.

These and other data show that the transformer responses are (1) highly linear, (2) reasonably similar in comparison with one another, and (3) in good qualitative agreement with the CW transfer function data presented in Section 4.2.3. The frequency-domain data show that significant differences in amplitude can be expected for different drive configurations, and this result is confirmed by the transient-response data. Comparison of the common- and differential-mode drive data plotted here shows the following:

- (1) Common-mode input or output configurations result in peak output signals that are approximately double those of differential-mode input or output configurations.
- (2) The peak output response varies by a factor of 2 or less from transformer to transformer.
- (3) Different secondary-winding configurations (i.e., series or parallel) have little effect on the secondary terminal-to-ground voltage.

4.3 NONLINEAR CHARACTERISTICS OF TRANSFORMERS⁷

4.3.1 TRANSFORMER RESPONSES

At primary excitation levels above about 42 kV, the 10-kV lightning arresters on the primary side of the transformers fire if the pulselwidth of the excitation waveform is large enough. At the threshold voltage of 42 kV, there is a time lag of 150 to 200 ns between the time of application of the voltage and the closure of the lightning-arrester spark-gap switch, but as the applied voltage increases, this time lag decreases. The transformer's secondary response to a primary-side excitation at levels above about 42 kV is therefore

influenced by the change in the excitation pulse when the lightning arrester fires, and by the variable time lag between the application of the exciting pulse and the closure of the lightning arrester.

The only nonlinear effect observed during the transformer tests with the lightning arresters installed was the lightning-arrester firing. No other arcing or flashover was observed inside or outside the transformer case (except when the secondary was driven). The nonlinear responses discussed here are, therefore, caused entirely by the lightning-arrester firing.

The effect of the lightning-arrester firing on the secondary voltage waveform is illustrated in Figure 4-23. As was observed in the discussion of the linear response of the transformers, the duration of the large-amplitude secondary voltage waveform is of the order of 200 ns, so that deviations of the excitation pulse after 150 to 200 ns should not have much effect on the peak voltage appearing at the secondary terminals. Indeed, the lightning-arrester firing did not have much effect on the peak secondary voltage until the time-to-fire was reduced appreciably from 200 ns. This is apparent from the secondary-terminal voltage waveforms shown in Figure 4-23 for excitation voltages above the lightning-arrester threshold. As the lightning arrester is more highly overvolted and the time-to-fire decreases significantly below 200 ns, however, the peak secondary voltage becomes a smaller fraction of the peak excitation voltage. When the time-to-fire is comparable to or less than the \approx 50-ns time-to-peak of the secondary voltage, the secondary-voltage limiting provided by the lightning arrester is quite effective, and the peak secondary voltage increases very little with increasing excitation voltage beyond this point.

In addition to limiting the peak secondary voltage, the lightning-arrester firing tends to reduce the width of the main secondary-voltage pulse. This is apparent in Figure 4-23, where it can be seen that as the excitation level increases, the time to reach the first zero crossing in the secondary-voltage waveform decreases and the negative undershoot increases. It is also noteworthy that the effect of the firing of the lightning arrester on the secondary voltage waveform is so subtle that its occurrence is very difficult to detect in the secondary waveform.

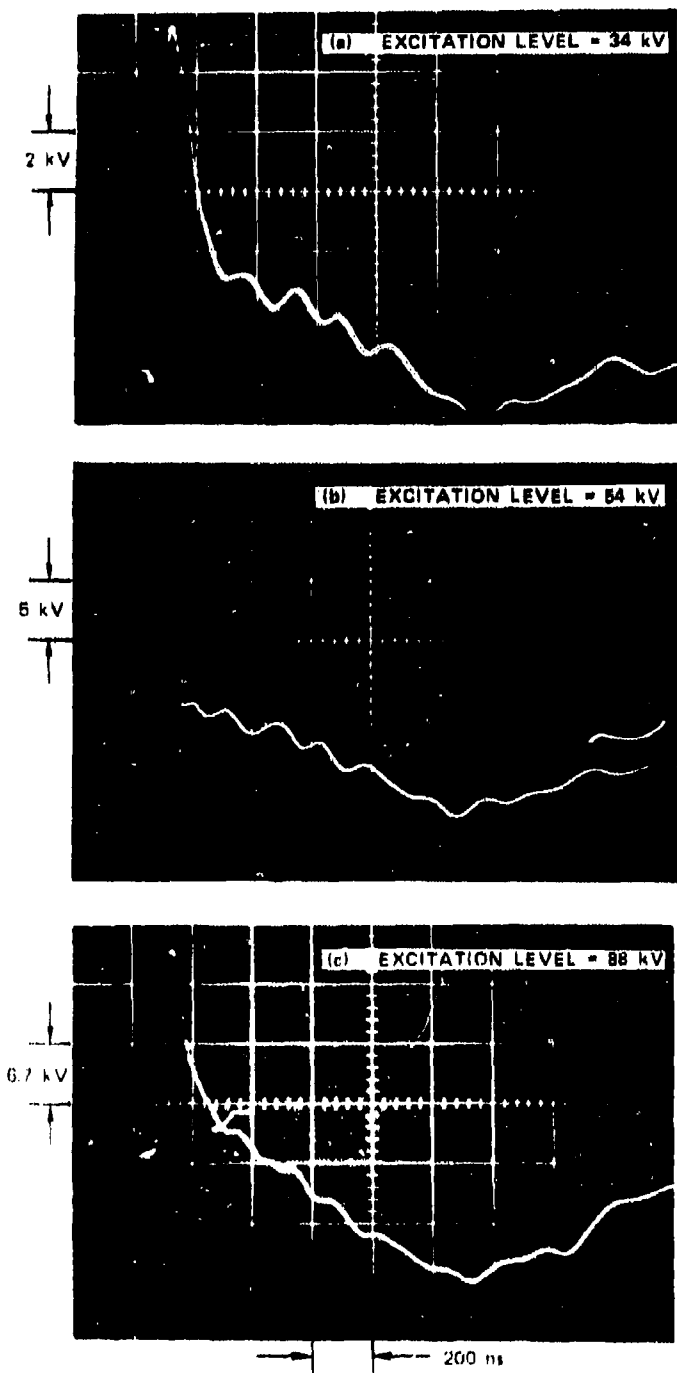


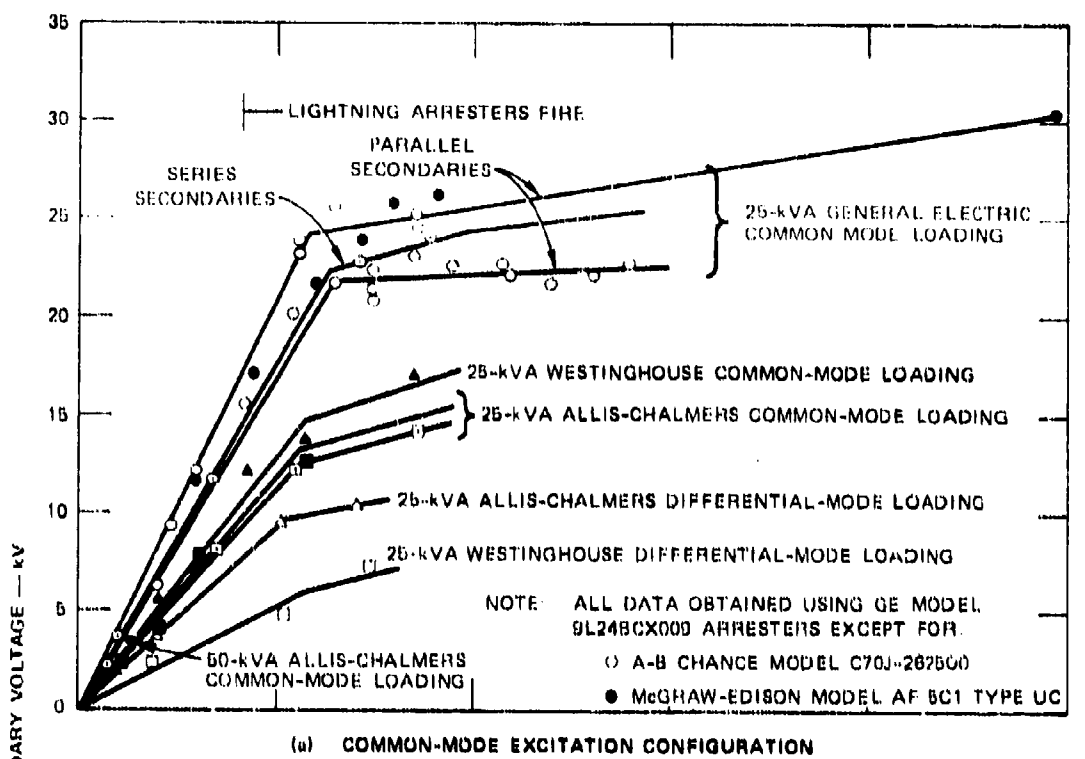
Figure 4-23 SECONDARY OUTPUT-TO-GROUND VOLTAGE OBSERVED AT X1 FOR COMMON-MODE EXCITATION AND LOADING (25-kVA GE unit; secondaries in series)

The secondary-voltage-limiting effect is illustrated in Figure 4-24, where the peak secondary voltage is plotted as a function of the peak excitation voltage for all four transformers and for both common and differential primary excitation modes. Here it is apparent that the secondary responses are quite linear with the excitation level until the peak excitation level reaches about 55 kV (30% above the lightning-arrester threshold), at which level the secondary voltage begins to level out. With the 250-kV excitation level (the highest level used) the peak secondary voltage was only 30 kV. This measurement was made on the 25-kVA G.E. transformer, which displayed the strongest coupling, and it was made in the configuration that displayed the strongest coupling. It should also be noted that, although the pulser was charged to 250 kV, the lightning arrester fired during the primary voltage rise and limited the voltage actually applied to the primary to only 100 kV.

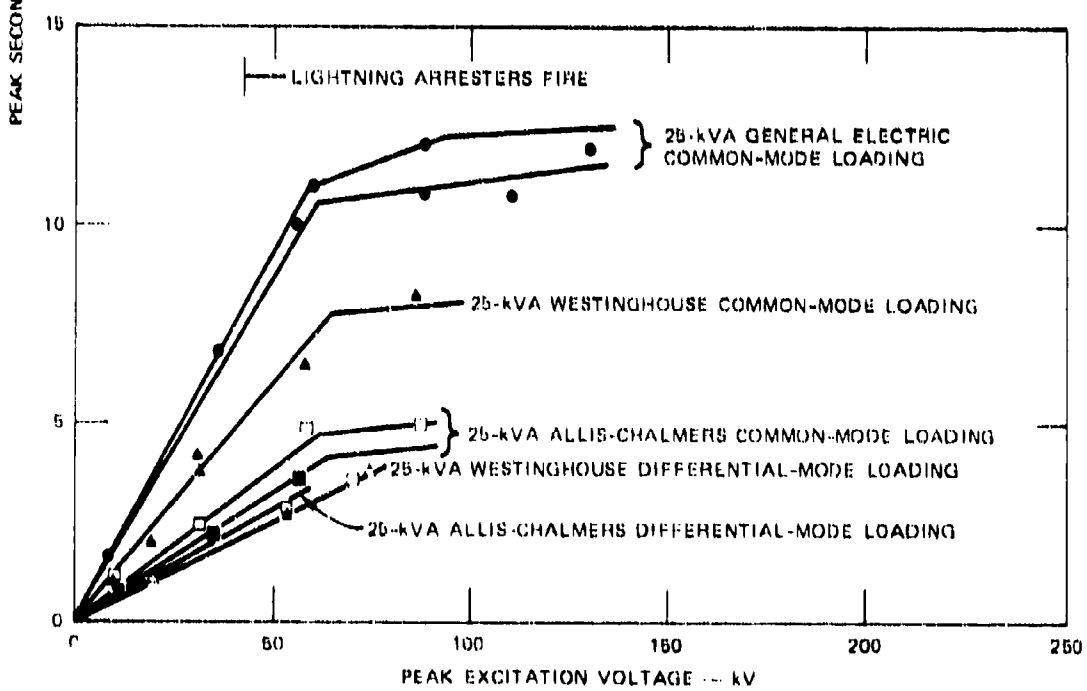
These tests were conducted with a low-impedance source, so that even when the lightning arresters fired, the excitation voltage at the primary terminals did not immediately change. When the source impedance was several hundred ohms, as it would be for an EMP-induced voltage wave incident on pole-mounted transformers driven by the distribution lines, the excitation voltage collapsed very rapidly when the lightning arrester fired. This value of source impedance causes the peak secondary voltage to be limited even more severely than was observed with the low-impedance sources used in the experiments described above. Since the transformer itself appears to remain linear, however, the effects of source impedance and primary excitation voltage can be simulated analytically and the secondary response determined from the linear transfer characteristics of the transformer.

4.3.2 LIGHTNING-ARRESTER FIRING CHARACTERISTICS⁷

The behavior of the 9-kV distribution lightning arresters used to protect the transformers was also obtained from the transient tests of the transformers with the lightning arresters installed. The lightning-arrester characteristics of primary importance in this evaluation are the time-to-fire and the firing voltage. These characteristics permit an estimate to be made of the peak voltage that might be applied to the transformer by a fast-rising transient.



(a) COMMON-MODE EXCITATION CONFIGURATION



(b) DIFFERENTIAL-MODE EXCITATION CONFIGURATION

Figure 4-24 PEAK SECONDARY VOLTAGE AS A FUNCTION OF PRIMARY EXCITATION FOR VARIOUS TRANSFORMER CONFIGURATIONS

The tests indicated that all three of the lightning arresters shown in Figure 4-4 were essentially identical in their firing characteristics. A plot of these firing characteristics is shown in Figure 4-25. The 9-kV arresters would normally be tested with the transient rate of rise of 100 kV/ μ s plotted in Figure 4-25; during the transformer tests, the maximum rate of rise achieved was about 2.5 kV/ns, or 25 times faster than that normally used to test lightning arresters of this voltage rating. With this rate of rise, which is also plotted in Figure 4-25, the firing voltage was 100 kV, or about 2.5 times the static firing threshold, and the time-to-fire was only 40 ns. In general, the trend of the lightning-arrester firing characteristics displayed in Figure 4-25 is that to be expected of spark-gap devices having large overvolted gaps.

The ability of the lightning arrester to protect the transformer under fast transients for which voltages of 100 kV are attained before the lightning arrester fires is believed to be related to two characteristics of the transformer. These are the ionization (or spark formation) time for bushing flashover and the impedance of the bushing and winding insulation. Because the arc formation time for the lightning arrester is less than the arc formation time for the bushing, the lightning arrester always fires before bushing flashover occurs. It is not apparent that this relationship should change even if greater rates of rise were encountered, since the lightning-arrester firing and bushing flashover involve similar gas-breakdown processes.⁹

The ability of the lightning arrester to protect the winding insulation against breakdown apparently depends on the fact that a finite time is required for the winding voltage to rise because of the winding-to-core capacitance and the bushing capacitance and inductance. For a typical transformer primary winding, the winding-to-core capacitance is a few hundred picofarads, the bushing capacitance is about 100 pF, and the bushing inductance is a few hundred nanohenries. Furthermore, as illustrated in Figure 4-7, the bushing inductance and bushing capacitance form a low-pass filter that limits the rate of rise of the voltage applied to the winding even if an infinite rate of rise is applied to the terminals. Therefore, even if the lightning arrester and bushing are subjected to very large rates of rise, the rate of rise of the voltage across the winding insulation is much smaller, thereby permitting the lightning arrester to reach its firing voltage before the voltage across the insulation reaches a dangerous level. Note that the CW-transfer-function data indicate that the high-frequency roll-off, which is believed to be caused primarily by the primary

bushing inductance and capacitance, begins at about 10 MHz, implying a 10-to-90% rise time of the order of 50 ns.

The rate of rise of the open-circuit voltage induced on power transmission lines by the EMP is of the order of a few $E_0 c$, where E_0 is the peak incident field strength and c is the speed of light (see Section 2.2.3). For realizable polarizations and angles of incidence, the maximum rate of rise of the open-circuit voltage is of the order of 50 kV/ns and the source impedance associated with this voltage is of the order of 300 ohms. This rate of rise is over an order of magnitude greater than the fastest rate of rise developed in the laboratory; however, the voltage actually applied to the transformer terminals is the fraction $Z_i/(Z_i + 300)$, where Z_i is the parallel input impedance of the transformers. Since $Z_i < 300$ ohms, at high frequencies (early times) only a fraction of the open-circuit voltage will actually be applied to the transformer windings.

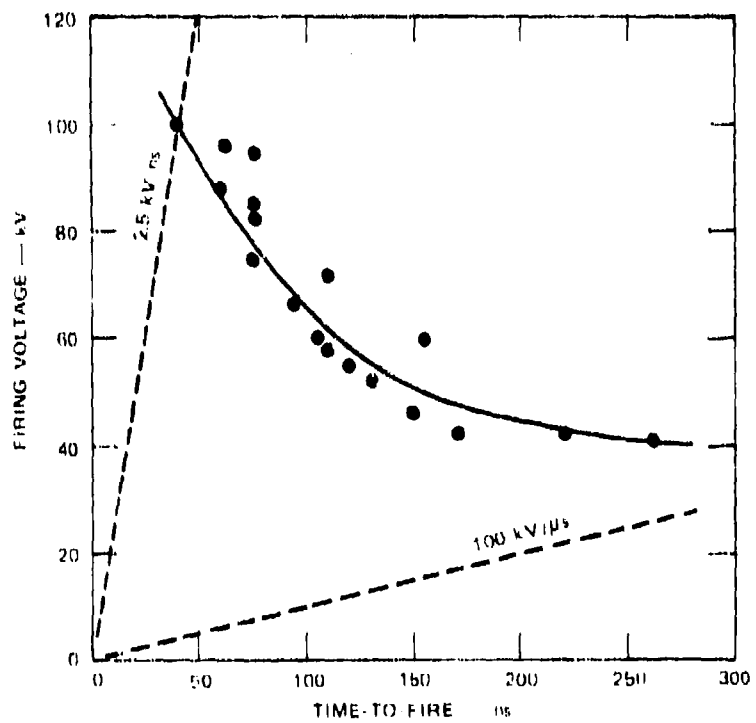


Figure 4-25 LIGHTNING-ARRESTER FIRING CHARACTERISTICS FOR FAST RATES OF RISE

4.3.3 SUMMARY OF TRANSFORMER AND LIGHTNING-ARRESTER PROPERTIES

Tests of selected lightning arresters and power transformers have demonstrated that at rates of rise up to 2.5 kV/ns the lightning arresters are effective in protecting the transformers from damage. It is believed that this protective capability should be applicable for even higher rates of rise, since the protection is based on (1) the lightning-arrester spark-gap ionizing and becoming conducting before other insulation breaks down, and (2) the bushing inductance and capacitance limiting the voltage between the primary windings and the core.

Studies of the transient throughput of the transformers with lightning arresters show that:

- (1) The bandpass character of the transformer slows the secondary-voltage rise-time to about 50 ns and limits the significant duration of the secondary response to less than 1 μ s.
- (2) When protected by lightning arresters, the transformer remains a linear device; all nonlinear activity occurs in the lightning arresters.
- (3) The key transformer parameters affecting the bandpass properties of the transformer are the primary bushing inductance and capacitance, and the interwinding- and winding-to-case capacitances.
- (4) There is little difference in the basic coupling characteristics among the different secondary-winding types or among the transformers from different manufacturers.
- (5) The peak secondary voltage is limited to a value of the order of 20 to 30 kV by the voltage-limiting action of the 9-kV lightning arresters for common-mode excitation.
- (6) Transients induced at the secondary terminals by the lightning arrester firing are barely detectable.

The test results show that the strongest coupling through the transformer occurs for common-mode excitation and common-mode loading, such as would occur if the 3-phase transformer bank were delta-connected at both primary and secondary sides. The weakest coupling occurs for differential mode excitation and loading, such as would occur for three-phase wye-connections at both sides.

The properties of the three models of 9-kV lightning arresters were virtually identical insofar as their firing characteristics are concerned. As the rate of rise of the voltage across the lightning arresters increases, the time-to-fire decreases, but with the maximum rate of rise available in these tests (2.5 kV/ns) the firing voltage was only 100 kV and the time-to-fire was only 40 ns. This rate of rise is 25 times that for which the lightning arresters are specified, while the firing voltage is only 2.5 times the static firing voltage. It is significant that as the rate of rise increases, the firing voltage increases, and as the time-to-fire decreases, the impulse /vdt passed by the lightning arrester does not change very much. Thus, the transformer's secondary voltage for fast rates of rise tends to be the impulse response and is relatively independent of the excitation voltage.

In operational systems, the use of lightning arresters between the primary terminals of the transformer and ground is recommended for all service transformers to protect the transformer, as well as to limit the high voltages induced on the transmission lines and coupled through the transformer.

4.4 CITED REFERENCES

1. *Electrical Transmission and Distribution Book*, 4th ed., 5th printing (Westinghouse Electric Corporation, East Pittsburgh, Penn., 1964).
2. W. W. Lewis, *The Protection of Transmission Systems Against Lightning* (John Wiley & Sons, Inc., New York, N. Y., 1950).
3. L. V. Bewley, *Traveling Waves on Transmission Systems* (Dover Publications, Inc., New York, N. Y., 1963).
4. R. Rudenberg, *Electrical Shock Waves in Power Systems* (Harvard University Press, Cambridge, Mass., 1968).

5. A. Greenwood, *Electrical Transients in Power Systems* (John Wiley & Sons, Inc., New York, N. Y., 1971).
6. E. F. Vance and S. Dairiki, "Analysis of Coupling to the Commercial Power System," Technical Report AFWL-TR-72-21, Contract F29601-69-C-0127, Air Force Weapons Laboratory, Kirtland Air Force Base, New Mexico (August 1972).
7. R. T. Bly, Jr., and E. F. Vance, "High-Voltage Transient Tests of Service Transformers, Lightning Arresters, and an Automatic Switching Unit," AFWL-TR-74-34, Contract F29601-69-C-0127, Air Force Weapons Laboratory, Kirtland Air Force Base, New Mexico (October 1973).
8. J. H. Marable, J. K. Baird, and D. B. Nelson, "Effects of Electromagnetic Pulse (EMP) on a Power System," Final Report, Interagency Agreement No. AEC 40-31-64 and OCD-PS-64-284, Work Unit #213C, ORNL 4836, Oak Ridge National Laboratory, Oak Ridge, Tennessee (December 1972).
9. J. D. Cobine, *Gaseous Conductors* (Dover Publications, Inc., New York, N. Y., 1958).

Chapter Five

LOW-VOLTAGE CIRCUITS

5.1 GENERAL DESCRIPTION OF THE LOW-VOLTAGE SYSTEM

5.1.1 INSTALLATION PRACTICE

The low-voltage circuits of concern in this chapter are those between the main circuit breaker and the loads (lights, appliances and equipment) in the consumer's facility. The source side of the main circuit breaker has been discussed in Chapters Two and Three. This part of the power system can be represented by a single (though, perhaps, multiconductor) transmission line whose characteristic impedance changes as its form changes from an aerial transmission line to a coaxial line at the service entrance. On the load side of the main circuit breaker, however, the circuits branch out to serve the various requirements of the consumer. The consumer's system may contain both single-phase and three-phase loads as illustrated in Figure 5-1, and in general the loads may require two or more voltages, necessitating more than one service entrance or transformer bank. The system shown in Figure 5-1 would be typical of a 120/208-V system in which single-phase circuits are operated on the 120-V between line and neutral and three-phase loads are operated from the 208-V

(line-to-line) system. If other three-phase or single-phase voltages are required, the low-voltage system may also contain power transformers or other power-conversion equipment. A more common practice where multiple voltages are required, however, is to bring the distribution voltage into a vault where the transformers required to supply all of the consumer's voltages are installed. Separate feeders from the transformer vault may then be used to supply the main circuit breakers for the various three-phase and single-phase systems in the facility. If the three-phase service is delta-connected, a zig-zag transformer may be included in

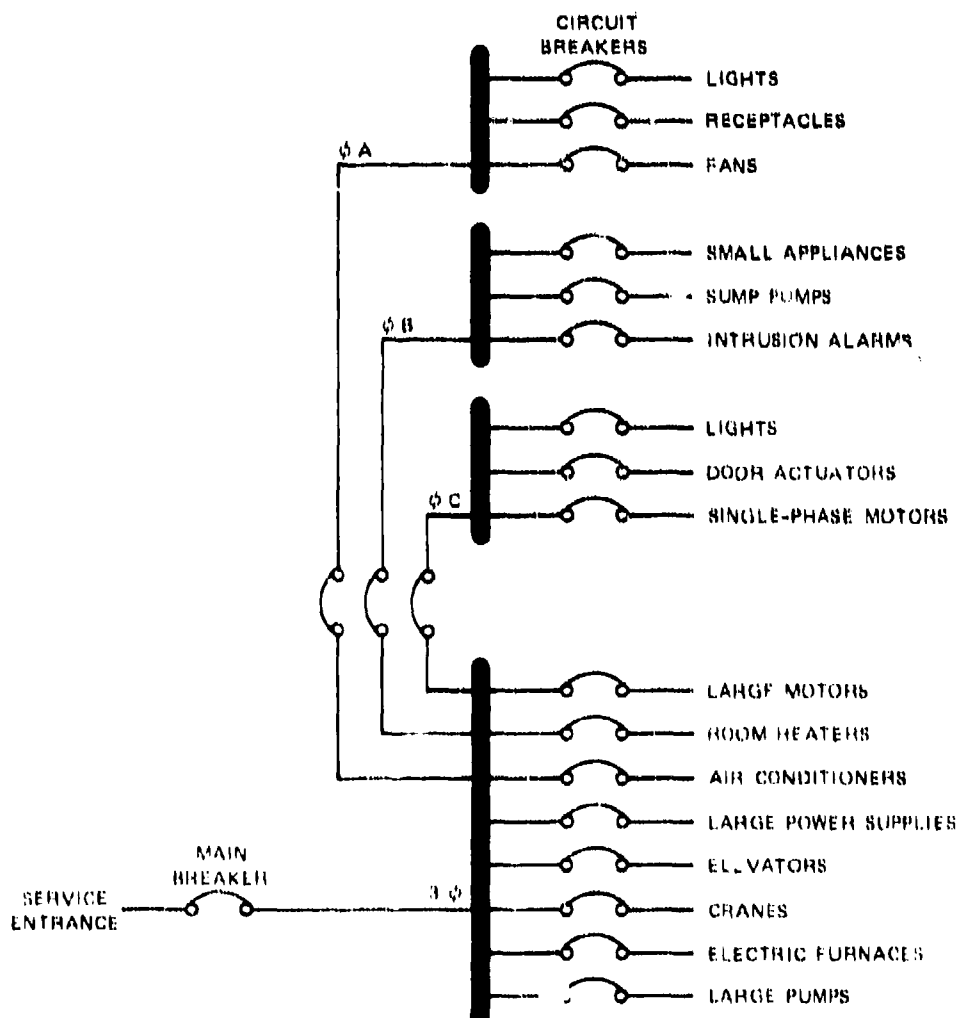
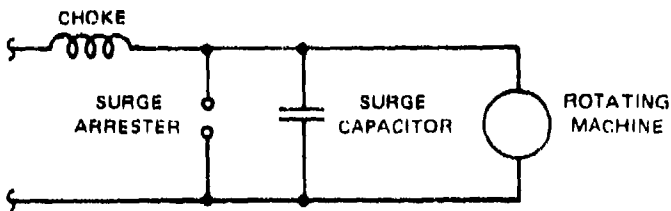


Figure 6-1 SINGLE-LINE DIAGRAM OF INTERNAL LOW-VOLTAGE CIRCUITS

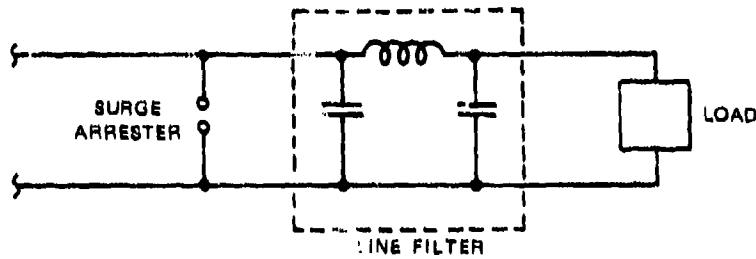
the low-voltage system to ground the low-voltage system. For some communications facilities the commercial power is used to drive a motor-generator set which, in turn, supplies the power for operating the facility. This system can provide excellent isolation of the consumer's circuits from transients on the power system if separate machines (connected only by the shaft) are used and appropriate separation of the power circuit and the low-voltage circuits is provided. Some large commercial computer installations use rectifier and storage-battery systems to provide surge protection and short-term standby power.

Other surge-protection equipment that may be found in commercial installations are secondary lightning arresters, surge limiting capacitors, and line filters. Secondary lightning arresters that operate at a few thousand volts may be installed at the transformer secondary, at the weatherhead, at the main circuit-breaker panel, on a circuit that requires special protection, or some combination of these. Surge capacitors are used to protect the windings of large rotating machines from the large rates of change in the leading edges of lightning-induced surges. Line filters are used to minimize the transients that can enter sensitive installations such as computer centers. As illustrated in Figure 5-2, combinations of these protective devices are often used. For example, a combination of lightning arresters and surge capacitors may be used to limit both the peak voltage and the rate of rise of the current, or a lightning arrester may be used to limit the voltage applied to the input terminals of a line filter.

The National Electrical Code¹ sets standards for materials and practices used in low-voltage wiring; in addition, states, counties, and cities have their own building codes that are often more restrictive than the national code. In spite of local variations, however, there is considerable uniformity in the wiring practices used in commercial steel and masonry buildings. The low voltage wiring in such facilities is usually installed in metallic conduit and raceways or gutters as illustrated in Figure 5-3. All metal conduit, gutters, circuit-breaker cabinets, outlet boxes, etc. are required by the national code to be "effectively bonded where necessary to assure electrical continuity . . .". The low-voltage wiring is thus fairly well enclosed in a metallic shield of sorts except at plug-in appliances (calculators, typewriters, coffee-makers, etc.), where the conductors are insulated but unshielded. We shall limit our discussion in this chapter to low-voltage systems with wiring in metal conduits.



(a) LIGHTNING ARRESTER AND CAPACITOR



(b) LIGHTNING ARRESTER AND LINE FILTER

Figure 5-2 SURGE-PROTECTION TECHNIQUES FOR LOW-VOLTAGE CIRCUITS

Vinyl- or neoprene-insulated copper conductors are used in applications where excessive heat or moisture is not a problem. These conductors are fished through the conduit between outlet boxes or cabinets, and extra wire is left at the ends to allow the craftsman to make the connections to the fixture terminals. Figure 5-4 illustrates the wiring inside a typical main circuit-breaker panel. The maximum number of wires that can be pulled through standard conduits is given in Table 5-1.¹ The dimensions of rigid steel conduit are given in Table 3-2, Chapter Three.

6.1.2 DISTRIBUTION OF THE EMP-INDUCED SIGNAL

In moderately well-shielded systems such as the electrical wiring in metal conduit, the signal induced in the exposed conductors (aerial transmission lines or entrance conductors in plastic conduit) and conducted into the shielded region is usually much larger than that penetrating directly through the shield to the conductors. Therefore the primary source



Figure 5-3 TYPICAL LOW-VOLTAGE WIRING IN RIGID STEEL CONDUIT

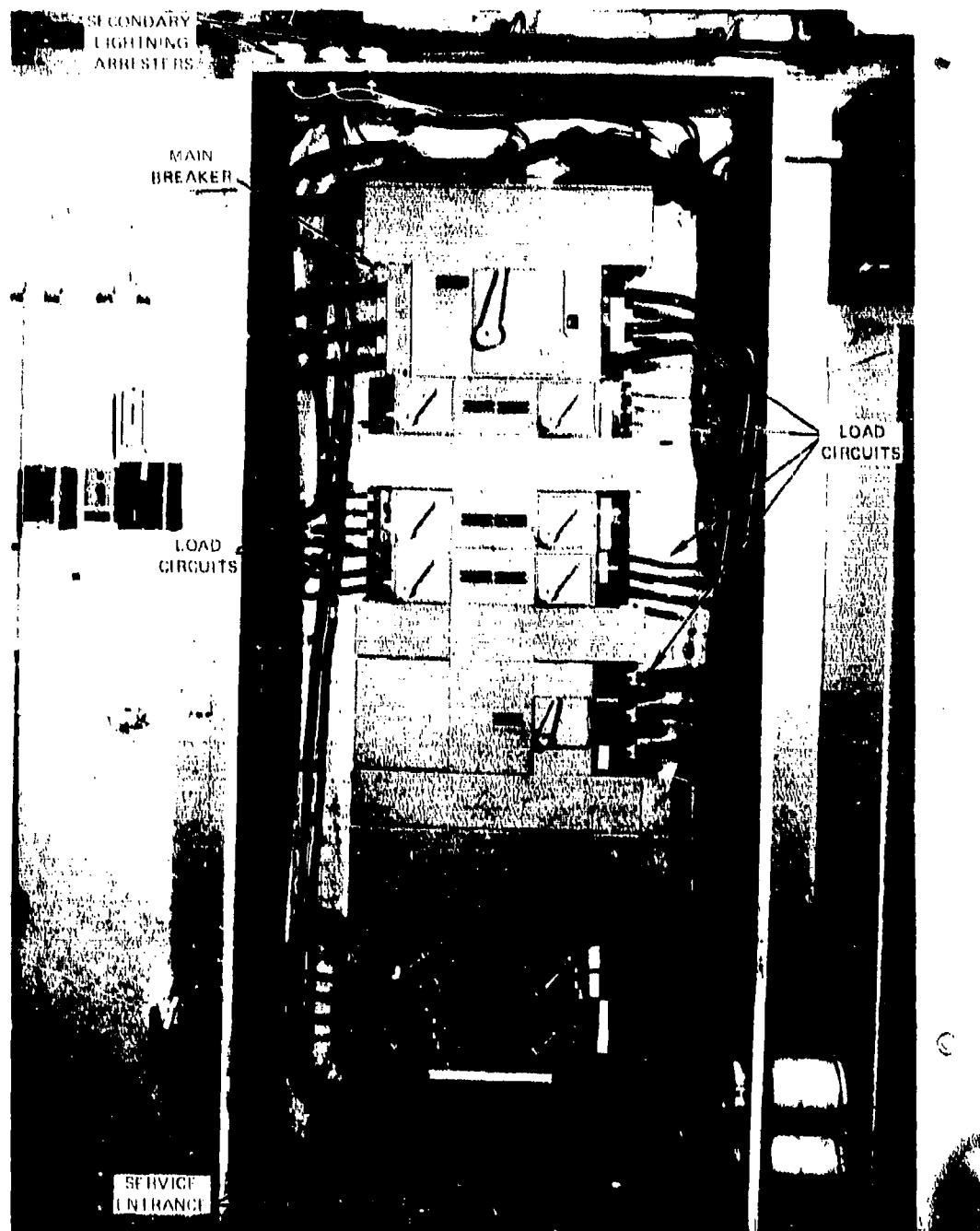


Figure 5-4 LOW-VOLTAGE WIRING INSIDE A MAIN CIRCUIT-BREAKER PANEL

Table 5-1
MAXIMUM NUMBER OF CONDUCTORS IN TRADE SIZE OF
CONDUIT OR TUBING¹

Conduit Trade Size (inches)		1/2	3/4	1	1 1/4	1 1/2	2	2 1/2	3	3 1/4	4	4 1/2	5	6
Insulating Type Letters	Conductor Size (AWG, MCM)													
TW, T, RUH, RUW, XHHW (14 through 8)	14	9	15	25	44	60	99	142						
	12	7	12	19	35	47	78	111	171					
	10	5	9	15	26	36	60	85	131	176				
	8	3	5	8	14	20	33	47	72	97	124			
RHW and RHH (without outer covering), THW	14	6	10	16	29	40	65	93	143	192				
	12	4	8	13	24	32	63	76	117	157				
	10	4	6	11	19	26	43	61	95	127	163			
	8	1	4	6	11	15	25	36	56	75	96	121	152	
TW, T, THW, RUH (6 through 2), RUW (6 through 2), PEPB (6 through 2), RHW and RHH (without outer covering)	6	1	2	4	7	10	16	23	36	48	62	78	97	141
	4	1	1	3	5	7	12	17	27	36	47	58	73	106
	3	1	1	2	4	6	10	15	23	31	40	50	63	91
	2	1	1	2	4	5	9	13	20	27	34	43	54	78
	1	1	1	3	4	6	9	14	19	25	31	39	57	
	0		1	1	2	3	5	8	12	16	21	27	33	49
	00		1	1	1	3	5	7	10	14	18	23	29	41
	000		1	1	1	2	4	6	9	12	15	19	24	35
	0000		1	1	1	3	5	7	10	13	16	20	29	
	250			1	1	1	2	4	6	8	10	13	16	23
	300			1	1	1	2	3	5	7	9	11	14	20
	350			1	1	1	1	3	4	6	8	10	12	18
	400			1	1	1	1	2	4	5	7	9	11	16
	500			1	1	1	1	1	3	4	6	7	9	14
	600					1	1	1	3	4	5	6	7	11
	700					1	1	1	2	3	4	5	7	10
	750					1	1	1	2	3	4	5	6	9

Key:

- T Thermoplastic
- TW Moisture-resistant thermoplastic
- THW Moisture- and heat-resistant thermoplastic
- RHW Moisture- and heat-resistant rubber
- RHH Heat-resistant rubber
- RUH Heat-resistant latex rubber
- RUW Moisture-resistant latex rubber
- XHHW Moisture- and heat-resistant cross-linked synthetic polymer.

of EMP-induced signal in the low-voltage wiring is usually the signal conducted in on the service entrance.

At the main circuit-breaker panel, the voltage and current entering from the service entrance are partially attenuated by the stray inductance of the wiring inside the circuit-breaker cabinet, and are partially transmitted to the load circuits. Because of the reflection, attenuation, and division of the power at the main circuit-breaker panel, the EMP-induced power transmitted to the load-circuit conduits is only a fraction of that incident from the service entrance. In addition, the stray inductances in the cabinets and junction boxes tend to suppress the high-frequency portion of the incident pulse spectrum, so that the rise time of the transient increases as the pulse propagates further into the low-voltage system. Each load-circuit is also shock-excited by the incident transient and tends to oscillate at its natural frequencies. This shock excitation leads to voltage waveforms in the load circuits moderately similar to the waveform shown in Figure 3-10(a). Needless to say, the EMP-induced waveforms at any point in the low-voltage system are quite complex and very difficult to calculate accurately. As a rough rule of thumb, however, the further from the main circuit-breaker panel, the smaller the peak voltage and the smaller the rates of change in the waveform.

5.2 LINEAR ANALYSIS OF CONDUIT CIRCUITS

5.2.1 TRANSMISSION-LINE ANALYSIS (COMMON-MODE)

Electrical wiring enclosed in metal conduit can be visualized as a transmission line. For a crude approximation, the power conductors can be considered the center conductor of a coaxial transmission line in which the conduit is the outer, or return, conductor. The low-voltage wiring system in the consumer's facility can then be represented as a network of transmission-line segments such as that illustrated in Figure 5-5. At the ends of the conduits where the wiring enters circuit-breaker cabinets, outlet boxes, etc., the wiring is more open and can be represented as a lumped inductance for short segments of, say, less than 2 m. Because the low-voltage systems contain many segments of transmission line with many branches and junctions, even this crude representation of the low-voltage wiring is very difficult to analyze without a computer. The analytical concepts required are quite

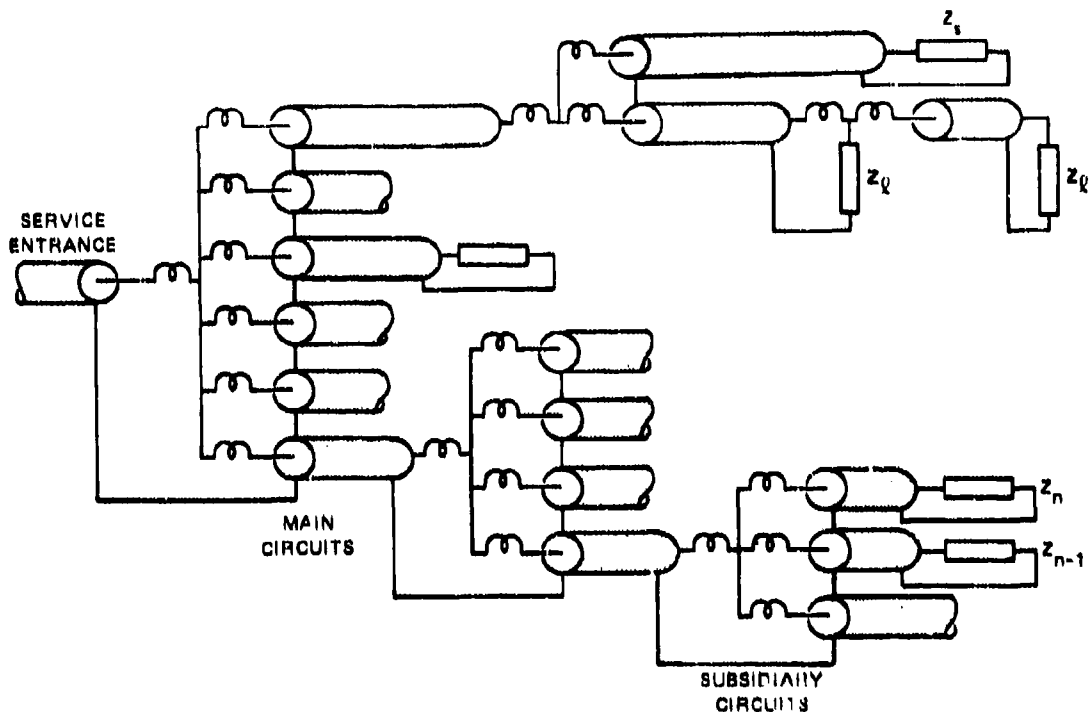


Figure 5-5 TRANSMISSION-LINE MODEL OF LOW-VOLTAGE WIRING IN METAL CONDUIT

simple; however, they must be applied to each segment and the results for the segments must be combined in an orderly fashion.

In the transmission-line network of Figure 5-5, for example, the upper branch of segments might represent a lighting circuit containing a wall switch (Z_1) and two ceiling lights (Z_2). This circuit contains four segments of transmission line downstream from the main circuit-breaker panel. A common occurrence in large facilities is represented by the bottom branch in Figure 5-5. In this case one circuit from the main circuit-breaker panel supplies a subsidiary circuit-breaker panel, which may, in turn, supply additional subsidiary circuits.

The general approach for analyzing such wiring as transmission-line networks is to transfer impedances along the segments from right to left in Figure 5-5 to obtain the load impedance on the service-entrance conduit. When this load impedance is known, the voltage or current in the load can be determined from the techniques described in Chapter Three. The voltage and currents can then be translated from left to right toward the loads at the right ends of the conduit circuits. At each junction of two or more conduits, the impedances translated from the right must be combined with the lumped impedances at the junction to

obtain the load impedance for the conduit to the left, and the current translated from the left must be divided among these impedances to obtain the current to translate to the right toward the loads.

Prior to performing this analysis it is necessary to determine

- (1) The characteristic impedances Z_{on} of the n conduit segments
- (2) The propagation factors γ_n for the n conduit segments
- (3) The lengths ℓ_n of the conduit segments
- (4) The load impedances Z_{Ln} at the right ends of the right-hand segments
- (5) The stray inductances L_n at the junctions of the conduit segments
- (6) The Thevenin or Norton Equivalent source representing the service entrance.

If these properties of the transmission line are determined, the load impedances at the right ends of the right-hand segments in Figure 5-6(a) can be translated to the left ends of the segments by

$$Z_{in} = Z_{on} \frac{1 + \rho_n e^{2\gamma_n \ell_n}}{1 - \rho_n e^{2\gamma_n \ell_n}} \quad (5-1)$$

where

$$\rho_n = \frac{Z_{Ln} - Z_{on}}{Z_{Ln} + Z_{on}} \quad (5-2)$$

This translation converts the original circuit of Figure 5-6(a) to the equivalent circuit of Figure 5-6(b). The input impedance Z_{in} at the left end of the conduit is then added to the impedance $j\omega L_n$ of the stray inductance at the junction, and the impedances $Z_{in} + j\omega L_n$

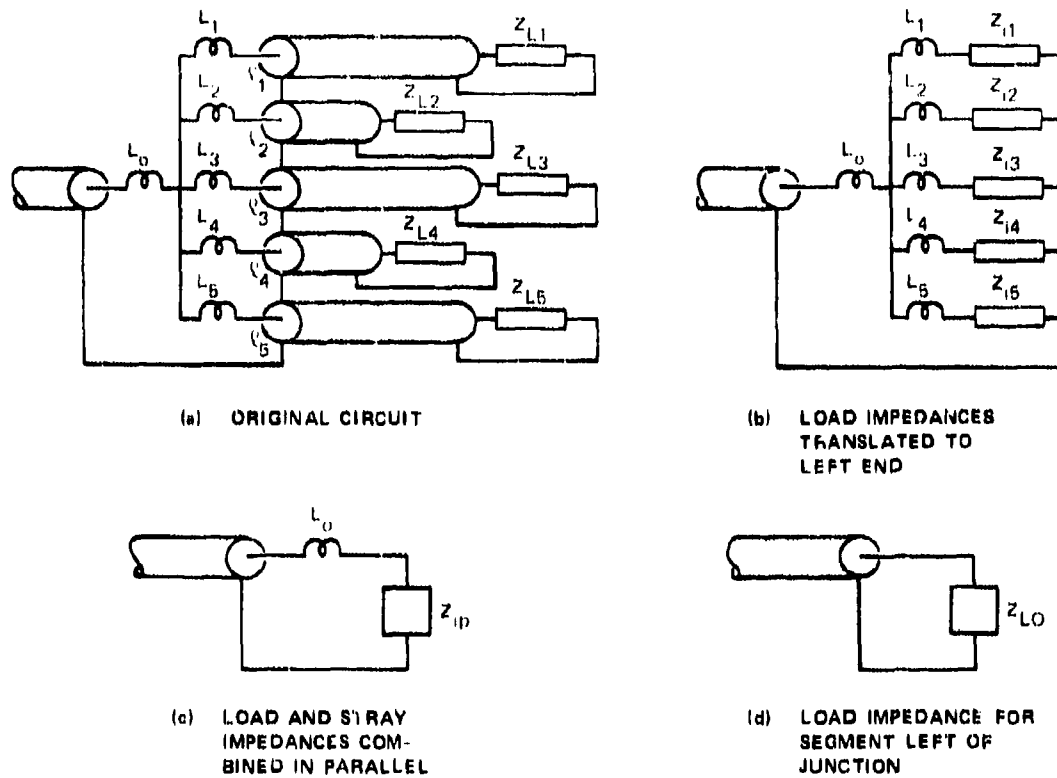


Figure 5-6 STEPS IN TRANSLATING LOAD IMPEDANCES TOWARD DRIVING SOURCE

are combined in parallel as illustrated in Figure 5-6(c). The load impedance on the right end of the conduit segment to the left of the junction (see Figure 5-6(d)) is then

$$Z_{lo} = j\omega L_0 + Z_{ip} \quad (5-3)$$

where

$$\frac{1}{Z_{ip}} = \frac{1}{j\omega L_1 + Z_{i1}} + \frac{1}{j\omega L_2 + Z_{i2}} + \dots + \frac{1}{j\omega L_n + Z_{in}}, \quad (5-4)$$

This cycle can then be repeated to translate the impedances toward the next junction to the left and so forth, until the load impedance at the end of the service-entrance conduit is established.

The object of the impedance translation is to combine the impedances of the branches to obtain the lumped equivalent load for the service entrance. The voltage and current translations involve a reversal of this process, in that the starting point is the Thevenin equivalent source representing the signal entering from the service entrance, and the object of the translations of the voltage and current from this source to the right is to determine how this signal fans out into the conduit network. Therefore we start with the Thevenin equivalent source and its load Z_{OL} in Figure 6-7(a) and calculate the junction voltage V_j and total current I_j as shown in Figure 6-7(b). The junction voltage is

$$V_j = \frac{Z_{ip}}{Z_1 + Z_{ip} + j\omega L_0} V_o \quad (6-5)$$

and the total current is

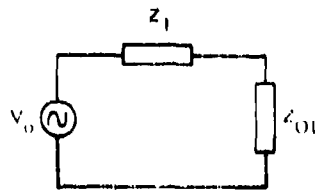
$$I_j = \frac{V_o}{Z_1 + Z_{ip} + j\omega L_0} \quad (6-6)$$

where V_o and Z_1 are open-circuit voltage and source impedance represented by the service entrance at, for example, the main circuit-breaker panel (see Chapter Three, Eqs. (3-7) and (3-8)). The voltage applied to each conduit to the right of the junction is a fraction of the junction voltage, however, as can be seen in Figure 6-7(c). The voltage V_n applied to the left end of the conduits is

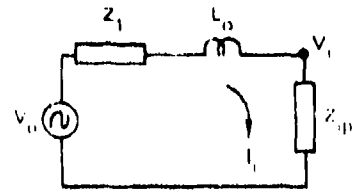
$$V_n = \frac{Z_{in}}{Z_{in} + j\omega L_n} V_j \quad (6-7)$$

and the current I_n in the conductors is

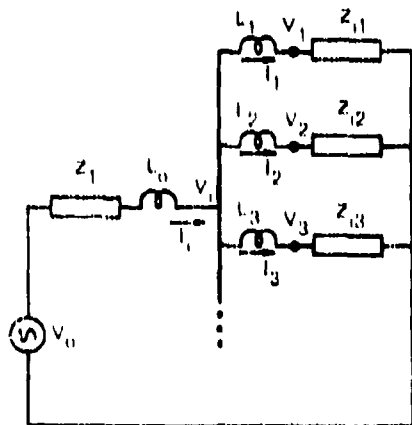
$$I_n = \frac{V_j}{Z_{in} + j\omega L_n} \quad (6-8)$$



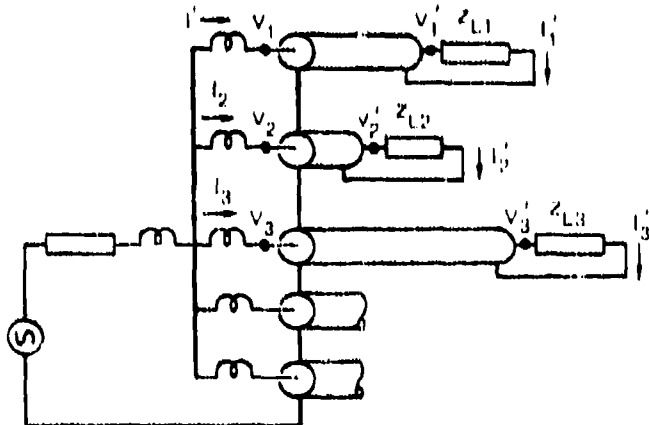
(a) LOAD DRIVEN BY SERVICE ENTRANCE



(b) JUNCTION VOLTAGE AND CURRENT



(c) CURRENT AND VOLTAGE LAUNCHED INTO CONDUITS



(d) CURRENT AND VOLTAGE TRANSLATED TO RIGHT ENDS OF CONDUITS

Figure 5-7 STEPS IN TRANSLATING DRIVING CURRENT AND VOLTAGE TOWARD LOADS

The current and voltage at the right ends of the conduits in Figure 5-7(d) are then

$$I'_n = I_n \frac{e^{-j\alpha n}}{1 - \rho_{1n} e^{-2j\alpha n}} \quad (5-9)$$

and

$$V'_n = V_n \frac{e^{-j\alpha n}}{1 + \rho_{1n} e^{-2j\alpha n}} \quad (5-10)$$

This cycle may be repeated for further translations to the right if it is observed that the source impedance at the right end of the conduit is

$$Z'_1 = \frac{V_n}{I_n} - Z_{Ln} \quad (5-11)$$

and the open-circuit voltage V'_o at the right end is

$$V'_o = I_n (Z_{Ln} + Z'_1) . \quad (5-12)$$

This Thevenin-equivalent source drives the junction (if any) at the right ends of the conduits.

5.2.2 DETERMINATION OF THE PROPERTIES OF CONDUIT CIRCUITS

In the introduction to the transmission-line analysis above, it was stated that six properties of the low-voltage system must be determined prior to performing the analysis of the low-voltage circuits. One of these properties — the equivalent source representing the signal entering on the service-entrance conductors — is the subject of Chapter Three. Another, the lengths of the conduit segments, can often be measured directly. The remaining four, the characteristic impedance Z_o , the propagation factor γ , the load impedance Z_L , and the stray inductance L may be measured, or they can be estimated by techniques discussed in this section.

5.2.2.1 Characteristic Impedance

Accurate formulas for the characteristic impedance of multiconductor transmission lines are available for only a few special geometries such as the symmetrical shielded pair and shielded quad shown in Figure 3-13. The electrical wiring fished through conduit rarely assumes the uniform symmetrical geometry postulated in these formulas; however, the formulas can provide estimates of the characteristic impedance of the conductors in

a conduit. The formulas for concentric or eccentric cylinders can also be used to estimate the characteristic impedance of a bundle of conductors in a conduit. The coaxial-cylinder formulas require an estimated effective radius for the wire bundle, but since the characteristic impedance varies as the logarithm of this radius, sizable error in the effective radius can be tolerated.

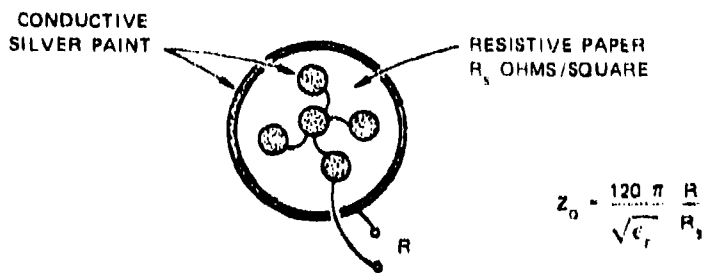
Simple experimental techniques can be used to determine the characteristic impedance of irregular geometries of uniform cross section. Resistance paper or a shallow electrolytic tank can be used as illustrated in Figure 5-8(a) to measure the resistance between the conductors (all in parallel) and the conduit. This resistance is related to the characteristic impedance of a transmission line having geometrically similar cross section by

$$Z_0 = \eta \frac{R}{R_s} = \frac{120\pi}{\sqrt{\epsilon}} \frac{R}{R_s} \quad (5-13)$$

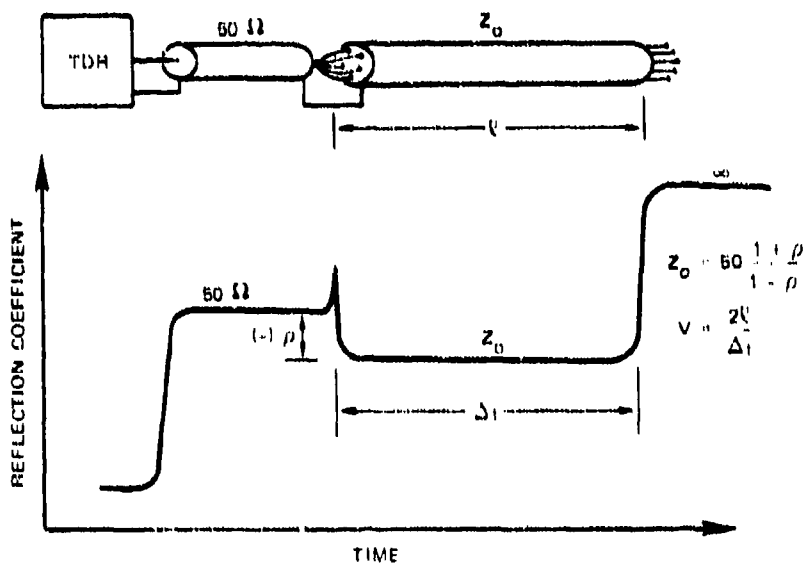
where R is the measured resistance between the simulated conductors and the conduit, and R_s is the resistance per square of the resistance paper or electrolyte. The resistance per square is the resistance (for uniform current) of the medium (paper or electrolyte) one unit wide and one unit long.

The time-domain reflectometer (TDR) is very useful for determining characteristic impedance and velocity of propagation *in situ* (with the 60-Hz power off). The TDR is essentially a fast-rising pulse source and an oscilloscope so arranged that the waveform of the voltage at the terminals of the pulse source can be observed as the reflections from discontinuities arrive. The oscilloscope is normally calibrated in units of reflection coefficient relative to a base impedance such as 50 ohms. From the TDR oscillogram (see Figure 5-8(b)), therefore, the reflection coefficient ρ and the round-trip propagation time along the conduit circuit can be determined. For a base impedance of 50 ohms, the characteristic impedance of the unknown transmission line is

$$Z_0 = 50 \frac{1 + \rho}{1 - \rho} \quad (5-14)$$



(a) RESISTANCE-PAPER METHOD



(b) TDR METHOD

Figure 5-8 TECHNIQUES FOR DETERMINING THE CHARACTERISTIC IMPEDANCE EXPERIMENTALLY

where ρ is the reflection coefficient obtained by attaching the unknown line to the end of the 50-ohm line. The velocity of propagation is

$$v = \frac{2L}{\Delta t} \quad (5-15)$$

where L is the length of the unknown line and Δt is the time elapsed between the arrival of

the reflections from the beginning and the end of the unknown line. The TDR method has the important advantage that it can measure the characteristic impedance and velocity of propagation regardless of how complex the geometry and the dielectric between the conductors and the conduit are.

5.2.2.2 Propagation Factor and Length

As indicated above, the velocity of propagation can be obtained from TDR measurements when the length of the conduit circuit is known. Since the attenuation of the short conduit circuits ordinarily found in low-voltage wiring is usually negligible, the propagation factor for these circuits is

$$\gamma \approx j\beta = j \frac{\omega}{v} . \quad (5-16)$$

When the conduit is buried or embedded in concrete, it may be difficult to determine its length. Then the TDR trace can give

$$\Delta t = \frac{2l}{v} \quad (5-17)$$

but a separate measurement is required to obtain γ and v explicitly. This measurement can be made on a similar circuit of known length, such as on one section of conduit with the same number and size of wires. Then the velocity of propagation is determined from TDR measurements on the sample of known length, and the length of the unknown circuit can be determined from Eq. (5-17) above.

5.2.2.3 Stray Inductance of Leads

The stray inductance of wiring in circuit-breaker cabinets, junction boxes, etc., can be estimated from the formulas for the inductance per unit length of a wire over a ground plane. The inductance per unit length of a wire over a ground plane is

$$L = \frac{\mu_0}{2\pi} \cosh^{-1} \frac{h}{a} \approx \frac{\mu_0}{2\pi} \log \frac{2h}{a} \quad \left(\frac{h}{a} \gg 1 \right) \quad (6-18)$$

where h is the height of the wire above the ground plane and a is the radius of the wire. A plot of the inductance per unit length as a function of the height-to-radius ratio h/a is shown in Figure 6-9. For h/a between 10 and 100, the inductance is between 0.5 and 1.0 $\mu\text{H}/\text{m}$. A convenient rule of thumb, allowing for some mutual coupling in coiled or folded wires in junction boxes, is 1 $\mu\text{H}/\text{m}$ for lead inductance.

5.2.2.4 Load Impedances

The load impedances represented by appliances and equipment are usually quite difficult to specify accurately over the spectrum of frequencies contained in the EMP. This difficulty arises from the fact that these loads are ordinarily specified and designed for their

60-Hz, three-phase or single-phase properties, whereas their common-mode, high-frequency properties are of primary interest in the EMP analysis. Therefore, an accurate determination of the high-frequency impedances of such equipment can be obtained only by direct measurement. The purpose of this section is to discuss the general nature of the common-mode impedances of selected loads and to present some examples of the impedances of three-phase and single-phase motors.

In general, the common-mode impedances of most electrical equipment can be represented as

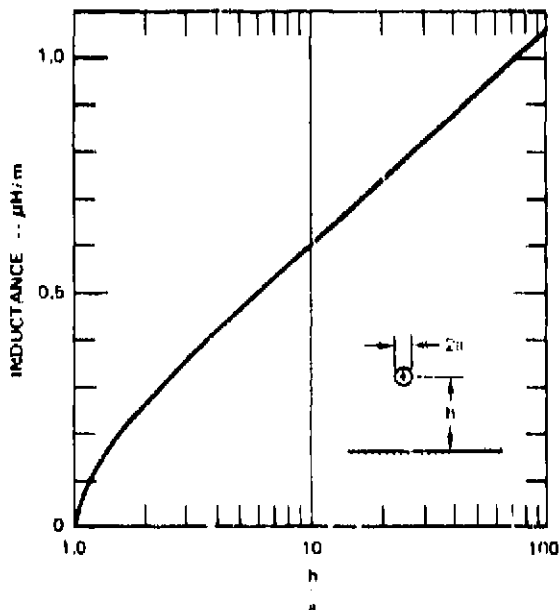


Figure 6-9 INDUCTANCE PER UNIT LENGTH OF A WIRE OVER A GROUND PLANE

transmission-line segments. If the total length of conductor protruding from the conduit is short and it is ungrounded, as is the case for an incandescent lamp mounted on an outlet box, the load will be capacitive. For such loads, the impedance is

$$Z_L \approx \frac{cZ_0}{j\omega\ell} \approx \frac{1}{j\omega Cl} \quad (\text{short, ungrounded}) \quad (5-19)$$

where ℓ is the length of the protruding conductor, Z_0 is its characteristic impedance, C is its capacitance per unit length, and c is the speed of light. If the length of the conductor is short and it is grounded, the impedance is

$$Z_L \approx j\omega\ell \frac{Z_0}{c} \approx j\omega L\ell \quad (\text{short, grounded}) \quad (5-20)$$

where L is the inductance per unit length of the protruding conductor.

If the protruding conductor is long and ungrounded, its input impedance is

$$Z_L \approx -jZ_0 \cot k\ell \quad (\text{long, ungrounded}) \quad (5-21)$$

where $k = \omega/c$, and if the conductor is long and grounded at its end, its input impedance is

$$Z_L \approx jZ_0 \tan k\ell \quad (\text{long, grounded}) \quad (5-22)$$

The inductance and capacitance per unit length, and the characteristic impedance for parallel-wire, conic, coaxial, and parallel-plate transmission-line configurations are plotted in

Figure 5-10. These data, the inductance data of Figure 5-9, and the formulas above are useful for estimating the common load impedances of power equipment such as lamps or heaters that have relatively small exposed conductors.

Because circuit elements with time constants shorter than 10 ns will probably have no effect on the response of the low-voltage system, we may neglect the inductance or capacitance of protruding conductors shorter than

$$l \approx \frac{10^{-8}c}{2} = 1.5 \text{ m (ungrounded)}$$

(5-23)

$$\approx \frac{10^{-8}Z_0}{L} \text{ (grounded)}$$

where Z_0 is the characteristic impedance of the conduit circuit, and L is the inductance per

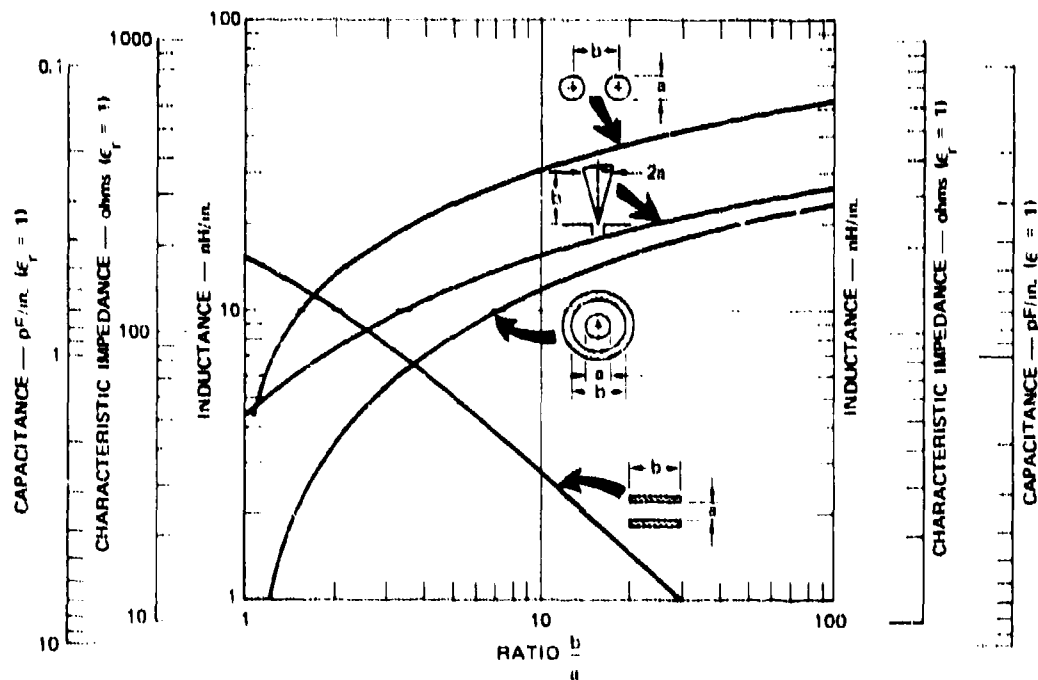


Figure 5-10 CHARACTERISTIC IMPEDANCE, AND CAPACITANCE AND INDUCTANCE PER INCH

unit length of the exposed conductor. Since Z_0 is typically of the order of 30 ohms for the conduit, and L is of the order of 20 nH/inch for openly protruding conductors, grounded conductors shorter than about 15 inches can be treated as short circuits. Ungrounded conductors shorter than 5 ft (10 μ s round-trip transit time) can be treated as open circuits. (The round-trip transit time, rather than the lumped capacitance, determines the "time constant" of ungrounded conductors unless the capacitance per unit length exceeds about 5 pF/inch.)

Three-phase and single-phase motors used to power pumps, blowers, etc., often represent the loads on conduit circuits. Measurements have been made of the line-to-case impedance and line-to-neutral impedance of two three-phase induction motors. The impedances between the three-phase conductors and the motor frame have been measured for both the 7-1/2-hp and the 1/2-hp three-phase motors. This impedance is shown in Figure 5-11 and 5-12. It is apparent that this impedance behaves as a capacitance at frequencies up to almost 10 MHz, although the value of the capacitance changes near 100 kHz. At 10 kHz, the capacitance of all three windings to the case is 0.0051 μ F for the 7-1/2-hp motor and 0.0013 μ F for

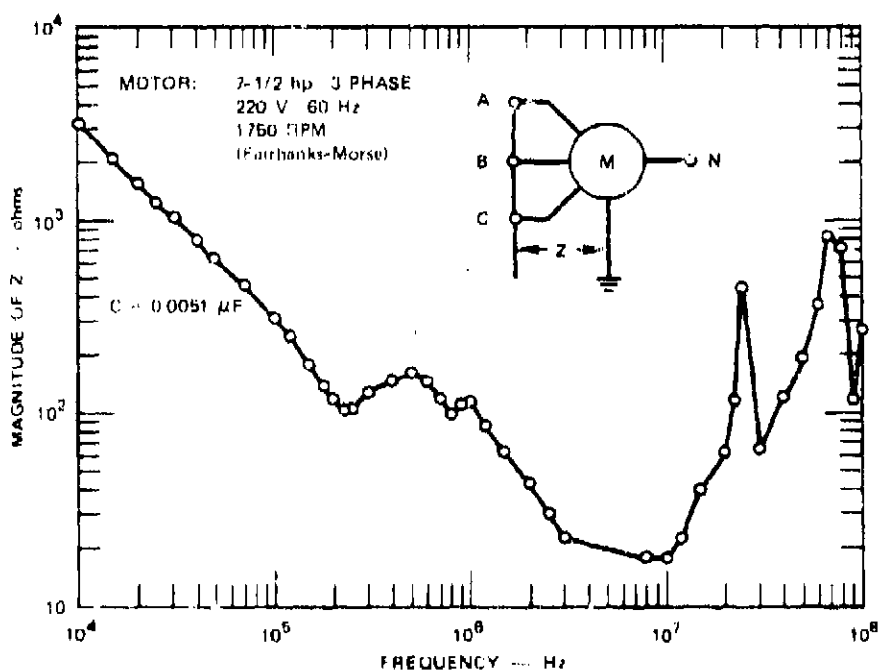


Figure 5-11 LINE-TO CASE IMPEDANCE OF 7-1/2-hp INDUCTION-MOTOR WINDING

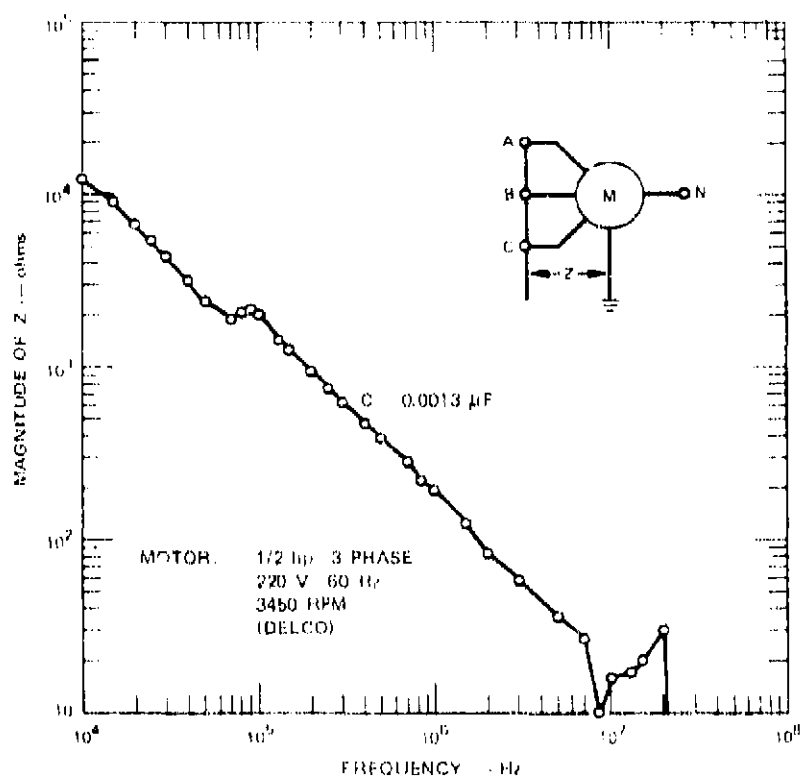


Figure 5-12 LINE-TO-CASE IMPEDANCE OF 1/2-hp INDUCTION-MOTOR WINDING

the 1/2-hp motor. Both motors have subsidiary resonances in the vicinity of 500 kHz and primary resonances near 10 MHz. The winding-to-case impedance has also been measured on a single-phase motor with the terminals connected together. This impedance is shown in Figure 5-13. As with the three-phase motors, this impedance behaves as a capacitance up to about 10 MHz, with some weak resonances along the way. At 10 kHz, the winding-to-case capacitance is $0.0014 \mu\text{F}$. From these data it appears that the winding-to-case capacitance, for example, increases with motor size, and the winding-to-case impedance can be represented fairly well by a lumped capacitance at frequencies up to 10 MHz. It should be pointed out that the 7-1/2-hp motor and the 1/2-hp three-phase motor are wound for different speeds. Interpretation of these data should also take into account motor speed as well as power and voltage rating, since different speed ratings imply a different way of combining windings that may affect the winding-to-case capacitance. It should also be pointed out that the measurements were all made with the windings unenergized and the rotors stationary. This condition

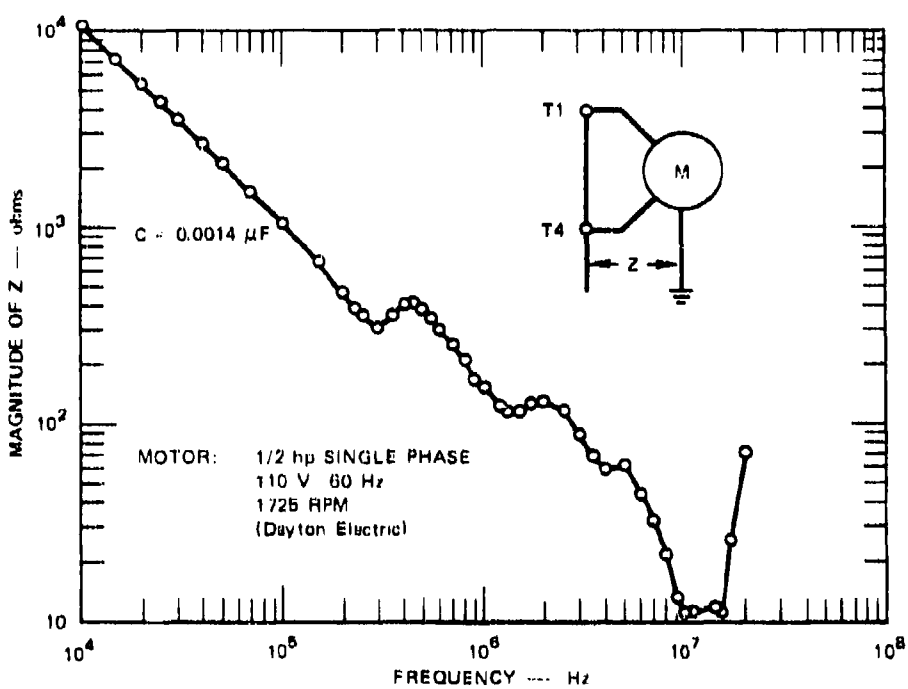


Figure 5-13 LINE-TO-CASE IMPEDANCE OF 1/2-hp SINGLE-PHASE CAPACITOR-START MOTOR WINDING

of measurement is no concern for the 3-phase induction motors, but for the single-phase capacitor-start motor it means that the measurements were made with the starting winding connected, and that the results may be different on a running motor with the starting winding disengaged.

5.2.3 MULTICONDUCTOR-TRANSMISSION-LINE ANALYSIS

A potentially more exact analysis of power conductors in conduits than the common-mode analysis described above treats the conductors as a multiconductor transmission line.²⁻⁴ Each conductor is then coupled to every other conductor in the conduit through mutual capacitances and mutual inductances, and loads at the ends of the conductors become networks of elements, rather than single elements as assumed in the common-mode model. Transmission-line voltages, currents, impedances, and admittances are represented by matrices in the multiconductor-transmission-line analysis. Evaluation of the voltages and currents

at points in the low-voltage wiring is very difficult if there are more than two conductors in each conduit. Because of the complexity of the multiconductor-transmission-line analysis, all applications of this method to power wiring have involved developing computer programs for performing the matrix manipulation and numerical evaluations.

Although the multiconductor-transmission-line analysis has the potential for providing more accurate results and for providing voltages between conductors as well as common-mode voltages, this potential can only be realized if the properties of the power circuits can be accurately specified. In practice, wiring fished through conduit meanders somewhat randomly along the circuit, so that the cross section of multiconductor circuit is not uniform along its length. Furthermore, to specify the load impedance of simple devices such as three-phase induction motors, a large number of measurements over a wide range of frequencies are required. It is questionable, therefore, that sufficient increase in accuracy can be achieved to warrant the large increase in complexity (or effort) required to perform the multiconductor-transmission-line analysis. Since power-system analyses are usually performed primarily to determine peak voltages that might damage insulation or components and to determine the type and quality of protection required for sensitive equipment, a very rigorous analysis is seldom required.

A less complex version of the multiconductor-transmission-line analysis is sometimes used. Because the neutral of a three-phase system or the center tap of a 120/240-V single-phase system is often grounded at the load as well as at the power ground near the service entrance, these conductors may behave quite differently from the ungrounded "line" conductors. Thus if the neutral or ground conductors are treated as one conductor and all the "line" conductors in common are treated as a separate conductor, the multiconductor circuits can be analyzed as three-conductor (two inner conductors and one conduit) transmission lines. This method of analysis offers some improvement over the common-mode analysis, yet because each conduit is presumed to contain only two conductors, it is much simpler than the complete multiconductor-transmission-line analysis. Some difficulty is encountered, however, where conductors from one conduit are separated and fed into two or more conduits, because such a branch does not constitute a solid junction of three-conductor transmission lines.

5.3 CITED REFERENCES

1. *National Electrical Code 1971*, (National Fire Protection Association, Boston, Massachusetts, 1971).
2. E. F. Vance and S. Dairiki, "Analysis of Coupling to the Commercial Power System," Technical Report AFWL-TR-72-21, Contract F29601-69-C-0127, Air Force Weapons Laboratory, Kirtland Air Force Base, New Mexico (August 1972).
3. S. Frankel, "The Differential Equations of a Transmission Line Excited by an Impressed Field with Axial Magnetic Component," Interaction Note 125, Air Force Weapons Laboratory, Kirtland Air Force Base, New Mexico (September 1972, unpublished report).
4. S. Frankel, "TEM Response of a Multiwire Transmission Line (Cable) to an Externally Impressed Electromagnetic Field: Recipe for Analysis," Interaction Note 130, Air Force Weapons Laboratory, Kirtland Air Force Base, New Mexico (February 1972, unpublished report).

Chapter Six

GROUNDING SYSTEMS

6.1 GENERAL DESCRIPTION OF GROUNDING SYSTEMS

6.1.1 POWER-SYSTEM GROUNDING

Grounding systems, although seemingly simple, are in fact quite complex and often controversial. The grounding system designed by the utility must be compatible with the lightning protection system, the protective relaying system, the system insulation, and the grounding systems of other utilities with which it is intertled.^{1, 2} The power grounding system required of the consumer by national or local electrical codes is specified primarily for personnel and property protection. The consumer's equipment grounding system may be designed primarily for interference reduction so that objectional crosstalk between subsystems is minimized. Therefore, there are at least three ground systems serving essentially different functions within the utility's and consumer's combined system.

Grounding in the transmission and distribution systems is necessary to prevent the conductors from "floating" to high potentials and inducing insulation failure. High potentials on floating systems can be generated by lightning, transients associated with switching or faults, leakage from a high-voltage system to a lower-voltage system, or from static electrification during snow, sleet, or dust storms. A system ground also facilitates fault detection and relaying because a fault on any phase can be detected and localized more readily if the grounding system is properly designed. A typical neutral grounding system for a three-phase transmission system is illustrated in Figure 6-1. The generators feeding the transmission bus are either ungrounded, or grounded through sufficient impedance that fault current through the generator is limited to a safe level. The transmission line is grounded at the neutral of the wye-connected transformer secondary, as is the subtransmission line and the distribution line. Transmission and subtransmission are normally over three-wire lines, while distribution lines serving both three-phase and single-phase loads are usually four-wire lines.

Not shown in Figure 6-1 is the overhead ground-wire system used for lightning protection on transmission and subtransmission lines. The overhead ground wires are usually grounded at each pole or tower, but they are not connected to the neutral except through the soil. The overhead ground wires thus form a separate ground system, essentially independent of the three-phase neutral.

At the consumer end of the distribution system the distribution transformers may be connected in any of the four possible delta and wye combinations shown in Figure 6-2. When the primary side is wye-connected and a four-wire distribution line is used, however, the neutral line is usually not connected to the neutral of the transformer bank. This is because a phase-to-ground fault would then place line-to-line voltage across the transformers on the unfaulted phases, with the consequent overvoltage and probable damage to the transformer and consumer equipment. To avoid this situation, the neutral of the distribution line is sometimes grounded one pole back from the transformers and the transformer neutral is grounded at the transformer pole so that the soil resistance limits the neutral current flow. However, this method has the disadvantage that large voltage gradients in the soil near the consumer's facility may accompany a phase-to-ground fault.

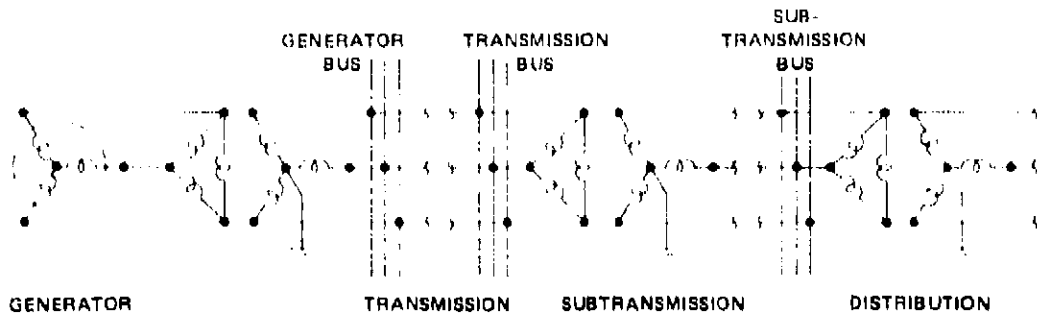
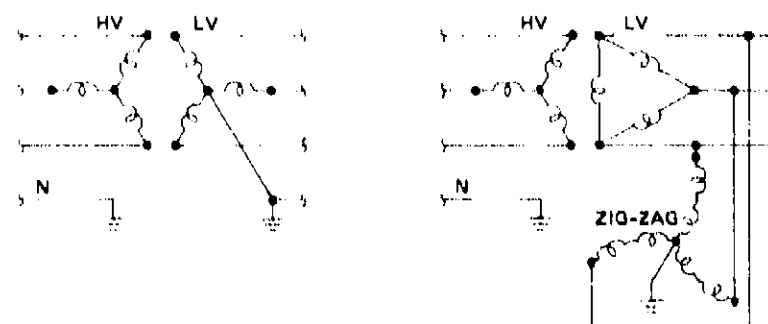
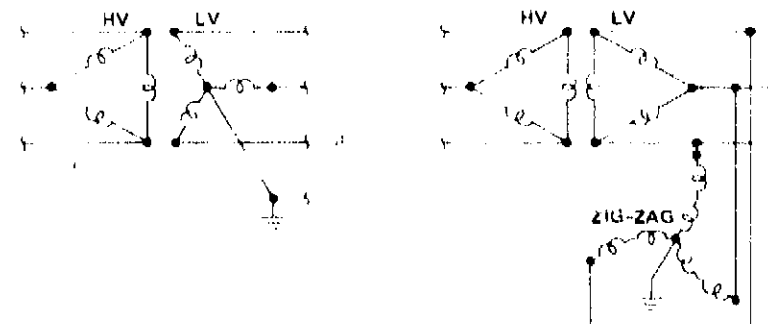


Figure 8-1 TYPICAL GROUNDING ARRANGEMENT FOR A TRANSMISSION SYSTEM



(a) WYE-WYE

(b) WYE-DELTA



(a) **DELTA-WYE**

(d) **DELTA-DELTA**

Figure 8-2 THREE-PHASE DISTRIBUTION TRANSFORMER CONNECTIONS

The delta-connected secondary shown in Figures 6-2(b) and 6-2(d) may be provided with a grounded neutral through a zig-zag transformer or some other means to meet the electrical codes. The delta-connected secondary is not uncommon, however, where 460 V (or higher) 3-phase service is required in addition to 120/240-V single-phase service.

6.1.2 GROUNDING LOW-VOLTAGE WIRING

The National Electrical Code requires all 4-wire, three phase circuits of 480 V or less to be grounded if the neutral is used as a circuit conductor.³ In general, if ground on any ac circuit can be achieved so that the voltage of the ungrounded conductors does not exceed 150 V the system must be grounded. Thus, one side of 120-V single-phase systems and the center tap of 120/240-V single-phase systems are grounded. A single-point ground is recommended (but not required), with the ground electrode being one of the following:

- (1) A water pipe or well casing at least 10 ft long
- (2) The metal frame of a building if effectively grounded
- (3) Gas piping (where permitted)
- (4) Other underground piping, tanks, etc.
- (5) Concrete-encased reinforcing bar of underground footings
- (6) Specially installed rod, pipe, or plate ground electrodes where resistance to ground does not exceed 25 ohms.

All metal conduit (rigid or flexible), raceways, gutters, metal equipment enclosures, and boxes must be bonded for electrical continuity. Although the national code establishes these bonding and grounding requirements, there are few quality-control checks to ensure that the requirements are met, and the requirements are often so vague as to be subject to a wide range of interpretations. The primary purpose of these requirements is to prevent personnel hazards and equipment damage that might result if ungrounded equipment cabinets

or outlet boxes inadvertently became energized; as they are practiced, the code requirements appear to be satisfactory for this purpose.

6.1.3 GROUNDING ELECTRONIC EQUIPMENT

If the consumer's facility contains extensive electronic equipment (e.g., a communications center or computer facility) additional grounding systems may be necessary. In these facilities it is not uncommon to find two to four ground buses that are interconnected only at one facility ground point (such as a well casing or a pipe driven expressly for grounding purposes).⁴ This grounding system is required to permit substantially balanced circuits to be used and segregated according to function served, so that mutual interference between ac power, dc power, and low-level-signal circuits can be reduced to a tolerable level. A separate tree system for each circuit class is usually claimed, although in practice there are usually some closed loops in the branches of the ground trees. The principal trunks and branches of a ground system for a telephone electronic switching center that contains four ground systems in addition to the ac power ground are illustrated in Figure 6-3.

6.2 EVOLUTION OF A FACILITY GROUNDING SYSTEM

As is pointed out in Section 6.1 above, the grounds for the transmission system, the building wiring, and the electronic equipment in the building are for quite different purposes. In general, the reasons for grounding are varied, and it would be presumptuous to attempt to specify grounding procedures without first establishing the reasons for grounding and the goals that the grounding system should achieve. These reasons and goals are usually based on system functional, safety, and RF interference considerations and are inherently prescribed by the system specifications. When the EMP is included as a consideration in the ground-system design, at least one more goal has been added (EMP hardness), but the reasons for grounding may remain unchanged. It is therefore prudent for the designer to avoid becoming so engrossed in the method of grounding the system that he forgets why it is grounded.

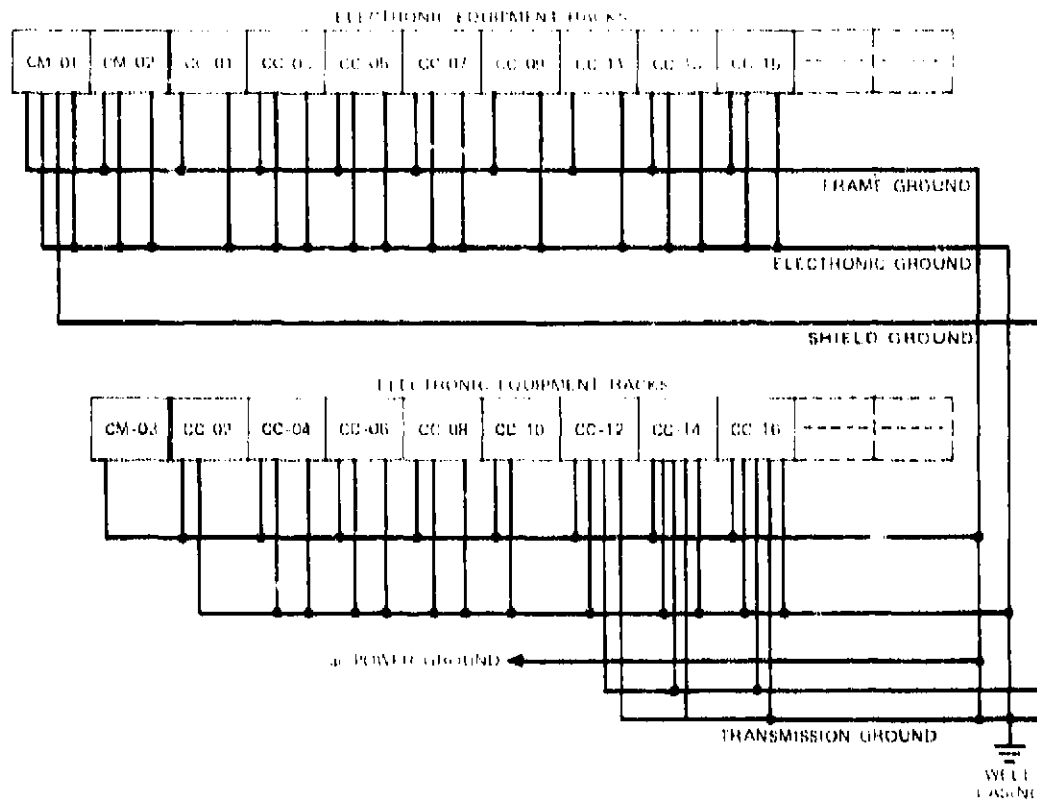
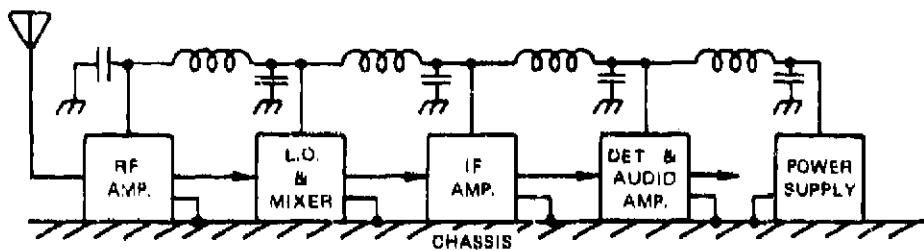
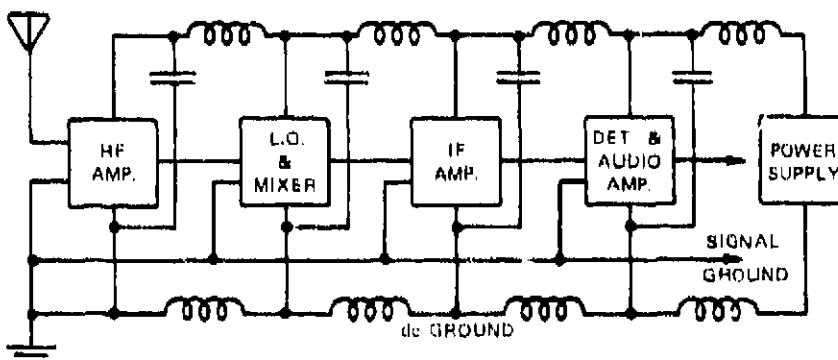


Figure 6-3 GROUNDING SYSTEM FOR A TELEPHONE SWITCHING CENTER

The basic reason for providing a "ground" in electronic equipment is to establish a firm reference potential against which signal and supply voltages are measured (or established). For small systems such as the home radio receiver illustrated in Figure 6-4(a), a metal chassis can be used as the reference even though it may not be "grounded" (there is no need to ground the chassis if it is so encased that there is no possibility of a shock hazard). The chassis potential is the same (almost) throughout the set, so that the power supply, the RF amplifiers, the mixer, the IF and audio amplifiers, etc. all share a common reference electrode and only a signal-carrying conductor and a power-supply conductor are needed to interconnect these stages. If the chassis were dielectric instead of metal, it might be necessary to provide two wires between stages for the signal and two for the dc power as illustrated in Figure 6-4(b). If one of the wires is used as a common reference for both power and signal,



(a) METAL CHASSIS AS GROUND FOR POWER SUPPLY AND RECEIVER CIRCUITS



(b) SEPARATE GROUNDS FOR SIGNAL AND dc POWER

Figure 6-4 EXAMPLES OF GROUNDS FOR A SIMPLE RADIO RECEIVER

fluctuations in power-supply current might induce $L \frac{di}{dt}$ voltages of objectional proportions in the "common" wire. Thus, the system has evolved into one requiring two references—one for signal and one for dc power. These two reference conductors must be connected together at one point, but the system may not operate if they are common throughout the system.

As a final evolution of the simple radio receiver, suppose the RF, IF, audio, and power-supply sections were built and packaged as separate modules that were physically separated and interconnected with cables as illustrated in Figure 6-5. Because the signal levels in the receiver are quite small, shielded interconnecting cables would be required to prevent ambient noise picked up on the interconnecting cables from degrading the performance of the receiver, and the modules would have to be shielded to prevent the interference on the cable shields from coupling to the signal conductors. Now a third reference system,

the shield, has been created. It must be connected to the signal and power-supply reference conductors to prevent excessive potential differences between the shield and the internal circuits, but if the shield and the other grounds are connected together at more than one

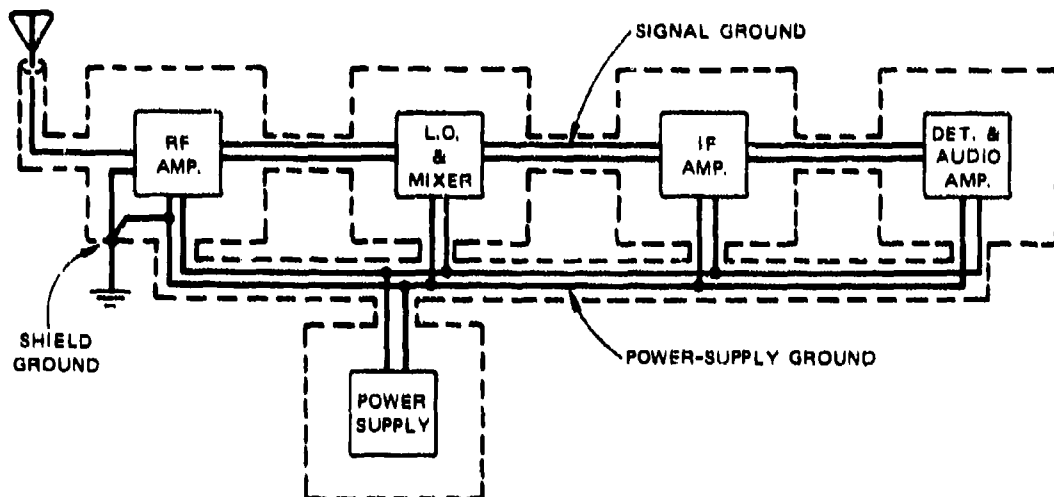


Figure 6-5 SIMPLE RECEIVER SEPARATED INTO MODULES INTERCONNECTED BY SHIELDED CABLES

point, voltage drops along the shield may induce malfunction of the receiver. In addition, because the shield is presumably exposed to operating personnel, it must be grounded to earth or building structure to prevent shock hazards. The originally simple receiver is now a complex, interconnected system with three "ground" systems.

The simple radio receiver, made complex by regressive evolution, provides an excellent example of the advantages of the popular single-point, tree ground system illustrated in Figure 6-6. The entire ground system is grounded at one point, and each subsidiary ground branches out from this trunk attached to the single ground point. If any of the branches had been connected to each other at more than one point there would be a reasonable doubt that the system could achieve the desired performance (even in the absence of extraneous influences such as the EMP). However, if we examine the shield system of Figure 6-5 carefully we observe a situation that poses a paradox for the tree concept of grounding. Although

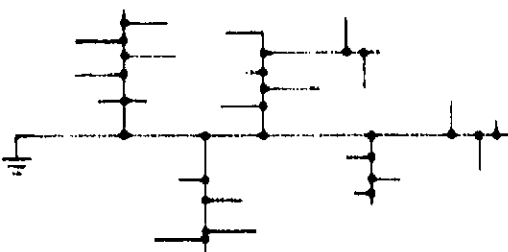
the signal and power-supply grounds follow the single-point, tree concept, the shield system does not, because there are loops between the shielded cables interconnecting each pair of modules. Thus, the shield system is a mesh, rather than a tree.

While it would be easy to redesign the simple radio receiver of Figure 6-5 to eliminate the loops in the shield system, in more complicated systems it is sometimes virtually impossible to eliminate all loops in all of the ground systems. Consider, for example,

a large system with a feedback loop such that the output of one module is operated on by a second module and fed back to an upstream module interconnected with the first. In this case it is likely that the shield, signal common, and power-system common will all contain loops. The problem can be even further complicated if the module enclosures are installed in a steel building so that each enclosure is grounded through its mounting

Figure 6-6 SINGLE-POINT TREE GROUND SYSTEM

hardware as well as through the shield system. The latter problem is illustrated in Figure 6-7(a) where two modules are interconnected through the cable shield and the mounting structure. Even if the cabinets are insulated from the metal floor, the capacitance between the cabinets and the floor would close the loop, as is suggested by the dashed capacitances in Figure 6-7(a). Opening the loop by breaking the shield, as indicated in Figure 6-7(b), does not eliminate the problem; it merely changes its form. Whereas the short-circuit current induced in the loop of Figure 6-7(a) flows in the cable shield, the open-circuit voltage induced in the loop can drive the internal circuits when the shield is broken as in Figure 6-7(b).



6.3 PRINCIPLES OF GROUNDING

6.3.1 SINGLE-POINT VS. DISTRIBUTED GROUND

The examples in the preceding section illustrate that implementing the single-point tree ground concept in systems with many racks mounted on a common metal structure or in systems with complex feedback loops may be very difficult or even undesirable. In this

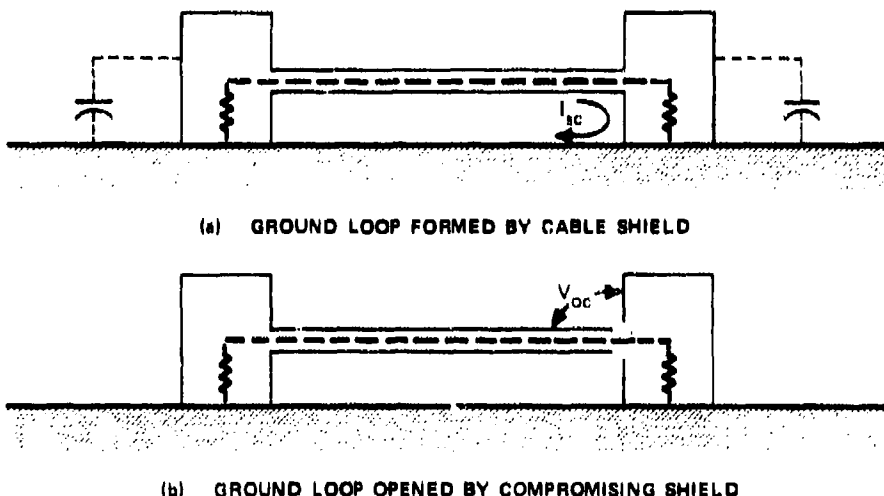


Figure 6-7 LOOP FORMED BY CABLE SHIELDS AND METAL FLOOR OR WALLS

section, an attempt will be made to evaluate the relative merits of the tree ground system and some violations of the tree ground. For this discussion, two aspects of the grounding systems will be considered: how it affects normal system performance, and how it affects coupling to the system from external effects such as the EMP.

Consider a single-point ground consisting of only the ground point and trunk as illustrated in Figure 6-8. The ground point is assumed to be a point on a metal plane, such as the steel liner of a shielded building, and the trunk is of length ℓ and of height h above the ground plane. If this ground trunk is illuminated with a plane wave, incident at an elevation angle ψ to the ground plane and an azimuth angle φ to the axis of the wire, the open-circuit voltage developed between the open end of the wire and the ground plane can be

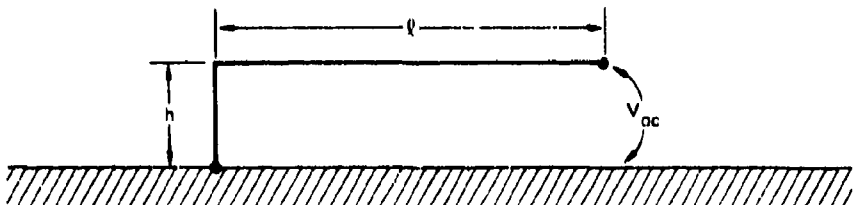


Figure 6-8 SINGLE-POINT GROUND AND ONE TRUNK

calculated from Eq. (2-18) with $\rho\ell = -1$ and $r_g \approx 0$. The impedance looking into the open end of the wire is

$$Z(0) = jZ_0 \tan \beta l \quad (6-1)$$

If perfect conductors are assumed and $l \gg h$,

At frequencies such that $l \ll c/f$, the impedance and open-circuit voltage expressions reduce to

$$V_{oc} \approx j\omega 2\mu_0 H_0 h l \left\{ \frac{\cos \varphi}{\sin \varphi \sin \psi} \right\} \quad (6-2)$$

$$Z(0) \approx j\omega \frac{\mu_0 l}{2\pi} \cosh^{-1} \frac{h}{a} \quad (6-3)$$

where H_0 is the incident-magnetic-field intensity, μ_0 is the permeability of free space, a is the radius of the wire, and the upper and lower trigonometric functions apply to vertical and horizontal polarization of the incident electric field, respectively. The voltage is just that induced in a loop of area hl by the magnetic flux $2\mu_0 H_0 \times$ (angular function) linking it. For a 1-V/m plane, vertically polarized wave incident at $\varphi = 0$, the open-circuit voltage induced at 1 MHz at the end of a conductor 2 cm in diameter, 2 cm high, and 3 m long is 2.5 mV, and its impedance is $j5$ ohms. If the right end of the wire were connected to the ground plane to form a closed loop, a circulating current of 0.5 mA would flow in the loop at 1 MHz. Thus, from the standpoint of induced effects, the question is, which is less desirable, the 2.5-mV potential difference between the ground tree and structural ground or the 0.5-mA current circulating in the ground loop?

The answer to this question will depend on the system requirements. If the ground tree is that formed by the interconnecting cable shields, the circulating current will usually be less objectionable than the potential difference because the cable shields eliminate much of the effect of this current on the conductors inside the shield. If the ground tree is the signal common, however, the same potential difference will be induced in the signal lead as is induced in the common lead, so that the potential difference between the signal and common leads is negligible. Unless the terminating impedance is balanced and the terminal circuits have adequate common-mode rejection, however, part of the common-mode induced voltage may be converted to differential voltage.

6.3.2 GROUND IMPEDANCE

From the standpoint of minimizing the impedance to ground of the equipment at the right end of the ground trunk shown in Figure 6-8, a direct connection to the ground plane is much superior. The impedance between two studs 2 cm in diameter welded to the ground plane 3 m apart is shown in Figure 6-9 for steel, aluminum, and copper ground planes that are thick compared to a skin depth. For comparison, the impedance of a ground cable 2 cm in diameter, 2 cm high, and 3 m long is also shown. The impedance of the cable is 10 to 100 times greater than that of the ground plane in the megahertz frequency range shown (except at the half-wave resonance frequencies for the cable). Thus if the objective of the ground is to firmly connect chassis or equipment frames to a low-impedance common bus, connecting these parts firmly to the ground plane by the shortest path possible provides the best solution.

In general the impedance of a wire ground connection varies widely with frequency. At low frequencies, such that the ground lead inductance is small compared to its internal impedance, the impedance of the ground is determined by the internal impedance of the lead and/or ground plane plus any contact resistance (in fact, the contact or junction resistance is often larger than the resistance of the metal). The low-frequency resistance applies for

$$f < \frac{R}{2\pi L} \quad (6-4)$$

where R is the resistance of the metal in the ground conductor and L is its inductance.

At high frequencies, the ground impedance is dominated by the inductance of the ground lead, which can be estimated from Figure 5-10 or from

$$L = \frac{Z_0 l}{c} \quad \left(\frac{R}{2\pi L} < f < \frac{c}{4l} \right) \quad (6-5)$$

where l is the length of the ground lead, Z_0 is its characteristic impedance as a transmission line, and c is the speed of light (3×10^8 m/s). Since wires over ground planes have characteristic impedances of a few hundred ohms, ground lead inductances are often about $1 \mu\text{H}$ per meter of length. The upper limit on the lumped-inductance behavior of the ground lead impedance indicated above is the frequency at which the length of the ground lead approaches a quarter wavelength. For high frequencies such that $f \gg c/4l$, the impedance of the ground lead changes radically with frequency, alternating between a very large value and a very small value as is illustrated by the cable impedance in Figure 6-9 for frequencies above 10 MHz. The impedance of the ground lead is then

$$Z_g = jZ_0 \tan \left(2\pi f \frac{l}{c} \right) \quad (6-6)$$

for perfect conductors, which varies between $-\infty$ and $+\infty$ as the frequency increases.

6.3.3 TREE GROUND

Suppose that two branches are added to the ground wire of Figure 6-8 so that we obtain a ground wire with a trunk and two branches as shown in Figure 6-10. Now if this ground tree is the signal ground for the system, and signal return currents I_1 and I_2 are flowing to the single ground point, their sum $I_1 + I_2$ must flow through the single trunk. The voltage V_0 developed by these return currents is

$$V_0 = (I_1 + I_2) Z_c \quad (6-7)$$

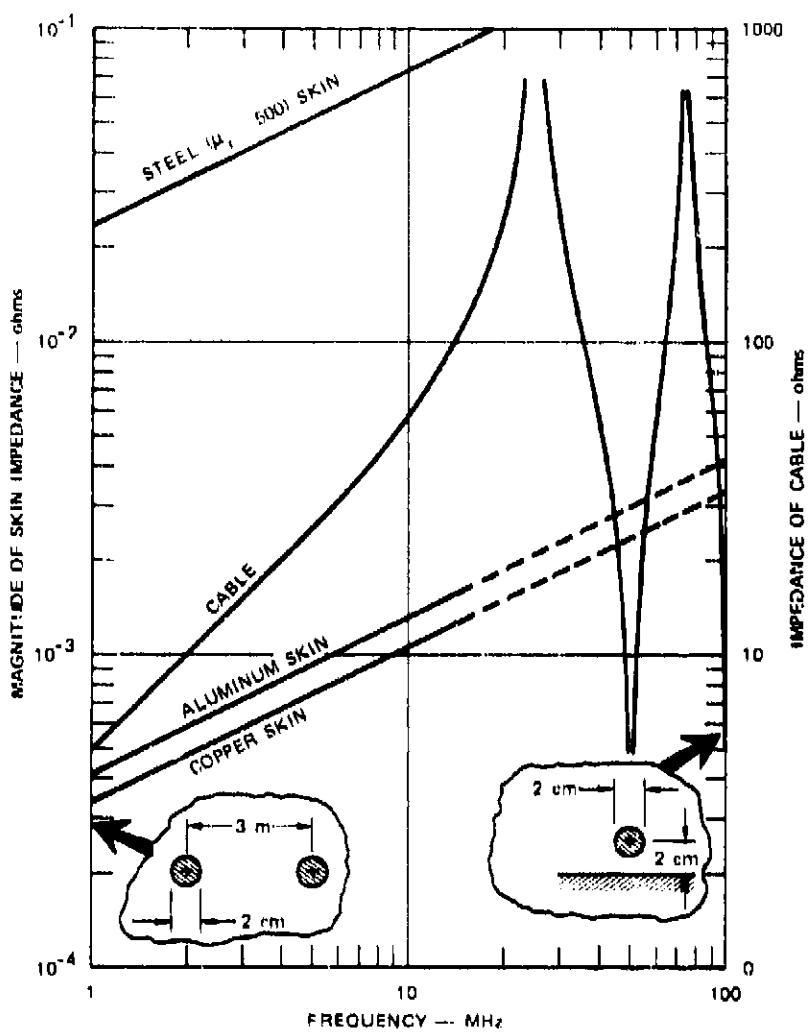


Figure 6-9 IMPEDANCE OF METAL GROUND PLANES (left scale) AND OF A GROUND CABLE (right scale)

where Z_c is the impedance of the line between the junction and the ground point. In addition, the voltages V_1 and V_2 between the right ends of the tree branches and the ground plane are

$$V_1 = I_1 (Z_1 + Z_c) + I_2 Z_c \quad (3-8)$$

$$V_2 = I_2 (Z_2 + Z_c) + I_1 Z_c \quad (6-9)$$

so that the signal-ground voltage at the end of Line 2 depends on the return current I_1 . If the numerical values obtained earlier are used, the impedance of the trunk and each branch is 5 ohms at 1 MHz, so that 1 A of return current in either branch will produce 5 V in the other branch, and vice versa. Thus, the common trunk has introduced mutual coupling between the subsystem at the end of Branch 1 and the one at the end of Branch 2. Such mutual coupling may be undesirable (or intolerable) from the point of view of system performance.

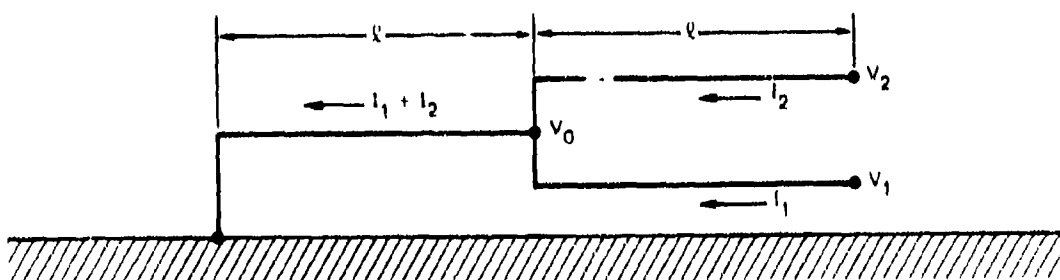


Figure 6-10 TREE WITH TRUNK AND TWO BRANCHES

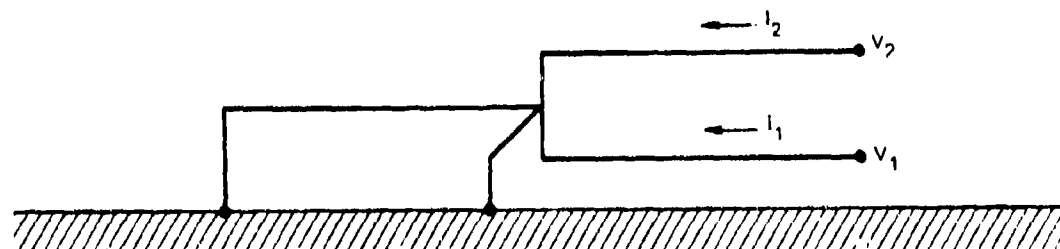


Figure 6-11 JUNCTION GROUNDED TO REDUCE COUPLING THROUGH TRUNK

6.3.4 DISTRIBUTED GROUND

The mutual coupling in the trunk can be greatly reduced by grounding the junction to the structure as illustrated in Figure 6-11. If the junction grounding lead is of length h , and radius a , its impedance will be

$$Z_n \approx j\omega \frac{\mu_0 h}{2\pi} \log \frac{2h}{a} \quad (6-10)$$

which is about h/l times the impedance of the trunk of length l ($l \gg h > a$). This reduction of coupling through the trunk has been achieved at the expense of forming a "ground loop" containing the trunk. This loop may be quite acceptable for many systems; however, it may be objectionable under either of the following conditions:

- (1) Grounding the signal common merely forces a common-mode signal conversion to take place at the junction (for either the desired signal or the externally induced signal).
- (2) The loop currents in the trunk can induce significant signals in the branches (e.g., if the trunk and branch are in the same cable or bundle).

6.3.5 STAR GROUND

An alternative method of reducing the coupling between the branches caused by the common trunk is to eliminate the common trunk by forming a "star" ground with three spokes as illustrated in Figure 6-12. For the simple example being considered here, the single-point star ground system would be preferred for a signal ground system in which there is negligible coupling between the branches (spokes). It should be pointed out, however, that if the three branches are in the same cable, there is a possibility of coupling (crosstalk) among them from both mutual capacitance and mutual inductance between the conductors.

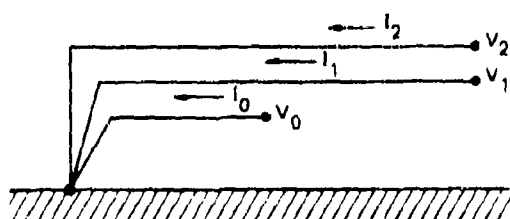


Figure 6-12 TRUNK ELIMINATED TO FORM A STAR GROUND

to the problem of potential differences between separate parts of the system (e.g., V_2 , V_1).

In practice, twisted pairs (or, if necessary, twisted shielded pairs) can be used for the signal and signal common leads to minimize cross-talk between the circuits in a common cable. For more complex systems involving feedback loops, the star ground with twisted pairs does not offer a solution

6.3.6 SOME GUIDELINES FOR SYSTEM DESIGN

It is evident from these discussions that one cannot *a priori* specify an optimum grounding system that is applicable to all systems or even to all parts of a given system. Each system and each part of a complex system has its own peculiar requirements based on functional and safety considerations. The design of the grounding system is therefore an integral part of the system design; it cannot, in general, be designed separately and added to the remainder of the system. Neither can rigid specification of a particular ground type ensure that the system will function properly or be immune to external interference such as the EMP. In the final analysis, it is the circuit (system) designer's responsibility to ensure that the system performs its intended function reliably and safely in the environments specified. The following guidelines are offered to assist the designer in achieving his objectives:

- (1) Use a tree or star ground system with twisted pairs and balanced signal circuits wherever practical.
- (2) When loops are formed by the interconnecting cables between separate modules, use balanced input and output stages with large common-mode rejection for the signal pairs.
- (3) Use separate ground returns for circuits that have large signal return currents or large rates of change of signal return currents to avoid mutual interference in common trunks or branches.

- (4) If the system is installed inside a welded steel (or other metal) shielded enclosure, bond all cabinets and equipment racks to the shield. The shields of shielded interconnecting cables should be connected to the cabinets (or racks) at both ends even if this forms a loop.
- (5) If the system is inside a closed shield, the walls of the shield should be used as the common ground for the system. The signal common should be connected to the inside of the shielded enclosure, and the ac power ground should be connected to the outside of the shielded enclosure (e.g., in an entry vault containing all other penetrations such as communications cables, antenna leads, etc.).
- (6) Avoid connecting the power neutral and external cable shields to the same point on the room shield that the signal ground is connected to. This will minimize the possibility of coupling large EMP-induced signals on these external conductors to the signal common through the ground-point impedance (see Items 3 and 5 above).
- (7) The building or site ground for the ac power (as required by the electrical code) should be connected to earth external to the facility shield. This earth connection may also serve as the external ground for the facility shield if the voltage drop between the shield and the earth is not a safety hazard or is not otherwise objectionable.
- (8) The use of balanced signal circuits with twisted pairs for interconnecting the subsystems and common-mode rejecting schemes (e.g., isolation transformers) on those circuits subject to externally induced signals, together with adequate overall shielding, can usually be implemented to minimize the effect of the EMP on the system.
- (9) The use of nonzero ground impedances (capacitances for high frequencies, inductances for low frequencies, and resistance for static-electricity bleeders) can often be used to advantage, particularly in view of the fact that zero-impedance grounds can be approached only at low frequencies. Often devices such as surge filters, chokes, and high-resistance bleeders can contribute to better overall system performance.

6.4 GROUNDING COUNTERPOISE

The use of a grounding counterpoise to reduce the surge impedance of the ground (earth) connection is a common practice for transmission lines and stations. For transmission lines, the counterpoise may be an array or grid of buried conductors fanning out from the tower footings, or it may be one or more continuous buried conductors under and parallel to the power conductors to which the towers are connected.^{1, 2, 5} For the transmission lines, a primary consideration is to obtain an impedance to ground sufficiently low that when lightning strikes the tower, the IZ drop at the tower footing does not exceed the flashover voltage of the line insulators. Another consideration is that gradients in the soil be minimized for safety reasons (particularly in populated areas) in the event of a line fault. Station grounds may be large buried grids, rings, or metal pipes. The station counterpoise serves the same general purpose as the transmission-line counterpoise as well as providing the reference for relaying and other protective and control systems.

Large communication stations such as telephone switching centers often use a counterpoise in the form of a well casing or a buried cable "ring" around the building, or both. Such a counterpoise serves a function similar to that served by the power-station ground; it provides a low-impedance ground reference for the communication equipment and it minimizes the gradients in the soil due to surges induced on the power and communication cable systems.

In an EMP environment, the counterpoise (or at least the common ground point) may have some effect in reducing potential differences between cable systems and power systems, but because of the lengths of the grounding conductors involved, this effect is usually secondary. In addition, the EMP induces gradients directly in the soil, so that the counterpoise does not reduce soil gradients in the same sense that it does for lightning surges; it merely distorts the gradients induced by the EMP. Finally, because the attenuation of currents conducted by buried conductors is very large at high frequencies, only a few meters of the counterpoise may be effective in grounding the system in the high-frequency part of the EMP spectrum. The attenuation constant α is

$$\alpha \approx \sqrt{\pi f \mu_0 \sigma} \quad (\sigma \gg we) \quad (6-11)$$

$$\alpha \approx \frac{\sigma}{2} \sqrt{\frac{\mu_0}{\epsilon}} \quad (\sigma \gg \omega\epsilon) \quad (6-12)$$

where σ is the soil conductivity, $\mu_0 = 4\pi \times 10^{-7}$, and ϵ is the permittivity of the soil. For average soil ($\sigma = 10^{-2}$ mho/m, $\epsilon = 8.85 \times 10^{-11}$ F/m), the attenuation constant is 0.14 m^{-1} at 1 MHz ($\sigma \gg \omega\epsilon$) and 0.60 m^{-1} above 18 MHz ($\sigma \ll \omega\epsilon$). Since $1/\alpha$ is the distance in which the current is attenuated by e^{-1} , this distance is only 7 m at 1 MHz and about 1.7 m at frequencies where the soil behaves as a lossy dielectric.

Because of this large attenuation, the input impedance of a single cable or well casing used as a counterpoise is essentially the characteristic impedance of the buried conductor. For a horizontal conductor a few feet deep, this impedance is

$$Z_0 \approx \frac{1 + j}{2\pi\sigma\delta} \log \frac{\sqrt{2\delta}}{\gamma_0 a} \quad (\sigma \gg \omega\epsilon) \quad (6-13)$$

$$Z_0 \approx \frac{j\omega\sqrt{\mu_0\epsilon}}{2\pi\sigma} \log \frac{2}{\omega\sqrt{\mu_0\epsilon}\gamma_0 a} - j\frac{\pi}{2} \quad (\sigma \ll \omega\epsilon) \quad (6-14)$$

where δ is the skin depth in the soil, a is the radius of the conductor, σ is the soil conductivity, and $\gamma_0 = 1.7811\dots$. For a horizontal conductor with the attachment point along the run, the impedances will be smaller by $\frac{1}{2}$ since there are then two impedances in parallel. For average soil ($\sigma = 10^{-2}$ mho/m, $\epsilon = 8.85 \times 10^{-11}$ F/m), the impedance of a 1-inch-dia meter horizontal cable is 26 ohms at 1 MHz ($\sigma \gg \omega\epsilon$) and 320 ohms at 100 MHz ($\sigma \ll \omega\epsilon$) if the cable is long compared to $1/\alpha$ (i.e., long compared to 7 m at 1 MHz). The surge impedance of the counterpoise at high frequencies is therefore large, independent of length, and relatively independent of conductor radius. Although the counterpoise impedance can be reduced by using multiple conductors in a grid, the high-frequency impedance of the counterpoise will still be tens of ohms in the vicinity of 100 MHz, so that 100-A surges will produce kilovolt potentials at the ground point.

The difference in the behavior of the counterpoise at high frequencies is illustrated in Figure 6-13. In Figure 6-13(a), the dimensions of the counterpoise are smaller than a skin-depth in the soil, so that the entire ring is effective in carrying and dissipating ground currents. Its surge impedance is low, and its "region of influence," taken as the area within one skin depth of the counterpoise conductors, is large. At high frequencies, however, the skin depth (or $1/\alpha$ if $\alpha \ll \omega t$) may be small compared to the dimensions of the counterpoise as illustrated in Figure 6-13(b). Then the surge impedance is large and the "region of influence" is small. Furthermore, only that part of the counterpoise within about a few skin depths in the soil is effective in carrying ground current; the remainder of the ring has

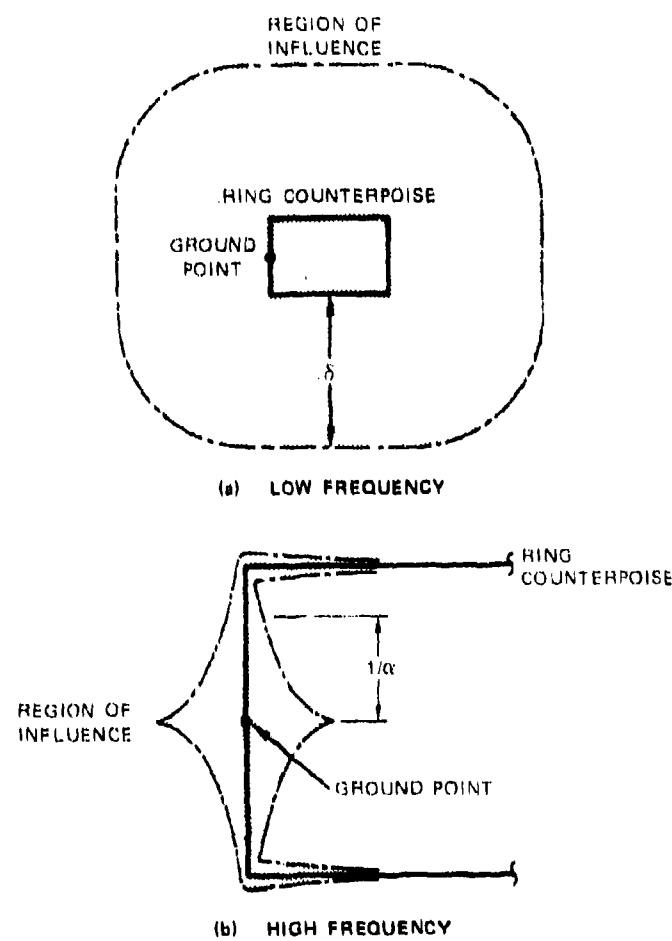


Figure 6-13 BEHAVIOR OF A RING COUNTERPOISE AT LOW AND HIGH FREQUENCIES

virtually no effect on either the surge impedance of the counterpoise or the ground-current distribution in the soil. Thus if two or more attachment points separated by several skin depths are used, each may behave as essentially independent ground points at high frequencies.

6.5 CITED REFERENCES

1. *Electrical Transmission and Distribution Reference Book* (Westinghouse Electric Corporation, East Pittsburgh, Pennsylvania, 1964)
2. A. E. Knowlton, Editor, *Standard Handbook for Electrical Engineers*, (McGraw-Hill Book Co., Inc., New York, N.Y., 1949).
3. *National Electrical Code 1971* (National Fire Protection Association, Boston, Massachusetts, 1971).
4. R. Morrison, *Grounding and Shielding Techniques in Instrumentation* (John Wiley & Sons, Inc., New York, N.Y., 1967).
5. R. Rudenberg, "Grounding Principles and Practice," *Electrical Engineering*, Vol. 64, pp. 1-13 (January 1945).

Chapter Seven

POWER-SYSTEM PRACTICES FOR EMP PROTECTION

7.1 INTRODUCTION

The protection of electric power systems from the effects of the EMP requires a determination of the EMP-induced transients in the system and an understanding of the tolerances of components of the system for these transients. At present, the transients induced by the EMP are better understood than are the tolerances of the power system to these transients — particularly the tolerances of the generation, transmission, and distribution systems. The tolerances of the distribution transformer, insulators, and lightning arresters, as presently understood, are discussed in Chapters Two and Four. The effect of the EMP-induced transients on supervisory-control systems, relaying equipment, and turbine control systems containing solid-state devices, or on other equipment in the generation and transmission portions of the power system is unknown. These components are apparently sufficiently tolerant to withstand normal switching and lightning transients (although early versions of some equipment containing silicon-controlled rectifiers were apparently susceptible to switching transients). However, one is inherently suspicious of equipment using solid-state electronics.

unless the electronic circuits are heavily protected from the direct EMP fields and from induced currents conducted into the electronic circuits.^{1,2}

The behavior of the consumer's end of the power system is considerably better understood because this portion of the system has been analyzed and tested in connection with several facility hardening and evaluation programs. The object of these programs has always been to protect the consumer facility from the effects of EMP on the power system, however, rather than to protect the power system from the EMP. In most such assessments, the commercial power system is considered expendable in the event of nuclear warfare; the primary concern is that EMP transients conducted into the facility on the power conductors do not cause vital equipment in the facility to malfunction. Such a hardening philosophy is the only prudent one to profess for critical communication and weapon systems that must function during or immediately after a nuclear engagement. For surface or air bursts of nuclear weapons, the blast and thermal damage will undoubtedly incapacitate power transmission and distribution equipment within a few kilometers of the burst.³

Weapons detonated at high altitudes do not produce significant blast and thermal effects at the surface, however. Their principal effect at the surface will be the EMP, which will be experienced over a large area (hundreds of kilometers) under the burst. Thus, while it will remain prudent for the designer of critical facilities to consider the commercial power system expendable, it may also be prudent to consider making the power system invulnerable to the EMP from a high-altitude weapon detonation — particularly if such hardening can be achieved in the course of providing protection from lightning and switching transients.

As has already been stated, there are insufficient data on the behavior of generation and transmission equipment to prescribe specific protection measures.⁴ For this reason, the protective measures described in this chapter are separated into two categories: measures that protect the consumer from transients conducted into his facility on the power lines, and some rather general measures for protecting the electric utility system from the effects of the EMP.

¹Studies are currently in progress under the auspices of the Defense Civil Preparedness Agency. Data from these studies may help to fill the present void.

7.2 PROTECTION FROM THE POWER SYSTEM

7.2.1 EMP PROTECTION OF THE CONSUMER

From the consumer's EMP-protection viewpoint, the power system is a large collector of the EMP that penetrates his facility. The objective of consumer EMP-protection is, therefore, to eliminate the EMP-induced transients on the power conductors before they reach sensitive components in the facility. Inasmuch as the open-circuit voltage induced on distribution lines may be of the order of megavolts, while some electronic circuits may be upset or damaged by volts, it is clear that some kind of protective measures will almost always be required for an electronic system that is to survive and operate immediately after the EMP.

As is evident from Chapters Two, Three, and Four, some of this protection will come from the power system itself. If the distribution transformers or potheads are protected with lightning arresters, the voltage delivered by the secondary of the transformer will be reduced to tens of kilovolts. Mismatches at the service entry also reduce the voltage that enters the low-voltage wiring, and the stray inductance of wiring in metering boxes and circuit-breaker panels slows the rise time of the transient. Thus, for facilities served by their own lightning-protected distribution transformers, the transient delivered to the main circuit breaker may have a rise time of 30 to 100 ns and a peak voltage of 10 to 50 kV. The task for the facility designer is then to suppress this remaining EMP-induced transient and provide a standby power source to carry the load if the commercial power source fails.

7.2.2 VOLTAGE LIMITERS AND FILTERS

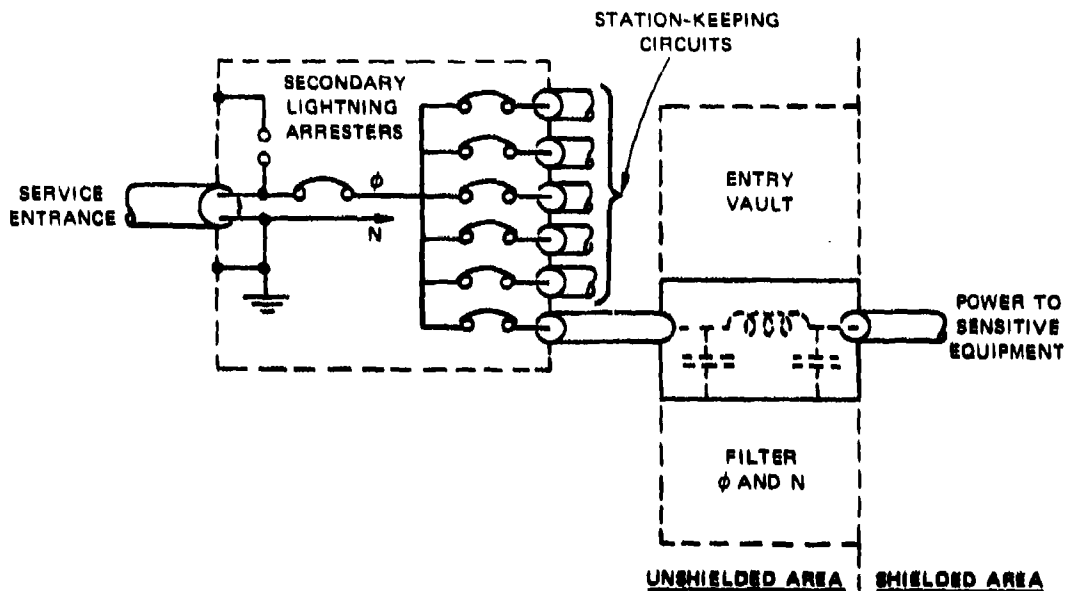
The residual 10 to 50 kV of EMP-induced signal can be adequately suppressed with a combination of voltage limiters and filters. Secondary lightning arresters that fire at voltages of 1 to 5 kV are available commercially for use on low-voltage circuits. The secondary arresters contain spark gaps and nonlinear resistances similar to the distribution type arresters, but they fire and extinguish at lower voltages. The arresters serve two purposes:

they prevent insulation breakdown in the low-voltage circuits (including the power-line filters) and they limit the low-frequency (late-time) content of the transient propagating beyond the arresters. Line filters suitable for use on circuits carrying up to 100 kVA are also available commercially. These filters are usually low-pass π -sections containing a series inductance with shunt capacitors across the input and output terminals. These filters usually have some specified minimum attenuation (e.g., 100 dB) at frequencies above a corner frequency such as 100 kHz so that they suppress the high frequencies passed by the lightning arresters.

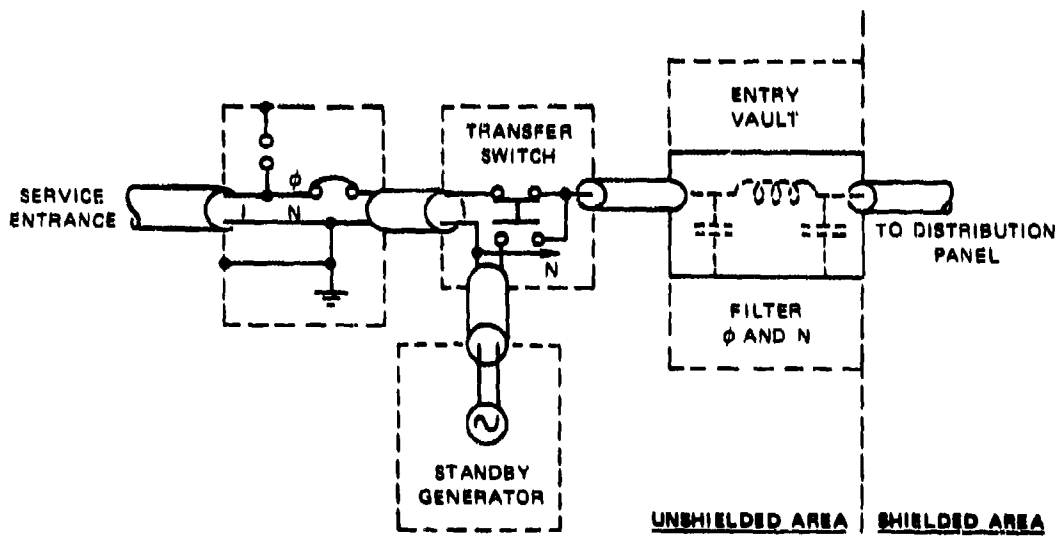
The placement of the secondary arresters and line filters will be determined to a large extent by the nature of the facility. Two possible applications are suggested in Figure 7-1. In Figure 7-1(a), a portion of the raw power is used for station-keeping equipment that is either expendable or insensitive to transients. Only the portion that is essential for sensitive and essential equipment is filtered, but all of the low-voltage circuits are protected by the voltage-limiting action of the secondary lightning arresters installed on the incoming conductors at the main circuit-breaker panel, since insulation damage must be provided even for the parts of the system that are not susceptible to transients. In Figure 7-1(b), all the incoming power is filtered upon entering the facility. A standby generator to provide power in the event of commercial power failure is also shown in Figure 7-1(b). Some or all of the external equipment shown in Figure 7-1(b) may be enclosed in the entry vault along with the line filters in some installations.

7.2.3 SELECTION AND INSTALLATION OF SURGE ARRESTERS

The secondary lightning arresters used for limiting transient voltage on the low-voltage wiring should be reliable, maintenance-free units designed for use on 60-Hz power circuits. Such components are commercially available and relatively inexpensive. They are designed to fire at voltages 5 to 10 times the peak 60-Hz voltage and will extinguish with the rated 60-Hz voltage applied. The latter property is important; surge arresters that conduct appreciable 60-Hz follow-on current tend to be short-lived because of the excessive electrode erosion and deformation caused by the follow-on current (failure then often occurs as a destructive short-circuit). In addition, the transient caused by the follow-on current



(a) SECONDARY ARRESTERS ON ALL POWER; SELECTED CIRCUITS FILTERED



(b) SECONDARY ARRESTERS AND FILTERS ON ALL POWER

Figure 7-1 USE OF SECONDARY LIGHTNING ARRESTERS AND FILTERS TO SUPPRESS EMP-INDUCED TRANSIENTS ON LOW-VOLTAGE CIRCUITS

flowing through surge arresters may be almost as objectionable as the original surge that triggered the arrester. The secondary lightning arresters should be essentially trouble-free for the life of the installation (unless a direct lightning strike to the low-voltage system is incurred).

The minimum firing voltage of secondary lightning arresters is determined by the 60-Hz voltage of the circuit being protected. Thus, for a 120-volt circuit the firing voltage of the secondary lightning arrester is usually at least 1000 V. The time-to-fire and the rate of rise of the current through the arrester are somewhat more variable in that they depend on the construction of the surge arrester and the wiring through which it is connected to the power conductor and ground. Adequate protection is usually obtained if the time-to-fire is less than 20 ns at twice the rated firing voltage of the arrester and if the effective time constant for the current buildup is 50 ns or less.

The time-to-fire is a property of the lightning arrester that can be determined experimentally by applying a fast-rising voltage step across the arrester and observing the time lag before conduction begins. However, the time constant for current buildup depends mainly on external-circuit properties, although the internal construction of the lightning arrester may also be a factor. For example, if the lightning arrester has an effective internal inductance of 60 nH and is connected to a long entrance conductor, whose characteristic impedance is 20 ohms, through 30 inches of lead (with 10 nH/inch), the current rise time constant is determined by the 360 nH of inductance and the 20-ohm source:

$$\tau = \frac{L}{R} = \frac{360 \text{ nH}}{20 \Omega} = 18 \text{ ns} . \quad (7-1)$$

Only the 60-nH internal inductance is attributable to the lightning arrester; the controlling resistance and external inductance are properties of the external circuits. It is evident, therefore, that the method of installing a secondary lightning arrester has a strong influence on its ability to dissipate short transients of current. A typical installation of secondary lightning arresters at the main circuit breaker panel is illustrated in Figure 7-2.

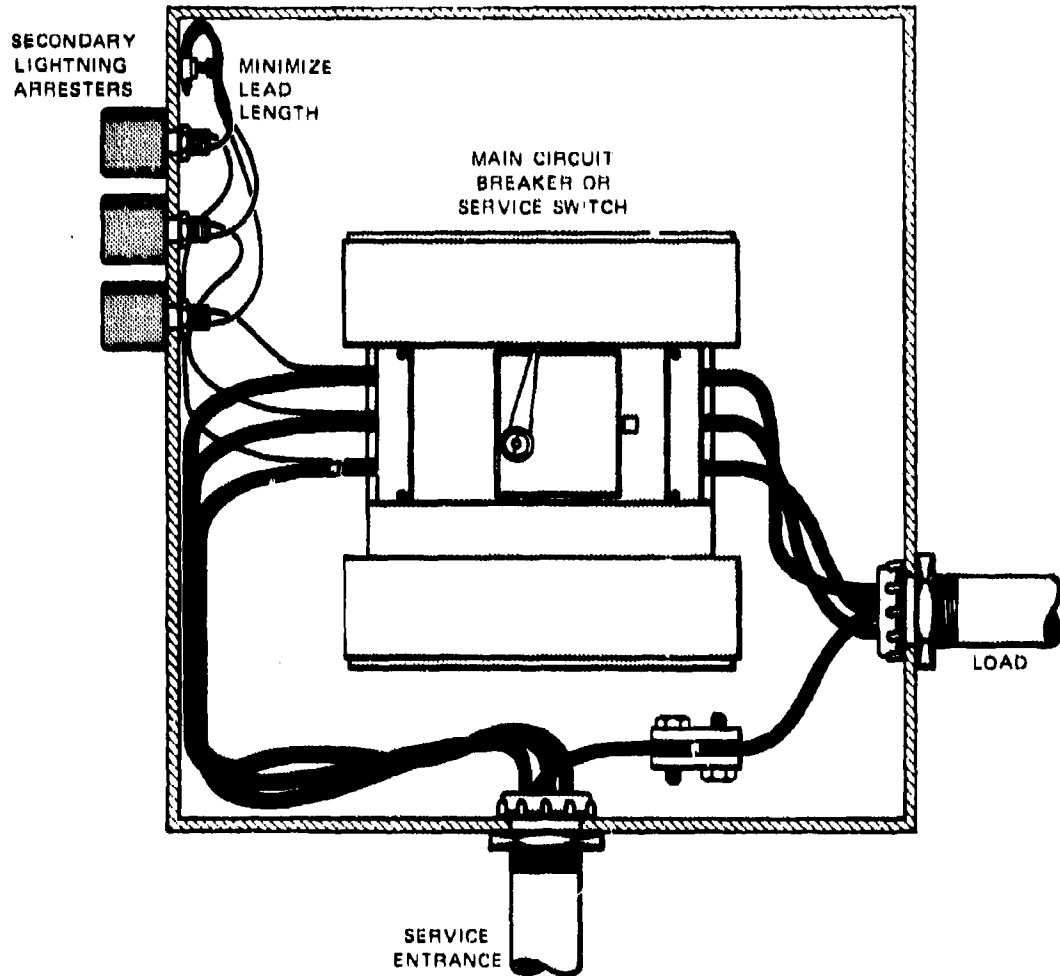


Figure 7-2 ILLUSTRATION OF SECONDARY LIGHTNING ARRESTERS AT THE MAIN CIRCUIT-BREAKER CABINET

The following guidelines are provided for the installation of secondary lightning arresters for EMP protection:

- **Use short leads.** The leads that connect the lightning arrester to the power conductor and to the ground should be as short as possible to minimize the external inductance in series with the arrester. This is particularly important for low source-impedance installations such as the main bus shown in Figure 7-1(a) where the lightning arrester is fed by many conduit conductors in parallel.
- **Use external ground.** The ground side of the lightning arrester should be connected to a ground point outside the shielded area (preferably to the circuit-breaker cabinet or service-entrance conduit). The surge-arrester discharge current should never be allowed to flow directly into the internal ground point used for sensitive electronics equipment inside the shielded area.
- **Install arresters on all phase conductors.** Arresters should be installed between each phase conductor and local ground. If the neutral or single-phase common are grounded (to the conduit or cabinet) in the main circuit-breaker cabinet, they will not need secondary lightning arresters. If the neutral or common ground-point is quite remote from the main circuit-breaker panel, or if the ground conductor is directly exposed to the EMP, secondary lightning arresters should be installed between these conductors and the cabinet or conduit in the main circuit-breaker cabinet.
- **Follow lightning arresters with filters.** Power supplied to sensitive electronic systems should always be filtered between the lightning arresters and the sensitive equipment. The lightning arrester only limits the transient voltage; it does not eliminate transients on the power conductors (sometimes the rates of change of the voltage or current are actually increased by the lightning arrester). Low-pass filters (either in the power system or in the equipment) are required to protect the equipment from the transient passed by the lightning arresters.

The discharge-current requirements for the secondary lightning arresters are also determined by the external circuit. For times less than the round-trip propagation time on the service-entrance conduit or cable, the current through the surge arrester is limited by the characteristic impedance of the conductor. Thus, for example, a 20-kV (open-circuit) transient entering on a 20-ohm conductor can deliver only 1000 A to a short-circuit until the discharge-current wave has propagated to the opposite end of the conductor and back to the discharge point. At later times, the discharge current will depend on the source impedance at the opposite end of the entrance conductor. This impedance is often tens or hundreds of ohms on phase conductors, however, so that peak surge-arrester currents seldom exceed the value obtained by dividing the open-circuit voltage by the characteristic impedance of the entrance conductor (see Chapter Three for more exact techniques for determining the short-circuit current at the end of the service entrance).

Since the duration of the high-level transient passed by the distribution transformers is usually less than 1 μ s, the total charge transferred through the surge arrester by an EMP-induced transient with a peak open-circuit voltage of tens of kilovolts is only tens of milli-coulombs. The current and charge transfer ratings required of secondary lightning arresters for EMP protection are thus lower than those required for lightning protection, for which longer pulses of similar magnitudes are usually specified.

7.2.4 SELECTION AND INSTALLATION OF LINE FILTERS

As has been discussed in the preceding sections, secondary lightning arresters can be used to limit the peak transient voltage to a few kilovolts so that insulation breakdown and flashover in the low-voltage wiring is limited. Transient voltages of a few kilovolts are permitted to propagate along the conductors beyond the lightning arresters, however, and fast-acting lightning arresters can cause fast-changing voltage and current transients in these circuits. The purpose of power-line filters is to remove these fast-changing components of the transient that remains after the lightning arresters have acted. Commercially available line filters are typically low-pass π -section filters with a large insertion loss at frequencies

well above the 60-Hz or 400-Hz power frequency, but fairly low-loss at the power frequencies. These filters can thus greatly suppress the large rates of change in current and voltage conducted past the lightning arresters.

Power-line filters should, like the secondary lightning arresters, be reliable and maintenance-free for the life of the installation except in extenuating circumstances such as a direct lightning strike to the low-voltage conductors or a short-circuit in the filtered circuit that is not cleared by circuit breakers or fuses. Most filters will tolerate sufficient temporary overcurrents that faults on properly protected circuits will not damage the filters. Thus, for example, a 100-A line filter on a circuit protected by a 100-A fuse or circuit breaker should not be damaged by the fault current required to blow the fuse or open the circuit breaker.

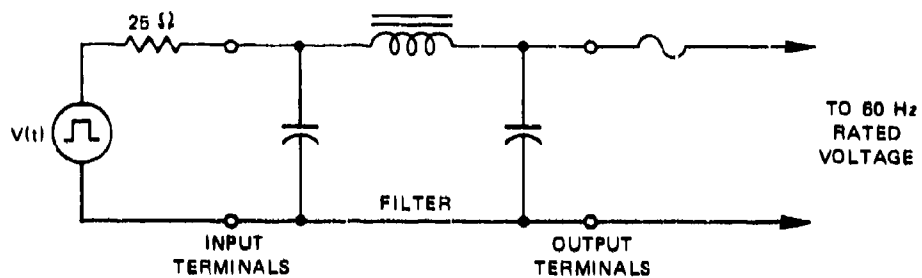
The primary factors, other than line voltage and current ratings, that influence the choice of line filters for EMP protection are the high-frequency attenuation and the insulation breakdown or flashover characteristics of the input terminals. The filter must be able to tolerate the peak voltage, rate-of-change of voltage, and rate-of-change of current passed by the secondary lightning arresters. π -section filters with shunt capacitors can usually tolerate large transients of short duration since the input capacitance of the filter can absorb the transient charges without large voltage changes. Their ability to do so, however, depends on the quality and size of the input capacitor. Very large capacitors that could, in principle, absorb large currents without big voltage changes, may, in fact, behave as inductors at high frequencies. Therefore, for EMP applications in which large amplitude, short-duration voltage transients may be delivered to the filter, the filter input characteristics must be carefully examined.

It is recommended that power-line filters for facility power applications such as those illustrated in Figure 7-1 be tested with a short, high-voltage impulse to determine that the input capacitance and insulation will withstand the fast, high-voltage transients passed by the secondary lightning arresters. A suggested test circuit and impulse waveform are shown in Figures 7-3(a) and (b) for filters expected to operate on 60-Hz voltages of 480 V or less. Note that the voltage waveform in Figure 7-3(b) is the open-circuit voltage behind the 25-ohm source impedance. Thus if the input capacitance of the filter is 1 μ F, the test pulse will increase the filter terminal voltage to only about 100 V. If the input capacitor behaves as inductance at early times, however, the terminal voltage may rise to several kV and permit the terminals to flash over or cause the capacitor dielectric to break-

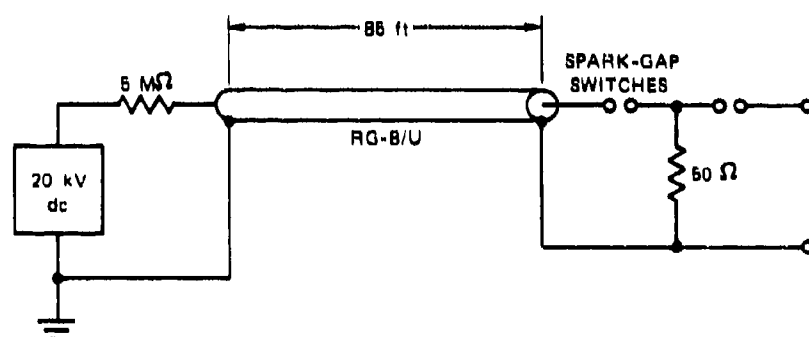
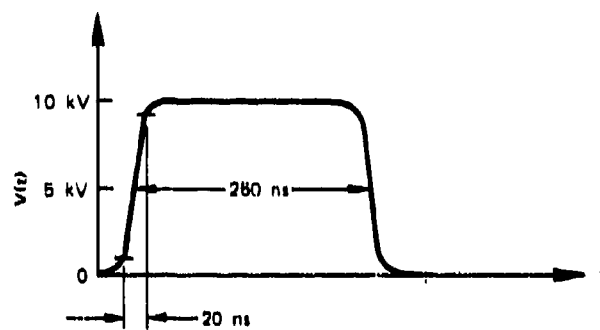
down. Because a dielectric breakdown in the input capacitor would be a catastrophic failure of the filter, it is recommended that the filter be tested with a fused 60-Hz source of rated voltage applied to the output terminals so that insulation failure resulting in 60-Hz follow-on current can be detected. A suggested pulser for generating the test pulse is shown in Figure 7-3(c).

The high-frequency attenuation of power-line filters is specified in terms of the insertion loss when the filter is placed in a 50-ohm circuit. The tests for measuring the insertion loss prescribed by MIL-STD-220-A are widely used in the manufacturing industry for specifying and evaluating line filters. The rudiments of this test are illustrated in Figure 7-4, where it is seen that the current through a 50-ohm load on a 50-ohm source is measured before and after the filter is inserted between the source and the load. The ratio of the unfiltered load current to the filtered load current (usually expressed in decibels) is the insertion loss of the filter. Insertion losses of 80 to 100 dB at frequencies above 100 kHz are common for commercially available line filters. It is widely recognized that the insertion loss measured in a 50-ohm circuit is not readily applicable to any other circuit impedance levels unless additional information on the filter is available. For high-current, 60-Hz, π -section power-line filters, however, the series inductance must be small (millihenries or less), to minimize the insertion loss at the power frequency, which implies that the shunt capacitors must be large ($\sim 1 \mu\text{F}$). In addition, many of the conduit-and-conductor transmission lines used in electrical wiring have characteristic impedances within a factor of 2 of 50 ohms, so that for many of the fast transients associated with the EMP, the 50-ohm impedance level is an appropriate mean value. Thus, for power-line filters, one can infer some of the properties of the filter, and it can be deduced that the attenuation with the 50-ohm impedance level is a reasonable approximation of the attenuation to be expected for the very rapidly varying components of the EMP-induced transients.

For EMP-protection of a shielded facility, filters should be installed on the neutral (or common) as well as on all phase conductors entering the shielded area. The ground sides of the filters should be connected to the outer surface of the shield — preferably by bolting the filter case directly to the shield. Only the output terminal of the filter should be permitted to enter the shielded area. A common practice is to install the filters in a closed metal vault attached to the shield as illustrated in Figure 7-5 so that exposed wiring and filter input terminals are shielded from the external environment.



(a) TEST CIRCUIT



(c) SUGGESTED PULSE SOURCE

Figure 7-3 IMPULSE TEST FOR EVALUATING POWER-LINE FILTERS FOR EMP APPLICATIONS

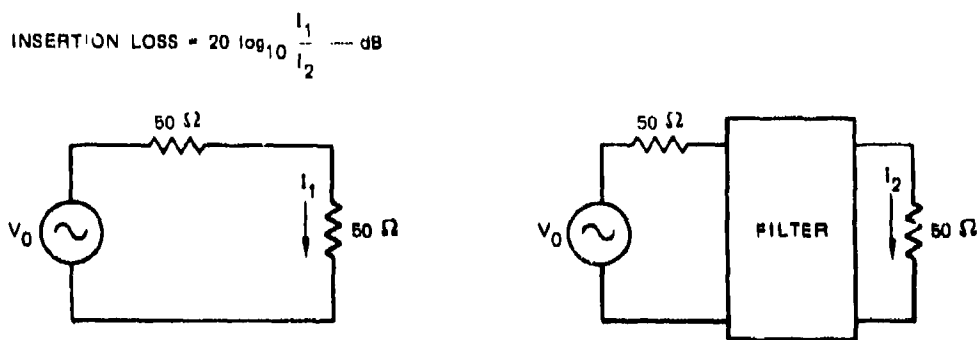


Figure 7-4 DETERMINATION OF THE INSERTION LOSS OF A LINE FILTER

7.2.5 AUXILIARY POWER SYSTEMS

7.2.5.1 Function of Auxiliary Power Systems

Installations requiring continuous and reliable power are usually operated from commercial power and provided with standby sources to provide power in the event of commercial power outage. Such systems are used in critical facilities such as hospitals, communication centers (civil and military), strategic military systems, power stations, and computer centers, and in similar facilities where power failure would cause loss of life, critical operating capability, or essential data. In many installations, even momentary loss of power or transients in the power system are intolerable. For example, computer centers and electronically controlled communication centers may lose stored data during a power outage or be upset by transients. Therefore the auxiliary power systems are usually designed to protect the facility from interference (lightning and switching transients) conducted in on the power lines as well as to provide stable and continuous electric power.

Auxiliary power systems for these applications usually consist of a combination of storage batteries and one or more engine-generators. The storage batteries are kept fully charged from the commercial power, so that when an outage occurs they can supply the facility operating power for a brief period (from a few minutes to a few hours). If the commercial power outage lasts longer than a few minutes, the engine-generator is started (usually

automatically) and the facility load is transferred from the commercial power service to the engine-generator. The engine-generators can supply power for days, or weeks, if necessary.

A schematic diagram of an "uninterruptible power system" is shown in Figure 7-6. The 60-Hz commercial power may be used directly for certain station-keeping functions such as outdoor lighting, and operating pumps, air conditioners, etc. The "uninterruptible" rectified power may also be used directly as the dc source for operating electronic equipment. "Clean" 60-Hz power for sensitive equipment is obtained from a motor-generator driven by the dc supply. In the event of commercial power failure, the storage batteries continue to supply dc power and drive the motor-generator to provide 60-Hz power while the engine generator is being started and brought up to speed. A properly designed power system of this type can provide a high degree of immunity to power outages and line transients for the system operated from the dc or "clean" 60-Hz power.

7.2.5.2 The Automatic Transfer Switch

A key component of an auxiliary power system is the automatic transfer switch. The function of an automatic transfer switch is to transfer a load from the normal (or preferred) power source to an emergency supply if normal voltage fails or is substantially reduced. Once the normal source is again in proper operating condition, the transfer switch should automatically restore the load to its original feeder lines, regardless of the condition of the emergency supply. A schematic of the automatic transfer switch is shown in Figure 7-7. This model is designed to provide full protection in 60-Hz, three-phase, 3-wire or three-phase, 4-wire solid neutral power services.

A properly designed transfer switch should be rugged, dependable, and rated for continuous duty, since failure of the unit might well create the hazard it is intended to eliminate — complete service outage. For similar reasons, it is desirable that the switch operate from the power source that is to be connected. Also, failure of a relay coil or control circuit in the transfer switch should not leave both normal and emergency contacts in the open position.

It is also necessary to provide suitable time lags in the switch's operation to allow for generator starting and warm up, and for the return of stable normal power or the

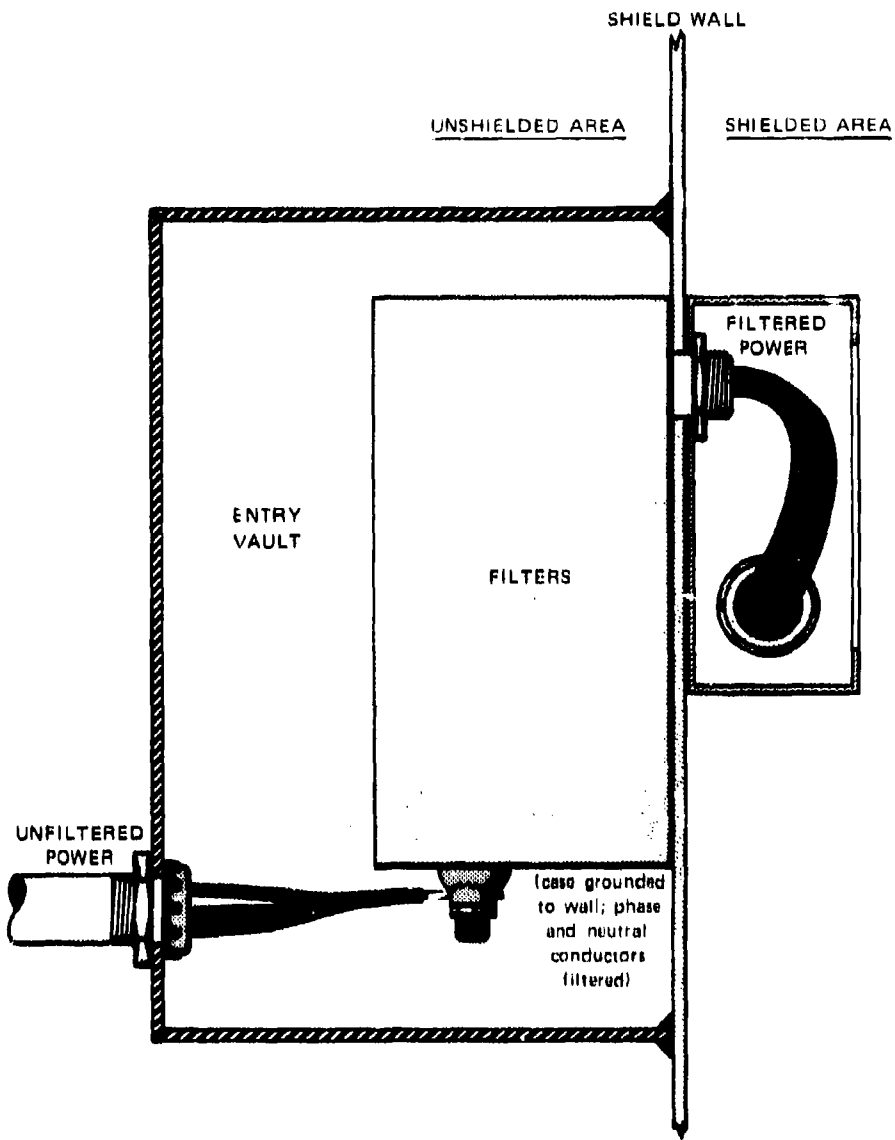


Figure 7-5 ILLUSTRATION OF POWER-LINE FILTERS IN AN ENTRY VAULT ON WALL OF SHIELDED STRUCTURE

shut-down of an emergency power source after a return to normal power. Time delays should be used to prevent unnecessary transfers due to momentary dips or transient outages. Switching, once initiated, should be fast (less than 10 cycles) to reduce contact burning and

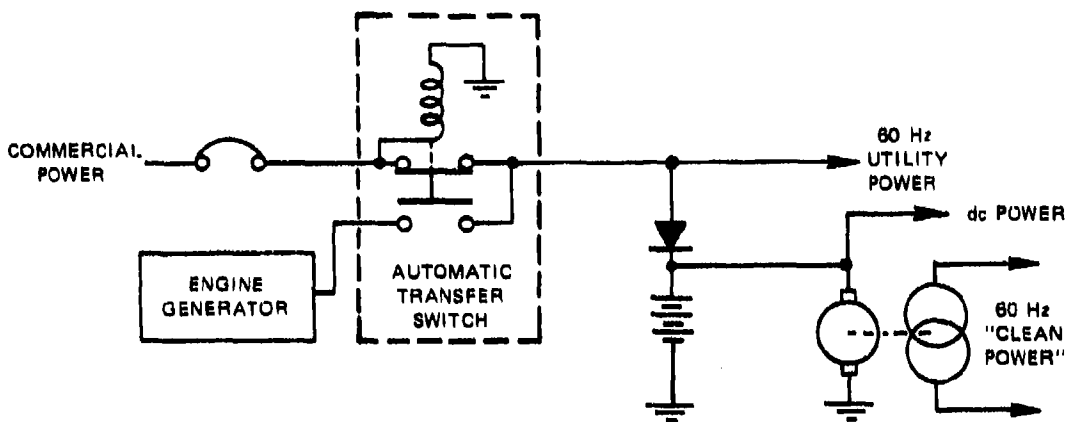
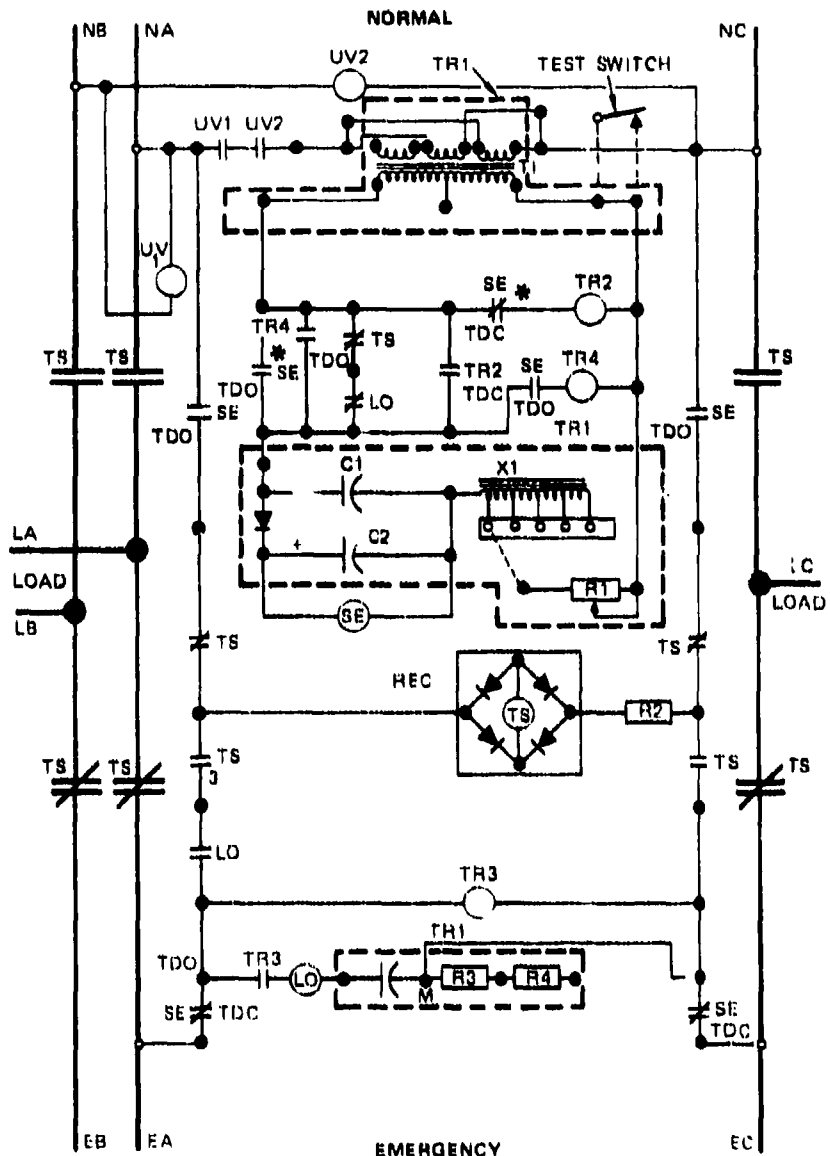


Figure 7-6 SCHEMATIC OF A SIMPLIFIED "UNINTERRUPTIBLE POWER SYSTEM" (UPS)

pitting during make and break operations. Other useful attributes of an automatic transfer switch include minimum maintenance, quiet normal operation, and minimum space requirements.

Because the automatic transfer switch must be located in the main or secondary branch circuits, the switch and its component parts may be subjected to the full magnitude of any EMP-induced voltages and currents coupled through the service transformer bank and service-entrance conduit to the main circuit-breaker panel. Therefore, the transfer switch must be resistant to the EMP-induced transients coming in on the power conductors. Transfer switches that contain only electromechanical relays for sensing and logic functions are usually relatively immune to EMP-induced transients that do not exceed the insulation strength of the switch components. However, there is a tendency to use solid-state electronic circuits for sensing and for providing time delays in modern transfer switches. Such components are much more susceptible to failure induced by the EMP transients. Therefore the transfer switch itself must be protected from transients on the commercial power system by voltage limiting and filtering if the switch is to function during or after an EMP environment.



NOTES

1. SWITCH WIRED ON FRONT OF PANEL AND SHOWN DE-ENERGIZED WITH EMERGENCY POLLS SHOWN CLOSED.
2. DEVICE SYMBOLS AND DESIGNATIONS ARE PER NEMA PUB. 1, #ICS 1-101-1970.
3. * INDICATES OVER LAPING CONTACTS.
4. TDC INDICATES TIME DELAY ON CLOSING; TDO INDICATES TIME DELAY ON OPENING.
5. NOMINAL 3 SECOND TIME DELAY TO OVERRIDE MOMENTARY POWER DIPS AND OUTAGES (INVERSE TIME CHARACTERISTIC WITH VOLTAGE).
6. TR1
7. LO RELAY. SENSITIVE TO VOLTAGE AND FREQUENCY.
8. CLOSE DIFFERENTIAL RELAY PROTECTION ON ALL PHASES PROVIDED BY THE SE RELAY. UV1 AND UV2. THE SE RELAY ALSO FUNCTIONS AS THE TRANSFER CONTROL RELAY.
9. TR2 - AN ADJUSTABLE TIME DELAY ON RETRANSFER TO NORMAL.
10. TR3 - AN ADJUSTABLE TIME DELAY ON TRANSFER TO EMERGENCY.
11. TR4 - AN ADJUSTABLE TIME DELAY ON ENGINE STARTING.

Figure 7-7 CIRCUIT DIAGRAM OF AN AUTOMATIC TRANSFER SWITCH

7.3 PROTECTION OF THE POWER SYSTEM

As was indicated in the beginning of this chapter, the tolerance of the power system to the effects of the EMP are largely unknown. It is suspected that transmission and distribution lines that are adequately protected against lightning will be relatively immune to the effects of the EMP.^{4, 5} Similar immunity is suspected in the case of transformers and electromechanical switch gear installed in accordance with modern lightning-protection practice. The principal uncertainty in these components is the ability of the solid dielectric to withstand the large EMP-induced voltages that might be developed before the lightning arresters fire. Insufficient testing has been conducted to provide assurance that the solid insulation is adequately protected by conventional lightning arresters, although the results to date suggest that conventional protection may be adequate. For the present, therefore, the primary EMP-protection policy for the transmission and distribution lines, transformers, and switchgear is an effective lightning-protection policy.^{6, 7} For utilities in areas of high lightning incidence, lightning protection is probably already practiced; utilities in areas of low lightning incidence may need to upgrade their lightning-protection systems to reduce vulnerability to the EMP.

Because very little is known about the vulnerability of many crucial parts of the power system, however, only the most general recommendations can be made. Modern supervisory control systems, turbine control systems, and relaying equipment, for example, use solid-state electronic components in varying degrees. It is strongly suspected that some or all of this equipment may be susceptible to damage from the EMP-induced transients, but no data on the nature or levels of susceptibility are available.

The utilities can, without expensive EMP testing, make a crude assessment of the vulnerability of their equipment by observing the types of equipment that fail and the nature of the failures in an environment of transient activity such as that accompanying thunder-storm activity or fault-clearing operations. Components that malfunction or are damaged in these environments may also be susceptible to the EMP transients. An occasional malfunction under severe lightning or fault conditions may be tolerable in one part of the system, but in the EMP environment, the entire utility system and most of its neighboring utilities may be exposed to the high level fast transient excitation. Thus, if a component is vulnerable,

all such components in the power network may malfunction simultaneously to cause a disastrous disruption of the system. Therefore in assessing the vulnerability of the system to the EMP, even rare malfunctions associated with severe transient activity may be significant.

Based on present understanding of the characteristics of high-voltage components and fast-pulse technology, it is assumed that the high-voltage components of the transmission and distribution systems are probably the least vulnerable to the transients induced by the EMP — particularly if good lightning-protection practice is employed. Low-voltage control circuits — particularly those with sensors (current or potential transformers) on transmission leads and those containing solid-state electronics — appear to be the most vulnerable to the EMP. Low-voltage circuits connected to instrument transformers are particularly suspect because the fast rise-time of the EMP-induced transient will be coupled through these transformers much more efficiently than the slower lightning and switching transients.

Improvements in the EMP protection of these low-voltage circuits can be achieved by following the principles used to protect sensitive equipment from transients conducted in on power leads.^{1, 2, 8} For systems already in existence, the basic hardening techniques are:

- (1) Making maximum use of existing shielding afforded by cabinets and housings through operating and maintenance procedures.
- (2) Installing voltage-limiting surge arresters on conductors that penetrate these shields.
- (3) Installing low-pass line filters on low-voltage conductors penetrating these shields.
- (4) Modifying operating characteristics of logic systems so that lockouts or lockups cannot be triggered by a single, wide-spread event.

For new systems and components, considerable EMP immunity can be incorporated in the design by taking precautions to ensure that housings, cabinets, etc. are designed for shielding integrity as well as mechanical protection, etc. In addition, surge filters and surge limiters can often be incorporated into new designs at little additional cost. Power-system components have the advantage, from the EMP-hardening point of view, that they must be

Inherently immune to lightning and switching transients. Hence, the additional protection required to reduce their vulnerability to the EMP-induced transients may be quite minimal.

7.4 CITED REFERENCES

1. "DNA EMP Awareness Course," DNA2772T Notes prepared by IIT Research Institute, Contract DASA 01-69-C-0095, Defense Nuclear Agency, Washington, D. C. (August 1971).
2. "EMP Protection For Emergency Operating Centers," Protection Engineering Management Note 8, Lawrence Livermore Laboratory, Livermore, Calif. (Originally issued by the Defense Civil Preparedness Agency as TR-DCA, July 1972).
3. S. Glasstone (Ed.) *The Effects of Nuclear Weapons*, U. S. Government Printing Office, Washington, D. C. (April 1962).
4. "EMP and Electric Power Systems," TR61-D, prepared by Oak Ridge National Laboratory for the Defense Civil Preparedness Agency, Washington, D. C. (July 1973).
5. G. E. Barker and W. B. Hull, "Characteristics of Commercial Power Systems," AFWL-TR-74-27, Contract F29601-69-C-0127, Air Force Weapons Laboratory, Kirtland Air Force Base, New Mexico (September 1973).
6. *Electrical Transmission and Distribution Book*, 4th Ed. (5th printing) (Westinghouse Electric Corporation, East Pittsburgh, Penn., 1964).
7. W. W. Lewis, *The Protection of Transmission Systems Against Lightning* (John Wiley & Sons, Inc., New York, N. Y., 1950).
8. *DASA EMP (Electromagnetic Pulse) Handbook*, DASA 2114-1 (DASA Information and Analysis Center, Santa Barbara, Calif., September 1968).

Chapter Eight

TESTS OF COMPONENTS AND FACILITIES

8.1 INTRODUCTION

The tests of power-system components and consumer facility and consumer component sensitivity to EMP-induced transients on the power system can be divided into three categories:

- (1) **Standard tests** — established by the IEEE and the American Standards Association and designed to determine transmission-system component insulation levels and tolerance to lightning and switching transients.
- (2) **Component tests** — with simulated EMP to determine the tolerance and transfer characteristics of power system and consumer components or items of equipment.

- (3) Facility tests - with simulated EMP transients injected at the service entrance to evaluate the tolerance of the facility wiring and components for the EMP-induced transients on the distribution system and to determine the excitation of internal equipment.

A fourth category of test could be postulated to determine the response of the power transmission and distribution network to the EMP. At present, however, no practical method of performing such a test has been proposed. Until such a method is developed, therefore, power network response must be assessed by a combination of direct-injection tests at the "nodes" (consumer facilities, switching centers, substations, etc.) and network stability analysis. It is quite likely that network assessment will never progress beyond this state because of the very serious technical and political problems associated with wide-area illumination of a power transmission network. In any event, much work remains to be done at the node and network analysis level before the implications of EMP interaction with power networks can be evaluated.

Tests of equipment and facilities are usually required to (1) determine the coupling between the incident EMP and a component or subsystem, (2) evaluate the sensitivity of the equipment to the coupled signal (i.e., threshold for damage or upset), and (3) assess the effectiveness of designs for reducing vulnerability to the EMP. The complexity of EMP tests varies from fairly simple laboratory tests of components to very complex tests of entire facilities. The nature of the test requirements is also influenced by the state of evolution of the system. Existing facilities that are to be upgraded usually require all forms of testing listed above, while new systems designed to be immune to the EMP may require primarily the design-effectiveness tests.

Experimental determination of the EMP tolerance and throughput is the only reliable means of obtaining these characteristics of most electrical systems because the broadband and nonlinear properties of most components are not well known. To illustrate this, consider a typical electric appliance designed to operate on 120 V, single-phase, 60 Hz. Its functional characteristics at 120 V, 60 Hz are usually well understood, but what can be said of its electrical properties at frequencies between 100 kHz and 50 MHz, and what will happen to the appliance if it is subjected to a 5-kV common-mode voltage transient on the power conductors? The nameplate data offer little help in answering these questions,

and often even the design data are of little value in evaluating the high-frequency and high-voltage characteristics of the appliance.

Because many items of equipment that are designed to operate from low-voltage, 60-Hz power are not designed to have specific high-voltage or high-frequency characteristics, these characteristics may also vary considerably among supposedly interchangeable items. This is attributable to the fact that manufacturing techniques and tolerances that affect the high-voltage and high-frequency characteristics are not controlled unless they also affect the 60-Hz performance. Because of this variability from unit to unit, it is important that the basic coupling mechanisms (or malfunction mechanisms) for each piece of equipment be understood, and that more than one item be tested, if possible, to ascertain that the same mechanism prevails in each case.

8.2. STANDARD INSULATION TESTS

The purpose of standard insulation testing is to demonstrate that the design, workmanship, and materials of electrical equipment are adequate. Such testing originated from the need to design and certify transmission and distribution system components capable of withstanding the transients associated with lightning and line switching. These tests are not nuclear EMP tests; they are quality-control tests established by the industry. They are described briefly here to illustrate the insulation standards used in the design of transformers, bushings, insulators, etc.

The insulation tests conducted by the power-component testing laboratories are of three types: (1) full-wave impulse tests with a pulse having a rise time of typically 1.5 μ s and a decay time (to half the peak value) of typically 40 μ s, (2) chopped-wave impulse tests in which the test waveform is truncated (chopped) after a few microseconds by shorting the source through a spark-gap switch, and (3) a low-frequency test at twice the rated voltage and at about twice the rated frequency for up to 1 minute.¹ These tests are not routinely conducted as a part of the manufacturing quality control; rather they are conducted as a part of the design qualification procedure, on samples of a new or altered component design. Thus, although a component has been designed and manufactured for

a basic insulation level, each individual component is not necessarily subjected to the tests specified for that basic insulation level.

The full-wave impulse test is conducted with a high-voltage pulse applied across the insulation. The pulse shape is basically an exponential pulse with a finite rise time such as that illustrated in Figure 8-1. The pulse is specified in terms of its crest value V , the time to crest T_r , and the time to half-crest $T_{1/2}$. The method of determining the time to crest and the time to half-crest is illustrated in Figure 8-1. The commonly-used impulse for insulation testing is the $1.5 \times 40\text{-}\mu\text{s}$ pulse, which means $T_r = 1.5\text{ }\mu\text{s}$ and $T_{1/2} = 40\text{ }\mu\text{s}$. The crest value V is a function of insulation class (voltage rating) of the equipment. Crest voltages for full-wave impulse tests are given in Tables 4-1 and 2-2 for most transmission and distribution voltages.

For chopped-wave tests, the waveform of Figure 8-1 is foreshortened by shorting the pulse source out after a predetermined time with a spark-gap switch. Tests with the chopped wave are conducted with slightly larger crest voltages, as can be seen in Table 4-1. However, the duration of the pulse is usually $3\text{ }\mu\text{s}$ or less.

The low-frequency tests of transformers and similar equipment are conducted at twice the rated frequency and at least twice the rated voltage of the equipment. At twice the rated frequency, the copper and iron losses are lower, so that the component can withstand the higher voltages without overheating. This test provides an evaluation of sustained ac overvoltage (test time is 1 minute or less) effects on the insulation between turns and between the winding and case.

8.3 EMP TESTS OF EQUIPMENT

8.3.1 PURPOSE OF EQUIPMENT TESTS

EMP tests of power-system or consumer facility equipment are usually conducted for one or both of the following purposes: (1) to establish the threshold for equipment malfunctions or failure, and (2) to determine the transfer function, or EMP throughput, of the equipment.^{2,3}

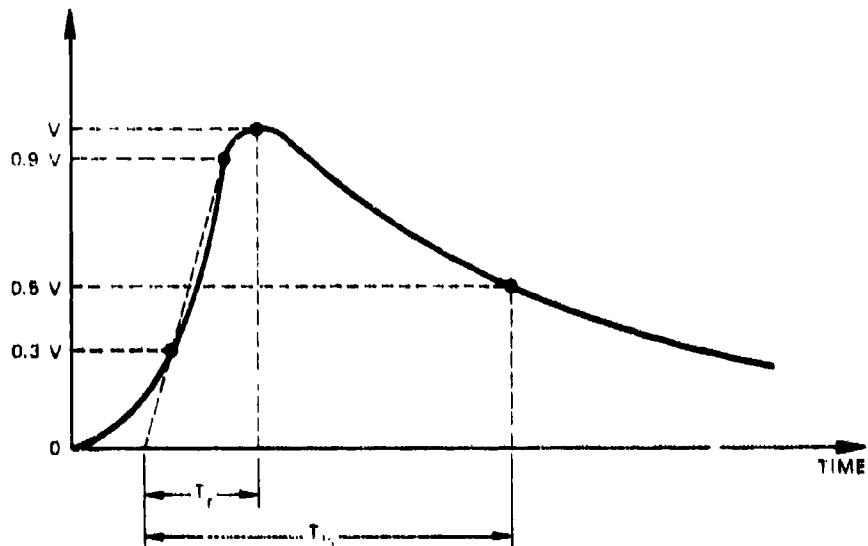


Figure 8-1 IMPULSE-TEST WAVEFORM SHOWING METHOD OF SPECIFYING RISE TIME AND TIME-TO-HALF-PEAK

The threshold for equipment malfunction is a measure of the tolerance of the equipment for the EMP-induced transient. This tolerance for the transients induced through the power system may be determined by injecting transients on the power leads supplying the equipment. In general, however, there may be several other coupling modes to which the equipment is sensitive, so the susceptibility to transients conducted on the power leads should not be considered the only susceptibility of the equipment. As is illustrated in Figure 8-2, the equipment may also have ground conductors and signal input and output conductors, and the equipment and its interconnecting conductors may be exposed to the incident EMP field or some fraction thereof. The equipment may be susceptible to the fields and to EMP-induced transients conducted on any (or all) of the other conductors. Thus although the emphasis of this handbook is on susceptibility to transients related to the power system, it is important to recognize that these other paths also exist.

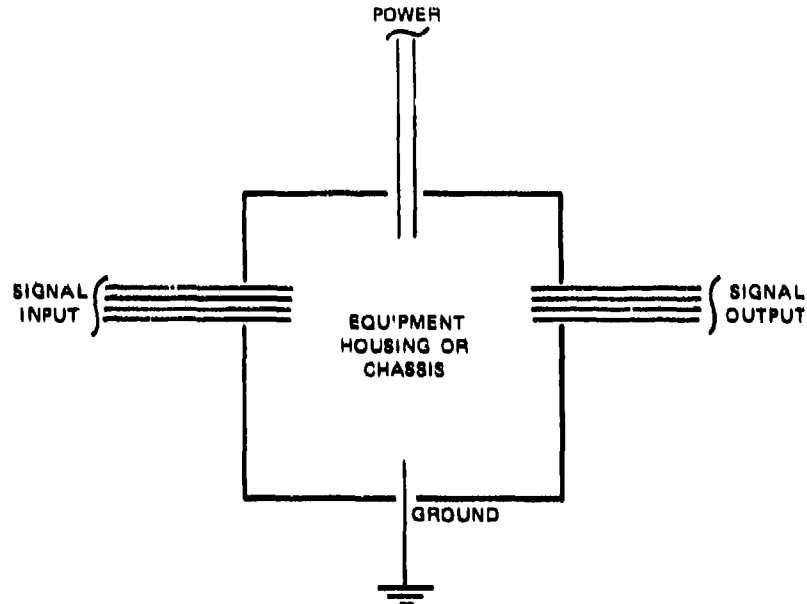


Figure 8-2 CONDUCTORS ENTERING OR LEAVING AN EQUIPMENT CABINET

The determination of the transfer function, or throughput, of certain types of equipment is often necessary to determine the nature of the EMP-induced transient passed through the equipment to more sensitive components downstream. Chapters Two through Five of this handbook describe techniques for determining the transfer functions for transmission lines, service entrances, and transformers so that, given the input fields or source characteristics, the voltages or currents at the output (downstream) terminals can be evaluated. Similar characteristics for other components of the power system or consumer facility may be required to evaluate the transients delivered to sensitive components. In Figure 8-2, for example, it may be necessary to determine the transient delivered to the input, output, and ground conductors by the EMP-induced signal conducted into the equipment on the power conductors.

8.3.2 DIRECT-INJECTION TESTS

Tests of equipment responses to transients conducted on the power conductors usually make use of some form of direct injection of the transient on the conductors. Some of the important considerations in performing such a test are:

- (1) What are the Thevenin or Norton source characteristics of the signal to be injected?
- (2) How are the other conductors (i.e., input, output, ground) terminated?
- (3) Is it important that equipment be energized when it is tested?
- (4) Is it necessary to establish and hold a particular state or operating mode during the test?
- (5) Is the equipment part of a system with feedback such that its output affects its input?
- (6) Are other environmental factors such as ambient pressure, temperature, humidity, illumination, or combustible vapors important to the test results?
- (7) Do transients conducted on other conductors or induced by the EMP fields affect the responses to the transients on the power conductors?

Most of these questions relate to specific properties or functional characteristics of the equipment to be tested and can be answered only when a particular item of equipment and its operating characteristics and environment are specified. This section will be confined primarily to techniques for injecting signals onto power conductors for the purpose of evaluating the tolerance or transfer characteristics of the equipment. However, the source characteristics of the excitation source can be defined from tests such as those described in Section 8.4.2.

For the case where one end of a power circuit is accessible for injection of test signals, a common-mode test voltage can be directly injected at the end through an impedance matrix as illustrated in Figure 8-3. The impedance matrix may simulate the

impedances usually connected between individual conductors and between the conductors and the conduit. In the case of a very long conduit, the voltage delivered to the conductors is:

$$V_{in} = \frac{Z_{in}}{Z + Z_{in}} V \quad (8-1)$$

where V is the source voltage, Z_{in} is the input impedance of the conductors with their normal load on the right-hand side (see Figure 8-3), and Z is the common-mode impedance of the terminating resistors between the source and the conductors. It should be noted that, if the righthand end of the conduit circuit is also terminated in its characteristic impedance, only half of the source voltage is applied to the conduit.

This method of driving power conductors is perhaps the most straightforward and commonly used of all the direct-injection methods. It can also be used with unshielded cables that are routed along a metal structure or are placed in metal cable trays. With unshielded cables of this type, the conductors are driven against the metal structure or trays rather than against the conduit. One disadvantage of this method is that the conductors being driven must be disconnected at one end; hence, the equipment may not be operating in its normal state during the test.

When one end of the circuit is not accessible, a different injection method must be used. Such cases arise where disconnecting the power precludes operating the system in its normal mode. In these cases, it may be necessary to accept some compromise in the quality of the simulation to perform tests economically. One approach that can be used under certain conditions is illustrated in Figure 8-4. At some suitable junction in the power system the excitation source is capacitively coupled to the conductors and permitted to drive them with respect to the local ground or conduit. As illustrated in the figure, however, the current injected at this point is divided into two parts, one flowing in each direction from the injection point. Because this method of distributing the current differs radically from the current distribution that would have resulted from the EMP excitation of the system, some care is required in designing a valid test using this approach.

A test using the injection method shown in Figure 8-4 will be valid only if the equipment response is not affected by the attachment of the energy source. Because the

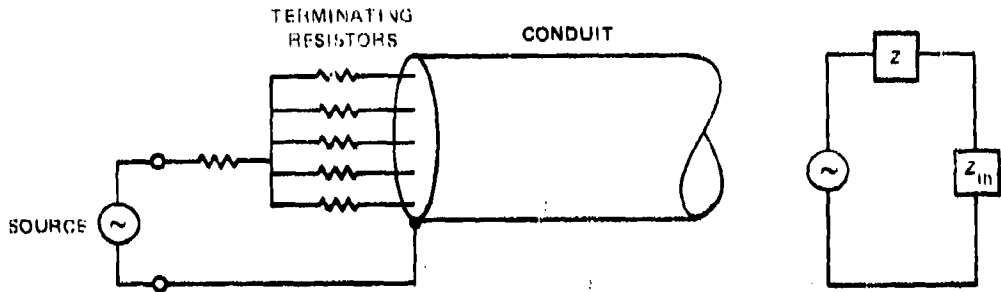


Figure 8-3 IMPEDANCE MATRIX USED TO INJECT COMMON-MODE VOLTAGES

equipment to the right of the injection point in Figure 8-4 is of primary interest in the test, for the test to be valid the portion of the current that flows to the left from the injection point must not be reflected back into the right-hand circuitry during the period when the system is being observed to determine its response to the EMP. This condition implies that no significant reflections should return from the left end of the circuit. Thus the circuit to the left must be very long (a round-trip transit time that is longer than viewing time), or very short (a round-trip transit time that is shorter than any response of interest), or it must be terminated in a matched load (no reflections).

If the driven conductors cannot be made very long, the stipulation that attachment of the excitation source should not significantly affect the system response usually implies that the coupling between the direct-injection source and the system conductors must be so loose that the system impedances are not significantly affected. It is important to observe that the loose-coupling requirement applies to the differential-mode impedances as well as to the common-mode, or line-to-ground, impedances. That is, the attachment of the energy source should, in general, disturb neither the line-to-ground impedances nor the line-to-line impedances of the power circuit at the injection point. The loose-coupling requirement usually requires that much of the source voltage be dissipated in the coupling network.

An alternative to the capacitive coupling method illustrated in Figure 8-4 is the inductive coupling method illustrated in Figure 8-5. In this method, the power conductors are made the one-turn secondary winding of a transformer by threading them through the window of a toroidal ferrite core with the conductor carrying the source current.

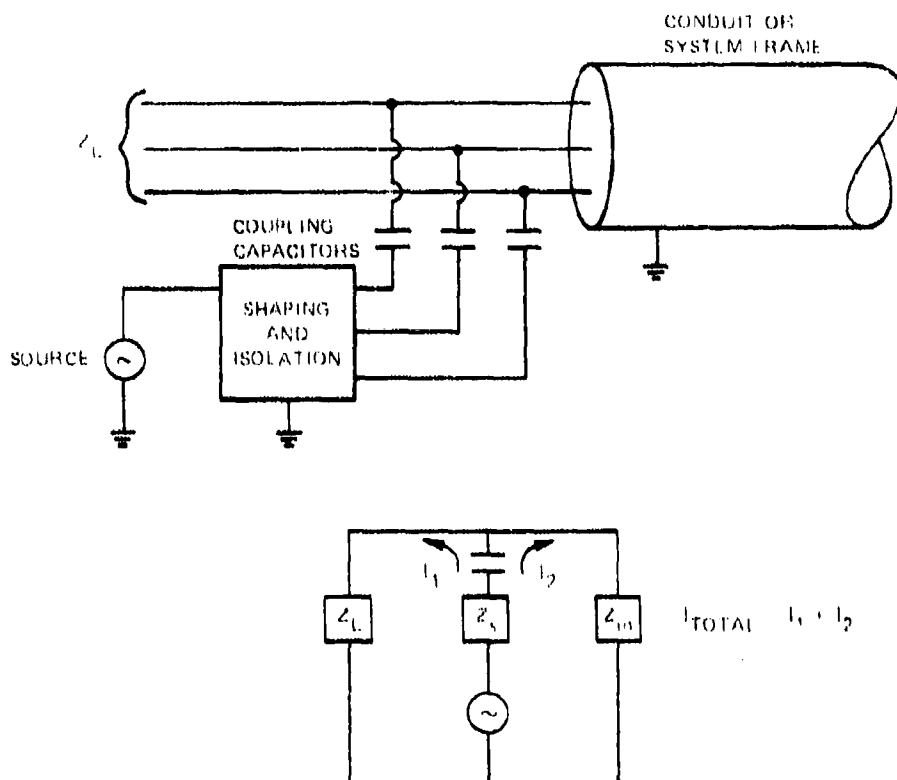


Figure 8-4 CAPACITORS USED TO INJECT COMMON-MODE VOLTAGES

This method has the advantages that the equipment can be operated with power on during the test, and the impedance added to the power conductors by the toroid is usually small enough that it can be ignored.

8.4 EMP TESTS OF FACILITIES

8.4.1 EXCITATION OF THE SERVICE ENTRANCE

Tests at the facility level are also performed primarily to establish thresholds for malfunctions and to determine transfer functions from the power service (e.g., the distribution lines or service entrance) to points of interest in the facility. For existing facilities, diagnostic testing may be performed to locate and rank malfunctions as well as to proof-test

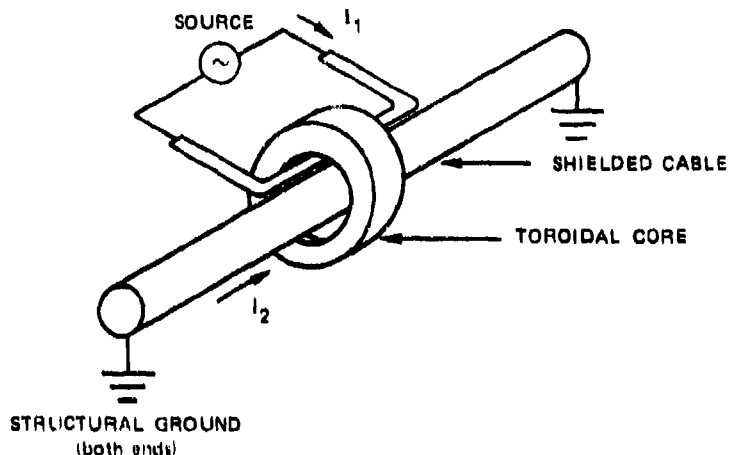


Figure 8-5 CURRENT TRANSFORMER TO INJECT CURRENT ON A GROUNDED CABLE SHIELD

the facility after modifications have been made to increase its tolerance for the EMP-induced transients. New facilities designed to be immune to EMP must also be tested to evaluate the success of the design.

In almost all cases in which EMP coupling into facilities is to be examined experimentally, it is necessary to perform the test without disconnecting the power. There is usually a significant change in the state of the circuits and equipment inside the facility when the commercial power is disconnected, because of relays becoming deenergized, automatic transfer switches becoming activated, and active electronic systems becoming dormant. Thus, unless the facility is very simple or totally passive in its function, it will probably be necessary to test with the power on to obtain valid results. For this reason, the capacitive or inductive coupling methods have been used for injection of the simulated EMP on the service-entrance conductors.

As with direct-injection testing of equipment, the effect of the excitation source impedance on the system response must be considered. At the facility level, however, there is often sufficient attenuation between the excitation source and the internal equipment that the source impedance is not a dominant factor. For economic reasons, the source impedance is often compromised to avoid the expense of loosely coupled megavolt pulse sources. Thus, for example, a 100 kV-tightly coupled source might be used where strict

adherence to preservation-of-impedance concepts might require a 10-MV loosely coupled source.

Because the insulation and coupler design requirements are more severe and the personnel hazards are greater if the pulse is coupled to the primary side of the distribution transformer, it is usually preferable to perform the injection on the secondary side. This often has the additional advantage that a substantially lower voltage is required. Because of the filtering action of the transformer and the mismatch between the aerial line and the conductors in the conduit, only a fraction of the open-circuit voltage induced in the distribution lines is transmitted into the service-entrance conduit. This is another reason that a low-voltage source (e.g., 100 kV) can be used to simulate the effect of several megavolts induced on the distribution lines.

The schematic of a capacitor discharge pulser with capacitive coupling to the power conductors is shown in Figure 8-6. This direct injection pulser was designed so that the high-voltage energy storage capacitor could be placed at ground level. The capacitive coupler unit is mounted near the service-entrance weatherhead and connected to the energy storage unit through four 50-ohm coaxial transmission lines operated in parallel. The reactance of the coupling capacitors is large enough that little 60-Hz current flows through them, but throughout most of the EMP spectrum, their reactance is so small that virtually all of the pulser voltage is applied to the power conductors. The coupler installed at the weatherhead (but not yet connected to the power conductor) is shown in Figure 8-7.

8.4.2 OBSERVATION OF THE SYSTEM RESPONSE

For the simplest form of proof-test, the system response may be judged on the basis of whether or not the system functions properly during and after the simulated EMP is injected into the service entrance. Visual and aural observations to detect any spurious arcing are usually included in such a test. It is more common, however, to provide some instrumentation to make quantitative measurements of selected internal currents and voltages so that the margin by which the system passed or failed the test can be determined.

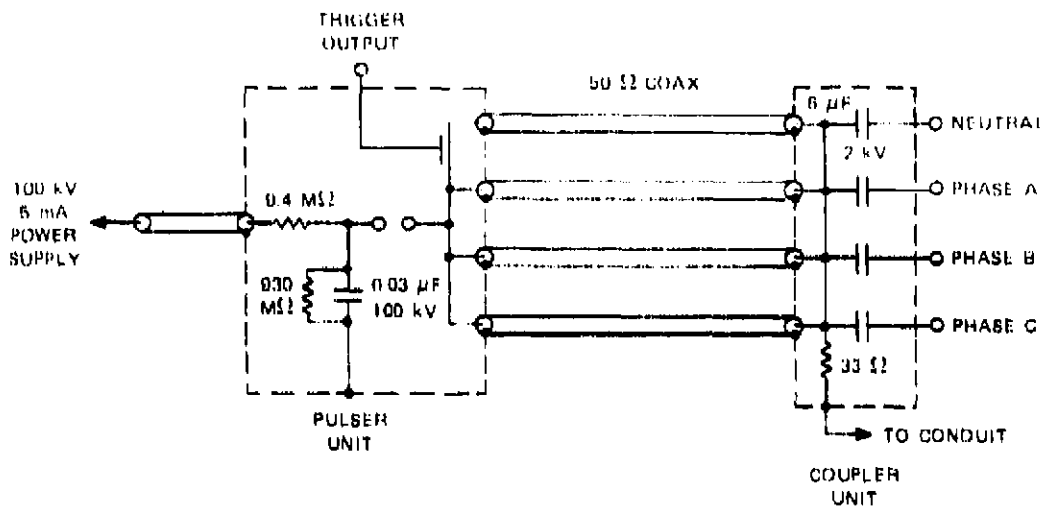


Figure 8-8 SCHEMATIC DIAGRAM OF POWER-LINE PULSER AND COUPLER

Such instrumentation is a necessity for those tests whose primary purpose is to determine the excitation levels to be used in the equipment tests described in Section 8.3.

The basic instrumentation required for measuring the system response is a selection of current probes, high-voltage probes, and a low-power, wideband oscilloscope with a camera capable of recording at fast writing rates (1 cm/ns). Commercial wideband (≥ 100 MHz), low-power (<150 W) oscilloscopes and cameras are readily available. If shielded operation is necessary, inverters for operating the oscilloscope in a shielded enclosure from a 12-V storage battery are also available. (One of the advantages of direct-injection testing is that large external fields and the instrumentation problems associated with them are not produced).

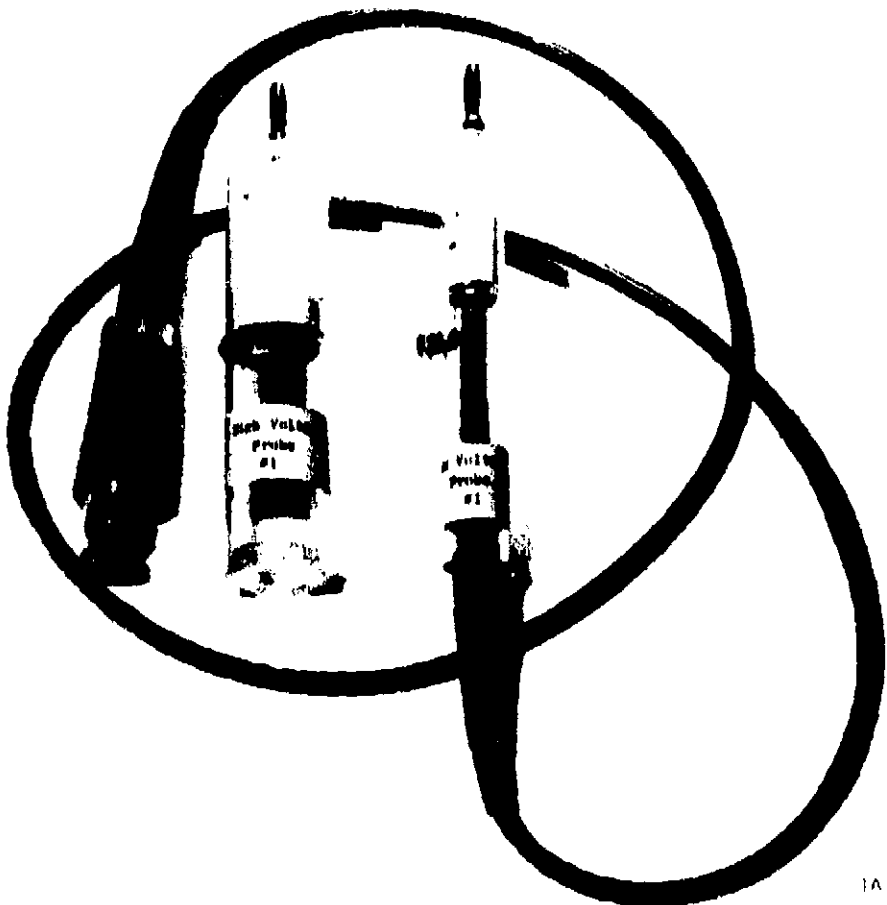
Current probes with a variety of window sizes, amplitude and frequency characteristics, and attachment provisions are also available commercially. Most of these current probes have transfer impedances (ratio of output voltage to current through the window) that decrease with decreasing frequency below a few kilohertz so that they tend to suppress the response to 60-Hz current in the power conductors. This property is desirable for making measurements of transients whose peak current value is equal to or less than the



Figure 8-7 POWER-LINE COUPLER UNIT

60-Hz current in the conductors. The hinged, clamp-on type of probe is also very convenient because it eliminates the necessity of disconnecting conductors to thread them through the window of the probe.

Passive wideband voltage probes are also available for measuring voltages ranging from a few hundred volts to about 30 kV. The high-voltage probes are excellent for measuring voltages with peak values greater than a few hundred volts on 120/240-V power



TA-7000-102

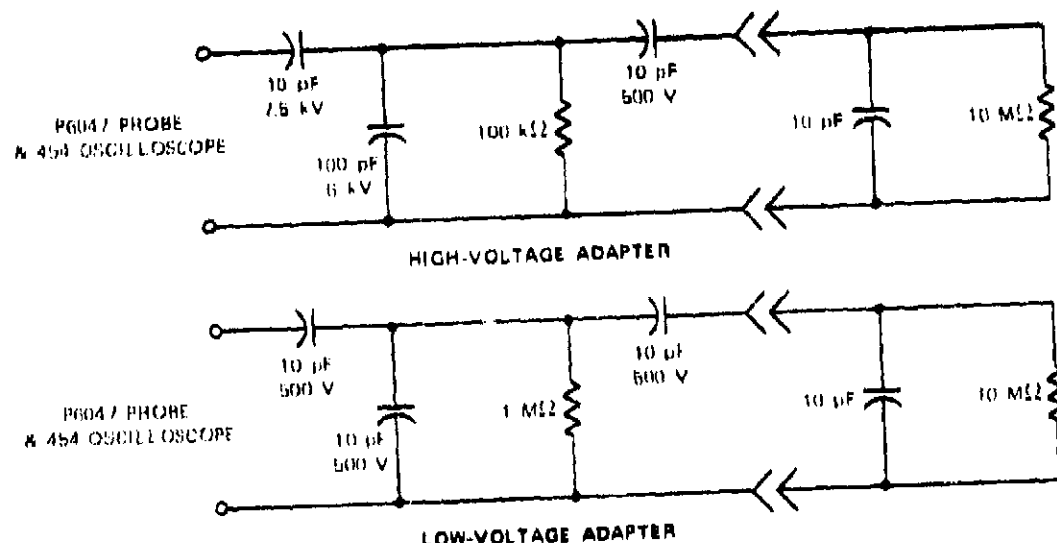


Figure 8-8 PROBE ADAPTERS FOR A TEKTRONIX P-6047 PASSIVE VOLTAGE PROBE

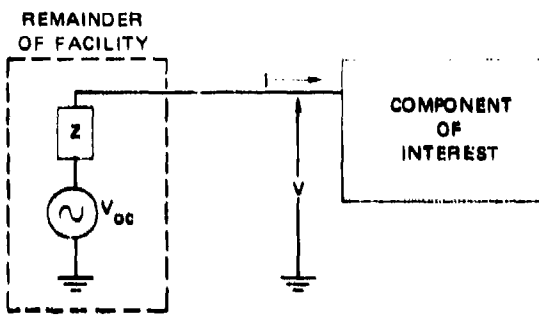


Figure 8-9 DEFINITION OF THE EXCITATION FOR AN INTERNAL EQUIPMENT COMPONENT

is to establish the excitation levels for later use in direct-injection tests of internal equipment, some consideration should be given to methods of specifying these excitation levels. These levels can be specified in terms of the *in situ* current and voltage on the conductors entering the equipment, or they can be specified in terms of a Thevenin (or Norton) equivalent source (see Figure 8-9). In the first case, the excitation source contains the unknown characteristics of the remainder of the facility (which must be simulated in a bench test of the component equipment). In the latter case, the characteristics of the remainder of the facility are contained in the Thevenin equivalent source voltage and impedance. The *in situ* measurements are usually easier to make than those necessary to specify the Thevenin equivalent source, but they may be inadequate to define the excitation source for laboratory or bench tests of the component. On the other hand, to define the Thevenin equivalent source, both the short-circuit current and the open-circuit voltage (or one of these and the source impedance of the circuit) at the excitation point must be measured. Measurement of open-circuit voltage and short-circuit current with the power on is often impossible, however.

This paradox can usually be resolved by acceptable estimates or approximations to the characteristics of the Thevenin equivalent source based on power-off measurements or circuit analysis. If it is necessary to specify the Thevenin source impedance more accurately, series inductance and shunt capacitance can be inverted at the terminals of the component to measure the open-circuit voltage and short-circuit current in the EMP spectrum with the power on.

conductors. For smaller transients, however, the 60-Hz voltage on which the transient is superimposed makes the measurement more difficult. This problem can be alleviated by making a high-pass-filter adapter for the probe so that the 60-Hz response of the probe is suppressed. Such adapters are shown in Figure 8-8.

When the purpose of the test

8.5 CITED REFERENCES

1. *Electrical Transmission and Distribution Book*, 4th ed., 5th printing (Westinghouse Electric Corporation, East Pittsburgh, Penn., 1964).
2. A. L. Whitson, "Engineering Techniques for Electromagnetic Pulse Testing," DNA 3332F, Stanford Research Institute, Contract DNA 3332F, Stanford Research Institute, Contract DNA001-71-C-0087, Defense Nuclear Agency, Washington, D.C. (November 1973).
3. *DASA EMP (Electromagnetic Pulse) Handbook*, DASA 2114-1, DASA Information and Analysis Center, Santa Barbara, Calif. (September 1968).

INDEX

Angle of incidence	61	Conductors, low voltage	264
Attenuation constant	57, 98	Conduit	29, 161
buried cable	189	dimension of	174
transmission line	57, 98	number of wires in	257
wave in lossy media	294	plastic	139, 264
Automatic transfer switch	311	steel	139
Auxiliary power systems	310	transfer impedance	173
Bend in transmission line	109	Core, transformer	202, 207
Branch in transmission line	106	Corona	46, 126
Bushing, transformer	203	threshold of conductors	133
capacitance	78, 213	Coupler, test	325, 326
inductance	216, 234	Coupling	58
Butt wrap, plate	29, 44	to vertical element	77
Cable	45	to conduit	161
serial	47	to shielded cable	185
shielded	139	through service entrance	146
Capacitance	39	through transformers	219
coupling	217	Counterpoise	46
motor windings	271	high-frequency performance	294
stray	270	Crest voltage	207
surge	264	Current transformer	33, 316
transformer windings	213	Differential-mode	116
transmission line	167	coupling to line	121
Carrier, power line	28	in transformers	222
Charge separation	22	in unbalanced systems	126
Chopped-wave test	207, 320	Diffusion constant	178, 180
Circuit breaker	32	Directivity function	57, 120
main	136, 251	Discharge	231
protection at	253	corona	132
Common-mode	49	lightning	25
excitation of transformers	222	Distributed source	51
on signal lines	292	Distribution system	33
Compton electrons	22	lightning arresters	209
Conductivity	39	line	43
air	22	transformer	204
soil	57, 62	Duct, fiber	138
conduit	173		

Electric field	24	Impedance, intrinsic	60
at wire height	54	Impedance, transfer	173, 194
in ground	171	of conduit	173
on a conductor	132	of tape-wound shield	196
Electromagnetic pulse (EMP)	22, 24	Impulse	177, 208
Electronic equipment	27	Impulse, test	208, 320
grounding	282, 293	Inductance	39
susceptibility	27	bushing	246
Entrance, service (see Service entrance)	29	shielded cable	198
Filter	306	stray	258, 260, 267
action of transformer	248	Induction motor	271
test of	307	Insulation	126
Firing voltage	244, 302	cable	139
Flashover	46	low-voltage	263
of insulators	126	transformer	204
Fourier transform	38	Insulators	48
Glimm- vs	22	flashover	126
Gap, spark	209	pin	48
Gradient control	139	post	48
Ground	276	suspension	48
butt wrap, plate	44	Ionization	22
counterpoise	294	by Compton electrons	22, 68
impedance	287	of lightning arrester	208, 248
rod	44, 86	Lightning	25
signal	283	Lightning arresters	29, 210
single-point	284, 286	distribution	141
wire	44	firing characteristics	129, 244
High-altitude EMP	22, 24	secondary	301
Impedance	39	Low-frequency test	208
of ground cable	289	Messenger cable	137
of ground connection	290	Multiconductor transmission lines	153
of motor windings	271	aerial	106
of transformers	219	conduit	273
Impedance, characteristic	60	model of transformer	213
calculation of	108, 117, 270	properties of	156
measurement of	265	Neutral	29, 308
of buried cable	187	grounding	29, 278, 308
of power line	60	conductor in conduit	274
of shielded cable	153, 159	Nuclear detonation	22

Periodically grounded line	91
Poles, wood	43, 46
Pothead	29, 138
Propagation factor	98
in free space	84
in soil	181
for aerial line	57, 98
for buried cable	181
Protection	298
lightning	45, 248
of low-voltage circuits	254
Reflection coefficient	54
Reflectometer, time-domain	268
Sag in transmission line	114
Saturation of conduit	182
Service entrance	138
analysis of	145
weatherhead	137, 140
effect on low-voltage circuits	143
Shielded cable	139
characteristic impedance	187
transfer impedance	194
Skin depth	100, 173
definition of	181
in soil	183
Source region	24
Step function	104
response of entrance cables	146
Surge arrester (<i>see</i> Lightning arresters)	210
Switched capacitor	231
Three-phase	33
transformer connections	279
grounding considerations	252, 277
Time constant	24
bushing capacitance	248
diffusion	174
of incident pulse	64
soil	67, 82, 162
stray inductance	303
Tower, steel	44
description	45
grounding	46, 294
Transfer function	146, 223
Transforms	38
Transformer	29, 202
classes	208
construction	203
distribution	204
transfer characteristics	219, 248
transient tests of	207
Transmission line	42
biconic	78
distributed source	51
formulas for	52
multiconductor	116
properties of	43
Transmission system	43
grounding	278
Uninterruptible power systems	311
Velocity of propagation	29
of light	86
measurement of	267
Vertical elements	77
Wave	27
incident	54
reflected	54
Winding, transformer	204
motor	271
Zero-sequence coupling	50